



POLITECNICO DI TORINO
Repository ISTITUZIONALE

NATURAL VENTILATION OF HIGH-RISE BUILDINGS
- A Methodology for Planning With Different Analysis Tools and Case-Study Integration

Original

NATURAL VENTILATION OF HIGH-RISE BUILDINGS - A Methodology for Planning With Different Analysis Tools and Case-Study Integration / Schulze, Tobias. - (2015).

Availability:

This version is available at: 11583/2637369 since: 2016-03-11T11:20:23Z

Publisher:

Politecnico di Torino

Published

DOI:10.6092/polito/porto/2637369

Terms of use:

Altro tipo di accesso

This article is made available under terms and conditions as specified in the corresponding bibliographic description in the repository

Publisher copyright

(Article begins on next page)

**ISTANBUL TECHNICAL UNIVERSITY ★ GRADUATE SCHOOL OF
SCIENCE ENGINEERING AND TECHNOLOGY**

POLYTECHNIC UNIVERSITY OF TURIN ★ DOCTORAL SCHOOL

**NATURAL VENTILATION OF HIGH-RISE BUILDINGS
A METHODOLOGY FOR PLANNING WITH DIFFERENT ANALYSIS TOOLS
AND CASE-STUDY INTEGRATION**

Ph.D. THESIS

Tobias SCHULZE

Department of Architecture - Construction Sciences Programme

Department of Energy - Energetics Programme

NOVEMBER 2015

contact

schulze-tobias@gmx.de

**ISTANBUL TECHNICAL UNIVERSITY ★ GRADUATE SCHOOL OF
SCIENCE ENGINEERING AND TECHNOLOGY**

POLYTECHNIC UNIVERSITY OF TURIN ★ DOCTORAL SCHOOL

**NATURAL VENTILATION OF HIGH-RISE BUILDINGS
A METHODOLOGY FOR PLANNING WITH DIFFERENT ANALYSIS TOOLS
AND CASE-STUDY INTEGRATION**

Ph.D. THESIS

**Tobias SCHULZE
(502082019 - 188938)**

Department of Architecture - Construction Sciences Programme

Department of Energy - Energetics Programme

**Thesis Advisor: Prof. Dr. A. Zerrin YILMAZ
Thesis Advisor: Prof. Dr. Marco PERINO**

NOVEMBER 2015

İSTANBUL TEKNİK ÜNİVERSİTESİ ★ FEN BİLİMLERİ ENSTİTÜSÜ

TORİNO POLİTEKNİK ÜNİVERSİTESİ ★ FEN BİLİMLERİ ENSTİTÜSÜ

**ÇOK KATLI BİNALARDA DOĞAL HAVALANDIRMA
FARKLI ANALİZ ARAÇLARI VE ÖRNEK ALAN ENTEGRASYONU İLE
PLANLAMA İÇİN BİR YÖNTEM**

DOKTORA TEZİ

**Tobias SCHULZE
(502082019 - 188938)**

Mimarlık Anabilim Dalı - Yapı Bilimleri Programı

Enerji Anabilim Dalı - Enerji Bilimi Programı

**Tez Danışmanı: Prof. Dr. A. Zerrin YILMAZ
Tez Danışmanı: Prof. Dr. Marco PERINO**

KASIM 2015

FOREWORD

While my name may be alone on the front cover of this thesis, I am by no means its sole contributor. Rather, there are a number of people behind this piece of work who deserve to be both acknowledged and thanked here.

First and foremost, I would like to express my deep appreciation and thanks to my supervisors, Prof. Dr. Ayşe Zerrin Yılmaz and Prof. Dr. Marco Perino for their valuable guidance, hospitality, support and encouragement throughout the research. I am very grateful for their patience, motivation, enthusiasm, and immense knowledge in building physics that, taken together, makes them great mentors. They have routinely gone beyond their duties to help me to overcome my worries, concerns, and anxieties, and gave me confidence in both myself and my work. It has been an honour for me to work with them.

I would also like to thank the members of Istanbul Technical University Faculty of Architecture for their contribution in my studies and for hosting me so generously in Istanbul. You all were so important to me while surviving and staying sane in graduate school. Thank you Feride Şener Yılmaz, Mine Aşçıgil Dincer, Meltem Bayraktar, Neşe Ganiç, Cem Taneri and all the others. In regards to the wind tunnel experiments, I thank Prof. Dr. Vildan Ok for great support. I would also like to thank my dissertation monitoring committee members including Prof. Dr. Ahmet Arisoy, Prof. Dr. Cem Parmaksızoğlu for all of their guidance through this process; your discussion, ideas, and feedback have been absolutely invaluable.

In the same vein, I would like to extend great thanks to the members of the Citynet group, who warmly offered their stories, support and commitment. This piece of research looks very different because of their input, influence and expert knowledge. It was a great opportunity for me to participate in this European PhD program on sustainable energy management, which received funding from the People Programme (Marie Curie Actions) of the European Union's Seventh Framework.

I would like to express my appreciation to all those who have offered me their time when I collected necessary data for my case study. Thank you Nimet Kara and Tuncer Kınıklı from the Kanyon building management.

My sincere thanks also goes to Prof. Dr. Ursula Eicker and the staff at Stuttgart University of Applied Sciences, Department of Building Physics, who has been a big support for me during my studies.

I thank all my friends in Turkey and Germany who have always been a big part of my life. They have helped me, one way or another, in my struggle to complete my Ph.D. Special mention goes to Silvine, for her generous encouragement. Thanks also to Vijay and Sarah for their fantastic support, to Anett for imparting presentation techniques and to Önder for having good times in Istanbul and for sharing the flat with me.

Finally, but by no means least I would like to appreciate my deepest thanks to my beloved family, my parents Ursula Hamm and Reinhardt Schulze and my brother Felix Schulze, who have always been a constant source of support to me throughout my life.

Along the way, I have received support from too many people to count. Though you may not see your names here, in black and white, know that your various contributions have not gone unnoticed or unappreciated. Thank you

September 2015

Tobias Schulze

TABLE OF CONTENTS

	<u>Page</u>
FOREWORD	vii
TABLE OF CONTENTS	ix
ABBREVIATIONS	xiii
NOMENCLATURE	xv
LIST OF TABLES	xvii
LIST OF FIGURES	xix
SUMMARY	xxv
ÖZET	xxix
1. INTRODUCTION	1
1.1 Design Methodology	2
1.2 Contributions of the Study	4
1.3 Hypothesis	5
1.4 Assumptions	7
1.5 Structure of the Thesis	8
2. LITERATURE REVIEW	11
2.1 High-Rise Office Buildings	13
2.2 Natural Ventilation	15
2.2.1 Driving forces	17
2.2.2 Ventilation strategies	20
2.2.3 Ventilation elements	24
2.2.4 Ventilative cooling	30
2.2.5 Design impact	33
2.2.6 Control strategies	35
2.3 Performance Indicators	38
2.3.1 Indoor air quality	38
2.3.2 Thermal comfort	39
2.3.3 Energy consumption	41
2.4 Airflow Modelling Approaches	42
2.4.1 Analytical approaches	42
2.4.2 Airflow networks	47
2.4.3 Computational fluid dynamics	48
2.5 Previous Research Projects on Natural Ventilation	49
2.5.1 PASCOOL (1992-95)	49
2.5.2 IAE Annex 28: Low Energy Cooling (1993-97)	50
2.5.3 AIOLOS (1993-97)	54
2.5.4 NatVent (1994-98)	58
2.5.5 IAE Annex 5: AIVC (ongoing since 1979)	64
2.5.6 IEA Annex 35: HybVent (1998-2002)	65
2.5.7 IAE Annex 62: Venticool (ongoing 2014 - 2017)	72

2.6 Regulatory Framework	72
2.6.1 BS 5925	73
2.6.2 EN 13779.....	75
2.6.3 EN 15251.....	75
2.6.4 EN 15242.....	78
2.7 Conclusions.....	79
3. METHODOLOGY	81
3.1 Conceptual Design	82
3.1.1 Natural ventilation.....	82
3.1.2 Solar heat gain reduction.....	85
3.1.3 Thermal mass activation.....	85
3.2 Preliminary Design and Tool Development	86
3.2.1 Ventilation model calculation method	89
3.2.2 Thermal model calculation method.....	102
3.2.3 Tool validation	113
3.3 Detailed Design Development through Energy Simulation	117
3.3.1 Simulation environment	118
3.3.2 Control strategies for the naturally ventilated offices	122
3.3.3 Final natural ventilation system sizing.....	129
3.4 Design Evaluation.....	130
3.5 Conclusions.....	132
4. THE KANYON CASE-STUDY BUILDING	135
4.1 Site	135
4.2 Office Tower.....	137
4.2.1 Introduction	137
4.2.2 Construction elements	138
4.2.3 Internal heat gains	142
4.2.4 Mechanical HVAC systems	144
4.2.5 Metered energy consumption.....	145
4.3 Conclusions.....	146
5. THE CLIMATE ASSESSMENT	147
5.1 Whole Year	149
5.1.1 Overview	149
5.1.2 Wind	150
5.1.3 Temperature	152
5.1.4 Adaptive thermal comfort limits	153
5.2 Cooling Period	154
5.2.1 Wind.....	154
5.2.2 Psychrometrics	155
5.2.3 Excess temperatures	157
5.2.4 Cooling potentials	159
5.3 Summer Design Days	161
5.3.1 ASHRAE cooling design day approach.....	161
5.3.2 ASHRAE summer design weeks.....	163
5.3.3 SWMD approach.....	164
5.4 Conclusions.....	167

6. THE APPLIED PASSIVE COOLING APPROACH.....	169
6.1 Conceptual Case-Study Design Adaptations	169
6.1.1 Natural ventilation.....	169
6.1.2 Solar heat gain reduction.....	171
6.1.3 Thermal mass activation	172
6.2 Preliminary Design	173
6.2.2 Case-study application	179
6.3 Detailed Design Development through Energy Simulation	181
6.3.1 Simulation setup.....	181
6.3.2 Final natural ventilation system sizing.....	189
6.4 Conclusions	195
7. DESIGN EVALUATION	199
7.1 Weekly Profiles	199
7.1.1 Mechanical approach	200
7.1.2 Passive approach	203
7.1.3 Hybrid approach.....	210
7.2 Annual Assessment.....	212
7.2.1 Ventilation rates	213
7.2.2 Thermal comfort.....	215
7.2.3 Energy consumption.....	227
7.3 Conclusions	232
8. CONCLUSIONS.....	237
8.1 Introduction.....	237
8.2 Summary and Conclusions from the Design Approach	238
8.3 Summary and Conclusions from the Design Evaluation.....	242
8.4 Limitations and Ideas for Future Work	244
8.5 Conclusion	247
REFERENCES	249
APPENDICES	259
CURRICULUM VITAE.....	293

ABBREVIATIONS

AFN	: Airflow Network
ACH	: Air Changes per Hour
BEPS	: Building Energy Performance Simulation
CFD	: Computational Fluid Dynamics
CHTC	: Convective Heat Transfer Coefficient
COP	: Coefficient of Performance
E+	: EnergyPlus Building Energy Simulation
EMS	: Energy Management System
FCU	: Fan Coil Unit
GWP	: Global Warming Potential
HVAC	: Heating, Ventilation and Air Conditioning
IEA	: International Energy Agency
NPL	: Neutral Pressure Level
OF	: Opening Factor
PEI	: Primary Energy Input
SHGC	: Solar Heat Gain Coefficient
SWMD	: Summer design Week Mean Day
IAQ	: Indoor Air Quality
TMY	: Typical Meteorological Year

NOMENCLATURE

Nomenclature

A	: area	m^2
ACH	: air change rate per hour	h^{-1}
c	: specific heat capacity	$J\ kg^{-1}\ K^{-1}$
C	: coefficient	dimensionless
C	: thermal capacity of a body	$J\ K^{-1}$
CO₂	: carbon dioxide concentration	ppm
d	: thickness	m
g	: acceleration due to gravity	$m\ s^{-2}$
h	: height of a construction element	m
HR	: humidity ratio	kg water per kg air
k	: external opening sizing factor	dimensionless
K	: internal opening sizing factor	dimensionless
l	: length	m
m	: mass	kg
\dot{m}	: mass flow	$kg\ s^{-1}$
p	: pressure	Pa
Q	: heat transfer	J
q	: heat flux	$J\ m^{-2}$
\dot{q}	: heat flux rate	$W\ m^{-2}$
Q	: heat transfer rate	W
R	: thermal resistance	$m^2\ W\ K^{-1}$
R	: flow resistance	$kg\ m^{-7}$
t	: time	s
T	: temperature	$^{\circ}C$
V	: volume	m^3
w	: width	m
v	: velocity	$m\ s^{-1}$
\dot{V}	: volume flow	$m^3\ s^{-1}$
z	: height above ground level	m
α	: window opening tilt angle	$^{\circ}$
β	: wind speed profile exponent	dimensionless
δ	: wind speed profile boundary layer thickness	m
ε	: exponential EMS control amplifier	dimensionless
λ	: linear EMS control amplifier	dimensionless
ρ	: density	$kg\ m^{-3}$
τ	: time constant	s
χ	: areal diurnal storage capacities of a body	$W\ h\ m^{-2}\ K^{-1}$

Subscripts

0	: reference
A	: supply chimney zone
air	: air
B	: exhaust chimney zone
b	: buoyancy
baro	: barometric
c	: convection
c1	: adaptive comfort limit category 1 according to EN 15251 standard
chi	: chimney
d	: discharge
dif	: diffuse radiation share
dir	: direct radiation share
E	: environment
eff	: fluidic effective share
ext	: external
I	: zone capital letter placeholder
i	: airflow opening number placeholder
i	: thermal mass layer number placeholder
in	: internal
m	: thermal mass
max	: maximum
met	: meteorological station location
min	: minimum
op	: operative
P	: in parallel
p	: pressure
r	: radiation
rm	: exponentially weighted running mean
S	: in series
s	: stack
se	: surface external
si	: surface internal
site	: site location
tot	: total or sum
v	: ventilation
w	: wind
win	: window
z	: local height from start height
τ	: window transmitted radiation

LIST OF TABLES

	<u>Page</u>
Table 2.1 : Recommended night cooling control strategies from different investigations. ..	37
Table 2.2 : Determination of natural ventilation rates reproduced from.....	74
Table 2.3 : Concentration levels of outdoor air and classification of indoor air quality.....	75
Table 2.4 : Description of the categories used in the adaptive thermal comfort model.....	78
Table 3.1 : Terrain-dependent coefficients.	90
Table 3.2 : Deviation from 10 h ⁻¹ design air change rate.....	115
Table 3.3 : Overview of the modelled natural ventilation controls.....	123
Table 3.4 : List of sensors for flow control in the EMS model.....	127
Table 4.1 : Thermal properties of the building construction elements also incorporated to the model.....	139
Table 4.2 : Thermal properties of the building construction materials also incorporated to the model.....	139
Table 4.3 : Thermal and visual properties of the window glazing.	140
Table 4.4 : Recommended equipment load factors for various office types.....	143
Table 4.5 : Natural-gas and electricity consumption of the Kanyon office tower in 2008.	145
Table 5.1 : Annual wind velocity and direction statistics for Istanbul, Turin, and Stuttgart.....	150
Table 5.2 : Cooling period wind direction statistics for Istanbul, Turin and Stuttgart.....	155
Table 5.3 : Cooling period wind velocity statistics for Istanbul, Turin and Stuttgart.....	155
Table 5.4 : Average temperature difference at day and night between external air, and indoor operative comfort criteria indicating the climatic ventilative cooling potentials.	160
Table 5.5 : Cooling peak temperatures and temperature ranges for design day calculations.	162
Table 5.6 : SWMD peak temperature and temperature range for design day calculations.	165
Table 5.7 : SWMD solar path information for design day calculations.....	166
Table 6.1 : Thermal properties of composition elements for three different levels of thermal mass	172
Table 6.2 : Inputs made for the flow path sizing pre-design with fixed boundary conditions.....	176
Table 6.3 : Brief overview of the simulation setup for the as-built and the adapted scenarios.....	182
Table 6.4 : Mean wind pressure coefficients as AFN input for ‘crack’ infiltration calculations.	188
Table 6.5 : Simulated derivation between the EMS target and reached ACH in the month with the highest target ventilation rates depending on the natural ventilation system size.	192
Table 6.6 : Floor area weighted average adaptive comfort criteria reached for the adapted base-case scenario during occupied hours depending on the natural ventilation system sizing.....	195
Table 7.1 : Extreme summer operative temperature reduction by design adaptations.....	210
Table 7.2 : Parametric solar gain reduction scenarios for the thermal comfort evaluation.	220

Table 7.3 : Passive cooling base-case comfort hours below and above category II when the adaptive temperature approach is applicable for 4 office zone orientations and in 3 climates.....	223
Table 7.4 : Primary energy input of electricity and natural gas in kWh primary energy per kWh end energy usage according to GEMIS database.	230
Table 7.5 : Electricity generation mix in 2010 according to GEMIS database.	231
Table 7.6 : Global warming potential of electricity mix and natural gas in kg CO _{2e} per kWh end energy usage in 2010 according to GEMIS database.....	231

LIST OF FIGURES

	<u>Page</u>
Figure 2.1 : Internal and external pressure distribution of buoyant flow causes airflow through a single large opening or through a lower and upper opening.	17
Figure 2.2 : Wind pressure distribution on a pitched roof building.	18
Figure 2.3 : Comparison of wind pressure coefficients on the façade for a low-rise building with different shielding conditions.....	19
Figure 2.4 : Single-sided single and double opening ventilation.	21
Figure 2.5 : Wind driven cross ventilation with two openings, one on each orientation. ...	22
Figure 2.6 : Buoyancy assisted cross ventilation with two openings.....	22
Figure 2.7 : Stack ventilation with solar and wind assistance.	23
Figure 2.8 : Central chimney ventilation.	23
Figure 2.9 : ‘Termite’ chimney ventilation example.	24
Figure 2.10 : Geometrical representations of horizontally and vertically movable sliding windows and their resulting effective opening area, height, and width.	25
Figure 2.11 : Effective areas with different height to width ratios scaled by the fully opened window with equal area according to van Paassen, and comparison with the EN 15242 polynomial approximation.	26
Figure 2.12 : Effective area for a wide and a narrow pivoted window scaled by the fully opened window with equal area according to van Paassen, and comparison with measured data reported by IES MacroFlo.	27
Figure 2.13 : Geometrical representation of a bottom-hung window and the resulting effective opening area and height.....	27
Figure 2.14 : Geometrical representation of a top-hung window and the resulting effective opening area and height.....	27
Figure 2.15 : Geometrical representation of a side-hung window and the resulting effective opening area and width.....	28
Figure 2.16 : Stack ventilation with sub-slab distribution.	28
Figure 2.17 : A characteristic airflow pattern and temperature stratification in a room with displacement ventilation.....	29
Figure 2.18 : Three types of aerodynamic device: wind scoop, wind extract, balanced ventilator.....	29
Figure 2.19 : Natural ventilation air change rates applied or measured.....	31
Figure 2.20 : Boundaries of outdoor air conditions within which indoor comfort can be provided by natural ventilation during the day, with indoor airspeed about 2 m/s (a very light breeze).....	32
Figure 2.21 : Typical surface temperature cycle of an office concrete slab using the thermal mass as a heat sink with a constant flow rate of 10 ACH.	33
Figure 2.22 : Three ventilation strategies for tall buildings: upward cross-flow with direct connection between floors; upward cross-flow with segmentation; isolated spaces.	35
Figure 2.23 : Monitored and allowed CO ₂ concentrations.....	39
Figure 2.24 : Pressure distribution and NPL for two openings buoyant flow with the same and different opening areas.	44
Figure 2.25 : Pressure distribution and NPL for multiple openings buoyant flow with different opening areas.	45

Figure 2.26 : Analytical results of a variant matrix for single-sided ventilation with small temperature differences between room and ambient air. The base-case is a room depth of 5,75 m and 2,8 m ceiling height with a total effective opening area of 0,88 m ²	47
Figure 2.27 : Control Strategy 1 - Setpoint Control.	53
Figure 2.28 : Effect of the control strategies.	61
Figure 2.29 : Graphical pre-design tool for night cooling.	62
Figure 2.30 : Feedforward control during occupied office time.	63
Figure 2.31 : Rule-based control of indoor air temperature (mixed-mode example).	70
Figure 2.32 : Design values of the operative room temperature for buildings without mechanical cooling as a function of the weighted ambient temperature.	77
Figure 2.33 : Effective area of a bottom-hung window scaled by the fully opened window with equal area.	79
Figure 3.1 : Maximum penetration depth for different ventilation strategies applied to a wide, exemplarily square shaped office-tower, which are wind driven cross ventilation, buoyancy driven single-sided ventilation and central void ventilation.	83
Figure 3.2 : Building segmentation of a high-rise building with multiple floors for each segment (here 5 storeys each) and with a commonly used exhaust stack.	84
Figure 3.3 : Simplified thermal-circuit model of the tool developed exclusive radiative heat transfer.	87
Figure 3.4 : Example of the steady state ventilation design major outputs for a 5-storey building segment with a internal chimney, sized for 13 air changes per hour.	88
Figure 3.5 : Example of the 'HighVent' design tool's major thermal outputs.	89
Figure 3.6 : Local wind speed profiles depending on terrain, meteorological wind speed, and height.	91
Figure 3.7 : Local external temperature profiles depending on the height.	93
Figure 3.8 : Local atmospheric pressure profiles depending on the height.	93
Figure 3.9 : Pressure drops across the whole flow path from the supply inlet to the exhaust outlet.	95
Figure 3.10 : Electric circuit and airflow analogy.	95
Figure 3.11 : Pressure head at differently sized openings depending on the volume flow according to Atkinson's equation for turbulent flow.	96
Figure 3.12 : Schematic overview of the exemplarily 5 storey per segment for volume flow calculations.	99
Figure 3.13 : Configuration for applying the electric analogy method to upward flow ventilation of a seven-cell model of a five storey building segment.	100
Figure 3.14 : Fixed sizing boundary conditions natural ventilation model exemplarily for a segment including two chimney and five storey cells.	101
Figure 3.15 : Schematic of the internal air heat balance.	103
Figure 3.16 : Schematic of the external wall heat balance model.	104
Figure 3.17 : Schematic of the external window heat balance model.	105
Figure 3.18 : RC-model for the windows.	105
Figure 3.19 : Schematic of the internal floor / ceiling adiabatic construction heat balance model.	106
Figure 3.20 : Schematic of the internal 'extra' mass construction heat balance model.	107
Figure 3.21 : Long wave radiation exchange at the interior surfaces.	108
Figure 3.22 : Long wave radiation exchange at the exterior surfaces.	108
Figure 3.23 : Direct solar beam distribution on interior surfaces.	109
Figure 3.24 : Diffuse solar beam distribution on interior surfaces.	109
Figure 3.25 : Internal heat gains distribution.	109
Figure 3.26 : Layers of the Lumped Capacity Model (LCM) construction.	110
Figure 3.27 : The heat flux balance at the surface node.	110
Figure 3.28 : Exemplary indoor air conditions together with predicted comfort limits for 0 W/m ² of solar radiation and different air velocities.	112

Figure 3.29 : Exemplarily indoor air conditions together with predicted comfort limits for 50 W/m ² of solar radiation and different air velocities.	112
Figure 3.30 : View from the inlet side on 12 zone AFN model representing one building segment.	115
Figure 3.31 : Tool validation dynamic environmental input parameters for Istanbul extreme summer design day.	116
Figure 3.32 : Tool validation dynamic internal output for Istanbul extreme summer design day and naturally ventilated base-case scenario.....	117
Figure 3.33 : Tool validation dynamic air change rate for Istanbul extreme summer design day.....	117
Figure 3.34 : Linear amplifier correction factor λ dependent on the external temperature.	125
Figure 3.35 : Ventilative cooling lower temperature limit for night-time ventilation in warm period.....	126
Figure 3.36 : Placement of the controlled openings.....	127
Figure 3.37 : EMS controlled air change rate for a typical spring week in Istanbul.	128
Figure 3.38 : Resulting EMS controlled air change rate for a typical summer week in Istanbul.	129
Figure 3.39 : Performance evaluation wheel developed to access simulated passive cooling design.....	131
Figure 4.1 : Location of the case-study site.	135
Figure 4.2 : Kanyon site with the office tower cross and longitudinal sections.	136
Figure 4.3 : Kanyon site plan at height of the residential / cinema floor.	136
Figure 4.4 : Pictures of the Kanyon multiplex including the office tower.....	136
Figure 4.5 : Kanyon office tower cross-section.	137
Figure 4.6 : Kanyon storey plan geometry.....	138
Figure 4.7 : Exemplary office plan.	138
Figure 4.8 : Exemplary office section.....	138
Figure 4.9 : Three pictures taken from an exemplary office storey interior.	138
Figure 4.10 : Shading devices from inside.....	141
Figure 4.11 : External shading device drawing detail.....	141
Figure 4.12 : Simulated effectiveness of the actual shading devices in a typical summer and winter week period according to the ASHRAE IEWC weather data.	141
Figure 4.13 : Mean actual internal heat gains modelled related to the total net storey area including the core and data centres.....	142
Figure 5.1 : The geographical locations of Istanbul, Turin, and Stuttgart shown on a Köppen climate classification map for Europe.	148
Figure 5.2 : Typical monthly average temperature, wind speed, relative humidity, and solar radiation for Istanbul, Turin, and Stuttgart at meteorological station... ..	149
Figure 5.3 : Annual wind speed frequency distribution for Istanbul, Turin, and Stuttgart.	150
Figure 5.4 : Average daily mean, daily maxima and daily minima wind velocity in Istanbul.	151
Figure 5.5 : Average daily mean, daily maxima and daily minima wind velocity in Turin.	151
Figure 5.6 : Average daily mean, daily maxima and daily minima wind velocity in Stuttgart.	152
Figure 5.7 : Average daily temperature swing between day and night.	152
Figure 5.8 : Adaptive thermal comfort boundaries for Istanbul.	153
Figure 5.9 : Adaptive thermal comfort boundaries for Turin.	153
Figure 5.10 : Adaptive thermal comfort boundaries for Stuttgart.....	154
Figure 5.11 : Boundaries of external temperature and humidity within which indoor comfort can be provided by natural ventilation during day at high air change rates with indoor airspeed at about 2 m/s and daytime climatic data for Istanbul during cooling period.	156

Figure 5.12 : Boundaries of external temperature and humidity within which indoor comfort can be provided by natural ventilation during day at high air change rates with indoor airspeed at about 2 m/s and daytime climatic data for Turin during cooling period.....	157
Figure 5.13 : Boundaries of external temperature and humidity within which indoor comfort can be provided by natural ventilation during day at high air change rates with indoor airspeed at about 2 m/s and daytime climatic data for Stuttgart during cooling period.....	157
Figure 5.14 : Excess frequency of fixed outdoor temperature limits.	158
Figure 5.15 : Excess frequency of outdoor temperature limits above climate specific upper adaptive comfort category limits.	158
Figure 5.16 : Daily cooling potentials in the cooling period for Istanbul.	159
Figure 5.17 : Daily cooling potentials in the cooling period for Torino.	159
Figure 5.18 : Daily cooling potentials in the cooling period for Stuttgart.	160
Figure 5.19 : Daily temperature multiplier profile.	162
Figure 5.20 : Dry-bulb temperature profile for Istanbul, Turin and Stuttgart climate according to the ASHRAE 2,0% occurrence value Cooling Design Day.	163
Figure 5.21 : Typical/extreme period according to the ASHRAE IEWC weather data and the related statistics for Istanbul climate.....	163
Figure 5.22 : Typical/extreme period according to the ASHRAE IEWC weather data and the related statistics for Turin climate.....	164
Figure 5.23 : Typical/extreme period according to the ASHRAE IEWC weather data and the related statistics for Stuttgart climate.....	164
Figure 5.24 : SWMD temperature profiles.....	165
Figure 5.25 : SWMD external horizontal direct solar radiation profiles.....	165
Figure 5.26 : SWMD external horizontal diffuse solar radiation profiles.....	165
Figure 5.27 : SWMD external humidity ratio profiles.	166
Figure 5.28 : Wind speed daily mean occurrence frequencies and 91 day period averages for the hottest 25% days of the year.....	167
Figure 6.1 : Maximum penetration depth for different ventilation strategies applied to the Kanyon, which are wind driven cross ventilation, buoyancy driven single-sided ventilation and central void ventilation.	170
Figure 6.2 : Modular five storey base-case natural ventilation building segment.....	170
Figure 6.3 : Side view of the enhanced shading window blind with horizontal slats showing slat geometry as modelled in the adapted base-case scenarios for passive cooling.....	171
Figure 6.4 : Simulated effectiveness of the controlled blinds compared to the actual shading devices in a typical summer and winter week period.....	171
Figure 6.5 : Effective heat capacity for a one day period of building elements for four different levels of thermal mass and classification.	173
Figure 6.6 : Total wind pressure difference across the flow paths from the inlet to the outlets.....	174
Figure 6.7 : Total stack pressure difference across the flow paths from the inlet to the outlet.	174
Figure 6.8 : Pressure drop across the flow paths from the supply inlet to the exhaust outlet for each storey of five segments with 5 storeys each, calculated according the unchanging design boundary conditions.	175
Figure 6.9 : Outputs for extreme summer conditions in Istanbul.....	177
Figure 6.10 : Outputs for typical summer conditions in Istanbul.....	177
Figure 6.11 : Outputs for extreme summer conditions in Turin.....	177
Figure 6.12 : Outputs for typical summer conditions in Turin.....	177
Figure 6.13 : Outputs for extreme summer conditions in Stuttgart.....	177
Figure 6.14 : Outputs for typical summer conditions in Stuttgart.....	177
Figure 6.15 : Outputs for extreme summer conditions in Turin.....	178
Figure 6.16 : Outputs for typical summer conditions in Turin.....	178

Figure 6.17 : Plan view of one storey of Kanyon including an central chimney.....	179
Figure 6.18 : Outputs of the flow path sizing pre-design with fixed boundary conditions for each segment and the three climates considered.....	180
Figure 6.19 : Geometrical representation of the simulation model.....	183
Figure 6.20 : Geometrical representation of the model zones and orientation.	183
Figure 6.21 : Comparison of the monthly metered (2008) and simulated energy consumption (typical year) of the as-built scenario.....	189
Figure 6.22 : Monthly simulated electricity consumption of the different consumers.	189
Figure 6.23 : Ventilation potentials and control targets for Istanbul climate.....	190
Figure 6.24 : Ventilation potentials and control targets for Turin climate.....	191
Figure 6.25 : Ventilation potentials and control targets for Stuttgart climate.....	191
Figure 6.26 : Floor area weighted average, zone minimum and zone maximum adaptive annual comfort criteria reached in respect to the three climates investigated for the naturally ventilated base-case scenario, a scenario without improved shading, and a scenario without thermal mass activation at the ceiling.....	193
Figure 6.27 : Natural ventilation system sizing sensitivity analysis in respect to the annual area weighted mean adaptive comfort distribution during occupancy.....	194
Figure 6.28 : Natural ventilation system sizing sensitivity analysis in respect to the annual area weighted mean adaptive comfort distribution during occupancy.....	195
Figure 7.1 : Design week simulation outputs of the as-built case in Istanbul.....	201
Figure 7.2 : Design week simulation outputs of mechanical ventilation only case without heating and cooling in Istanbul.	202
Figure 7.3 : Design week simulation outputs of the base-case scenario for passive cooling but with uncontrolled ventilation and without heating in Istanbul... ..	203
Figure 7.4 : Simulation results of the base-case scenario for passive cooling but with night-time ventilation only and without heating in Istanbul.....	204
Figure 7.5 : Simulation results of the base-case scenario for passive cooling but with daytime ventilation only and without heating in Istanbul.	205
Figure 7.6 : Simulation results of the base-case scenario for passive cooling but with fixed-setpoint ventilation and without heating in Istanbul.	206
Figure 7.7 : Simulation results of the base-case scenario for passive cooling with adaptive temperature amplifier control but without heating in Istanbul.....	207
Figure 7.8 : Simulation results of the base-case scenario for passive cooling with adaptive temperature amplifier control but without heating in Turin.....	208
Figure 7.9 : Simulation results of the base-case scenario for passive cooling with adaptive temperature amplifier control but without heating in Stuttgart.....	209
Figure 7.10 : Extreme summer design week simulation results for the southwest zones indicating the effectiveness of the passive cooling conceptual design adaptations.....	210
Figure 7.11 : Design week simulation outputs of the base-case scenario for hybrid cooling and ventilation in Istanbul.	211
Figure 7.12 : Simulated controlled air change rates over the course of an year.	214
Figure 7.13 : Comfort analysis for the passive cooling approach in different climates according to EN 15251 comfort categories during occupancy.....	216
Figure 7.14 : Comfort analysis for the passive and hybrid cooling approach in different climates according to the internal relative humidity level during occupancy.....	217
Figure 7.15 : Thermal mass distribution scenarios sensitivity analysis w.r.t. the annual area weighted average adaptive comfort distribution during occupancy.	219
Figure 7.16 : Thermal mass convective heat transfer sensitivity analysis w.r.t. the annual area weighted average adaptive comfort distribution during occupancy.	219

Figure 7.17 : Protection of external heat gains sensitivity analysis w.r.t. the annual area weighted average adaptive comfort distribution during occupancy.....	220
Figure 7.18 : Prevention of equipment heat gains sensitivity analysis w.r.t. the annual area weighted average adaptive comfort distribution during occupancy.....	221
Figure 7.19 : Heat maps of comfort hours for the passive cooling base-case scenario when adaptive comfort criteria from EN 15251 is applicable in Istanbul.	222
Figure 7.20 : Heat map of comfort hours for the passive cooling base-case scenario when adaptive comfort criteria from EN 15251 is applicable in Turin.	223
Figure 7.21 : Heat map of comfort hours for the passive cooling base-case scenario when adaptive comfort criteria from EN 15251 is applicable in Stuttgart. ...	223
Figure 7.22 : Heat map of comfort hours for an inappropriate passive cooling scenario with the actual as-built shading devices and without thermal mass activation at the ceiling when adaptive comfort criteria is applicable in Istanbul.	224
Figure 7.23 : Simulation results of the office space psychrometrics during occupancy and in the cooling period for Istanbul climate.	225
Figure 7.24 : Simulation results of the office space psychrometrics during occupancy and in the cooling period for Turin climate.	226
Figure 7.25 : Simulation results of the office space psychrometrics during occupancy and in the cooling period for Stuttgart climate.	226
Figure 7.26 : Simulated energy consumption of the as-built Kanyon building base-case. .	228
Figure 7.27 : Simulated electricity consumption of the mechanically and passively cooled base-case scenarios.....	228
Figure 7.28 : Simulated natural-gas consumption of the mechanically and passively cooled base-case scenarios.....	229
Figure 7.29 : Comparative whole building annual primary energy input analysis.....	230
Figure 7.30 : Comparative only HVAC system annual primary energy input analysis.	230
Figure 7.31 : Comparative whole building annual global warming potential analysis.	232
Figure 7.32 : Comparative only HVAC system annual global warming potential analysis.	232

NATURAL VENTILATION OF HIGH-RISE BUILDINGS A METHODOLOGY FOR PLANNING WITH DIFFERENT ANALYSIS TOOLS AND CASE-STUDY INTEGRATION

SUMMARY

Natural ventilation of buildings has the potential to significantly reduce energy consumption related to cooling and fanning. This can be achieved by (i) providing good indoor air quality without any electricity demand and (ii) improving thermal comfort in the summer through increased daytime airspeed and high night ventilation rates. In high-rise office buildings, however, natural ventilation is still not a widely preferred means of ventilation.

The main reason is the lack of information on the required system design. There are neither standards nor tools and instrument that support planners in the design of natural ventilation systems. Evaluation tools and instruments that are usually applied for effective vent sizing during preliminary planning are not suitable for complex flow path design. Only few results, if any, are available on the performance of naturally ventilated high-rise office buildings, especially where energy conservation is considered. In addition, a passive cooling approach can rely not only on intense natural ventilation but also on the reduction of heat gains, and on night cold storage systems. Considering these aspects together, there is a definitive need for research on the flow path design taking vent sizing for the provision of good indoor air quality and thermal comfort into account..

The current thesis is predicated on the above mentioned research gap. Towards this end, the thesis sets out to explore the concept of natural ventilation with focus on office buildings as a major application area. Emphasis is laid on the cooling potential of natural ventilation. The existing barriers for practically implementing passive technologies can be lowered by creating a quantifiable framework that accounts for all the relevant input parameters in the design process. In order to reach this goal, a planning and simulation approach is developed for the required system design, and the functionality is subsequently evaluated. The results of simulations are compared to those of a reference case-study.

The 28-floor Kanyon high-rise office tower, situated in Istanbul, Turkey, is selected to demonstrate the applicability as it is considered to be a representative, state-of-the-art building. From the energy metering, it is concluded that mechanical cooling and ventilation result in significant electricity consumption. Detailed information on the building and its operation has been made available by the building management. In addition to the primary case-study, a comparative assessment of the impact of three different moderate climate locations, viz., Istanbul, Turin and Stuttgart, is systematically analysed.

The primary objectives of the thesis can be stated as (i) the development of a design approach, and (ii) the investigation of the feasibility of the proposed design, based on an existing case-study building virtually adapted specifically for this purpose.

The approach is developed in three steps, including (i) conceptual design considerations with focus on the architectural consequences on the building type of concern, (ii) the original development of a preliminary design tool based on electrical circuit analogies for sizing the natural ventilation system, and (iii) a more detailed design development based on annual building energy performance simulations including custom ventilation control.

In the first step, an architectural concept is developed for passive cooling in wide-shaped high-rise buildings where it is impossible to realise simple cross ventilation or single-sided ventilation. During the conceptual design process several challenges emerged. Conceptual adaptations addressing the flow path design are (i) a central chimney strategy in respect to the building width, (ii) isolated, modular segments, as each can then be treated as a medium-rise building and (iii) opposed, wind adapting openings to guarantee the intended flow direction and to maximise the wind pressure differences. Other solutions proposed for passive cooling are (iv) improved external shading devices (v) activation of the structural mass for night-time ventilation.

In the second step of the design approach, the originally developed ‘HighVent’ planning tool is introduced with the aim to determine the design air change rate and system sizes necessary for climate specific summer design days. Simple electrical circuit analogies, for both ventilation and thermal models, are found to be suitable in supporting the passive system planning. As it is concluded that the classic design day conditions for mechanical plant sizing are too strict for passive cooling system design, meaningful design boundary conditions are provided. Openings can be sized automatically by the inverse solver method including an optimization process. For the Kanyon building, the pressure distribution is deduced from wind tunnel measurements. The program first calculates the flow-path design for a given airflow rate with unchanging boundary conditions. These values are then provided to the thermal module, which calculates the dynamic thermal comfort. The procedure is then repeated till the system size is sufficient for passive cooling. The tool outputs include advice if certain adaptive thermal comfort criteria can be reached for a summer design day.

In the third step, the annual performance is exemplarily modelled with EnergyPlus building energy performance simulations including airflow networks. This includes the ‘HighVent’ tool preliminary ventilation design outputs, further ‘post-processed’ as model inputs, the conceptual adaptations made for improved shading and thermal mass activation, and the remaining features of the as-built Kanyon building in accordance with the data provided by the building management. It allows the users to perform sensitivity analysis for the investigation of the impact of specific parameters. The custom ventilation control dynamically targets to achieve (i) good indoor air quality according to EN 13779, and (ii) stay within adaptive comfort limits category II according to EN 15251. Annual thermal comfort is the most crucial indicator for evaluating passive cooling concepts, and is therefore proposed for final decision making. As the volume of a building is an expensive resource, the designer needs to do a weighting between the expected comfort and the size of the natural ventilation system.

The applicability of the ‘3-step’ design approach is then further evaluated by comparing the fully mechanical operated as-built Kanyon building with an operation based on passive and the hybrid control. The assessment is carried out with the help of performance indicators, and the results are intended to assist decision making in the design phase. Indicators proposed to evaluate the functionality are the energy consumption compared to that of mechanical ventilation and cooling systems, and compliance with the thermal comfort limits; additional aspects are the ventilation rates and the indoor air quality reached.

A significant result of this comparative study is that control over the openings is crucial for all the scenarios when it comes to natural ventilation applications; otherwise ventilation rates can get too high and the office rooms tend to cool down way too much even during summer. It is shown that the ‘adaptive temperature amplifier’ control algorithm developed is more robust than simplistic controls. Furthermore, simulation results indicate that properly designed and controlled natural ventilation shows a good functionality and the comfort limits are rarely exceeded. However, differences in climate among geographical regions have a varying impact on the simulation results. For example, in the climate of Stuttgart, further adaptations to the preliminary design of the ‘HighVent’ tool or hybrid cooling are not necessary, whereas in Istanbul adaptations might be reasonable. However, to satisfy the comfort expectations in Turin, there is a necessity for further passive design adaptations or a hybrid cooling concept. That humidity values meet comfort expectations must be discussed and accepted by all project stakeholders, else a hybrid operation approach might be a good alternative. Nonetheless, in all controlled scenarios, high indoor air quality is achieved.

To systematically study the possible energy conservation while maintaining thermal comfort, the energy consumption of identical buildings with different variants (passive/hybrid/active) is compared and benchmarked against the as-built scenario. Results show that the primary energy input for the Kanyon office-tower building can be reduced by approximately 30% to 40% for passive operation and by 28% to 34% for hybrid operation. For passive cooling including controlled natural ventilation, there is even no energy consumption for cooling and ventilation required, while energy usage for pump operation is limited only to the heating season. The hybrid strategies are found to be capable of exploiting the biggest share of passive cooling and ventilation energy conservation by providing a maximum operative temperature limit of 26 °C. This verifies the initial assumption that energy conservation of purely passively cooled and ventilated office spaces is significant, especially when compared to highly energy consuming state-of-the-art office towers.

The results of this research work are intended, on the one hand, to support building planners in better understanding and implementing passive cooling measures and, on the other hand, to contribute to further development of sustainable building practices.

ÇOK KATLI BİNALARDA DOĞAL HAVALANDIRMA FARKLI ANALİZ ARAÇLARI VE ÖRNEK ALAN ENTEGRASYONU İLE PLANLAMA İÇİN BİR YÖNTEM

ÖZET

Doğal havalandırma, binalarda, soğutma ve hava üflemeyle ilişkin elektrik enerjisi tüketimini azaltma potansiyeline sahiptir. İki ana fonksiyonu: (i) havanın hareket ettirilmesi için elektrik harcanmadan iyi bir iç mekan hava kalitesi sağlanması ve (ii) gün içinde hava hızının artırılması ve gece boyunca yüksek havalandırma oranları aracılığıyla yaz aylarında konfor sıcaklığının iyileştirilmesidir. Esas fayda, dışsal enerji gereksinimine ihtiyaç duymaksızın, yaz aylarında soğutma için gerekli olan yüksek havalandırma oranlarına ulaşılması olasılığıdır. Ancak ana sorun, kış aylarında, ılık oda sıcaklığından ısının geri kazanılmasıdır. Doğal havalandırma, çok katlı ofis binaları için hala yaygın olarak tercih edilen bir havalandırma yöntemi değildir. Konfor sıcaklığı kestirimlerindeki belirsizliklere bağlı olarak, mimar ve mühendisler, pasif teknolojilerin uygulanmasına hala çekinceli yaklaşmaktadırlar.

Bunun nedeni, klima tesisatı olmadan iyi bir konfor sıcaklığı ve iç mekan hava kalitesinin elde edilebilmesi için gerekli olan elverişli sistem tasarımı konusunda sınırlı düzeyde bilginin var olmasıdır. Plancıları doğal havalandırma sistemlerinin tasarımı konusunda destekleyebilecek, hazır standartlar bulunmamaktadır. Hava deliklerinin efektif olarak boyutlandırılması için ön değerlendirme araç ve aygıtları bulunsa da, bunlar sadece bazı bina ve havalandırma tasarımları için geçerlidir ve karmaşık akım yolu tasarımlarında kullanılmak için elverişli değildir. Doğal olarak havalandırılan çok katlı ofis binalarının, özellikle enerji korunumu ile ilgili performansları konusunda, yok denecek kadar az sonuca rastlanmaktadır. Akım yolu tasarımının içerdiği öğelerin boyutları ve havalandırma stratejilerinin araştırılması konusunda nihai bir ihtiyaç bulunmaktadır. Pasif soğutma yaklaşımının sadece sağlam bir doğal havalandırmaya değil, aynı zamanda ısı kazanımlarının azaltılmasına ve gece soğüğünün depolanması sistemlerine de dayandığı görülmüştür.

Bu tez, bahsi geçen araştırma açığına dayanmaktadır ve dolayısıyla amaçlanan, ılıman Avrupa iklimlerinde enerji korunumu sağlanabilmesi için doğal havalandırmadan faydalanılmasının elverişliliğini incelemektir. Bu amaç doğrultusunda tezin başlangıç noktası, doğal havalandırma için büyük bir uygulama alanı olan ofis binalarına yoğunlaşarak, doğal havalandırma kavramını incelemektir. Buradaki ana önerme, pasif teknolojilerin etkin şekilde uygulanması yoluyla, sürdürülebilir binalar tasarlanması ve inşa edilmesinin mümkün olduğudur. Esasen, doğal havalandırmanın soğutma potansiyeli üzerine vurgu yapılmaktadır. En önemli kapsayıcı hedef, yeni binaların tasarlanması ve mevcut olanların geliştirilmesi ile bağlantılı enerji tasarrufu önlemleri konusundaki bilimsel anlayışı derinleştirmektir. Tasarım süreciyle ilgili bütün girdi parametrelerini tanımlayan, ölçülebilir bir çerçeve yaratılması aracılığıyla, pasif teknolojilerin pratik olarak uygulanabilmesi

önündeki mevcut engellerin azaltılması sağlanabilir. Bu hedefe ulaşmak amacıyla, gerekli sistem tasarımı için bir planlama ve simülasyon yaklaşımı geliştirilmiş ve ardından, kontrollü doğal havalandırmanın fonksiyonelliği değerlendirilmiştir. Simülasyon sonuçları, referans alınan örnek alan ile karşılaştırılmıştır.

İstanbul / Türkiye’de yer alan çok katlı ofis kulesi Kanyon (28 kat), yüksek konfor beklentileri ve karmaşık mekanik sistemleri ile en son teknoloji ile inşa edilmiş bir bina olarak temsili özellikler taşıması nedeniyle, uygulamayı göstermek amacıyla seçilmiştir. Binanın ölçülen enerji tüketiminden yola çıkarak, solar ve içsel ısı kazanımı ile temiz hava kontrolünün, mekanik soğutma ve havalandırma için önemli düzeyde elektrik tüketimine neden olduğu sonucuna varılmıştır. Bina ve işletme konusundaki detaylı bilgi, bina yönetimi tarafından sağlanmıştır. Esas alan araştırmasına ek olarak, üç farklı ılıman iklim konumunun etkisi üzerine bir karşılaştırmalı değerlendirme yapmak üzere, İstanbul, Torino ve Stuttgart sistematik olarak analiz edilmiştir. Bu değerlendirme, farklı iklim koşullarının, tasarım ve performans üzerindeki etkilerini daha iyi anlamak için gerçekleştirilmiştir. Kapsamın bu şekilde genişletilmesi ile öngörülen, pasif soğutma sistem tasarımları için anlamlı sınır koşullarının sağlanmasıdır.

Tezin başlıca hedefleri şu şekilde sıralanabilir: (i) çok katlı ofis binalarının pasif soğutma ve havalandırması için bir tasarım yaklaşımı geliştirmek, (ii) önerilen tasarımın fizibilitesini incelemek adına, özellikle bu amaç için sanal olarak uyarlanmış mevcut bir binaya dayalı alan araştırması gerçekleştirmek.

Doğal havalandırma tasarımının farklı analiz araçları ve örnek alan entegrasyonu ile planlanması için bir yaklaşım geliştirilmiştir. Yöntem üç aşamadan oluşmaktadır: (i) ilgili bina tipi üzerindeki mimari sonuçlara odaklanan kavramsal tasarım değerlendirmesi, (ii) havalandırma sistemini boyutlandırmak için elektrik devresi analogilerine dayalı özgün bir ön tasarım aracının geliştirilmesi ve (iii) isteğe bağlı havalandırma kontrolünü de içeren, yıllık bina enerji performansı simülasyonlarına dayalı daha detaylı bir tasarım geliştirilmesi.

İlk aşamada, basit çapraz havalandırma ya da tek yönlü havalandırma uygulamalarının imkânsız olduğu geniş yapıları çok katlı binalarda, pasif soğutma için genel bir kavram geliştirilmiştir. Tasarım yaklaşımına ilişkin araştırma sorusu mimari sonuçlar üzerine yoğunlaşmıştır. Bulgular, dikkate alınan spesifik bina türünün incelenmesine ek olarak, örnek alan olan Kanyon binasının ve iklim değerlendirmesinin incelenmesinden elde edilen bulgulara dayanmaktadır. Kavramsal tasarım sürecinde bir takım zorluklar ortaya çıkmıştır. Akım yolu tasarımına yönelik kavramsal uyarlamalar şunlardır: (i) bina genişliğine bağlı olarak merkezi baca stratejisi, (ii) her biri orta yükseklikte bir bina olarak değerlendirilebilecek izole, modüler parçalar ve (iii) istenilen akım yönünü garantilemek ve rüzgâr basınç farklılıklarını maksimize etmek için karşılıklı, rüzgâra göre ayarlanmış açıklıklar. Pasif soğutma için önerilen diğer kavramsal tasarım çözümleri şunlardır: (iv) binaya giren solar radyasyon miktarını düşürme kapasitesine sahip, iyileştirilmiş dışsal gölgelik aygıtları ve (v) gece havalandırması için binanın yapısal kütlelerinin aktive edilmesi.

Tasarım yaklaşımının ikinci aşamasında, iklime özgü yaz gündüz tasarımı için gerekli olan hava değişimi oranını ve sistem boyutunu belirlemek amacıyla özgün olarak geliştirilmiş ‘HighVent’ (‘YüksekHavaDeliği’) planlama aracı tanıtılmıştır. Basit elektrik devre analogileri, hem havalandırma hem termal modellerde, doğal havalandırma sistemleri odaklı pasif sistem planlamasını desteklemek için uygun

görülmüştür. Sonuçların geçerliliği, 'EnergyPlus' bina enerjisi simülasyon programı ile karşılaştırmalı doğrulama yapılması yoluyla kanıtlanmıştır. Mekanik tesis boyutlandırması ile ilgili klasik gündüz koşulları tasarımının, pasif soğutma sistem tasarımı için fazla katı olduğu ve uyarlanmış konfor yaklaşımını yansıtmadığı sonucuna varılması neticesinde anlamlı tasarım sınır koşulları, yaz günü profillerinin özgün olarak geliştirilmesi aracılığıyla sağlanmıştır. Yaklaşım, aşırı sıcak ve normal yaz dönemleri için ortalama hava sıcaklığı, nem oranı, radyasyon ve rüzgâr bilgisini organize etmektedir. Açıklıklar, optimizasyon sürecini de içeren ters çözücü yöntemi ile otomatik olarak boyutlandırılabilirler. Yöntem, arazi ve kat yükseklikleri için düzeltme faktörü önermektedir. Varsayılan basınç dağılımı ve akım dirençleri düzenlenebilmektedir. Kanyon binası için, basınç katsayıları, rüzgâr tüneli ölçülerinden elde edilmiştir. Program öncelikle, değişmeyen sınır koşulları ile verilmiş hava akımı oranına göre akım yolu tasarımını hesaplamaktadır. İlk modülden alınan bu değerler, dinamik konfor ısını hesaplayan termal modüle aktarılmaktadır. Ardından, işlemler, sistem boyutu pasif soğutma için yeterli olana dek tekrarlanmaktadır. Bina, hava sızdırmazlığı, yönelim, solar kontrol, parlama oranı, ısı kütlesi, konumu ve içsel ısı kazanımları gibi tasarım seçenekleriyle tanımlanabilmektedir. Termal modeli de içeren dinamik gündüz simülasyon tasarımları, tek bölge modeli için yürütülmektedir. Bu tasarımlar, seçilen havalandırma stratejisi ve boyuta göre binanın termal davranışı üzerindeki etki değerlendirmesinin yapılmasına olanak tanımaktadırlar. Araç sonuçları, eğer yaz günü tasarımları için belirli bir uyarlanmış konfor ısı ölçütü elde edilebilirse, öneriler de içermektedir.

Üçüncü aşamada, uyarlanmış Kanyon binasının yıllık performansı, hava akımı ağlarını da içeren EnergyPlus bina enerji simülasyonları ile örnek oluşturacak şekilde modellenmiştir. Model, 'HighVent' aracının ilk havalandırma tasarım sonuçlarını, 'işlem sonrası' model girdilerini, iyileştirilmiş gölgelik ve ısı kütle aktivasyonları için yapılmış kavramsal uyarlamaları ve bina yöneticileri tarafından sağlanmış veriler doğrultusunda Kanyon binasının uygulama çizimlerine ilişkin diğer özelliklerini de içermektedir. Belirli parametrelerin etkilerinin incelenebilmesi için kullanıcılara duyarlılık analizi yürütme olanağı tanınmaktadır. Programlanmış isteğe bağlı havalandırma kontrolü ile dinamik olarak elde edilmeye çalışılan: (i) EN 13779'a bağlı yüksek iç mekân hava kalitesi elde edilmesi ve (ii) EN 15251 kategori II'ye bağlı olarak uyarlanabilir konfor sınırları içerisinde kalmasıdır. Hedeflenen hava değişimi oranı, uygulanması amaçlanan hava miktarını temsil ederken, ulaşılan hava değişimi oranı, simülasyonda ortaya çıkan havalandırmanın küçük olan miktarıdır. Yıllık konfor ısı, pasif soğutma kavramlarının değerlendirilmesi için en önemli göstergedir; dolayısıyla son karar alma aşaması için önerilmiştir. Bina hacminin pahalı bir kaynak olmasından dolayı, tasarımcının, beklenen uyarlanabilir konfor ve doğal havalandırma sistem boyutu arasında bir önem değerlendirmesi yapması gerekmektedir. Tasarım özelliklerinin görece etkisinin araştırılması için duyarlılık analizi yapılması suretiyle sistem yeniden boyutlandırılabilir. Karma bir yaklaşımın benimsenmesi durumunda, mekanik sistem donanımı ve enerji tüketim parametrelerinin de dikkate alınması gerekmektedir.

Yöntem yaklaşımının uygulanabilirliği, mevcut Kanyon ofis kulesinin sanal olarak uyarlanması yoluyla tanıtılmış ve değerlendirilmiştir. Sanal izleme, modelleme ve simülasyon aracılığıyla, yöntem, hava sıcaklığı dağılımı ve hava akımı örüntülerini, doğal olarak havalandırılan bir ofis kulesi binasının prototipinde öngörebilmektedir. İşleyiş düzeyi, bina enerji performansı simülasyon sonuçlarının Avrupa standartları

veya diğ er referans ölçütlerine göre sınıflandırılabilmesi için performans göstergelerinin kullanılması yoluyla tasdik edilmektedir. Farklı iklimsel koşulların etkisi, üç farklı iklimsel konumdaki örnek binanın karşılaştırmalı performans değerlendirmeleri aracılığıyla ortaya koyulmakta, böylece, Avrupa Birliği'nin, Bina Enerji Performansı Yönergesinde belirlenen iddialı hedefler desteklenmektedir.

Açıklıkların kontrol edilmesinin bütün örneklerde önemli olduğu görülmüştür; aksi takdirde, havalandırma oranları fazla yükselerek, yaz aylarında bile ofis odalarının fazla soğumasına neden olmaktadır. Haftalık tasarım simülasyonlarının karşılaştırılması ile geliştirilen 'uyarlanabilir hava sıcaklığı yükselticisi' kontrol algoritmasının, aşırı soğuma olmaksızın ve sıklıkla yüksek ayarı yapılmasına gerek kalmaksızın pasif soğutma için gerekli akım oranlarının uyarlanmasında, basit kontrollerden daha dirençli olduğu gösterilmiştir.

Sonuçlar, doğru tasarlanan ve kontrol altındaki doğal havalandırmanın iyi işlediğini ve EN 15251 kategori II'deki uyarlanmış konfor sınırlarının nadiren aşıldığını göstermektedir. Stuttgart ikliminde, ileri tasarım uyarlamalarına ya da karma soğutmaya ihtiyaç olmadığı sonucuna varılmıştır. İstanbul'da, %3 ile %5 arasında ortalama bir aşma sıklığı ile ileri tasarım uyarlaması ya da karma soğutma makul ancak zorunlu değildir. Ancak, Torino'daki konfor beklentilerinin karşılanması için, daha fazla tasarım uyarlaması veya bir karma soğutma kavramına ihtiyaç olduğu saptanmıştır. Duyarlılık analizi, parlama alanı ya da teçhizat ısı kazanımının yarıya indirilmesi veya binanın ağır olması durumunda, Torino'daki ortalama aşma sıklığının %3'ün altında bir değ ere düşürülebileceğini göstermektedir. Nem değerlerinin konfor beklentilerini karşılaması tartışılmalı ve tüm proje taraflarınca kabul edilmelidir, aksi takdirde karma operasyon yaklaşımı iyi bir alternatif oluşturabilir.

Kontrol edilen tüm örneklerde, EN 13779'a uygun olarak, dış mekân havası üzerinde 400 ppm'nin altında CO₂ seviyesine rastlanmış, yüksek iç mekân hava kalitesine erişilmiştir. Bunun nedeni, bir saniyede kişi başı en az 14 litre ile tanımlanan gerekli hava akım oranlarının sağlandığı, mekanik ve doğal havalandırma sistem boyutunun yeterli olmasıdır.

Konfor ısısının devamlılığı sağlanırken olası enerji korunumunun incelenebilmesi için, simülasyon aracılığıyla, birbiriyle aynı olup varyantları (pasif/karma/aktif) farklı olan binalar karşılaştırılmıştır. Enerji tüketimi için uygulanmış senaryolar referans alınmıştır. Kanyon ofis binasının başlıca enerji girdisi, pasif işlem için yaklaşık olarak %30-40 arasında ve karma işlem için %28-34 arasında düşürülmüştür. Kontrollü doğal havalandırmayı da içeren pasif soğutmada, soğutma ve havalandırma için enerji tüketimi yoktur ve pompa işlemi ısıtma sezonuyla sınırlandırılmıştır. Bu durum, ilk başta yapılan varsayımı doğrulamaktadır; tamamen pasif olarak soğutulan ve havalandırılan ofis mekânları için enerji korunumu kayda değerdir, özellikle de yüksek enerji tüketen son teknoloji ofis kuleleri ile kıyaslandığında. Karma stratejilerin, işlem için maksimum 26 °C hava sıcaklığı sınırı sağlanması nedeniyle, pasif soğutma ve havalandırma kaynaklı enerji korunumunda en yüksek paya sahip olduğu görülmüştür. Yıllık küresel ısınma potansiyelinde azalmanın, yaklaşık olarak, Stuttgart'ta 1 200 ton CO₂'ye, Torino'da 1 300 CO₂'ye ve İstanbul'da 1 700 ton CO₂'ye eşdeğer olduğu görülmektedir.

1. INTRODUCTION

Natural ventilation of buildings has the potential to save significant electrical energy consumption related to cooling and fanning. The main advantage of natural ventilation is the possibility of achieving high ventilation rates in summer for cooling without external energy requirements. The main drawback, though, is the difficulty of winter heat recovery from the warm room air. For high-rise office buildings, natural ventilation is still not a widely preferred means of ventilation. This is because only limited information is available on suitable system design required to achieve good thermal comfort and indoor air quality, without air conditioning. There are no readily available standards which support planners in the design of natural ventilation systems. Few results, if any, are available on the performance of naturally ventilated high-rise office buildings, especially where energy conservation is concerned.

The current thesis is predicated on the above mentioned research gap, and therefore aims to investigate the feasibility of exploiting natural ventilation as a means of achieving energy conservation for moderate European climates. Emphasis is laid on the cooling potential of natural ventilation. The overarching goal is to deepen the scientific understanding of the associated energy saving measures both in the design of new buildings and the improvement of existing buildings. In order to reach this goal, a planning and simulation approach is developed for the required system design, and the functionality of controlled natural ventilation is subsequently evaluated. The focus is on office buildings as a major application area of natural ventilation. The results of simulations are compared to those of a reference case-study – an office tower with mechanical ventilation and cooling systems.

The thesis first summarises the findings of previous studies on natural ventilation and hybrid design, control strategies, energy consumption, and performance indicators. The approach to the development of proposed methodology is then explained, followed by its virtual application through simulations. The 28-floor Kanyon high-rise office tower, situated in Istanbul, Turkey, is selected to demonstrate the applicability as it is considered to be a representative, state-of-the art building with

high comfort expectations and high energy consuming mechanical systems. Detailed information on the building and its operation has been made available by the building management for this research work.

In addition to the primary case-study, a comparative assessment of the impact of three different moderate climate locations, viz., Istanbul, Turin and Stuttgart, is systematically analysed. This is to deepen the understanding of design and performance consequences as a function of different climates. This extension is also envisaged to provide meaningful boundary conditions for passive cooling system design.

1.1 Design Methodology

The proposed passive cooling approach is based on three steps as follows. The Kanyon office tower is virtually adapted accordingly.

Step 1: Passive cooling is conceptually realised by intense day and night natural ventilation, flanked by a reduction of solar heat gains, and by thermal mass activation to store night cold in the building fabric. The idea of night-time ventilation in office buildings is to use the thermal mass of a building as a heat sink. The structure is cooled by convection during the night and is able to absorb heat in the occupied hours. In principle, cool night air passes over a heavyweight building fabric and cools the thermal mass. The warmer daytime air will then be reduced in temperature when passing over that cooled slab. Therefore, night ventilation is particularly suited to offices, which are unoccupied during the night. In this way, relatively high air changes can be used to provide maximum cooling effect without creating thermal discomfort or mechanical heating in the morning. This strategy provides attenuation of peaks in cooling load and modulation of internal temperature with heat discharge at a later time. The natural ventilation design is especially developed for wide-shaped high-rise buildings where it is impossible to realise simple cross ventilation or single-sided ventilation.

Step 2: A 'HighVent' preliminary design planning tool is developed based on existing models of electrical analogies of flow and thermodynamics. This is intended to support the passive system planning with emphasis on the size and distribution of flow paths. The cross-sectional areas of openings for a building segment with up to

ten storeys are determined for (i) target air change rate with fixed boundary conditions, and (ii) expected wind velocities in accordance with the climate assessment. The design is then tested with dynamic, summer design day boundary conditions. The results will indicate whether the passive cooling system sizes are appropriate to obtain a good comfort level for the climate considered or if the target air change rate or other measures have to be further adapted. Other measures include reducing solar and internal heat gains (e.g., better shading/smaller windows, and less equipment or loads from lights, respectively), and activating additional thermal mass for night-time ventilation using the building as a heat sink (e.g., making the building heavier by removing internal claddings).

Step 3: In the third step of the passive cooling approach development, the preliminary design outputs are utilised as inputs for detailed annual simulations. This is realised by using integrated building energy performance and airflow network simulations. In contrast to the sizing tool developed in Step 2, the overall annual performance for a specific climate including the mechanical systems and controls can be considered. Simulation outputs further guide the designer to modify the initial sizing parameters gathered from the ‘HighVent’ design tool if necessary.

Finally, in the design evaluation section, more coupled airflow network- and dynamic building simulations are carried out to determine the annual thermal comfort and the energy savings. Parametric results for the three chosen moderate climate locations show that summer cooling potential and thermal comfort strongly depend on the natural ventilation strategy. Good results can be expected only if ventilative cooling is applied along with other passive cooling measures, which in this study are the reduction of solar heat gains and the activation of the building thermal mass as a heat sink for night-time ventilation. Control over the openings is crucial for all the cases; otherwise ventilation rates can get too high, and the office rooms tend to cool down way too much even in summer conditions.

1.2 Contributions of the Study

The primary objectives of the thesis can be stated as follows:

- 1) Development of a design approach for passive cooling and ventilation of high-rise office buildings, and
- 2) Investigation of the feasibility of the proposed design, based on an existing case-study building adapted specifically for this purpose.

The design approach to reduce heat gains and to use the building's mass as a heat sink, has the focus on controlled natural ventilation. The developed methodology conceptually considers the special building shape as tall and wide. It is intended to provide fundamental understanding on how the building space can be naturally ventilated by maximally exploiting the natural driving forces, viz., wind and buoyant forces, for volume flow. Bearing this in mind, the original 'HighVent' program, which is based on electrical analogies of flow and thermodynamics, is developed as a planning tool for the distribution and dimensioning of complex flow paths. This tool has been developed with a view to preparing for a suitable extension of the existing standards, and to support the planning of ventilation applications even in non-residential, high-rise buildings. This means of creation of controlled natural ventilation concepts had to be resorted to, as actual standards and guidelines in practice were found to be ill-suited for the building type concerned.

To evaluate the developed design, and to identify the existing design parameters to be changed, outputs of the 'HighVent' tool are further utilised as inputs for a complex energy performance simulation of the building. Since the functionality of controlled natural ventilation is highly dependent on the control methodology, new adaptive temperature amplifier controls are developed as part of the energy management system controls. In this study, the openings for natural ventilation are controlled at night and day in a way that ensures good indoor air quality, best possible thermal comfort conditions, and energy efficient building operation. Detailed EnergyPlus [1] simulations are intended to yield information on the functionality of passive cooling. The most important factors influencing passive and hybrid cooling performance such as ventilation rates, controls, heat gains, building mass, and climatic conditions are evaluated. Design week profiles give insight into the functioning of natural ventilation systems, and also serve to analyse the opening

control and the quality of indoor air. Annual assessment gives insight into the overall functionality of controlled natural and hybrid operation throughout the year. Indicators used to evaluate the functionality are the energy consumption compared to mechanical ventilation and cooling, and especially compliance with the thermal comfort limits for the users. Annual simulations are intended to indicate the period when adaptive comfort can hardly be reached, and also provide information on the influence of different design parameters.

Specific and systematic statements on annual energy savings achievable through natural ventilation are rare. The saved electrical energy consumption for mechanical ventilation, the possible cooling energy by night ventilation with increased air changes rates and the energy losses due to missing heat recovery in winter must be considered as well as the auxiliary energy, e.g., system pumps. Here two identical buildings with different variants (passive/active) must be compared by simulation, because the setpoint temperatures are different for naturally ventilated buildings than in air-conditioned buildings. For a more systematic study of the possible energy conservation while maintaining thermal comfort, further parametric annual simulations coupled with airflow network simulations are carried out. The savings on energy, and the consequent environmental impact are then determined. This is done by comparing the corresponding effects of the proposed natural ventilation strategies with those of an identical building for which mechanical ventilation is used.

1.3 Hypothesis

From the metered energy consumption of the Kanyon office building, it is concluded that the building's solar- and internal heat gains as well as its fresh air control result in significant electricity consumption for mechanical cooling and ventilation. Systems that consume energy for fresh air supply to provide comfort can be reduced or eliminated with the use of passive or hybrid technologies. For sustainable use of energy, thus, there is a huge potential for passive systems, whenever they are capable, to maintain a good indoor environment for the building occupants.

The two main functions of natural ventilation are: (i) provision of good indoor air quality without any electricity demand for moving the air, and (ii) improvement of thermal comfort in summer through increased daytime airspeed and high night ventilation rates. Especially for commercial buildings, night-time ventilation seems

to be a simple and energy efficient approach to improve thermal comfort in summer [2]. Additionally, passive systems such as self-adapting solar shading elements or the use of thermal mass as a heat sink can help to temper the internal environment.

Hybrid operation combines the use of natural and mechanical systems to cool and ventilate buildings. These systems offer opportunities to take advantage of the external conditions when appropriate, but have a mechanical backup system to maintain the indoor environment during periods when the external conditions are not adequate [3].

Understanding the climate of a specific site can create more liveable buildings that require lower maintenance and utility costs. In moderate climates, by reducing the amount of supplementary cooling and fresh air needed to maintain occupant comfort and health, the approach of passive technologies may result in adequate building design without the need for any mechanical systems.

However, due to uncertainties in the prediction of thermal comfort, architects and engineers are still hesitant to apply passive technologies to wide, tall, and complex buildings such as the Kanyon tower. In order to reduce uncertainties, the most important parameters affecting the summer passive design performance need to be identified. This thesis derives its motivation from this premise, and aims to lower the barriers for implementation of passive technologies in high-rise buildings. This thesis provides a unique opportunity for the passive system design in high-rise office buildings as performance modelling is carried out at different design stages, and is thus integrated into the design decision-making.

The results of this research work are intended to help the building planner to better understand and implement passive cooling measures. It is envisioned that recommendations for sustainable building practices can be put forward through this thesis by devising the following:

- 1) a passive system design and sizing tool,
- 2) natural ventilation control algorithms, and
- 3) a method for detailed design evaluation through energy performance simulations.

As a result, builders can possibly build smaller mechanical cooling plants, or even leave them out, and the buildings can be operated more efficiently, while providing

the users with improved thermal comfort. Moreover, it is hoped that this thesis will be helpful for researchers in their search for better solutions to the problem of designing and constructing sustainable buildings.

1.4 Assumptions

The approach developed contains multiple assumptions for model inputs as well as for the thermodynamic concepts, so that complex interrelations can be simplified and managed. The assumptions made while developing the 'HighVent' design tool vary to some degree when compared to those made in the context of more detailed building energy performance simulations with EnergyPlus. Building energy performance simulation is typically used to compare design alternatives, rather than to predict the actual energy performance of buildings. The list below is intended to point the most relevant assumptions made:

- Typical meteorological year weather data used for simulations is gathered at meteorological stations outside the city centre, and is based on long-term measurements from the past.
- Wind pressure is estimated according to wind tunnel experiments (pressure coefficients) and the power-law estimation, which calculates the local wind speed depending on the height of the opening and the terrain roughness.
- Flow resistance of orifices is described by the discharge coefficients with values from literature, which are mostly obtained from laboratory tests under still-air conditions.
- Simplified approaches for infiltration and natural ventilation are based on electrical analogy models.
- Internal heat loads from equipment and lighting are approximated, based on interviews with the building management, and partly on electricity metering.
- Solar heat loads are computed by simple performance parameters, taken from the technical specifications defined by the glazing production company.
- Convective heat transfer is strongly simplified and computed for cases without mechanical cooling with values from the EN ISO 13791 standard, although for mechanically operated reference cases, the EnergyPlus default TARP algorithm is employed.

- Well-mixed zone air assumption is employed with spatially uniform temperatures.
- Model validation of the as-built reference scenario is based on energy bills and metering data for electricity and natural gas consumption from the years 2008 and 2009. As the metering data does not provide all levels of detail necessary to validate each type of consumer separately, their shares of consumption are mostly approximated according to the model inputs.

1.5 Structure of the Thesis

The thesis is organised as follows.

Chapter 2 contains the literature review, also identifying the research problem. It first gives a brief overview of the trends in high-rise office building operation. It then summarises the principles of natural ventilation, e.g., driving forces, strategies, elements, controls, performance indicators, and air flow modelling approaches. An overview is given on the major findings of past and ongoing research projects. The regulatory framework complements this chapter by providing the area relevant codes across European countries.

Chapter 3 introduces the passive cooling design approach developed with focus on wide-shaped office-towers. An electric analogy software tool named ‘HighVent’ is developed to design and size natural ventilation systems. It is capable of designing flow paths and evaluating the comfort performance with a relatively small number of input parameters. The tool outputs are then further ‘post-processed’ as inputs for detailed building energy performance simulations including airflow networks. EnergyPlus simulations are intended to access annual information about the comfort reached. This detailed design development also includes the model calibration and original natural ventilation controls.

Chapter 4 investigates the existing Kanyon office tower located in Istanbul. Detailed data including the building’s energy consumption gathered from the building management is presented. The geometry, the construction elements, and the building usage are analysed and processed towards reliable building energy performance simulation model inputs.

Chapter 5 reviews the climate of the three locations considered based on ‘typical meteorological year’ weather data. As the focus is on passive cooling and comfort during summer, the cooling period is further evaluated to infer the climatic cooling potentials. Summer design weeks are analysed and then further processed to generate meaningful design days for passive cooling as input for the developed ‘HighVent’ design tool.

Chapter 6 explains the passive cooling design approach through virtual case-study integration. The Kanyon building is adapted for the climates of Istanbul, Turin and Stuttgart. The HighVent’ tool is utilized to design and size the passive system components. For the detailed design development of the passive approach including the controls, a BEPS model of Kanyon tower is simulated on annual basis along with the preliminary passive design outputs from the tool.

Chapter 7 evaluates the design approaches developed by comparing the fully mechanical Kanyon building operation with an operation based on controlled passive and hybrid cooling. The most important factors influencing passive and hybrid cooling performance are evaluated and design alternatives are analysed and discussed for different climates. The assessment is carried out with the help of performance indicators, and the results are intended to assist decision making in the pre-design phase. For the estimation of energy conservation and environmental benefits, simulation outputs for the passive and the hybrid scenarios are compared to those with mechanical ventilation and cooling systems.

Finally, in Chapter 8 a summary of the research work is given and conclusions of the research are drawn. Suggestions for areas of improvement and perspectives for further research work are also presented.

Appendix A contains wind pressure coefficient data from wind tunnel tests carried out for the Kanyon building including adjacent buildings. The building is modelled with a scale of 1:300. 98 points of the building façade structure correspond to 14 nodes on each storey and on seven height levels. The measurements are repeated for eight wind directions. The data is used as input for the ‘HighVent’ design tool and for dynamic AFN simulations with EnergyPlus.

Appendix B gives supplementary information about the ‘HighVent’ tool underlying the dynamic calculation method. It provides pre-simulated solar transmitted heat

gains for different shading configurations, used as tool input. The construction library provides lumped capacity model constructions with different levels of mass.

2. LITERATURE REVIEW

Major challenges for the 21st century are a secured long-term energy supply as well as the sustainable protection of earth's atmosphere to limit the climate change to less than 2 °C by the end of the century. Scientists estimate that 2 °C of warming is the limit of safety, beyond which climate change becomes catastrophic and irreversible [4]. It was recognised that deep cuts in global greenhouse gas emissions are required, vitally essential from ecology and economic point of view. The International Energy Agency (IEA) estimates that buildings account for 30-40% of the worldwide energy use, which is equivalent to 2,500 Mtoe (million tonnes of oil equivalent) every year [5]. The built environment sector therefore has a huge potential for energy savings. These reductions are fundamental for achieving the IAE's target of a 77% reduction in the planet's carbon footprint against the 2050 baseline. Stabilized CO₂ levels are called for by the Intergovernmental Panel on Climate Change (IPCC).

Increasing population density in cities is now widely accepted as necessary for achieving more sustainable cities. Keeping in mind that the United Nations (UN) forecasts more than six billion people in urbanised areas by 2050, widespread megacities will require much more land usage and higher energy demand for infrastructure and mobility. A higher density of population may be reached by high-rise buildings; besides the lower land usage, such buildings have the benefit of higher building volume to envelope area ratio, creating less heat losses and requiring less material usage. But there are also potential disadvantages such as the increasing lighting demand and lower natural ventilation potentials due to a lower envelope area to floor area ratio. These may negate the benefits together with the fact that building structures at heights need greater material sizing to counteract greater environmental pressure [6].

Globally, more and more legislative instruments are being introduced to control the energy consumption level of buildings. With the Energy Performance of Buildings Directive (EPBD) [7], the European Union (EU) has set ambitious goals to improve the sustainability of the built environment (see § 2.6). However, regulations like

codes and standards prescribe how to construct new developments and how to restore energy efficiency in real estate assets; but, they seldom address passive techniques with the same technical emphasis compared to active measures. Normally, single efficiency measures are considered, which cannot achieve possible primary energy savings with an integrated passive approach.

Bioclimatic architecture responds to the regional climate and conditions, and can provide comfort even without expensive heating or cooling [8]. Designers can learn to adapt their buildings, making use of solar energy and other environmental sources [9]. However, it is often tried to use superior, modern types of construction, which can end up relying on costly climate control systems, especially in warm locations. Architects often resist energy efficiency for competitive and social reasons, and mostly their expectations for efficiency are often much too low for achieving substantial energy savings. Especially, office buildings with their high requirements on lighting, thermal comfort, and air quality, as well as their often highly glazed facades have high-energy demand, which is to be questioned.

Building ventilation is the intentional process of supplying fresh air from the outside to the inside of a building and keeping interior air circulating. Ventilation is used to provide high indoor air quality, and is a crucial parameter for thermal comfort conditions. The air change is necessary to control temperature, to replenish oxygen, and to remove moisture, odours, smoke, dust, airborne bacteria, and carbon dioxide. The circulation of air within the building prevents the interior air from stagnation. Ventilation systems supply and remove air either naturally and/or mechanically. Different types of ventilation may operate in different areas of the building. The air change rates achievable through natural ventilation with correct sizing of the openings are significantly higher than those with mechanical ventilation for night cooling and without electrical energy input. Building infiltration due to an untight envelope is unintentional airflow, and therefore treated separately from building ventilation. 'Build tight, ventilate right' is said to be a good builder's motto. Good ventilation in many cases is also subject to a legal minimum requirement. The choice between natural and mechanical ventilation depends on different criteria, such as discussed in the British Standard 5925 [10].

2.1 High-Rise Office Buildings

Historically, by the end of the 19th century the first high-rise office buildings were built naturally ventilated. They were constructed relatively narrow to control the indoor environment passively by exploiting daylight and fresh air from outside to naturally ventilate and cool the buildings. The only simple mechanical systems focused on heating the building in winter. Natural ventilation systems from that period do offer only limited control, and therefore do not provide comfort expectations for modern buildings. Very well-known examples of buildings of this period still relying on natural ventilation are the Chrysler Building and the Empire State Building in New York [6].

More complex mechanical systems were established by the 1950s due to cheap energy and technical progress in terms of the ability to control the indoor environment mechanically with air conditioning systems. As a consequence of their widespread usage, architects were no longer 'restricted' by the central concern to consider passive strategies to provide good indoor environment as they were when designing the first generation of skyscrapers in the beginning of the 20th century. From this time, architects had the possibility to design light and highly transparent offices with deep floor plans. This glass box style, together with the lack of solar control, created increased cooling and heating demands depending on the season.

After the energy crisis in 1973, building regulations aimed to decrease the heating and cooling energy consumption of buildings. Regulations mainly focused on the building insulation, air tightness, and heat recovery. In this period, buildings were designed to be isolated from the outdoor environment, and the energy consumption suffered from high solar heat gains. Another aggravating factor was the increase in internal heat gains from office equipment, low-efficiency lighting systems, and high staff densities. While reducing the heating demand, many existing office buildings are still either overheated in summer, or use excessive amounts of energy to maintain acceptable temperatures [3]. The poor indoor air quality and the growth of mould due to high humidity levels and bad maintenance of the Heating, Ventilation and Air Conditioning (HVAC) systems spread illnesses; this is well known as the 'sick building syndrome'.

Starting from the 1980s, designers considered energy efficient buildings, which also provided a healthier indoor environment. Architects started to reconsider and revitalise natural ventilation as a response to a number of challenges in the built environment. An integrated design aims to utilise and interact with the outdoor environment. The focus slowly moved towards optimal use of sustainable technologies such as solar gains, natural light and ventilation, and passive cooling. To a certain extent and depending on the expectations of occupants, the climate, the building use, the design and the location, sustainable technologies are able to supply heating, lighting, and cooling. Yet, supplementary active systems are often needed to support the passive technologies. This is especially true in the case of high-rise office buildings where a pure passive approach for ventilation and cooling is seldom implemented [6]. Even sustainable, passive technologies have been better understood in the last few decades, in recent years a trend towards increasing cooling demand has been observed, especially in commercial type buildings [11]. Higher internal and solar heat gains and increased comfort expectations, as well as global warming and the ‘heat island’ effect in big cities increase the cooling demand. The HybVent project [3] investigated that *‘in well-insulated office buildings, which are becoming more and more common in IEA countries, ventilation and cooling account for more than 50% of the energy requirement’*. It was concluded that a well-controlled and energy efficient ventilation system is required to achieve low energy consumption. Moreover, it is stated that adequately controlled natural ventilation and passive cooling are energy efficient and sustainable technologies.

Although the emphasis in this thesis is on passive ventilation to minimise energy consumption by maximizing the airflow rates, the reality is that high-rise office buildings are almost always operated with mechanical ventilation systems or sometimes with mixed-mode ventilation. However, mechanical ventilation systems in commercial buildings usually include air distribution ducts with centrally located fans to control the indoor air quality. In addition, mechanical ventilation systems usually also incorporate filters, space heating, cooling, and heat recovery. The use of mechanical ventilation and air conditioning systems does have an energy demand and a related energy cost. The more complex the system is in terms of duct length, filters, and heat recovery (high pressure drops), and the higher the airflow rate to be generated, the higher is the fan power necessary to move the air. The main advantage

of mechanical ventilation in terms of energy conservation is winter heat recovery from the warm room air. The main drawback is the restricted possibility of achieving high outside air ventilation rates in summer. Besides the initial costs for these systems, regular system maintenance is required to secure bacterial safety. Moreover, complex mechanical systems often have high space requirements for the central units and ductwork.

2.2 Natural Ventilation

Natural ventilation, also known as passive ventilation, is the most energy efficient technique for the provision of good indoor air quality. This is accomplished without any electricity demand for moving the air and improving the thermal comfort in summer by increased daytime airspeed and high night ventilation rates. The air change rates achievable through natural ventilation with correct sizing of the openings are significantly higher than those with mechanical ventilation for night cooling. Generally, controlled natural ventilation offers excellent potential for single-sided ventilation, and of course also for cross ventilation and stack ventilation due to the possibility of large opening cross-sections. The simplest form of natural ventilation is through open windows, or through window trickle vents.

In the design of ventilation strategies, natural ventilation is often not considered since there are very few standards and guidelines available for supporting planners in the design of natural ventilation, especially for high-rise office buildings.

The purpose of this section is to outline the physical processes which govern natural ventilation, to introduce the different ventilation strategies and elements, and to illustrate these for simple cases. Equations describing the volume flow (see § 2.4.1 and § 2.6.1) can be combined with meteorological data and flow path characteristics in models, which allow natural ventilation rates to be calculated. These models may be used to provide guidance on the areas of opening required to ensure that airflow requirements are satisfied.

The NatVent project [12] (see § 2.5.4) identified the lack of experience and know-how of the main stakeholders such as architects, engineering consultants, and building developers as the main barriers for the use of natural ventilation. Moreover, the project concluded that design tools and simulation codes were missing. Many

research projects have since been trying to develop simplified methods for passive cooling applications in order to handle the complex task of simulating airflow rates under changing external pressure and temperature [13-16].

Monitoring projects mainly analyse the indoor air quality and thermal comfort of naturally ventilated buildings, e.g., a study of 19 naturally ventilated buildings [12]. While the indoor air quality in most of the buildings was acceptable, eight of the buildings had serious overheating problems particularly caused by solar gains. Two design strategies for naturally ventilated buildings were identified:

- 1) When indoor air quality is the main priority, airflow rates tend to be low.
- 2) When summer comfort is the priority, much higher airflow rates are required and significant thermal mass needs to be present for night ventilation.

Simulations showed that natural night ventilation is only suitable in buildings with sufficient and accessible thermal mass of about 75-100 kg per square meter of floor space. The internal gains have to be limited to 30 W per m² of floor area. Night ventilation reduced the mean room temperature by 1,2 °C during working hours for a building in Freiburg/Germany [17], and between 1,5 and 2 °C in La Rochelle/France compared to a reference room [18].

The average reduction of temperature in an office building in Greece was predicted between 1,8-3 °C using night ventilation [19]. Monitoring projects show that night ventilation works well in climates with large diurnal temperature differences, but cannot be recommended for humid climates with humidity ratios above 15 g per kg air.

Natural ventilation can reach much higher ventilation rates than mechanical ventilation systems that are especially designed for fresh air supply. A range of studies using measurements and simulations in schools and offices showed air change rates between 5 and 22 per hour for cross ventilation and 1 to 4 per hour for single-sided ventilation [20-24]. The World Health Organization (WHO) recommends the use of natural ventilation in hospital isolation rooms with very high air change rates of 24 changes per hour, while general hospital areas should be ventilated with 8 air changes per hour [25].

2.2.1 Driving forces

The driving forces for natural ventilation of rooms and buildings are pressure differences caused by buoyancy or wind, or by a combination of these acting together or against each other. Ventilation rates (calculation see § 2.4.1) are dependent on the magnitude and direction of these forces and the flow resistance of the flow path. Air is forced to flow into the building where the external pressure across the enclosure orifices of a building is higher than the internal pressure. Orifices can be tiny cracks (infiltration) or large openings like windows (controllable building ventilation).

Physically, wind on a building envelope creates a pressure field with positive pressure on the windward side and negative pressure on the leeward and mostly all other sides. Buoyant pressure mechanisms arise where gravity acts on density differences due to temperature differences (e.g., mostly when the internal temperature is higher than the external temperature). Buoyancy induced ventilation is also known as ‘stack-effect’ or ‘chimney-effect’.

2.2.1.1 Buoyancy

The volume flow caused by buoyancy forces through a single large opening (i.e., open windows rather than cracks) or multiple openings in the building envelope is proportional to the square root of the pressure difference, and depends on the room air and the external air temperature as well as on the stack height. Density differences due to temperature differences create a density gradient. Below the neutral pressure line (NPL), the air will flow from the cold side to the warm side, and above the NPL from the warm side to the cold side.

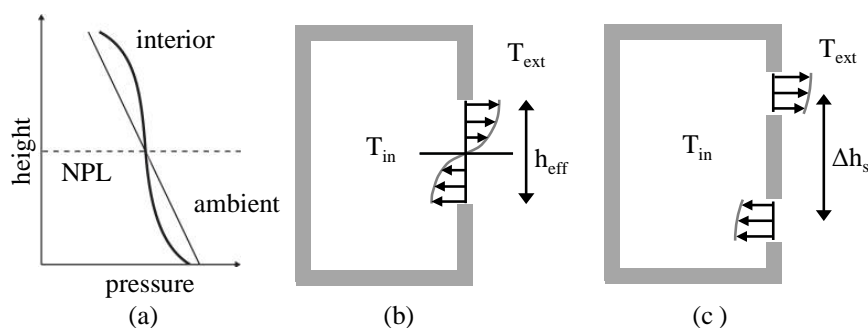


Figure 2.1: Internal and external pressure distribution of buoyant flow (a) causes airflow through a single large opening (b) or through a lower and upper opening (c).

An overall measure of the stack buoyancy pressure difference with two openings on different height levels h_s (stack height) is:

$$\Delta p_b = \Delta \rho_{\text{air}} \cdot g \cdot \Delta h_s \quad (2.1)$$

For the subsequent flow rate calculations or the sizing of opening areas, it is important to use a relatively accurate value for the density difference $\Delta \rho$. The absolute value for the density ρ or the average density $\bar{\rho}$ is less important. Therefore, it is common practice to express the density difference in terms of the temperature difference in Kelvin [26]:

$$\frac{\Delta \rho}{\bar{\rho}} = \frac{\Delta T}{\frac{T_{\text{in}} + T_{\text{ext}}}{2} + 273} \quad (2.2)$$

2.2.1.2 Wind

The airflow due to wind pressure differences has similar physical relationships as the buoyant driven flows, except that the pressure differences here are wind induced across the building.

Wind pressure differences Δp_w are dependent on the pressure coefficients C_p and on the local wind velocity v_z at the height of the openings. The surface pressure p_w will vary with the square of local wind velocity:

$$p_w = 0,5 \cdot \rho_{\text{ext}} \cdot C_p \cdot v_z^2 \quad (2.3)$$

Values of the wind pressure depend on the building shape, the wind speed and direction, the location and surroundings, and the specific location on the building surface.

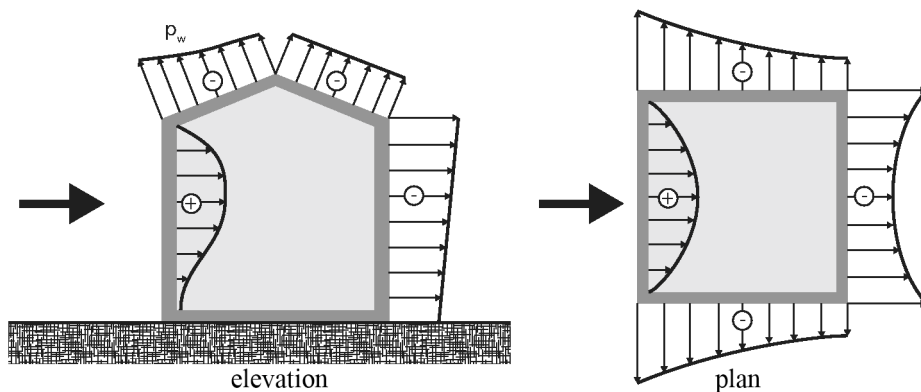


Figure 2.2: Wind pressure distribution on a pitched roof building.

The wind pressure difference between two points (e.g., inlet and outlet openings) may be calculated according to:

$$\Delta p_w = |p_{w,1} - p_{w,2}| \quad (2.4)$$

Wind pressure coefficients

Values of the pressure coefficient depend on four parameters, which are the spatial location on the building envelope (e.g., height and distance from the middle), the building shape, the surroundings (e.g., nearby buildings and vegetation), and the wind direction [27]. The static pressure coefficient is dependent on the wind pressure p_w at the point at which pressure coefficient is being evaluated, the pressure in the freestream p_∞ , the air density ρ_{air} , and the air velocity v_z :

$$C_p = \frac{p_w - p_\infty}{0,5 \cdot \rho_{\text{air}} \cdot v_z^2} \quad (2.5)$$

C_p data can be obtained from primary or secondary sources. Primary sources are expensive and time intensive full scale measurements, wind tunnel measurements, or Computational Fluid Dynamics (CFD) simulations. Less reliable secondary sources are tables such as those in the EN 15242 standard [28] and ASHRAE Fundamentals Handbook [27], or C_p -generators which are based on interpolation and extrapolation of generic knowledge and previously measured data and are therefore best applicable on standard building geometries. Costola [29] gives a good overview of such sources.

The following diagram exemplarily shows pressure coefficient data from a secondary source. The values are extracted from investigations made by Orme *et al.* [30].

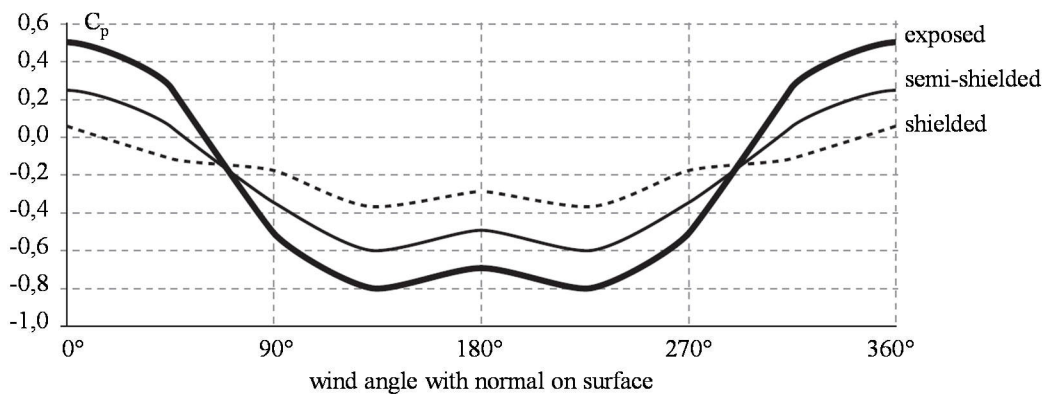


Figure 2.3: Comparison of wind pressure coefficients on the façade for a low-rise building with different shielding conditions [30].

2.2.2 Ventilation strategies

The term ‘ventilation strategy’ refers to the principle on how (driving force) and where on the envelope (opening configuration) air is introduced in the building. Ventilation strategies used to exploit the natural driving forces can be divided into three types: single-sided, cross, and chimney (stack) ventilation.

2.2.2.1 Single-sided ventilation

Single-sided ventilation typically serves a single room and occurs if the outside air enters and leaves the room on one side of the enclosure. Relative to other ventilation strategies, single-sided ventilation offers the least attractive solution for reaching high ventilation rates, and is only suitable together with a relatively low spatial depth.

Single-sided ventilation for ventilative cooling can be considered as well-designed in two variants: by a single tall opening, or with a double opening at different heights. If the opening is reasonably tall or two openings are on different height levels, the main driving force is typically the difference between inside and outside temperatures. Wind forces may influence the air change rate due to turbulences depending on the wind speed, but may also slightly decrease the airflow rate as the wind pressure rises with altitude due to the wind profile as described in § 3.2.1.1, and therefore counteract the buoyant flow. The double opening variant may enhance the stack effect by maximizing the height difference up to a room-scale. Even when increasing the penetration depth, care is needed in positioning any low level inlet if the external temperature is cold as it may create draughts. A winter solution could be to only open the upper opening for fresh air supply, while the lower opening can enhance summer ventilation at lower temperature differences. With only one opening, the airflow enters and leaves at a single large opening, and the flow rates are usually lower. The neutral pressure plane in both variants is typically close to the centre.

As compared to other strategies, the ventilation rates are typically lower, and the ventilation air does not penetrate as far into the space. As a rule of thumb, it is commonly stated that for effective ventilation, the room depth should not be higher than maximum 2,5 times the room height [26].

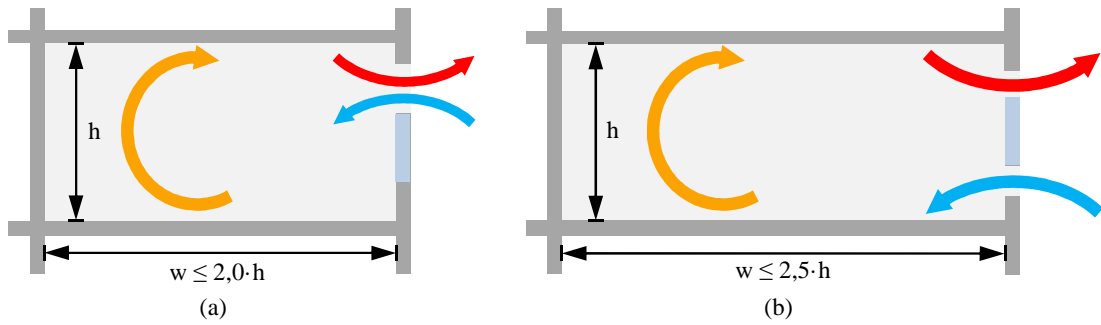


Figure 2.4: Single-sided single (a) and double (b) opening ventilation.

2.2.2.2 Cross ventilation

Cross ventilation can serve a single room or multiple rooms in series, and occurs if the outside air enters and leaves the building on different sides of the enclosure.

Relative to other ventilation strategies, cross ventilation typically offers an excellent solution for reaching high ventilation rates. But because of large and rapid variations in wind, the airflow is more difficult to control.

Even if cross ventilation can be assisted by thermal driving forces, wind is mostly the primary driving force, especially in the cooling season with low temperature differences between inside and outside. Positive pressure on the windward facade and negative pressure on most other orientated surfaces of the enclosure create a pressure field around the building. With the inlet and outlet on both sides of the room, directly or via a flow path connected to different sides of the enclosure, high flow rates can be usually achieved. If multiple rooms are connected, the resistance to airflow needs to be considered carefully. Thermal effects may assist if the openings for inflow and outflow are positioned on different height levels as shown in **Figure 2.6**. This is of special importance if there is no wind present.

The depth for effective ventilation has to be limited to prevent from the build-up of pollutants and heat. As air is crossing the room and reachable ventilation rates are higher than in the single-sided variant, larger room depths can be ventilated. In literature, as a rule of thumb, it is commonly stated that the flow path depth should not be higher than 5 times the ceiling height [26]. This implies a relative narrow plan depth of the building of typically not more than 15 m.

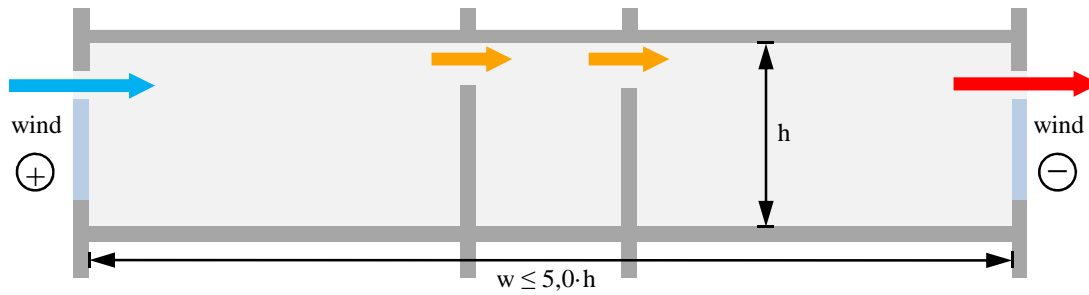


Figure 2.5: Wind driven cross ventilation with two openings, one on each orientation.

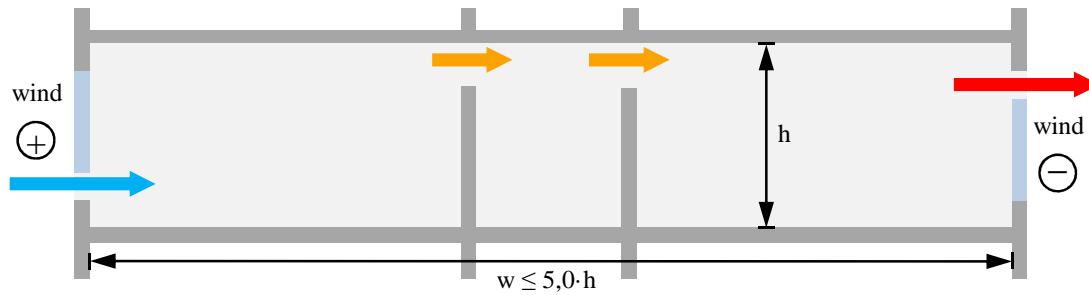


Figure 2.6: Buoyancy assisted cross ventilation with two openings, one on each orientation.

2.2.2.3 Chimney ventilation

Chimney ventilation, like cross ventilation, can serve a single room or multiple rooms. Chimney ventilation, also referred to as stack ventilation, occurs if fresh cool air enters the ventilated space at low level openings, leaving vertically towards a high level chimney exhaust, commonly situated above the roof. As far as the occupied space is concerned, chimney ventilation can be treated like cross ventilation with occupied space depth of maximum 5 times the ceiling height.

The strategy is mainly thermally driven by the difference in density between the warm chimney air column and the cold supply air, and can be further assisted by wind if the chimney outlet is in a region of wind-induced negative pressure as described in § 2.2.1.2. Due to large height difference between the inlet and the outlet up to a multi-storey scale, chimney ventilation offers a good ventilation potential. Solar gains to the chimney space can further increase the ventilation rate and stabilise the upward flow direction. If multiple storey levels are connected to a single commonly used exhaust stack, great care has to be taken when determining the different sizes of the ventilation openings on each storey of the building. For equal ventilation rates, the openings at lower floors need to be smaller compared to those near the chimney exhaust opening. This fact also has to be considered for the opening control.

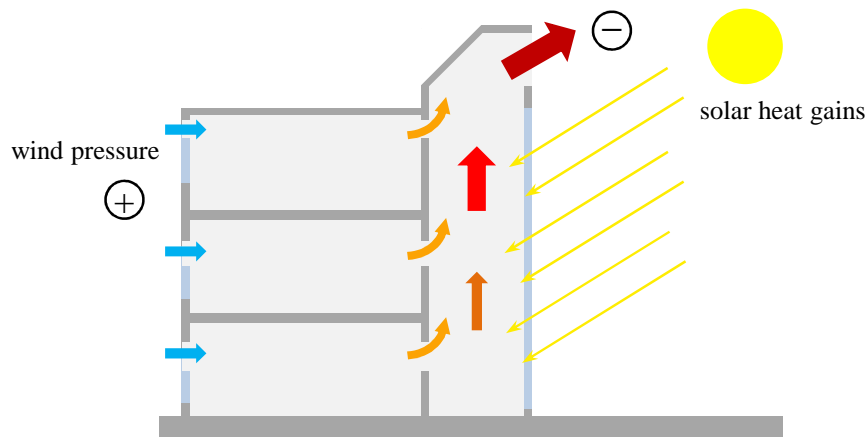


Figure 2.7: Stack ventilation with solar and wind assistance.

The air may flow from the edges to the centre of the building, to be exhausted via a central chimney or atrium. Chimney ventilation is therefore especially suited for wide building shapes with a central spine of chimneys as shown in Figure 2.8. But considering the wind pressure distribution at the inlet openings, it will be not uniform on the different envelope orientations, and therefore the flow direction and magnitude is difficult to control.

An atrium can be considered as a wide chimney. It is typically a rectangular, usable space for social interaction in the centre of a building, which is accessible from the surrounding rooms. A modern glass-roofed atrium, besides other functions, provides ventilation and daylight. The atrium design is a variant of the chimney ventilation principle and is suitable for wide plan, low- to medium height buildings. Hence, it is not considered further in the context of this study focusing on high-rise buildings.

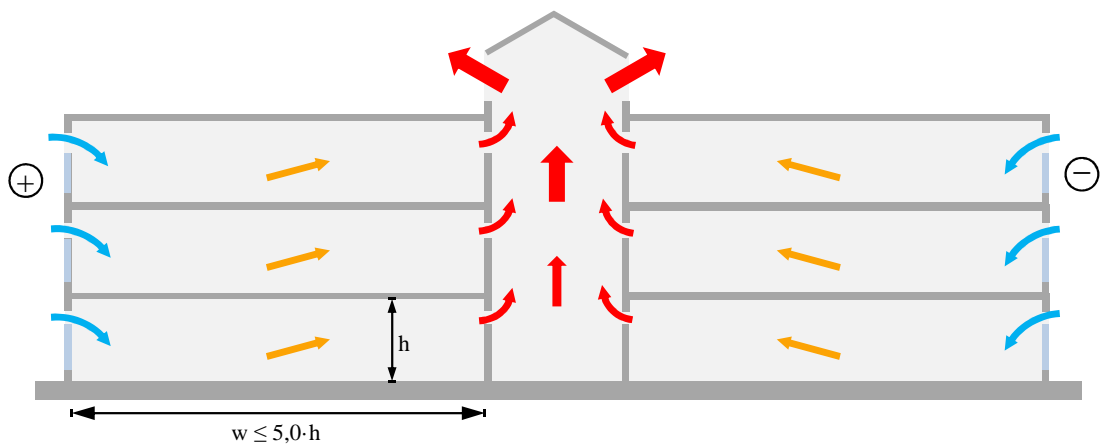


Figure 2.8: Central chimney ventilation.

A special chimney ventilation strategy worth mentioning is the so called ‘termite mound’ design shown in Figure 2.9. As a variant of the chimney ventilation strategy

it utilises a central exhaust air chimney, and also supplies air by a central void to provide fresh-air entry. In the example below, the cool air supply chimney can be integrated together with the exhaust air chimney by a constant chimney diameter. With a ‘termite’ strategy, air may be introduced at a central inlet point, which can be of special interest if underground earth tubes are intended to precool the supply air, and/or if central filters and/or supply air fans are intended to support the passive ventilation system. Disadvantages are the higher flow resistance and the smaller opening sizing possibilities. An existing example of the design is the Eastgate centre in Zimbabwe [31].

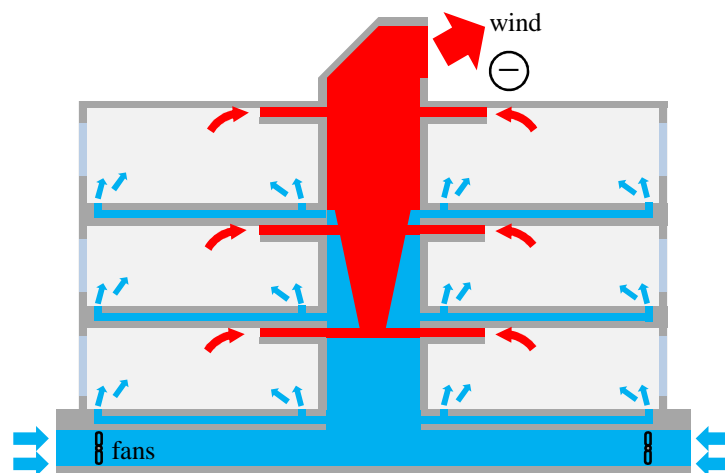


Figure 2.9: ‘Termite’ chimney ventilation example.

2.2.3 Ventilation elements

Precise parameterisation of flow through openings is necessary in order to model natural ventilation strategies. In this section, the most important elements forming the flow path are introduced.

2.2.3.1 Window Openings

Well-established opening types in naturally ventilated buildings are windows with rotating axis such as bottom- or side-hung windows. Due to the complexity of their geometries, simple analytical airflow calculations and airflow networks typically do not include their full geometry as input parameters; they include an effective area and height together with a discharge coefficient (see § 2.4.1.3) to describe the equivalent area of the rectangular orifice that would have the same flow as the pivoted window opening. The full geometry is typically described in a simplified way, but mostly

little guidance is provided on selecting airflow parameters such as the flow effective area and the discharge coefficient.

The flow effective opening area A_{eff} and height h_{eff} have to be first determined by the full geometry of windows (height, width, angle of tilt, opening factor, etc.). However, the definition of effective opening area is not standardised in literature – some authors include the tilt angle to the (effective) discharge coefficient [32], while others do not [16], depending on the focus of their work. In this study, the effective opening areas are dependent on the tilt angle, and the discharge coefficient stays constant. Depending on the ventilation strategy, typical opening cross-sections are approximately 1-3% of the floor area [16].

Sliding windows

Geometrically, the sliding (sash) window type is a rectangular opening without tilting or rotating elements. For the estimation of the flow rates, the effective area corresponds to the geometrical area together with an Opening Factor OF . The effective height is also dependent on the motion axis and whether the window moveable parts are controlled horizontally (Eq. (2.6)) or vertically (Eq. (2.7)):

$$h_{\text{eff}} = h \quad (2.6)$$

$$h_{\text{eff}} = OF \cdot h \quad (2.7)$$

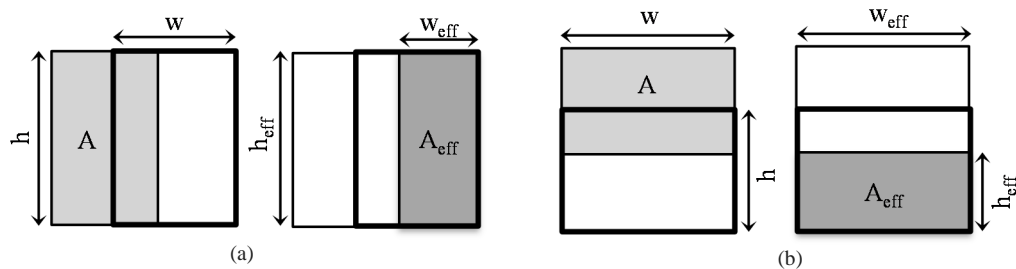


Figure 2.10: Geometrical representations of horizontally (a) and vertically (b) movable sliding windows and their resulting effective opening area, height, and width.

Pivoted windows

Simplified methods for the effective area calculation of bottom-hung windows can be found in literature [16,28]. Coley [33] investigated how to better represent bottom-hung windows in thermal models regarding the flow effective height of an opening, which is of special importance considering single-sided ventilation strategies. Subsequently, these methods gathered from literature are further adapted here for representing different tilted window types.

However, Hall [34] states in her dissertation that the determination of the resulting opening areas for bottom- and top-hung tilted windows requires further investigation in order to reach a better general validity for the simulation. She experimentally determined smaller effective opening areas for bottom-hung windows with reveals.

The European standard EN 15242 [28] (see § 2.6.4) makes the very simplified assumption that the volume flow through a tilted window depends only on the tilt angle and is independent of the ratio of height to width.

A more accurate formula was developed by van Paassen [16] in the context of the NatVent study (see also § 2.5.4). It fits reasonably well with the EN 15242 formula for low height windows. This expression, besides the tilt angle, also reflects the opening geometry as a function of height and width (cf. Figure 2.11):

$$A_{\text{eff}} = \frac{1}{\sqrt{\frac{1}{(h \cdot w)^2} + \frac{1}{\left(2 \cdot h \cdot w \cdot \sin\left(\frac{\alpha}{2}\right) + h^2 \cdot \sin(\alpha)\right)^2}}} \quad (2.8)$$

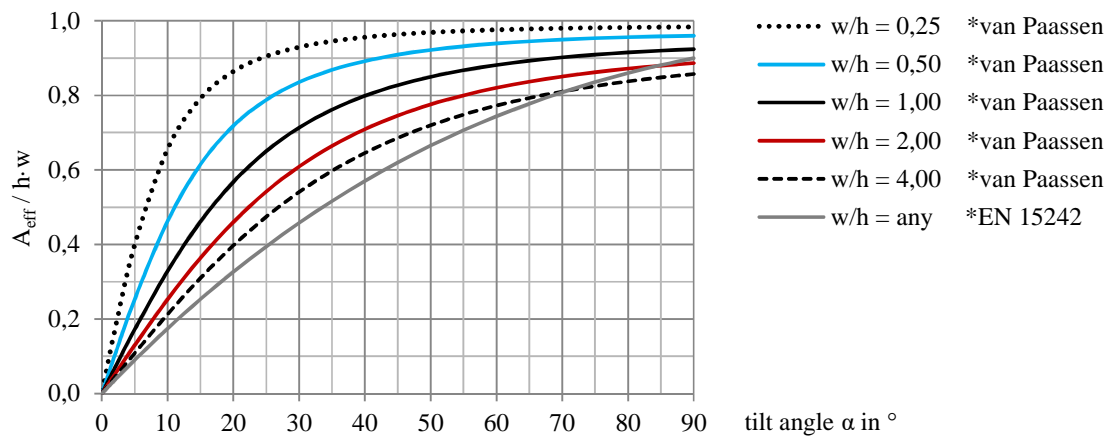


Figure 2.11: Effective areas with different height to width ratios scaled by the fully opened window with equal area according to van Paassen [16], and comparison with the EN 15242 [28] polynomial approximation.

Figure 2.12 also shows the effective area from the manufacturer's test data of flow through top-, bottom- and side-hung windows as provided in the IES MacroFlo documentation [35]. IES lists the effective discharge coefficient by window angle and window aspect ratio, and interpolated values for C_d . The data here was normalised by the effective discharge coefficient at 90 degree opening angle as described by Hult *et al.* [36]. Relatively close agreement was found especially for

narrow windows between the data from window manufacturers and the effective areas calculated according to van Paassen.

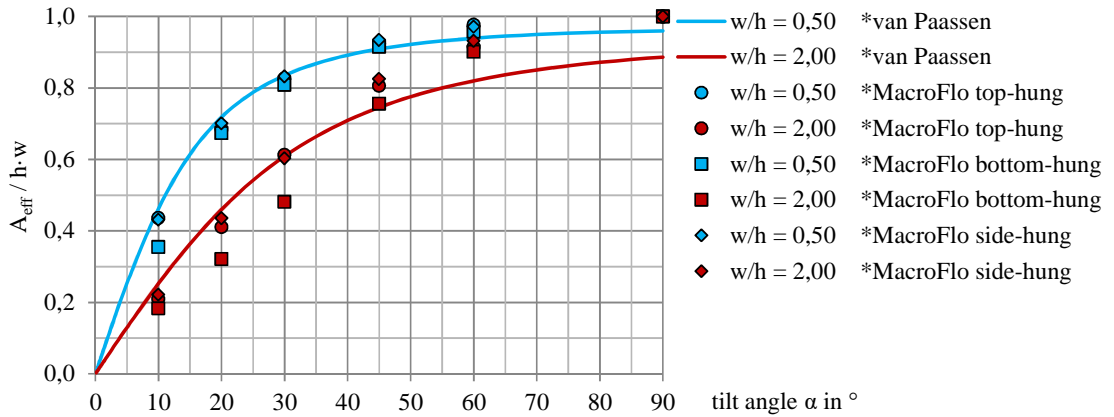


Figure 2.12: Effective area for a wide and a narrow pivoted window scaled by the fully opened window with equal area according to van Paassen [16], and comparison with measured data reported by IES MacroFlo.

The effective opening height for a bottom-hung window is determined according to Coley [33] by the following formulation:

$$h_{\text{eff}} = \frac{A_{\text{eff}}}{w} \quad (2.9)$$

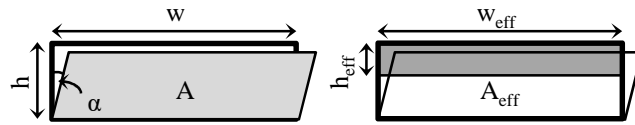


Figure 2.13: Geometrical representation of a bottom-hung window and the resulting effective opening area and height.

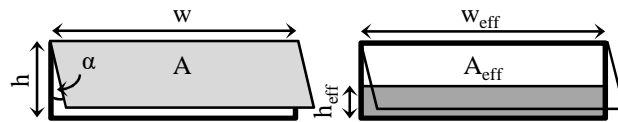


Figure 2.14: Geometrical representation of a top-hung window and the resulting effective opening area and height.

The effective opening area of side-hung windows as shown in Figure 2.15 can be calculated similarly as in the bottom-hung formula shown before (Eq. (2.8)). The adapted formula for the calculation of the effective area of side-hung windows is:

$$A_{\text{eff}} = \sqrt{\frac{1}{\frac{1}{(w \cdot h)^2} + \frac{1}{\left(2 \cdot w \cdot h \cdot \sin\left(\frac{\alpha}{2}\right) + w^2 \cdot \sin(\alpha)\right)^2}}} \quad (2.10)$$

The effective height for the single-sided ventilation here however equates to the geometrical height of the opening (cf. Figure 2.15).

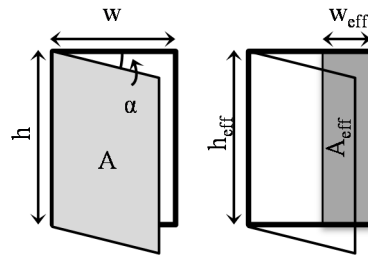


Figure 2.15: Geometrical representation of a side-hung window and the resulting effective opening area and width.

2.2.3.2 Sub-slab distribution

As already shown in the termite example in § 2.2.2.3, another possibility for air supply other than simple window inlets is sub-slab, also referred to as underfloor air distribution. This air supply type uses an underfloor supply plenum, e.g., located between the concrete slab and the raised floor to supply external air into the occupied zones of the building. The approach provides greater control of air distribution across the building section [37]. The flow path can be designed to take air directly from the envelope (Figure 2.16), and also from the building's internal chimneys (Figure 2.9). The airflow resistances in the airways are strongly dependent on the design as they depend on whether the flow is laminar or turbulent, and on the dimensions of the airways. Specially designed floor diffusers are usually used as supply outlets.

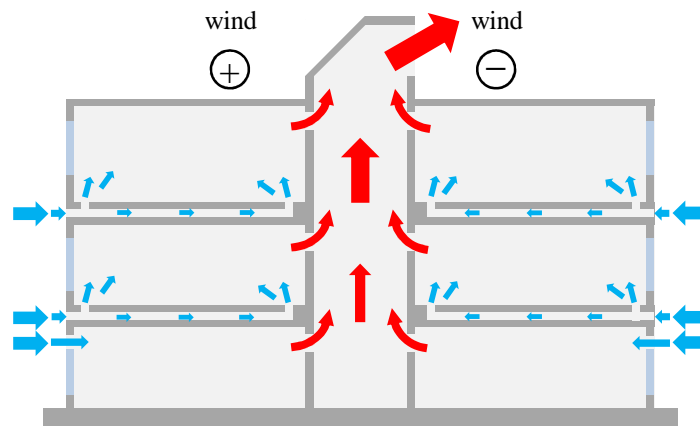


Figure 2.16: Stack ventilation with sub-slab distribution.

Vertical temperature stratification is a well-known phenomenon and will result here as sub-slab supply can be considered similar to displacement ventilation [38].

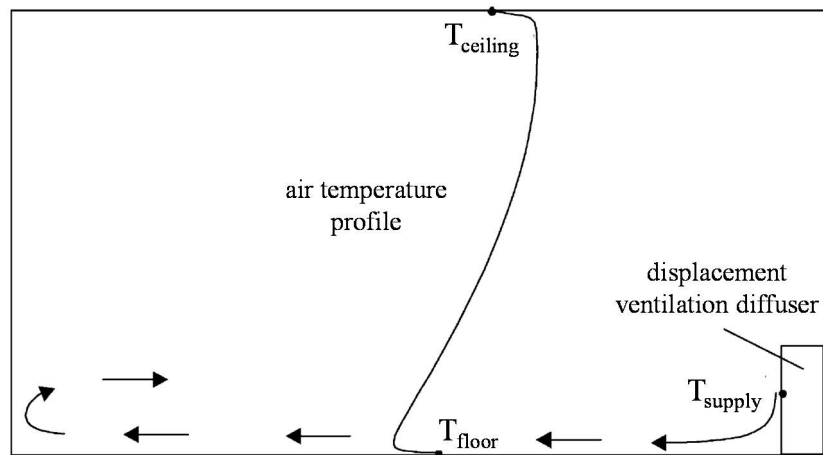


Figure 2.17: A characteristic airflow pattern and temperature stratification in a room with displacement ventilation (adapted from [38]).

2.2.3.3 Chimney openings

Considering the wind pressure field around a building as shown in Figure 2.2, chimney openings for air intake or exhaust require care when designing the position and form. Chimney inlets (wind-scoop) are best positioned windward, and chimney exhausts (wind-extract) in most other directions. A chimney device, which is opened on two or four sides, is capable of acting as scoop and extract. A pair of partitions is usually placed diagonally across each length. This ventilation system has been part of the building design for already hundreds of years in the Middle East, and is known as ‘wind-catcher’ or ‘badgir’ [39].

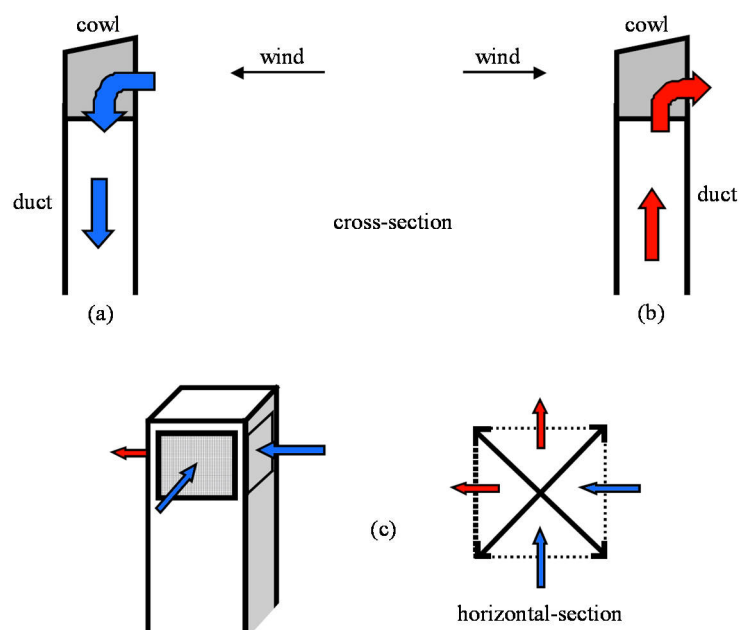


Figure 2.18: Three types of aerodynamic device: (a) wind scoop, (b) wind extract, (c) balanced ventilator (adapted from [40]).

2.2.4 Ventilative cooling

To reach thermal comfort conditions in the warm period, an effective ventilation strategy for temperature control (cooling) comprises measures that act to reduce the internal and solar gains as far as possible and to absorb heat in the fabric of the structure. The protection from intense heat gains may involve landscaping, building form, layout and external finishing, solar control and shading of building surfaces, thermal insulation, and the control of internal gains.

The aim of ventilation is to achieve high flow rates of cooler outside air through the building. Ventilation as a heat dissipation technique can deal with the potential for disposal of excess heat of the building to an environmental sink of lower temperature, which here is the external air. The dissipation of excess heat generally depends on the availability of an appropriate environmental heat sink, and of an appropriate thermal coupling between the building and the sink as well as sufficient temperature differences for the transfer of heat. The potential of heat dissipation techniques strongly depends on climatic conditions.

For the control of temperatures, passive daytime cooling or night cooling can then be very effective in moderate climates. This requires rather high flow rates, with a factor of 3 to 12 times the flow required for indoor air quality reasons in a medium-densely occupied office. This substantial difference leads to completely different systems for passive cooling, although the ventilation system for indoor air quality control may assist the control of temperatures during warm periods. The ventilation system for indoor air quality control will almost never be sufficient to take over the function of temperature control. With mechanical ventilation, the necessary system size and electricity demand is in opposition to the necessary flow rate.

Naturally ventilated buildings can offer good thermal comfort even in hot summer conditions. For example, in the summer of 2003 the office building Lamparter had less than 10% of the hours of use above 26 °C, but atriums can easily overheat [24].

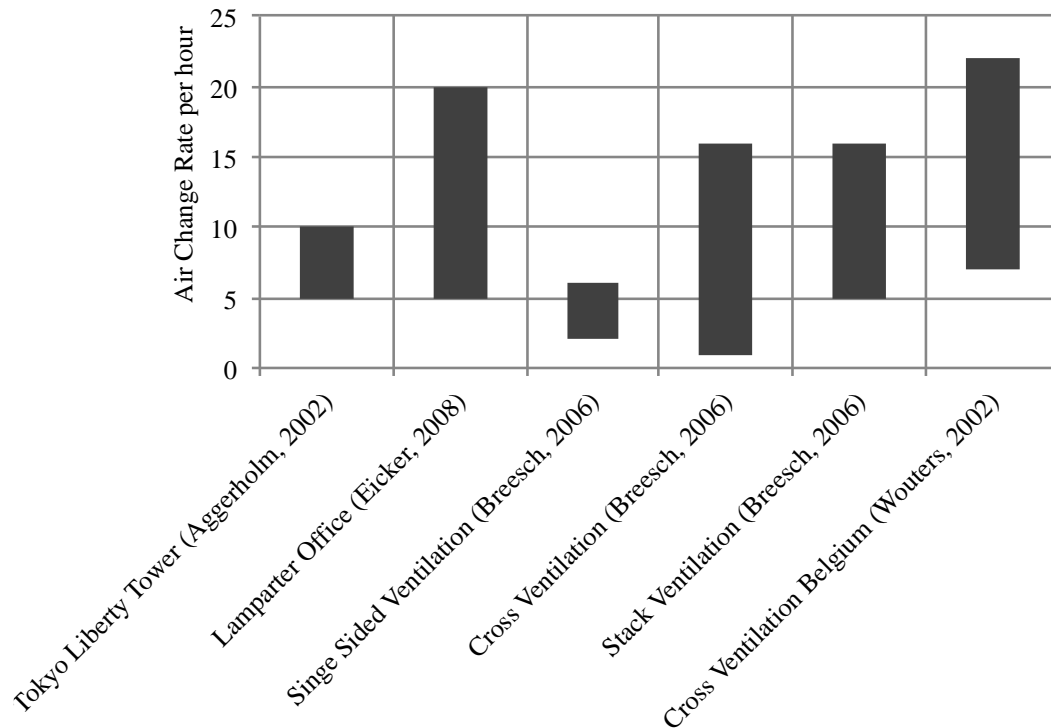


Figure 2.19: Natural ventilation air change rates applied or measured [20,23,24].

2.2.4.1 Diurnal ventilation

Daytime ventilation is a simple strategy to enhance comfort by direct personal cooling. When internal temperature is felt too warm at still air, increased air velocities can compensate for higher room temperatures to achieve comfortable conditions by wind-chill. The increased airflow of outdoor air increases the limits of acceptable temperature and humidity as it affects evaporation and convection around the human body. High airflow rates are particularly useful when relative humidity is high as the higher air velocity increases the rate of sweat evaporation from skin, thus increasing heat losses in the thermal balance of human body [41].

Direct advective cooling with high flow rates replaces the warm internal air by cooler external air, and therefore the internal air temperature may closely follow the ambient air temperature.

Daytime ventilation can only be applied in an acceptable way if the indoor comfort may be achieved with outdoor air temperatures and with acceptable indoor air velocities. The distinct operation control regime should be considered with relatively high ventilation rates of the order of 5 to 10 ACH for direct ventilative cooling when appropriate.

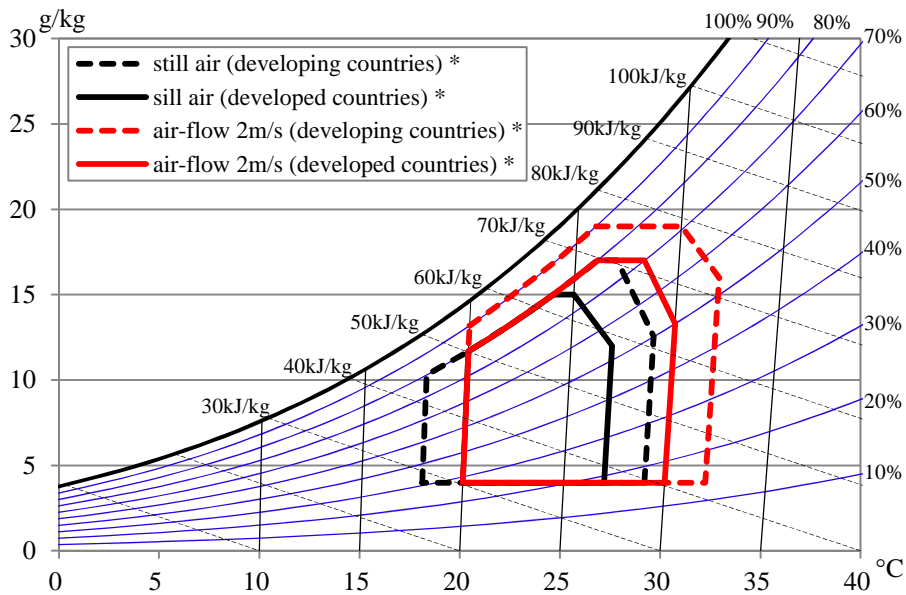


Figure 2.20: Boundaries of outdoor air conditions within which indoor comfort can be provided by natural ventilation during the day, with indoor airspeed about 2 m/s (a very light breeze) [8].

2.2.4.2 Night-time ventilation

The idea of night-time ventilation in office buildings is to use the thermal mass of a building as a heat sink. The structure is cooled by convection during the night and is able to absorb heat in occupied hours. In principle, cool night air passes over a heavyweight building fabric and cools the thermal mass. The warmer daytime air will then be reduced in temperature when passing over the cooled slab. Therefore, night ventilation is particularly suited to offices, which are unoccupied during the night so that relatively high air changes can be used to provide maximum cooling effect without creating thermal discomfort. This strategy provides attenuation of peaks in cooling load and modulation of internal temperature with heat discharge at a later time (Figure 2.21). The larger the outdoor temperature swings, the bigger the influence of such storage capacity. The cycle of heat storage and discharge must be combined with means of heat dissipation, so that the discharge phase does not add to overheating.

Controlled night cooling must continue till the building is adequately cooled or occupied again. If the building structures are cooled to a too low level, the cooling process has to be interrupted before the end of the night in order to regain acceptable surface temperatures before the start of occupation. Night-time ventilation is an effective low energy cooling technique, especially in climates with relatively low

peak summer temperatures during the day and medium to large diurnal temperature differences.

The distinct operation control regime should be considered with high ventilation rates when required. Typical ventilation rates for night cooling (typically of the order of 5 to 15 ACH) will exceed minimal rates needed for indoor air quality control, which during unoccupied hours may fall well below 1 ACH. Thus again, air quality control other than moisture control will usually not be needed to be considered during night-time ventilation.

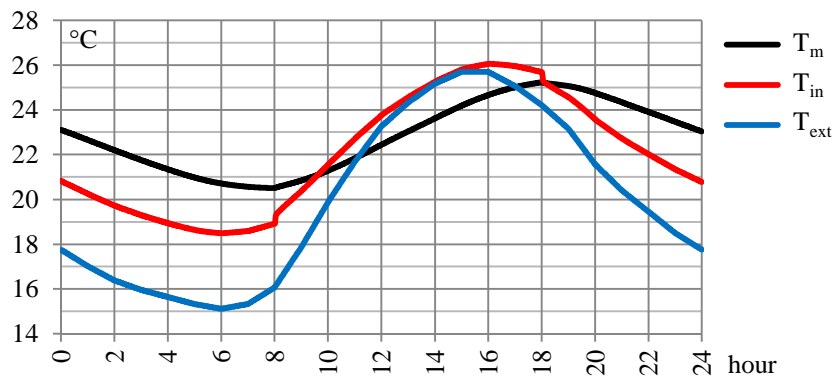


Figure 2.21: Typical surface temperature cycle (black line) of an office concrete slab using the thermal mass as a heat sink with a constant flow rate of 10 ACH during night and day.

Night ventilation can be operated passively, e.g., window ventilation, or mechanically with fans. Natural night ventilation has the advantage of higher flow rates without fan electricity demand. Night ventilation can operate not only along with passive diurnal ventilative cooling strategies, but also with mechanical cooling. Thus, night ventilation, if not a pure passive approach, is also of importance to reduce the energy consumption for mechanical cooling in summer.

2.2.5 Design impact

Natural ventilation principles will result in buildings with very little visible conventional ventilation equipment, as the building itself mostly provides the ductwork. The investment in mechanical equipment will be shifted towards a larger investment in the building itself: increased room air volume per person, a shape favourable for air movement, a more complex facade/window system, optionally with underground intake air culverts, extract air stacks, etc. Thus, modern natural and hybrid ventilation systems will have a large impact on the building design, making

close cooperation between the architect, the civil engineer and the HVAC engineer a necessity [3], providing the possibility of 'form-follows-function' stylistic elements.

For high-rise building shapes, the challenges in terms of designing the envelope and its openings are greater, primarily because the potential magnitudes of driving forces become bigger, and their relative magnitudes can vary over a wider range. For a buoyant driven chimney strategy where multiple storeys are connected to one single stack, the pressure differences at the lowest storey openings are great, especially when the temperature differences are high (in winter). For example, for a building with 200 m height and with a temperature difference of 20 °C between inside and outside, the pressure drop across the envelope at the ground level would be in the range of 140 Pa (without internal resistance) [42]. Besides high unintended infiltration rates, this force is unacceptable for controlling (open and close) windows and doors. Another difficulty is the range of opening sizes. The pressure drop at the lower level of the building can be many times more than that at the highest level. At the upper storeys, the opening sizes for pure buoyant ventilation as well as the chimney size tend to be too large to be realised in practice. Internal flow path resistance can reduce the peaks in pressure drop around a single orifice, but the overall system size would be enhanced (e.g., the resulting chimney diameter). In contrast, the wind pressure at the highest storeys is generally much higher than that on the lower floors. This is because of the urban terrain roughness, the resulting wind profile (see § 3.2.1.1) and local wind shielding, e.g., by other buildings (see § 2.2.1.2). The resulting opening sizes are thus very different to the sizes intended for thermal ventilation. Also, the forces of wind and buoyancy may oppose each other depending on the flow path design, which makes the control over external air supply difficult. To overcome these difficulties, Etheridge [43] proposes the design of isolated spaces (single zones or storeys) or building segmentation (part of the building up to few storeys) as vertical passages will suffer less from the difficulties mentioned above. Each isolated zone, storey or segment can then be treated as a low-rise design (Figure 2.22).

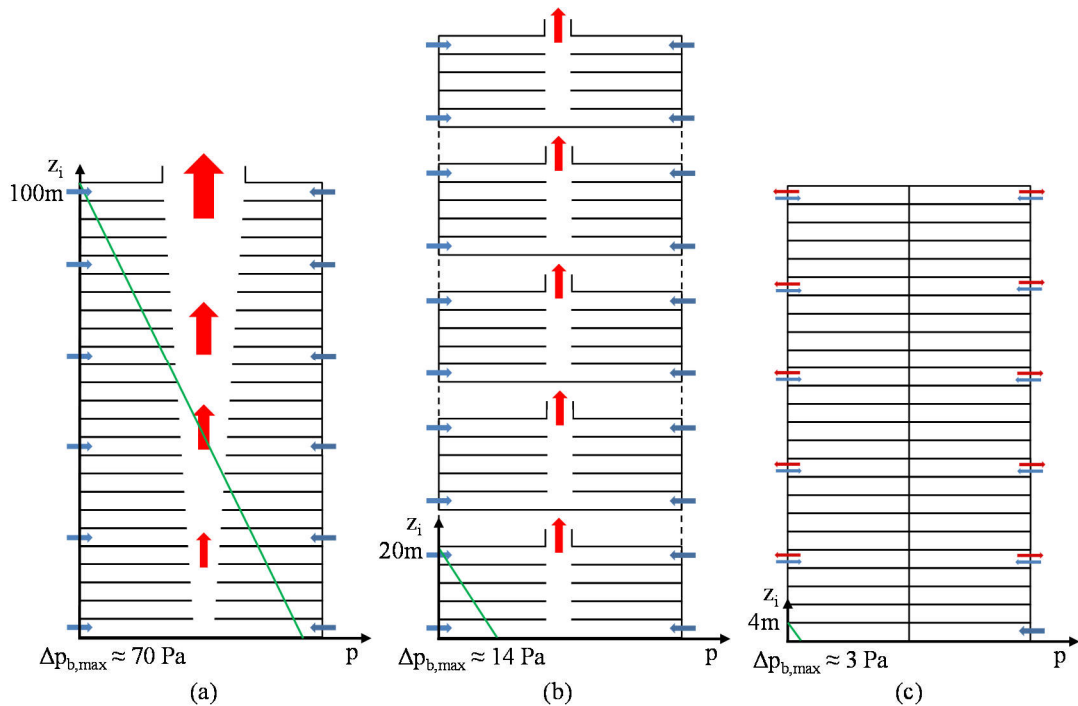


Figure 2.22: Three ventilation strategies for tall buildings: (a) upward cross-flow with direct connection between floors; (b) upward cross-flow with segmentation; (c) isolated spaces. Note: The flow pattern is the same for each floor, so only a few flow arrows are shown. The resulting pressure drops are due to buoyancy at 20 °C temperature difference without internal resistance. Source: adapted from [42].

2.2.6 Control strategies

The control of natural ventilation openings either focuses on indoor air quality, on indoor temperature levels for free cooling modes, or on a mix of both. It is important that both ventilation rates and air distribution must be considered. Manual or automatic control can be achieved whenever the building is occupied. The relatively simple control of indoor air quality is discussed in § 2.3.1.

Surveys that tried to identify manual control actions for direct ventilative cooling have shown that occupants in general will accept wider thermal comfort bands when occupant control is available [41,44-48], and is generally preferred. Therefore during occupation, it is best to allow building occupants to control (overwrite) the flow rate (opening factor) as manual control appears to be strongly related to productivity [26]. Nevertheless, there are some obvious pitfalls with manual control, especially concerning problems of unintentionally high ventilation rates. Thus, automatic overrides may have to be used in practice [49]. During occupancy, a distinction is made between cellular and landscaped offices [50]. While user control functions well in cellular offices, in landscaped offices automatic control is also necessary during the

day. However, the correct control strategy is not easy to establish and users should still be able to override the automatic control.

Results from twelve office and educational building case studies showed that during non-occupancy, automatic control is necessary to cool down the building structure with the help of night ventilation [20]. Night-time ventilation (see § 2.2.4.2), due to its dynamic nature, represents a great challenge as it can lead to overheating, overcooling, and moisture entrainment. It affects the indoor conditions during the next day by [51]:

- 3) peak air temperatures reduction,
- 4) air temperature reduction throughout the day and, in particular in the morning hours,
- 5) slab temperature reduction, and
- 6) time lag creation between the occurrence of external and internal maximum temperatures.

Good control needs to forecast future conditions. Consequently, due to the absence of occupants and also for security reasons (i.e., sudden change of weather), night ventilation is best controlled automatically. A great number of researchers highlighted the problem of developing effective night cooling control strategies (references may be found in [49]). Axley [49] recommended and compared three such simple control strategies developed (summarised in Table 2.1). In the third column, different night control strategies (Opt. A-E) either based on room air temperature setpoints, floor slab temperature levels, degree hours, or daily cooling uptake were analysed and compared for an office building, and showed very comparable results. The setting of the control parameters was shown to be more important than the strategy itself. The main parameter was to provide high enough airflow rates for night ventilation and limit the internal gains [15,16].

Table 2.1: Recommended night cooling control strategies from different investigations [49].

Kolokotroni [52]	Martin & Fletcher [53]	van Paassen <i>et al.</i> [16]
enable night cool criteria		
<ul style="list-style-type: none"> • if peak zone temp. > 23 °C or, • if average daytime zone temp. > 22 °C or, • if average afternoon outside air temp. > 23 °C or, • if slab temp. > 23 °C. 	<ul style="list-style-type: none"> • if peak zone temp. > 23 °C or, • if average daytime zone temp. > 22 °C or, • if average afternoon outside air temp. > 20 °C or, 	<ul style="list-style-type: none"> • Opt. A: if peak zone temp. > 24 °C and if daytime zone degree hours, base 21 °C is positive or, • Opt. B: if average afternoon outside air temp. > 18 °C or, • Opt. C: if slab temp. > 23 °C. • Opt. D: PI vent control on peak zone temp. to (18 – 22)^a °C or, • Opt. E: manual control based on weather forecast.
operate night cool criteria		
<ul style="list-style-type: none"> • if zone temp. > outdoor temp. and • if outside air temp. > 12 °C and • if zone temp. > zone heating setpoint. 	<ul style="list-style-type: none"> • if zone temp. > outdoor temp. +2 °C and • if outside air temp. > 12 °C and • if zone temp. > zone heating setpoint. 	<ul style="list-style-type: none"> • if zone temp. > outdoor temp. and • if outside air temp. > 12 °C.
operation period		
<ul style="list-style-type: none"> • enable operation 7 days a week • enable operation during entire non occupied period 	<ul style="list-style-type: none"> • enable operation 7 days a week • enable operation during entire non-occupied period • continue operation two additional nights when activation & operation criteria are no longer satisfied if operated for 5 or more consecutive nights. 	<ul style="list-style-type: none"> • enable operation 7 days a week • enable operation during entire non-occupied period

In recent years, fuzzy control algorithms have also been successfully used for combining acceptable indoor air quality and thermal comfort [54]. Another study in the UK showed that complex algorithms do not perform better than simple ones, but it is recommended not to overcool the buildings especially in the transition months May, June, September, and October [53].

2.3 Performance Indicators

2.3.1 Indoor air quality

The main reason ventilation is required to maintain a reasonable level of indoor air quality is the fact that people are in buildings. Their bio-effluents have to be removed and diluted. The required flow rates are therefore normally expressed in volume per person. Sensors may also directly control the demand based on the CO₂ concentration, and can improve the air quality while saving energy. The operation control regime should be considered for the control of ventilation rates and air distribution to maintain acceptable indoor air quality. Typically, minimal ventilation rates for air quality control (background ventilation, i.e., of the order of 1 ACH during building occupancy) will be less than those required for direct ventilative cooling (see § 2.2.4). The minimal ventilation rate is reasonably controlled automatically, as personal detection of air quality conditions is generally too subtle to be considered [49]. The control is critical in winter conditions and can have significant energy consequences.

Thus, air quality control will normally not be an issue during direct ventilative cooling. To reduce heat losses to a minimum without heat recovery in winter, it is favourable to restrict the ventilation intervals (to a few minutes). Higher ventilation rates can supply the total required amount of air in a shorter time period. During these short time periods, the building heat losses are smaller because most of the heat is stored in the building fabric, and the entering fresh air quickly heats up again.

In a number of cases with the so-called ‘sick building syndrome’ symptoms, people rely on the strategy to ventilate more because of high emissions from the building, the furniture materials and the badly maintained mechanical ventilation systems. This is not very energy efficient. The goal must be to keep emissions as low as possible. The strategy therefore is source and product control, but not ventilation.

Indoor air quality is usually evaluated by the CO₂ concentration indicator. Unfortunately, there is no agreement on the limit values for good air quality (see Figure 2.23). According to EN 13779 [55] high indoor air quality (IAQ) is achieved with less than 400 ppm above the level of outdoor air, medium IAQ in a range between 400 to 600 ppm, moderate IAQ from 600 to 1000 ppm, and low IAQ above 1000 ppm. The German Federal Ministry for the Environment, Nature Conservation

and Nuclear Safety considers 1000 ppm in schools as hygienically good, from 1000 to 2000 ppm as hygienically noticeable, and above 2000 ppm as not acceptable. EN 15251 [41] uses 1000 ppm as the upper limit for the design of ventilation systems. According to the Commission Delegated Regulation (EU) No 244/2012 [56], ‘energy efficiency measures ... shall be compatible with air quality ... levels according to CEN standard 15251 on indoor air quality or equivalent national standards’.

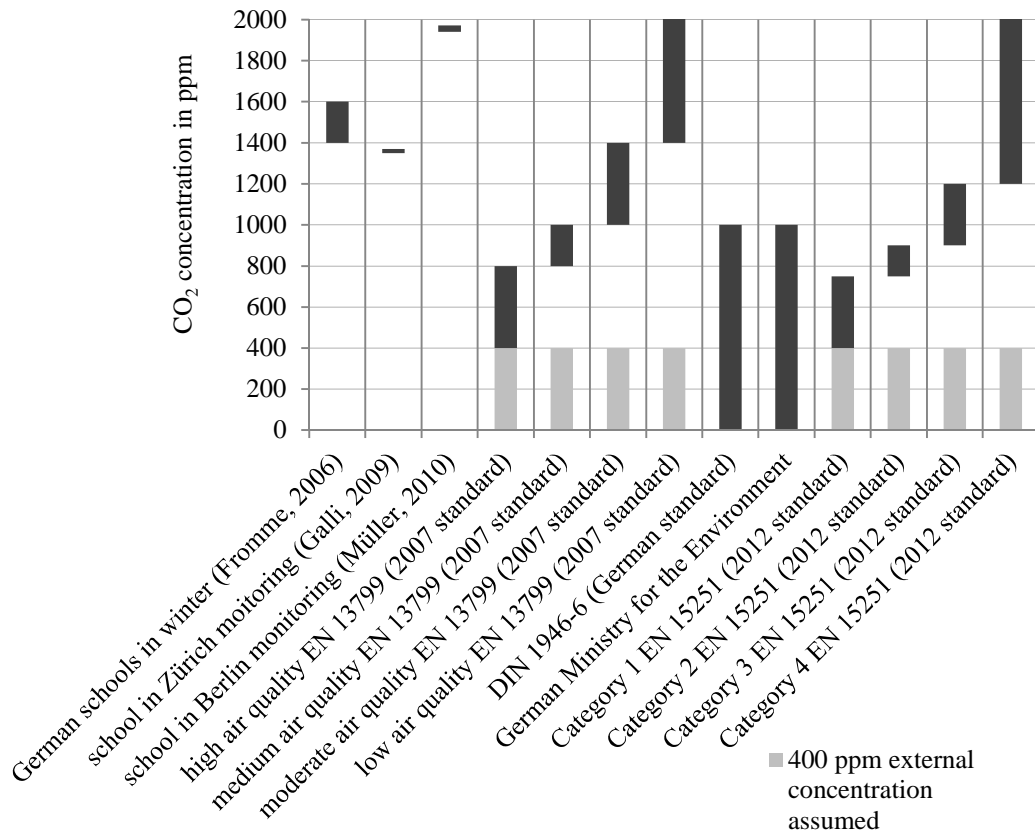


Figure 2.23: Monitored and allowed CO₂ concentrations [21,41,55,57-59].

2.3.2 Thermal comfort

Thermal comfort is seen as a state of mind that expresses satisfaction of the occupants. It is assessed by subjective evaluation [60] since the occupants will desire differently based on their physiology and psychology. Besides the psychological parameters such as individual expectations, thermal neutrality is maintained when the heat generated by human metabolism is in thermal equilibrium with the surroundings. The main factors that influence thermal comfort are the metabolic rate, the clothing insulation, the air temperature, the mean radiant temperature, the air velocity, and the relative humidity.

The Predicted Mean Vote (PMV) model [60] is one of the most recognised thermal comfort models, and has been incorporated into a number of standards and design codes (e.g., ISO-7730 [61]). But the PMV method should be applied only to air-conditioned buildings, while the adaptive model can be generally applied only to passively operated buildings where no mechanical systems have been installed. The adaptive model was developed with the idea that outdoor climate influences indoor comfort as occupants dynamically interact with their environment. The operative room temperature is allowed to increase in naturally ventilated, non air-conditioned buildings with rising ambient air temperatures. Occupants in the warm period control their thermal environment by means of clothing, controllable natural ventilation, fans, and shading elements [62]. Extensive field studies showed that the occupants of naturally ventilated buildings do accept and even prefer a wider range of temperatures than in air-conditioned buildings because their preferred temperature depends on outdoor conditions.

Adaptive comfort models are implemented in standards such as European EN 15251 and ISO 7730 standard, and slightly different in the American ASHRAE 55 standard. Contrarily to the ASHRAE 55 standard [63], and in accordance with the EN 15251 standard [41], the adaptive approach can be applied to hybrid (mixed-mode) buildings whenever the mechanical systems are not running. In contrast to the PMV model, the adaptive model does not reflect the influence of humidity. According to the Commission Delegated Regulation (EU) No 244/2012 [56]: *'energy efficiency measures ... shall be compatible with ... indoor comfort levels according to CEN standard 15251.... In cases where measures produce different comfort levels, this shall be made transparent in the calculations.'*

The temperature excess method cumulates the hours with room air temperatures above a given setpoint and compares them with limiting values, e.g., 5% of all office hours.

In this thesis, the acceptable temperature setpoints were calculated following the adaptive comfort limits, which are defined in the European standard EN 15251 [41]. Depending on the exponentially weighted running mean of the daily mean ambient air temperature series of the previous week, recommended operative temperatures are calculated for different comfort categories (for details see § 2.6.3). The criteria were obtained through investigations in office buildings with user operated windows [48].

2.3.3 Energy consumption

The HybVent project investigated that ‘in well-insulated office buildings, which are becoming more and more common in IEA countries, ventilation and cooling account for more than 50% of the energy requirement’ [3]. Due to passive cooling and controlled natural ventilation, there is no energy consumption for cooling and ventilation. It is assumed that if thermal comfort can be guaranteed without air conditioning, then significant cooling and ventilation energy conservation can be achieved [64]. Energy savings by natural ventilation can mostly only be evaluated when simulation tools are used, as two identical buildings with different ventilation or climatisation strategies are rarely available for monitoring. The savings on venting, heating, and cooling energy can be determined by comparing natural ventilation strategies (while maintaining thermal comfort) with an identical office building for which mechanical ventilation is used (e.g., utilizing building energy simulation tools).

A 30% reduction of the cooling energy consumption and 40% reduction of the installed cooling capacity was predicted for a UK low energy office building with a stack driven night ventilation air change rate of 10 per hour [51]. 40% reduction of the daily cooling demand was simulated for a high thermal mass office building in Belgium [65]. Blondeau investigated that night ventilation with air change rates of 8 per hour can reduce cooling requirements by 12 to 54%, depending on the temperature setpoint [18].

The primary energy consumption of naturally ventilated office buildings in Denmark was compared with that of mechanical ventilation systems [66]. The naturally ventilated buildings consumed 40 kWh/m² per year, whereas the consumption of mechanical ventilation systems varied from 50 kWh/m² per year (VAV system) to 90 kWh/m² per year (CAV system). The primary energy conservation for naturally ventilated office buildings in Belgium was calculated to be 8 kWh/m² per year [23]. Studies conducted on the 23 storey Liberty Tower of Meiji University in Tokyo [3] showed that about 17% of energy consumption for cooling is saved by using the natural ventilation system.

2.4 Airflow Modelling Approaches

The driving forces for natural ventilation of rooms and buildings are pressure differences caused by buoyancy and wind (see § 2.2.1). Ventilation rates are dependent on the magnitude and direction of these forces, and the flow resistance of the flow path (see § 2.2.2 and § 2.2.3).

Simplified calculation methods for cross ventilation can be applied when the pressure conditions at inlets and outlets are the same or at least similar for each orientation, and thus a relatively constant pressure difference can be supposed. For thermally driven ventilation, the inlets and outlets should each be located at the same or at least a similar height level; for wind induced ventilation, the wind pressure coefficients and the wind speeds at the opposing openings should each have a similar value.

Occasionally, one will encounter configurations that cannot be covered by simple equations as presented in § 2.4.1. Examples are solar chimneys or atriums with inlets on different floors and with a common outlet or complex wind pressure conditions at different façade orientations. In such cases, it is advisable to calculate the airflow for the most effective flow path. If this is no longer possible due to the complexity of the flow paths, it is recommended to utilise the more complex, but still explicit ‘Envelope-flow’ method [26,43] or dynamic multi-zone flow models [67,68], which are included in programs such as TRNSYS or EnergyPlus [1]. As a unique tool, Computational Fluid Dynamics (CFD) predicts the airflows at all points of the space defined including the flow momentum, but computation time is excessive.

The analytical calculation methods described below can be utilised for sizing openings or to validate the airflow network simulation or CFD simulation results for simple situations. For complex flow path configurations, the flow rate can be estimated by AirFlow Networks (AFN) [69], the Envelope Flow Model (EFM) [70] or by the electrical analogy approach developed in this thesis (see § 3.2.1.2).

2.4.1 Analytical approaches

The flow rate through a flow path also referred as to airway configuration, depends on the opening areas in series and parallel (§ 2.4.1.3), the discharge coefficients (flow resistance) of the openings (also § 2.4.1.3) and the pressure differences (see driving forces § 2.2.1). A flow path configuration may range from only one opening

for single-sided ventilation up to multiple external and internal openings of different size, height level, and orientation. Simple analytical equations presented here cannot reflect all but some of the more simple configurations.

2.4.1.1 Cross ventilation

Simplified empirical formulae estimate the volume flow rate of a single opening dependent on the effective area. The basic equation for the volume flow can be expressed by:

$$\dot{V} = C_d \cdot A_{\text{eff}} \cdot \sqrt{\frac{2 \cdot |\Delta p|}{\rho_{\text{air}}}} \quad (2.11)$$

The pressure difference across an opening for combined wind Δp_w and buoyant Δp_b pressure differences may be evaluated by:

$$\Delta p = \Delta p_w \pm \Delta p_b = \left| \frac{C_{p,1} \cdot v_{z,1}^2 - C_{p,2} \cdot v_{z,2}^2}{2} \pm \frac{\Delta T}{\frac{T_{\text{in}} + T_{\text{ext}}}{2} + 273} \cdot g \cdot h_s \right| \quad (2.12)$$

It is assumed that the reference air density ρ_0 for wind induced pressure is the outside air density ρ_{ext} , and for the buoyant share the mean air density is from inside and outside $\bar{\rho}$. The solution (\pm) depends on whether the opening level on the windward side is located higher than that on the leeward side (-) or not (+).

With $A_{S,\text{eff}}$ as the effective area of the whole flow path (see § 2.4.1.3), the basic equation for the volumetric flow can then be expressed by:

$$\begin{aligned} \dot{V} &= A_{S,\text{eff}} \cdot \sqrt{\frac{2 \cdot |\Delta p|}{\rho_0}} = A_{S,\text{eff}} \cdot \sqrt{2} \cdot \sqrt{\left| \frac{\Delta p_w}{\rho_{\text{ext}}} \pm \frac{\Delta p_b}{\bar{\rho}} \right|} \\ &= A_{S,\text{eff}} \sqrt{\left| \frac{C_{p,1} \cdot v_{z,1}^2 - C_{p,2} \cdot v_{z,2}^2}{2} \pm \frac{\Delta T}{\frac{T_{\text{in}} + T_{\text{ext}}}{2} + 273} \cdot g \cdot h_s \right|} \end{aligned} \quad (2.13)$$

This equation can also be used to exclusively estimate wind induced flow or thermally induced flow by setting the respective shares to zero.

2.4.1.2 Buoyant ventilation

For the ventilation through identical lower and an upper openings as shown in Figure 2.24, the pressure drop on each is assumed to be the same, but acting in opposite directions. With the same effective opening area, the height in which the pressure gradients intersect (i.e., the NPL) is midway between the two openings [26]. If two openings on different heights are differently sized and with a temperature difference between inside and outside, the resistance of the bigger opening is smaller than for the smaller opening. To fulfil the mass conservation (inflow = outflow), the pressure drop around the bigger opening must decrease compared to the smaller opening until the mass flow equalises on both openings. The Neutral Pressure Level (NPL) here moves towards the bigger sized opening [26].

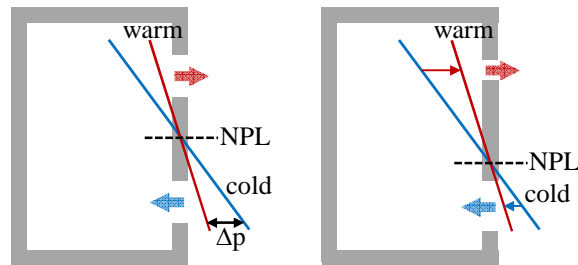


Figure 2.24: Pressure distribution and NPL for two openings buoyant flow with the same and different opening areas.

The volumetric flow can be assumed with the same equation as that for cross ventilation by setting wind pressure share to zero. The flow rate may be estimated by the following equation (again, $A_{s,eff}$ is described in § 2.4.1.3):

$$\dot{V} = A_{s,eff} \sqrt{2 \cdot \frac{\Delta T}{\frac{T_{in} + T_{ext}}{2} + 273} \cdot g \cdot h_s} \quad (2.14)$$

It is important to note again that differently sized openings influence the position of the NPL, which can be especially important in multi-storied buildings with a common flow path. The required ventilation rates of each level may be adapted (e.g., set equal) by sizing the openings depending on their height level. The sum of all inflows may balance the exhaust flow of a single high level opening, if the NPL is forced above the height of the highest inflow opening (sizing the exhaust big and high enough). The driving pressure at a low level here is much higher than on upper levels, and the openings should be sized accordingly (cf. Figure 2.25) [26].

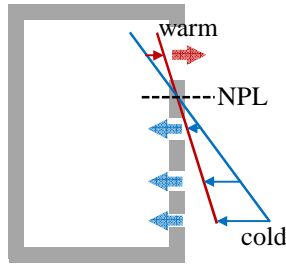


Figure 2.25: Pressure distribution and NPL for multiple openings buoyant flow with different opening areas.

The buoyant flow through a single opening such as a window is bidirectional as shown in Figure 2.1 (b). For cold ambient conditions, the warm room air exits at the upper part of the opening and the colder ambient air enters at the lower part of the opening. If the ambient air is warmer than the room air in summer conditions, the flow reverses. The flow direction changes at the height of the neutral pressure plane. The integration of the flow profile over the height results in a constant of 1/3 in the following equation, as only part of the window opening area A_{eff} is available as air inlet, and the neutral pressure plane is assumed at half the effective opening height h_{eff} level. Any influence of wind (e.g., due to turbulence) is not initially considered here. For single-sided ventilation with a single large opening, the flow rate caused by buoyancy can be expressed through the following equation [71]:

$$\dot{V} = \frac{C_d \cdot A_{\text{eff}}}{3} \sqrt{\frac{\Delta T}{\frac{T_{\text{in}} + T_{\text{ext}}}{2} + 273}} \cdot g \cdot h_{\text{eff}} \quad (2.15)$$

2.4.1.3 Flow path

A building can be regarded as a series of discrete cells connected to outside air and to each other by opening elements of the types discussed. Cells can be connected in series and in parallel. Together they form a flow path with a specific flow resistance, which for the whole airway can be described by a global effective opening area.

Opening discharge coefficients

The discharge coefficient of an orifice C_d is the ratio of the actual flow to the ideal flow without the effects of friction and flow contraction (flow resistance). According to the British standard BS 5925 [10], it is conventional to assign a value to the discharge coefficient, corresponding to that of a sharp-edged orifice. Typical values of sharp-edged external openings such as windows lie between 0,60 and 0,65

[26,32,72-74]. Previous research showed that the discharge coefficient of an opening did vary to some degree with Reynolds number, but only little variation was detected with external large openings appropriate for building ventilation [73]. The current practice of using values obtained from laboratory tests under still-air conditions may not be appropriate when the ventilation is influenced by wind. There are several wind tunnel investigations that show C_d varying with wind direction (e.g., [75]). The value taken in the BS is 0,61, which is also the value used further in this work.

For internal openings in partitioned buildings, which are much larger than the external openings, the discharge coefficient is close to 1 [76], because if the rooms are connected by very large openings, they effectively form a single zone.

Flow path resistance (total effective area of a flow path)

For multiple openings in a flow path, a global effective area $A_{S,eff}$ including the discharge coefficients has to be calculated for the entire flow path.

For openings in a parallel arrangement, the effective opening surface area $A_{P,eff}$ is obtained from the sum of discharge coefficients and area products:

$$A_{P,eff} = C_{d,1} \cdot A_{eff,1} + C_{d,2} \cdot A_{eff,2} + \dots + C_{d,n} \cdot A_{eff,n} \quad (2.16)$$

For openings in serial arrangement, the effective surface $A_{S,eff}$ is estimated as follows:

$$\frac{1}{A_{S,eff}^2} = \frac{1}{A_{P,eff,1}^2} + \frac{1}{A_{P,eff,2}^2} + \dots + \frac{1}{A_{P,eff,n}^2} \quad (2.17)$$

2.4.1.4 Example calculations and EnergyPlus validation

The analytical calculation methodology described has been validated against the widely recognised building energy simulation software with integrated AFN EnergyPlus [1]. The relative deviation of the simulated flow rates with same opening configuration and fixed boundary conditions as in the examples before is 3,2% for the single-sided ventilation scenario and 0,04% for the cross ventilation scenario. The validation methodology can be found in another article by the author of this thesis [77].

2.4.1.5 Ventilative potential

The potential of natural ventilation for different openings and room geometries were originally analysed in the context of a different study by the author of this thesis, and published in ‘Energy and Buildings’ [77]. Here, the term ‘ventilation potential’ is utilised, as the flow rates are not only dependent on the size of the openings, but also on the ventilation strategy including flow resistances and the achieved pressure differences from buoyancy and wind with fixed boundary conditions.

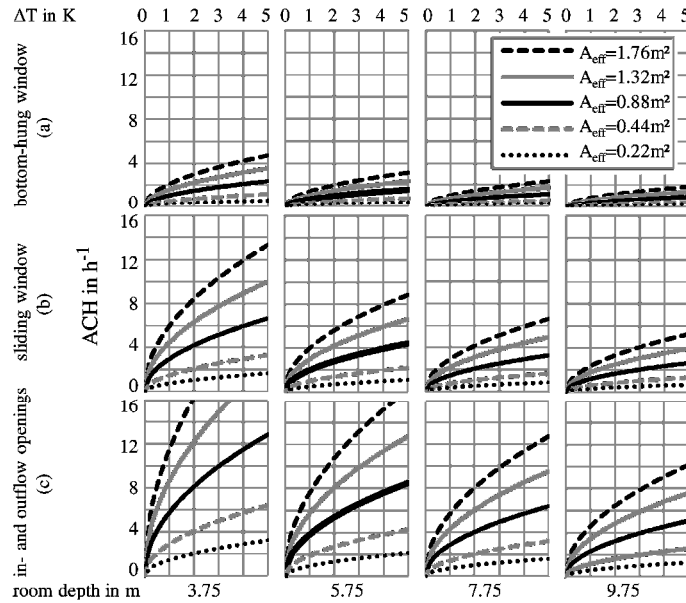


Figure 2.26: Analytical results of a variant matrix for single-sided ventilation with small temperature differences between room and ambient air. The base-case is a room depth of 5,75 m and 2,8 m ceiling height with a total effective opening area of 0,88 m² (3% of the net floor area).

2.4.2 Airflow networks

Airflow Network (AFN) simulation models have been developed to quickly solve the airflows and contaminant distributions in buildings. Buildings are represented by well-mixed zones, assuming a uniform temperature and contaminant concentration, connected by airflow paths. Air momentum effects are neglected. The flow calculation is based on the assumption that indoor airflows reach steady state at each timestep. Multizone airflow network models can simulate several airflow components i.e., cracks, ducts, duct fittings, fans, flow controllers, vertical and horizontal large openings (windows, doors and/or staircases), and passive stacks. AFN consists of a set of nodes linked by such components and represents a simplified airflow model. The flow elements correspond to openings and calculate the airflow rates; buoyancy flows are calculated by air density differences. Mathematically, matrix equations are constructed and numerically solved using the

Bernoulli equation. Convergence is reached when the sum of all mass flow rates through all components of a flow path converges to zero.

AFNs are often coupled to thermal dynamic simulation models to evaluate the whole building performance, including the thermal mass of building elements. EnergyPlus contains such a fully integrated network model (primarily COMIS [69], then replaced by AIRNET/CONTAM [67]) for calculating building airflows and their impact on building energy use as described in § 3.3.1.2 and by J. Huang *et al.* [78]. Other examples for AFN integration into Building Energy Performance Simulation (BEPS) are ESP-r, LESOCOOL and TRNSYS. Different coupling approaches such as the onion and ping pong coupling are possible [79].

However, AFN models are based on assumptions and simplifications [80] and the local air velocities in rooms cannot be computed. Pseudo steady state AFN simulations were compared with analytical models with very good agreement [77]. Johnson [81] compared the predicted airflows from different AFN models against measured airflow from laboratory experiments. The different simulation programs yielded similar predictions, which are within 30% error for the simple cases evaluated. Care must be taken in case of single-sided ventilation with relative strong wind, since the AFN calculations do not consider the turbulent air exchange as reflected in BS 5925 [10].

2.4.3 Computational fluid dynamics

Computational Fluid Dynamics (CFD) methods provide numerical solutions of the partial differential equations governing airflow and related physical processes. Solving the Navier-Stokes equation in a fluid domain, the technique is particularly suited for air movement and contaminant distribution analysis in [26,82] and around [83,84] buildings. CFD allows the airflow patterns inside a ventilated space to be analysed in great detail, but computation effort is extensive. Detailed information can be visualised for air velocity, and temperature and pressure distribution at each point of the zone. This provides the user with a vast amount of information, and it is theoretically possible to know the temperature, and the flow and concentration fields throughout the whole area of interest with the desired spatial and time resolution. The geometrical domain under analysis is subdivided into a large number of small cells (typically from some thousands up to some millions) over which the equations

of conservation of mass, energy and momentum (and, if needed, of any scalar of interest) are written, discretised and iteratively solved.

Usually, commercially available CFD codes as well as user-developed tools are capable of performing both steady state and transient analyses and special subroutines are frequently included in order to take into account a wide variety of other physical phenomena, such as particle settling and thermal radiation. Some CFD codes that use unstructured grids can also handle very complex geometries.

However, CFD simulations are also much more time-consuming than a multi-zone approach. Because of limitations in computer power, in practice it is not possible to simulate a whole building with a large number of rooms. CFD is therefore more suited to produce ‘snapshots’ of how a design would work at a certain moment. Given the long calculation time and the high dependency on boundary conditions, CFD simulations are usually only applied at a detailed design level to verify indoor comfort [26].

Thermal domain and detailed airflow domain simulation can also be coupled to achieve better results by providing boundary conditions. For instance, a BEPS program can provide building heating/cooling load and interior surface temperatures of building envelopes to CFD as boundary conditions, while CFD can determine surface convective heat fluxes for BEPS.

2.5 Previous Research Projects on Natural Ventilation

2.5.1 PASCOOL (1992-95)

2.5.1.1 Introduction

The PASCOOL project [85] investigated the tools necessary to promote passive cooling in buildings. Based on this, design tools and design guidelines for passive cooling of buildings were developed. The project operated from late 1992 to 1995 and was funded in part by a sub-programme (energy conservation and utilisation) of the European non-nuclear energy programme JOULE II.

2.5.1.2 Results

The LESOCOOL tool

The 16 bit Windows program LESOCOOL [86] developed by the Solar Energy and Building Physics Laboratory of the EPA in Lausanne, was intended for the pre-design evaluation of natural or mechanical ventilative cooling potentials. It is a simplified multi-zone ventilation simulation model in combination with heat storage and heat transfer. Limitations are that it allows simulation only for a single flow path without branches, and also that the thermal model is based on infinitely thick walls. The required input parameters are the wall first layer material and surface, the position and dimensions of the openings, and the time schedules for heat gain, ventilation, and external temperature.

The PASSPORT-AIR tool

The software Passport-Air [86] complements LESOCOOL as a network model for airflow calculations. It was developed to calculate the airflow rates in naturally ventilated buildings.

The CpCalc+ tool

The tool CpCalc+ [87] is based on empirical data from wind tunnel experiments, and allows the calculation of pressure coefficients on buildings. This C_p -generator (based mostly on interpolation and extrapolation of measured data) was developed because Passport-Air relies on wind pressure coefficient distribution on surfaces as the inlets and outlets for cross ventilation.

2.5.2 IAE Annex 28: Low Energy Cooling (1993-97)

2.5.2.1 Introduction

The objective of the IEA Task 28¹ was to provide design tools and guidelines on the application of low energy cooling strategies. Besides the ventilative night cooling for commercial buildings, other technologies were also addressed but will not be reviewed here. Outputs of the IEA annex include technology reviews, technology selection guidance, tools for early and detailed design, and case-study descriptions. The detailed design tool NiteVent was finally published within the NatVent study, and is presented in Section 2.5.4.2.

¹ <http://www.ecbcs.org/annexes/annex28.htm#p>

2.5.2.2 Results

Climatic considerations

Even the technology review [88] states that hot or moderate climates with large diurnal temperature swings between day and night over summer are best suited for ventilative night cooling. The technical synthesis report [89] claims that ventilative night cooling is appropriate for moderate climate conditions in which high mid-day dry-bulb is not common (e.g., usually $< 31\text{ }^{\circ}\text{C}$), whereas the technology selection guidance [90] indicates hot climate ($\text{SDT}^2 > 28\text{ }^{\circ}\text{C}$ and $\text{SNT}^3 > 20\text{ }^{\circ}\text{C}$) as low feasible, warm climate ($\text{SDT} > 28\text{ }^{\circ}\text{C}$ and $\text{SNT} < 20\text{ }^{\circ}\text{C}$) as low suitable, and cool climate ($\text{SDT} > 28\text{ }^{\circ}\text{C}$ and $\text{SNT} < 20\text{ }^{\circ}\text{C}$) as medium suitable.

The technology review states that the humidity ratio of the air should be less than 15 g per kg dry air since the technology primarily provides sensible cooling. The technology selection guidance declares all humidity levels from humid ($\text{MC}^4 > 14\text{ g/kg}$) to dry as medium suitable.

Thermal mass application

To increase the storage performance and to provide the desired daily cooling cycle, the thermal mass of the building must be in direct contact with the cool night ventilation air. The mass should therefore not be isolated by lightweight finishes, such as dry lining or suspended ceilings. It has been found that any thickness of dense concrete greater than about 50 mm has very little effect on the diurnal temperature cycles, although these larger thicknesses may become significant in weekly or seasonal variations.

Cooling load and heat gain limitations

Simulations indicated that depending on the climate and building, ventilative night cooling is capable of providing cooling for up to 40 W/m^2 of internal heat gains. On an average, night cooling will offset $\sim 20\text{-}30\text{ W/m}^2$ of heat gain for heavy-weight constructions. Therefore the technology is capable of satisfying only moderate cooling loads. Beside the provision of accessible thermal mass, ventilative night cooling should be planned in combination with good thermal insulation to the building envelope and also together with external shades over windows as they are

² SDT summer peak design temperature

³ SNT summer night minimum design temperature corresponding to summer peak design temperature

⁴ MC summer design moisture content

crucial in preventing higher solar heat gains. To minimise the internal heat gains, low energy appliances and their smart control, and taking advantage of natural daylighting are important. Moreover, it was indicated that the most appropriate application is in buildings which are unoccupied during night-time, with regular cycles of heat gains.

Comfort assessment

Computer simulations indicated that night-time ventilation can reduce the daytime peak temperatures in heavyweight buildings in the order of 2-3 °C; but controls are needed to monitor the outside and indoor conditions to prevent from overcooling and discomfort in the early morning hours. Also, as cooling occurs, the relative humidity should be maintained at less than ~ 60%. Thus, in humid climates care must be taken not to bring in too much moisture at night which would cause discomfort during the following day.

Air change rates

Night-time ventilation is particularly suitable for commercial buildings that remain unoccupied at night and where high airflows can be used. Typical night air change rates needed for cooling are between 5-20 ACH. The daytime ventilation rate needs to be minimised to the rate needed for IAQ requirements when the outdoor air temperature is greater than the thermal mass surface temperature.

Control algorithms

In the description of the detailed design tools [91], three night cooling control algorithms for commercial buildings have been identified: the setpoint control, the slab temperature control, and the degree hours control.

In general, night ventilation should be initiated if the peak zone temperature is above 23 °C, and/or the average daytime zone temperature is above 22°C, and/or the average afternoon outside air temperature was above e.g. 20 °C and/or the slab temperature is above 23 °C.

Night cooling should continue if the zone temperature is above the outside air temperature (for natural ventilation), and the outside air temperature is above 12 °C (to prevent any risk of condensation).

If setpoint controlled, the zone temperature may drop at night to 16 °C before the vents close. Once this has occurred, the building will then slowly increase in

temperature due to heat gains re-emitted from the building fabric. The vents remain shut until the second hysteresis setpoint (e.g., 19 °C) allows opening again. This alternating cooling and heating process continues until such time as the ‘preheat’ period is reached. The preheat period is the time at which the inlet and outlet vents must shut in order that the space reaches the heating setpoint (e.g., 19 °C) by the start of occupation without overcooling the building. In the preheat period, the radiative and convective heating rates may be calculated in order to predict if the desired occupancy temperature will be reached in the morning hours even if the openings remain open. Although it is not anticipated to occur, the heating system should be enabled to ensure that any overcooling will not affect the comfort conditions.

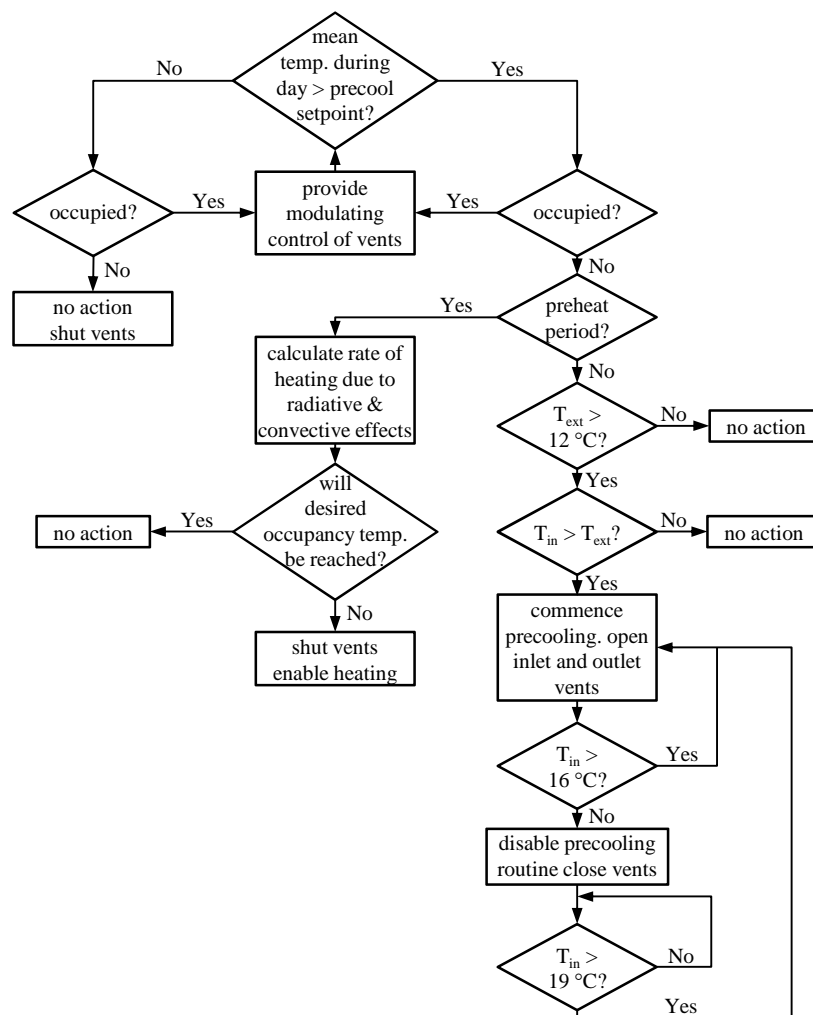


Figure 2.27: Control Strategy 1 - Setpoint Control [91].

The precooling strategy to cool the slab to a predefined slab temperature setpoint during the night is described for a hybrid ventilation strategy. The mechanical ventilation system may briefly assist the natural ventilation if the low night

electricity tariff may be exploited and the slab temperature setpoint is not reached. The calculation of slab temperature setpoint is self-learning, and is based on equalising the slab temperature, the room temperature, and the slab temperature setpoint. An adjustment factor is provided in order that a cooling effect is still available from the slab towards the end of the occupancy period. If at a certain time of the night the slab temperature has not achieved the slab setpoint, the time is calculated so that fan -assisted cooling is enabled to achieve the slab temperature setpoint. This calculation is based upon the difference between the internal and the external temperatures, and the rate of change of the slab temperature using fans under these conditions. For mechanical or hybrid ventilation, cooling benefits must be balanced against the use of fan energy and the temperature shift of the incoming air due to the fan induced heat gains.

The degree hours control strategy aims to calculate the daytime heat gains and the cooling gains at night to maintain equilibrium. The decision as to precool or not is based upon the number of hours that the internal temperature is above the room temperature setpoint. If at the end of the occupied period the degree hours are greater than 3, then the night precooling is activated. The openings then modulate to maintain the space temperature at the precool setpoint (e.g., 18 °C) till the degree hours of night cooling gains are equal to those of the daytime heating gains. The control system also calculates the time to raise the space temperature back to the comfort setpoint by the start of occupation period. It may then terminate the night ventilation before the equilibrium between the building fabric temperature and the space temperature of the next day is reached.

2.5.3 AIOLOS (1993-97)

2.5.3.1 Introduction

The European-funded project AIOLOS has been coordinated by Mat Santamouris and involved experts in numerous European countries. The project was carried out within the framework of the ALTENER Programme, which focused on the promotion of renewable energy sources of the European Commission. The goal of the project was to create educational material on the efficient use of passive ventilation. The project deliverables were published in the book 'Natural Ventilation in Buildings: A Design Handbook' [14]. An accompanying CD-ROM contains the

design performance evaluation AIOLOS software for the calculation of the airflow in natural ventilation configurations.

2.5.3.2 Results

Empirical methods

Eight simplified empirical methods for the prediction of the airflow rates [10,92-94] and the air velocity inside a building [95-98] are presented.

Airflow network model and experimental validation

The second approach is the network model (see § 2.4.2) where the building is represented by a grid that is formed by nodes (zones with a pressure value) and linkages (flow paths through openings). The mathematical approach is presented and results gathered from different simulation tools (AIRNET, ESP, BREEZE, PASSPORT-AIR, COMIS) were compared against each other and against the measured data.

Experiments were performed in Athens (single-sided ventilation), Lyon (cross ventilation) and Lausanne (stack driven ventilation).

For the single-sided scenario, all five network tools predicted very similar airflow rates. But the predictions were initially not in good agreement with the experimental values. It was found that the experiments were characterized by high wind speeds and small temperature differences, but the network modelling with PASSPORT-AIR neglected the wind effect in the case of single-sided ventilation. Therefore an additional algorithm was developed [99] and introduced via a correction factor to the model. This factor depends on a correlation between the Grashof number and the Reynolds number. The correlation coefficient between experiments and simulation then was close to 0,75.

The cross ventilation experiments with rather low wind speeds (~ 3 m/s) were carried out in two rooms connected by a door and with sliding windows on opposite, sheltered facades. Simulations were realised using the COMIS model, and measured wind speed was modified by a wind profile model [100] for the calculation of local wind speed at the level of the windows. The value of the external discharge coefficient of the windows was taken to be equal to 0,85, while the internal door discharge coefficient was set at 0,65. The pressure coefficients at the two facades were calculated using a simplified model for low rise-buildings [100]. It was found

that that the AFN model estimated the flow rates reasonably well, but that inaccuracies in pressure and discharge coefficients caused notable error.

The stack driven experiments were carried out in the LESO building for six different, relatively simple flow paths and different temperature differences. The building's staircase here acts as an up to 12 m high chimney. Simulations were carried out with the absence of wind using PASSPORT-AIR. The internal door connecting the office with the staircase was open. All discharge coefficients were set at 0,7. The comparison of measured and predicted airflow rates showed good agreement.

Methodologies for sizing openings

The methods described for sizing openings are based on simplified empirical methods or on computerized iterative AFN methodologies. Five empirical methods and one AFN method are discussed. By estimating the opening area, a certain airflow rate is targeted. Calculations are performed with unchanging driving forces, which are the local prevailing wind speed and direction or the mean expected indoor-outdoor temperature difference. They do not reflect the thermal mass of the building, the climatic region, the comfort criteria, and the solar and internal heat gains; they also do not give recommendations about the desired airflow rate. The empirical methods treat the building as only one zone without internal resistance.

Two empirical methods developed by the Florida Solar Energy Centre calculate the window area for cross ventilation with a design wind speed from the closest weather station, which is then adapted for the local wind speed. The first method [101] calculates the gross window area including 20% framing and screening with a porosity of 0,6. The method proposes correction factors for the wind incidence angle, the terrain, the wind shielding by neighbouring buildings, and the floor height (only ground or first floor). The second method [102] introduces pressure coefficients from a simple table, which replace the factors for the wind incidence angle and the terrain. The inlets and outlets may be designed here in different size. Also the porosity of the windows can be adapted by choosing from different insect screens and window types.

A very simple method proposed by ASHRAE [103] is also discussed, which can be used for wind or temperature driven ventilation, but not for a combination. If the flow is mainly due to wind, and the openings are sized equal, the area is a product of the design flow rate, the local wind speed, and a factor that accounts for the

effectiveness of the opening based on the wind direction. If the airflow is mainly due to the temperature difference, the area may be calculated from the design flow rate, height difference between inlets and outlets, and the temperature difference. If the inlets and outlets are not equal in size, then the percentage of the desired flow may be increased according to a diagram.

The Aynsley [93] and the British Standard (BS) methods [10] both estimate the surface area of the openings for wind-driven ventilation based on the same equation:

$$\dot{V} = v_z \sqrt{\frac{(C_{p,1} - C_{p,2})}{\frac{1}{A_1^2 \cdot C_{d,1}^2} + \frac{1}{A_2^2 \cdot C_{d,2}^2}}} \quad (2.18)$$

The BS-method in addition proposes an expression to calculate the opening sizes due to buoyancy:

$$\dot{V} = C_d \cdot A_s \sqrt{\frac{2 \cdot \Delta T \cdot g \cdot \Delta h}{\frac{T_{in} + T_{ext}}{2} + 273}} \quad (2.19)$$

where:

$$\frac{1}{A_s^2} = \frac{1}{A_1^2} + \frac{1}{A_2^2} \quad (2.20)$$

Additionally the BS-Method provides criteria to define whether the flow is mainly due to wind pressure or buoyancy (see also § 2.6.1).

The sixth method described is based on computerized network simulation. Openings can be sized by realizing a sensitivity analysis to study the relative impact of the design characteristics (e.g., the opening areas and their location). AFN models are capable of calculating combined thermal and wind pressure differences; they can also model multi-zone buildings with internal openings (flow resistances). This method therefore overcomes some of the limitations of the empirical methods.

AOILOS tool

The dynamic, airflow network (AFN) modelling based AOILOS software is focused on the calculation of airflow rates in multi-room buildings for a run period of up to 30 days. It is suitable for the calculation of airflow rates in each simulated room zone

and also for calculating the airflow through each opening involved. It allows the users to perform sensitivity analysis for the investigation of the impact of specific parameters. It includes an optimization process for the opening sizing in terms of optimum airflow rates. The openings are controlled (open or closed) by user-defined schedules, which are the same for each day in a given simulation period. It also includes a single zone thermal model for the whole building. This allows the assessment of the impact of the chosen ventilation strategy on the thermal behaviour of the building. The program first calculates the global airflow rates of the building with a given internal air temperature. These values from the first module are then provided to the thermal module, which calculates the cooling loads and the thermal comfort with a fixed design temperature. Comfort is calculated by means of the temperature excess method in degree hours.

2.5.4 NatVent (1994-98)

2.5.4.1 Introduction

The NatVent project was a seven nation pan-European project aiming to reduce primary energy consumption of office type buildings in urban areas. Like PASCOOL it was partly funded by the European Commission JOULE program, and was targeted at countries with low winter temperatures and moderate summer temperatures.

The work was divided into three work packages (WP). The first work package identified the barriers that prevented the uptake of natural ventilation, based on interviews with leading designers, architects, and building owners and developers. The second work package evaluated the performance of 19 existing and naturally ventilated low energy buildings. Temperature, humidity, carbon dioxide and ventilation rates were measured during both winter and summer periods to determine the shortcomings and advantages of different strategies. In the third work package, 'smart' technology systems and component solutions were investigated to overcome the identified barriers. This included passive air supply components for use with high external pollution and noise loads, 'smart' constant air inlets for IAQ and thermal comfort, heat recovery systems with acceptable energy consumption, and especially 'smart' systems integration for optimum year round performance.

2.5.4.2 Results

Barriers

Conclusions from the interviews of 107 designers and decision makers in the final perceived barriers report [104] show that the interviewees showed a lack of knowledge about ad hoc designed natural ventilation compared to what they knew about mechanical ventilation. But it was also indicated that they worked with traditional natural ventilation. The interviewees noticed that there were only few available good sources of information (e.g., natural ventilation guidelines) for products especially when compared to those pertaining to mechanical ventilation systems. They expected the same level of user satisfaction for naturally and mechanically ventilated cellular offices, but less for open plan offices. In contrast, they expected mechanical ventilation systems to perform better with regard to cooling effectiveness, draught minimisation, ability to remove and prevent ingress of odours, and insulation against external noise. Most interviewees expected much lower installation, running and maintenance costs for passive ventilation than for mechanical ventilation. If mechanical systems were installed, they would have to account for a significant proportion of the total costs of the building.

Recommendations included the development of simple, energy efficient, low-cost natural ventilation system concepts. Standards and guidelines must be developed so that there is a more favourable technical and legal framework for naturally ventilated office buildings. Simple design tools like diagrams or easy-to-use computer programmes have to be developed. Components and control systems for natural ventilation, and the general knowledge need improvement.

Experiences from the monitored buildings

The final performance monitoring report [12] from WP2 stated that the measured CO₂ levels in most of the 19 buildings were acceptable, but eight buildings suffered from serious overheating problems, which was the most common user complaint. On the contrary, studies on several buildings proved that it was indeed possible to achieve an acceptable thermal summer comfort without mechanical cooling. A clear distinction between natural ventilation for IAQ and summer comfort is essential to avoid confusion. Natural ventilation for IAQ aims to control the indoor air quality during office hours with a rather low air change rate from 0 to 1,5 ACH, since large

ventilation flows mean large energy losses. Advanced control strategies instead of manually opening windows were found to considerably reduce ventilation losses.

In contrast, to achieve good thermal comfort in summer, the airflow rates should be controlled as high as possible if the internal temperature is warmer than the external temperature. In addition, accessible thermal mass is required. The optimum solution is found in buildings with exposed heavy ceilings, floors and walls. Exposed ceiling or (half) open lowered ceiling also achieves acceptable results but not optimal. Recommended airflow rates without specific problems (from 5 to 10 h⁻¹) aim cooling down the thermal mass of the building especially at night. Monitoring the results showed that the control of airflow rates for summer comfort is in most cases not as critical as it is for IAQ ventilation. Automatic control has the possibility of optimizing the opening and closing, but it is recommended taking a relatively simple and stable control, as a detailed study [16] of different control algorithms showed the impact of the control strategy as limited. Undercooling during the early morning hours should be avoided. During the office hours, it is preferable that the users can overrule the automatic control. But if the openings are controlled manually, it is essential to provide a clear instruction for the use of the ventilation openings, also in combination with the shading devices, the lights, and the radiators.

Another key message from the monitoring report is that summer comfort requires much more than just intensive ventilation. In many of the monitored buildings, there was a problem of overheating due to very high solar gains. The recommended design elements to control solar heat gains are shading devices, and the intelligent choice of glazing type surfaces and orientation. A high insulation level can limit indirect solar gains through opaque surfaces. Low energy equipment and well-controlled lighting systems can minimise the internal gains.

Control strategies and opening sizing

In WP 3.4, two methods for the calculation of effective vent opening areas were developed for the early stage of design [16]. They were based on a comprehensive parametric analysis carried out with an ad hoc developed SIMULINK dynamic thermal and ventilation network tool. The aim was to investigate the control strategies and the required ventilation opening area for a representative three zone office model with two office zones (22 m² each) and a corridor (9 m²). Simulations were carried out for single-sided, cross and stack ($h_s = 5$ m / exhaust fan-assisted)

ventilation. The comfort criterion was evaluated by the temperature excess method. No more than 100 hours in a year with indoor temperatures above 25,5 °C, and no more than 15 h above 28 °C were accepted. The effective opening area is dependent on the opening angle of the window (calculation according to § 2.2.3.1). The weather data represented the months May till September, and was from De Bilt in the Netherlands from 1964. Parameters investigated were the building orientation, mass (low = 55 kg/m², medium = 75 kg/m², high = 100 kg/m²), internal heat gains (20 to 40 W/m²), solar gains (different shades and window areas) and the control strategy. The area density of the thermal mass is the sum of half the weight of the side walls, the back wall, the floor and the ceiling, and the entire weight of the façade, divided by the net room floor area. The control during office hours (8 am till 6 pm) tries to keep the room air temperature at the cooling setpoint (22 °C) when $T_{in} > T_{ext}$ and $T_{ext} > 12$ °C. It was shown that the various predictive night control strategies proposed in literature produce nearly the same results (Figure 2.28) and concluded that the setting of the control parameters was more important than the strategy itself. The strategy used for further analysis was the predictive cooling day control, where if during the previous day vents were open for cooling, the night setpoint was decreased by 2 °C. The start value was 22 °C and the minimum was 18 °C.

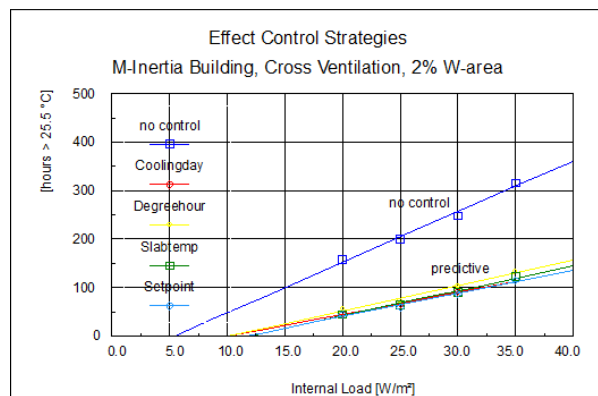


Figure 2.28: Effect of the control strategies [16].

The first method designed was an easy-to-use selection chart (Figure 2.29) to determine the ventilation system and effective opening areas that can be applied.

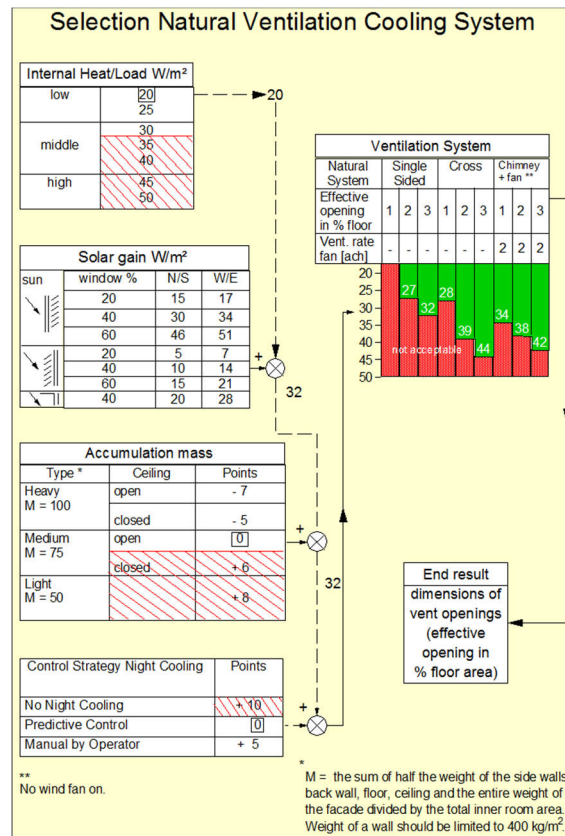


Figure 2.29: Graphical pre-design tool for night cooling [16].

The second method was intended also to calculate the effective opening area with similar inputs as in the graphical tool, but was based on simplified equations and could be used in a spreadsheet [16].

Controlled airflow inlets

The project conducted a market breakdown [105] in European countries for several types of air inlets, controlled by pressure differences, humidity, pollutants, and temperature. The purpose of pressure controlled air inlets is to maintain a constant airflow independent of wind and buoyant pressure differences, where pressure differences across air inlets are normally in the range of 1 to 20 Pa. An ideal constant airflow inlet gives a constant flow independent of the pressure difference, and can also compensate for increased airflow from leakage.

Besides the market analysis, the FlexNightVent prototype [106] was designed and tested with promising results for fresh air supply, but mainly focusing on night cooling. The cross ventilation design consists of a motorised trickle vent with sound attenuation for fresh air supply, a motorized window that could be set in any position for night cooling and a control unit for connecting the ventilator system with a building management system and for manual overriding. An optional presence sensor

saves energy in the heating season by closing the trickle vents. The ventilation openings were dimensioned by the method mentioned in § 2.2.3.1. The motorized window control for cooling is divided into three subroutines [107]. During occupation, no feedback control was applied because field tests showed that the inhabitants would not accept frequent adjustments. Therefore, a feedforward control (Figure 2.30) was applied, whose aim was to find a position that was most likely the best for the next period. Adjustments were dependent on the indoor air temperature and the time of the day, and were made in periods without occupation. Further, the opening area was decreased by a correction factor dependent on the external temperature to avoid the risk of draught.

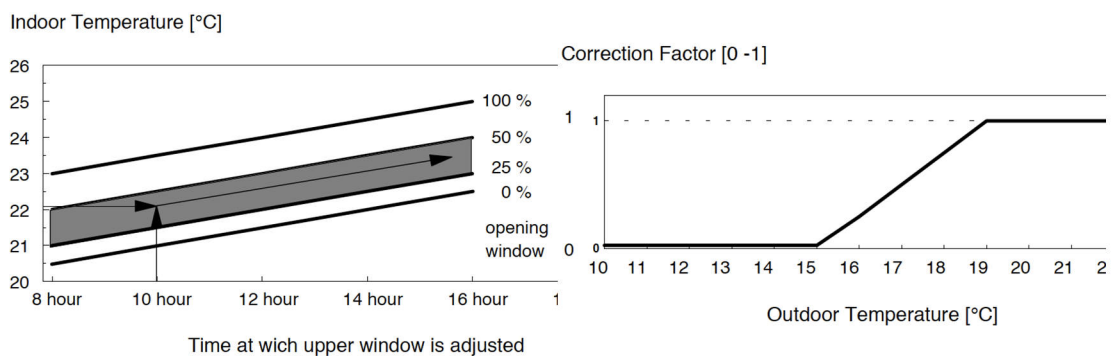


Figure 2.30: Feedforward control during occupied office time (source: [106]).

Without occupation, a self-adapting feedback algorithm is active, which tries to keep the temperature at the cooling setpoint. Without considering current comfort due to the absence of inhabitants, the window position is the result of a proportional integral algorithm divided by the temperature difference.

Night cooling was realised by the predictive cooling day control as mentioned above, but with a starting setpoint of 24 °C, which in the second night of operation was then decreased to 20 °C, and in the third night further down to 18 °C.

NiteCool tool

NiteCool [108] is an easy to use night ventilation pre-design tool especially developed for UK office buildings. It was programmed with the objective to keep the user input at minimum and to facilitate fast simulation time for the tool-integrated sensitivity analysis.

The tool combines heat transfer (third-order lumped-parameter method [109]) and ventilation and is based on a pre-configured single zone model with dimensions 10 m width, 6 m depth and 3 m height in the middle of a row of offices on the middle floor

of a 3-storey building. The building can be described by design options such as air tightness, orientation, solar control, glazing ratio, thermal mass, site location, and internal heat gains.

Dynamic simulations are either carried out for a month or over the cooling season from May to September. Internal temperatures are only simulated for seven days each month, and energy data is then multiplied by using factors. The hourly weather data is calculated from data in the CIBSE guide [110]. Sinusoidal external temperatures can be adapted for each weekday by editing the daily minimum (night) and maximum (day) temperatures or by setting percentage risk factors for excess temperatures.

It covers a range of natural ventilation strategies, which are single-sided single opening, single-sided double opening, cross ventilation, and stack ventilation (buoyancy and wind). To achieve certain airflow, openings for all strategies can be sized automatically by the inverse solver method [111,112] or by user-specifications of size and position. Default pressure coefficients can be edited.

It is possible to choose cooling systems for day and night separately. Besides the four natural ventilation systems described earlier, there are three mechanical ventilation and two active cooling systems available, which are characterized by their fan power, system performance, and setpoint temperature.

The tool allows the user to customise the control strategy of the night cooling system by setting operation times, system initiation rules (e.g., previous day peak, average or initial temperature for inside, outside, or slab) and system continuation to avoid overcooling.

Energy savings can be evaluated by setting a reference HVAC system (displacement ventilation or fan coil units), which is considered to be a standard solution with no night cooling. The setpoint can be a constant temperature or the program can choose a setpoint similar to the resulting internal temperature calculated for the low energy design strategy.

2.5.5 IAE Annex 5: AIVC (ongoing since 1979)

In 1979, the 'Air Infiltration and Ventilation Centre' (AIVC) started as the 5th IAE research project (Annex 5) in the context of the Energy in Buildings and

Communities Programme (EBC), running even today. Originally focusing on the energy impact of air infiltration in buildings, ventilation was introduced in the mid-80s as the interest moved towards indoor air quality concerns. Today, AIVC serves as a source of information (AIRBASE), holds annual conferences and workshops, publishes papers and reports, maintains a large database of publications, and shifted its focus to networking activities of multiple stakeholders. The centre also collaborates with the venticool programme (see § 2.5.7), focusing on ventilative cooling strategies in buildings.

Since its creation, the AIVC has produced a series of publications such as the guidebook ‘A Guide to Energy Efficient Ventilation’ [113], and the important and comprehensive book ‘Building Ventilation - The State of the Art’ [114].

2.5.6 IEA Annex 35: HybVent (1998-2002)

2.5.6.1 Introduction

Annex 35 HybVent ‘Hybrid Ventilation in New and Retrofitted Office Buildings’ was a worldwide research project with about 30 research institutes, initiated by the IEA Implementing Agreement ‘Energy Conservation in Buildings and Community Systems (ECBCS)’.

Targets of the project were the development of control strategies and performance predicting methods, the selection of measurement techniques, and the promotion of hybrid ventilation systems for offices and educational buildings.

These objectives were met by the production of various publications. The state-of-the-art report reviewed hybrid ventilation technologies, controls, and analysis methods. It identified barriers and the lack of knowledge, and contained a survey of 22 buildings. As a final product of the research project, the booklet ‘Principles of Hybrid Ventilation’ [50] was intended for newcomers. Several technical reports and research papers give detailed information on the topic.

The project was divided into three subtasks, each devoted to a specific area of interest. Subtask A focused on the development of control strategies. Subtask B emphasised theoretical and experimental methods for performance analysis. Subtask C investigated monitoring results of case studies. The buildings surveyed are low to medium-rise buildings, and the Meiji University Tower in Tokyo.

The International Energy Agency Annex 35 aimed to develop control strategies for hybrid ventilation systems for newly built and retrofitted office and educational buildings. Various control strategies for hybrid ventilation and their integration in building management systems were analysed [3], and different simulation tools were evaluated [115].

2.5.6.2 Results

Principles

Hybrid ventilation is defined as a two-mode system using both natural and mechanical ventilation [50]. It can switch between or combine these two modes to exploit the benefits of each mode while maintaining the desired airflow rate and airflow pattern. Hybrid ventilation systems all aim to provide fresh air for the IAQ aspects, and some also contribute to passive cooling for the establishment of thermal comfort in warm periods. An intelligent control system is intended to minimise the energy consumption and to provide acceptable indoor air quality and thermal comfort. Compared to mechanical ventilation and air conditioning systems, energy savings can be achieved mainly because of a very substantial reduction in energy use for fans and active cooling by using mechanical forces only when natural potentials do not suffice.

The mechanical systems in a hybrid-ventilated building can range from simple exhaust fans to balanced ventilation or even to full air conditioning systems depending on the climate, the building behaviour, and the comfort requirements.

In cold climate, the natural ventilation mode in a hybrid system most probably dominates the summer temperature control, while in warm climate the passive cooling potential is mainly exploitable in the intermediate season, and may assist active summer cooling by night ventilation [3].

The three main hybrid ventilation principles are:

- The natural and mechanical ventilations as two autonomous systems, where the control switches between the modes depending on the season or occupation of the building;

- The fan-assisted natural ventilation, where natural ventilation is combined with a supply or exhaust fan. Here the fan assists the system by enhancing the pressure differences during periods with weak natural driving forces or increased demands;
- The natural driving forces can partly account for the necessary pressure differences in wind-assisted and stack-assisted mechanical ventilation systems with low-pressure losses.

Controls

The ‘Principles of Hybrid Ventilation’ booklet [50] summarises the research findings and the lessons learned from the case studies [116] as follows: *‘The main challenge in the design of control systems for hybrid ventilated buildings is to find the right balance between implementation costs, operation costs, energy use, indoor climate, comfort, users’ satisfaction and robustness. The development of an “optimal” control strategy for a specific building will depend not only on technical parameters ... but also on parameters such as dress code, user attitudes and user expectations.’*

Manual versus automatic control

- Individual control should be maintained even if it can conflict with guaranteeing a specific level of indoor thermal comfort or air quality;
- During occupancy, automatic control is beneficial to support the user;
- Users are more tolerant with respect to thermal climate if controlled by themselves;
- Automatic control is required in times of non-occupation to save energy and to precondition the rooms;
- Automatic control is necessary to reset manual controls;
- Rooms occupied by several people (e.g., landscaped offices) need a higher degree of automation;
- Automatic control during working hours was discovered to be difficult for user acceptance due to high draught risks;
- The control strategy should be easy to understand by the users and by the maintenance staff;
- Users want rapid feedback of the system when they manually change the conditions.

Climate and season

- The control strategy should be separated in different modes for summer, winter and intermediate season;
- Winter control (during heating season) focuses on IAQ issues;
- Summer control (during cooling season) concerns the maximum temperature;
- Intermediate season control occasionally switches between IAQ and temperature concerns;
- The control strategy is strongly influenced by the climate;
- In cold climate the control concentrates to minimise energy consumption for fresh air supply and to achieve good thermal comfort in summer without mechanical cooling;
- In warm climate the strategy should focus on reducing the energy consumption for mechanical cooling in summer.

IAQ control during occupancy

- Flow rates for IAQ can be either controlled manually by the occupants, time control via a schedule, presence detection, IAQ measurement or by a combination of these;
- CO₂ sensors indicate IAQ where people are the governing pollution source;
- In small rooms with few people, the users are capable of controlling the IAQ manually;
- For large rooms (e.g., landscaped offices) with many people and for occasionally used rooms (e.g., meeting room), automatic IAQ control is necessary;
- Energy consumption for IAQ control can be reduced by limiting the operating hours and the ventilation rate according to the occupancy pattern;
- Good user control in combination with automatic back up based on IAQ is the optimum strategy, but might be expensive.

IAQ control during non-occupancy (only for tight buildings)

- Necessary to remove build-up pollution from day;
- Necessary to supply fresh air before occupation;
- Necessary to remove pollution from materials and cleaning.

Temperature control during occupied hours in summer

- Manual control in small rooms is possible because people do have a clear sense of their own thermal comfort;
- May only have a limited cooling potential, if ΔT between T_{in} and T_{ext} is small;
- High air change rates can assist the body cooling potential (evaporation chill);
- Ventilation may increase T_{in} , if $T_{ext} > T_{in}$;
- In combination with automatically controlled mechanical cooling, there is a risk that once activated the system will stay in active mode;
- Automatic control is necessary if the mode is mechanical cooling and/or ventilating.

Temperature control during summer nights

- Is very important to achieve thermal comfort in buildings without mechanical cooling;
- Is very important to reduce energy consumption in buildings with mechanical cooling;
- Aim is to cool down the building structure as much as possible without creating discomfort at the start of occupation;
- It is possible but not recommended to manually control night ventilation (only if the users receive clear and easy-to-understand instructions);
- Can be established for a room or can be central for a group of rooms or for the entire building;
- If a representative room is chosen to control several rooms, the room selection is of great importance;
- If mechanical ventilation is on, the cooling potential (depending on ΔT) must be weighed against the fan power consumption.

Additional control systems

- The supply air may be preheated to reduce the risk of draught (even when cooling is needed) based on temperature control (T_{ext}) but should be treated separately from the room heating;
- During severe weather conditions (e.g., storm, rain) normal controls must be overwritten by closing the windows and raising the external sunshades;

- Sunshades should be user overwritable, automatic controlled based on solar radiation intensity on the façade.

A technical report on advanced control strategies [117] introduces different strategies briefly, stating that the performance of control is particularly sensitive to the quality of sensor information, the efficiency of actors, and the quality of controls to meet the objectives of the system. The advanced controls listed are (1) rule based control, which is most frequently implemented in Building Energy Management Systems, (2) the optimum and predictive control, (3) neural networks, and (4) the fuzzy logic control.

Rule based controls can simultaneously browse and control several parameters, and they are based on e.g., IF, OR, AND, THEN commands. The definition of rules depends on expert knowledge, and is a good opportunity for combined control of mechanical and passive components. Figure 2.31 exemplarily shows a rule based control over the room air temperature control based on a hybrid strategy taking control over active heating and cooling, mechanical and natural ventilation, active heating, and controlled solar shading devices.

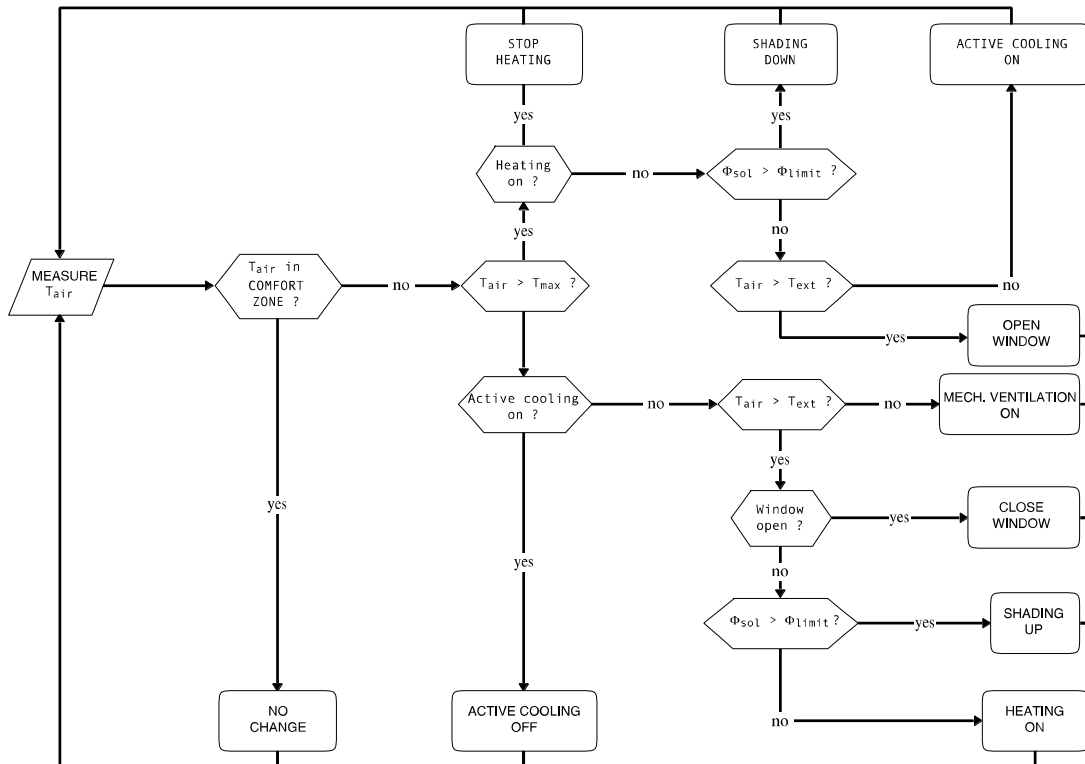


Figure 2.31: Rule-based control of indoor air temperature (mixed-mode example) [117].

At the time of the report, optimum and predictive controls were not widely implemented as no industrial development followed the scientific research. Optimum control is based on a mathematical model of the system to be controlled such that certain optimality criterion is achieved. It deals with finding a control law for a given system via differential equations describing the cost paths of the variables that minimises the cost function (in the context of hybrid ventilation, it is the balance between energy and comfort). Model predictive control includes a forecast of external, climatic variables based on a statistical analysis of meteorological data gathered, or on the weather forecast. This control is very effective for improving night ventilation and to avoid overcooling in the morning hours due to time-shifted heat exchange of thermal mass.

Early stage design tool

Fracastoro *et al.* [118] developed a simple tool to assess the feasibility of hybrid ventilation systems in the early stages of building design. The procedure aims to determine suitable ventilation design from a few known building parameters and the local climate data for the heating season. It includes a statistical prediction technique for estimating the relationship between two variables, where regression analysis is applied. The efficient pressure difference among the envelope as a function of the temperature difference between inside and outside, and the wind speed was found using the AFN simulation engine COMIS [69]. These two parameters again depend on the building typology and surrounding terrain.

The procedure is to first calculate the frequency distribution of pressure difference across the envelope for each hour with typical weather data TRY [119]. In the second step, the required minimum effective pressure difference, depending on a typical building tightness value, is determined to achieve a certain air change rate as a function of the building's envelope area and gross volume. Next, the time percentage for which the required ventilation rate will be satisfied by natural ventilation can be evaluated. Finally, if the time percentage by natural ventilation is too low, the permeability should be increased by additional openings, or a mechanical system should be introduced, or both these options should be employed.

2.5.7 IAE Annex 62: Venticool (ongoing 2014 - 2017)

The IEA Energy in Buildings and Communities programme (IEA EBC) recently approved Annex 62 Ventilative Cooling ‘Venticool’. This new Annex is an ongoing worldwide research project with about 13 countries participating from Europe, Japan, China, and the US. It refers to the new challenges in design and construction towards nearly-zero energy buildings, and the increased need for cooling in highly insulated and airtight buildings. Focusing on energy efficient ventilative cooling solutions, the research aims to develop design methods and tools to predict, evaluate and eliminate the risk of overheating in buildings. One of the objectives of the ‘IEA ECBCS Annex 62 Ventilative cooling’, started in 2014, is to give guidelines for integration of ventilative cooling in energy performance calculation methods and regulations (e.g., DIRECTIVE 2010/31/EU [7]).

2.6 Regulatory Framework

Buildings greatly contribute to the climate change, since 40% of the energy is used in buildings. With the Energy Performance Buildings Directive (EPBD) DIRECTIVE 2010/31/EU [7] the European Union has set ambitious goals to improve the sustainability of the built environment. The aim is to move towards new and retrofitted nearly-zero energy buildings by 2020, and by 2018 in the case of public buildings. It also targets the application of a cost-optimal methodology for setting minimum requirements for both the envelope and the technical systems.

Article 9 requires that *‘Member States shall ensure that by 31 December 2020 all new buildings are nearly zero-energy buildings; and after 31 December 2018, new buildings occupied and owned by public authorities are nearly zero-energy buildings’*. Member States shall furthermore *‘draw up national plans for increasing the number of nearly zero-energy buildings’* and *‘following the leading example of the public sector, develop policies and take measures such as the setting of targets in order to stimulate the transformation of buildings that are refurbished into nearly zero-energy buildings’*.

Building airtightness and energy efficient ventilation systems will implicitly become a mandatory point of attention. The usage of natural ventilation to improve thermal

comfort and/or reducing cooling need (ventilative cooling), and to assure indoor air quality will significantly increase.

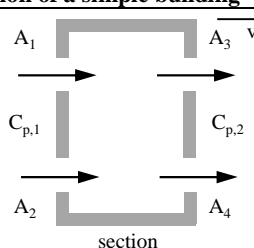
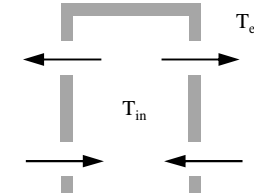
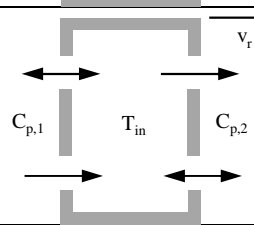
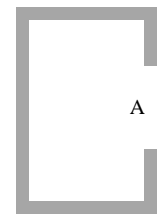
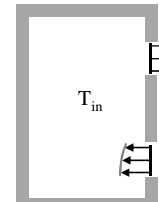
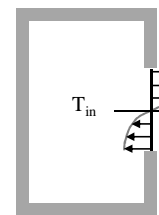
However, the existing European standards consider natural ventilation mainly as a measure to provide good indoor air quality but not as a cooling strategy. The following subsections provide a summary of the codes focusing on the area relevant to naturally ventilated buildings across several European countries.

2.6.1 BS 5925

The British Standard BS 5925: 1991 [10] gives recommendations for designing natural ventilation systems. It outlines the main reason for building ventilation, and recommends quantitative airflow rates. The standard provides basic factors which influence the choice between natural and mechanical systems. A comprehensive section examines the design of natural ventilation systems.

This includes the basic physics of natural ventilation including the flow characteristics of openings, the generation of pressure differences, the definition of meteorological variables, and gives equations for the determination of natural ventilation rates. This relatively old standard is the only one with clear focus on natural ventilation including ventilation requirements and flow rate calculations. The standard provides analytical solutions for wind and buoyancy induced ventilation for simple buildings without internal flow resistance, or for a space with openings on one orientation only (Table 2.2). For a space with openings on one orientation only, the resulting flow rate is the maximum value of either wind or buoyancy.

Table 2.2: Determination of natural ventilation rates [10] reproduced from [120] (unit symbols adapted according to the nomenclature of this work).

natural ventilation of a simple building	
(a) wind only	 $\dot{V}_w = C_d \cdot A_w \cdot v_r \sqrt{\Delta C_p}$ $\frac{1}{A_w^2} = \frac{1}{(A_1 + A_2)^2} + \frac{1}{(A_3 + A_4)^2}$
(b) temperature difference only	 $\dot{V}_b = C_d \cdot A_b \cdot \sqrt{\frac{2 \cdot \Delta T}{\frac{T_{in} + T_{ext}}{2} + 273}} \cdot g \cdot \Delta h$ $\frac{1}{A_b^2} = \frac{1}{(A_1 + A_3)^2} + \frac{1}{(A_2 + A_4)^2}$
(c) wind and temperature difference together	 $\dot{V} = \dot{V}_b$ <p>for $\frac{v_r}{\sqrt{\Delta T}} < 0,26 \cdot \left(\frac{A_b}{A_w}\right)^{1/2} \cdot \left(\frac{H_1}{\Delta C_p}\right)^{1/2}$</p> $\dot{V} = \dot{V}_w$ <p>for $\frac{v_r}{\sqrt{\Delta T}} > 0,26 \cdot \left(\frac{A_b}{A_w}\right)^{1/2} \cdot \left(\frac{H_1}{\Delta C_p}\right)^{1/2}$</p>
natural ventilation of spaces with openings on one wall only	
(a) due to wind	 $\dot{V} = 0,025 \cdot A \cdot v_r$ <p>because of the turbulent nature of the airflow</p>
(b) due to temperature difference with two openings	 $\dot{V} = C_d \cdot A_w \cdot \left[\frac{\epsilon \sqrt{2}}{(1+\epsilon) \cdot (1+\epsilon^2)^{1/2}} \right] \cdot \sqrt{\frac{\Delta T}{\frac{T_{in} + T_{ext}}{2} + 273}} \cdot g \cdot \Delta h$ $\epsilon = \frac{A_1}{A_2}$ $A_w = A_1 + A_2$
(c) due to temperature difference with one opening	 $\dot{V} = \frac{C_d \cdot A}{3} \cdot \sqrt{\frac{\Delta T}{\frac{T_{in} + T_{ext}}{2} + 273}} \cdot g \cdot h$ <p>if an tilted opening is present</p> $\dot{V} = \frac{C_d \cdot A}{3} \cdot J(\Phi) \cdot \sqrt{\frac{\Delta T}{\frac{T_{in} + T_{ext}}{2} + 273}} \cdot g \cdot h$ <p>where J(Φ) is varied with the opening angle for side-hung centre-pivoted windows (further details see [10])</p>

* v_r = reference wind speed

BS 5925 also provides:

- an approach to calculate the vertical wind profiles depending on the roughness of the terrain and cumulative frequency of meteorological wind speed;
- mean surface pressure coefficients for vertical walls of rectangular buildings;
- values for the metabolic rate of different activities (W/person);

- the production rate of carbon dioxide depending on the metabolic rate of the occupants (0,00004 litres/W);
- correction to the dry resultant upper temperature limits to take account of air movement.

However, the design of mechanical ventilation systems is not included.

2.6.2 EN 13779

The European Standard EN 13799: 2007 [55] focuses on achieving a comfortable and healthy indoor environment with mechanical ventilation systems.

The standard indicates typical CO₂ concentration levels in outdoor air for different locations (e.g., city centres), together with a suggestion on how to categorize the quality. The standard also classifies the indoor air quality from IDA 4 (low IAQ) up to IDA 1 (high IAQ), typically by determining the CO₂ concentration. CO₂ is the product of human respiration, and is therefore good indicator of effective ventilation, but not of absolute air quality. Another approach established is to specify the rate of outdoor air supply for each person in litres per second and person.

These values in practice are often used to size the mechanical ventilation systems, but can also be utilised to size and control natural ventilation systems together with CO₂ sensors or flow rate estimations based on analytical flow rate calculations according to the BS 5925 (see § 2.6.1).

Table 2.3 lists the typical ranges for CO₂ levels and the recommended flow rates for external air supply to realise different categories of indoor air quality.

Table 2.3: Concentration levels of outdoor air and classification of indoor air quality [41].

external air description of the location	typical CO ₂ concentration level in ppm	indoor air quality classification category	description	CO ₂ concentration level in ppm above external air	outdoor airflow rate in litre·s ⁻¹ ·person ⁻¹
rural areas with no significant sources	350	IDA 1	high IAQ	< 400	20
		IDA 2	medium IAQ	400 - 600	12,5
smaller towns	400	IDA 3	moderate IAQ	600 - 1000	8
city centres	450	IDA 4	low IAQ	> 1000	5

2.6.3 EN 15251

The EN 15251: 2012 [41] specifies indoor environmental input parameters for design and assessment of energy performance of buildings addressing indoor air quality, thermal environment, lighting, and acoustics. It includes comfort criteria for the

implementation of the European Directive for Energy Performance of Buildings (EPBD) according to the Commission Delegated Regulation (EU) No 244/2012 [56]: *'The selected energy efficiency measures shall be compatible with air quality and indoor comfort levels according to CEN standard 15251 on indoor air quality or equivalent national standards. In cases where measures produce different comfort levels, this shall be made transparent in the calculations.'*

Describing the philosophy behind EN 15251, Olesen states [48]: *'The energy consumption of buildings depends significantly on the criteria used for the indoor environment, which also affect health, productivity and comfort of the occupants. An energy declaration without a declaration related to the indoor environment makes no sense. ... energy-saving measures should not sacrifice people's comfort and health.'*

According to the standard, the comfort criteria for naturally ventilated buildings without active cooling systems can be specified differently than those with mechanical acclimatisation. This is because of the fact that the expectation of occupants regarding the room climate is different; moreover, the occupants adapt according to the prevailing conditions. The categorisation of acceptable summer temperatures is used for the building design in terms of finding suitable measures against overheating. Passive measures involve appropriate building orientation, suitable shading elements, and the effective use of thermal mass and natural ventilation with sufficient ventilation rate.

Acceptable temperature setpoints should be calculated following the adaptive comfort limits, which are defined in the standard as operative zone temperatures, which are the arithmetic mean of the zone mean air and the zone mean radiant temperature. This is because radiation is an important physical factor that influences comfort, as people standing in the sun, under a hot ceiling, or near hot walls feel hotter than what the air temperature alone indicates.

The operative room temperature is allowed to increase in naturally ventilated, non air-conditioned buildings, with rising ambient air temperatures. Depending on the exponentially weighted running mean of the daily mean ambient air temperature series of the previous week, recommended operative temperatures are calculated for different comfort categories. The criteria were obtained through investigations in office buildings with user-operated windows.

The running mean daily ambient temperature T_{rm} is obtained from the mean external temperatures of the day before, and the weighted temperatures of the previous days of the week.

Using this mean temperature makes the calculations of admissible lower and upper boundaries of the operative temperature for different categories possible.

category 1 upper limit: $T_{c1,max} = 0,33 \cdot T_{rm} + 18,8 + 2$ (2.21)

category 1 lower limit: $T_{c1,min} = 0,33 \cdot T_{rm} + 18,8 - 2$ (2.22)

category 2 upper limit: $T_{c2,max} = 0,33 \cdot T_{rm} + 18,8 + 3$ (2.23)

category 2 lower limit: $T_{c2,min} = 0,33 \cdot T_{rm} + 18,8 - 3$ (2.24)

category 3 upper limit: $T_{c3,max} = 0,33 \cdot T_{rm} + 18,8 + 4$ (2.25)

category 3 lower limit: $T_{c3,min} = 0,33 \cdot T_{rm} + 18,8 - 4$ (2.26)

Outside the limiting values of $T_{rm} < 10 \text{ }^\circ\text{C}$ or $T_{rm} > 30 \text{ }^\circ\text{C}$ for the upper limits, and $T_{rm} < 15 \text{ }^\circ\text{C}$ or $T_{rm} > 30 \text{ }^\circ\text{C}$ for the lower limits, a fixed and non-adaptive boundary temperature is assumed.

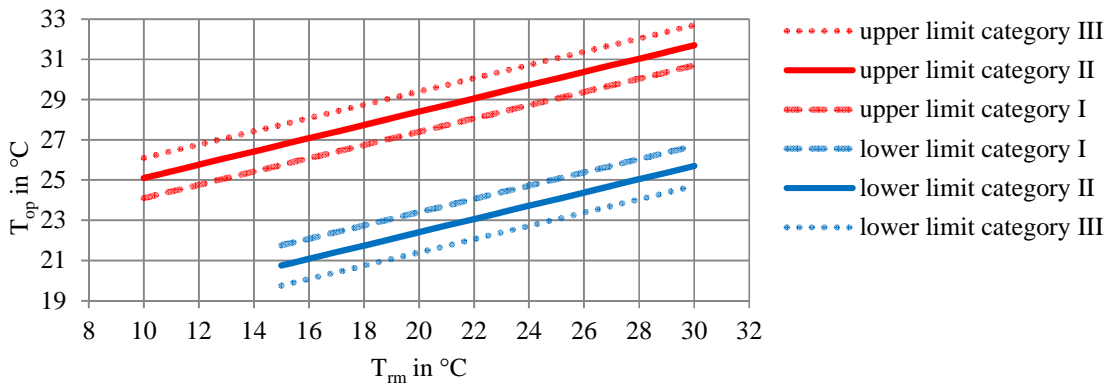


Figure 2.32: Design values of the operative room temperature for buildings without mechanical cooling as a function of the weighted ambient temperature according to [41].

A short description of the categories is shown in Table 2.4.

Table 2.4: Description of the categories used in the adaptive thermal comfort model [41].

Category	Explanation
I	High level of expectation and is recommended for spaces occupied by very sensitive and fragile persons with special requirements, e.g., handicapped, sick, very young children and elderly persons
II	Normal level of expectation and should be used for new buildings and renovations
III	An acceptable, moderate level of expectation and may be used for existing buildings
IV	Values outside the criteria for the above categories. This category should only be accepted for a limited part of the year

This thesis will consider category II as comfort limit temperatures. As examples, the annual adaptive thermal comfort limits were calculated with the ASHRAE IWEC ‘typical’ climate data for three reference locations Istanbul / Turkey, Turin / Italy and Stuttgart / Germany (see § 5.1.4). In Istanbul and Turin, operative temperature levels over 30 °C are briefly allowed for hot ambient air summer conditions.

2.6.4 EN 15242

The European standard EN 15242: 2007 [28] defines the way to calculate airflows due to the ventilation system and infiltration.

It specifies a direct method for calculating manually operated, single-sided ventilation through open windows for airing or achieving thermal comfort in summertime. The method is intended for calculating the opening angle for a given bottom-hung window. The formulae below are only suitable for the single-sided volume flow calculations. The volume flow rate \dot{V}_{EN} is calculated using three coefficients for wind turbulence ($C_t = 0,01$), wind speed ($C_w = 0,001$), and thermal buoyancy ($C_{st} = 0,0035$):

$$\dot{V}_{EN} = 3,6 \cdot 500 \cdot A_{EN} \sqrt{C_t \cdot C_w \cdot v_{met} \cdot C_{st} \cdot h_{eff} \cdot |\Delta T|} \quad (2.27)$$

Subsequently, the necessary structural area A_{EN} of a bottom-hung window is calculated according to:

$$A_{EN} = C_k(\alpha) \cdot A \quad (2.28)$$

with $C_k(\alpha)$ as a polynomial approximation (cf. Figure 2.33):

$$C_k(\alpha) = 2,60 \cdot 10^{-7} \cdot \alpha^3 - 1,19 \cdot 10^{-4} \cdot \alpha^2 + 1,86 \cdot 10^{-2} \cdot \alpha \quad (2.29)$$

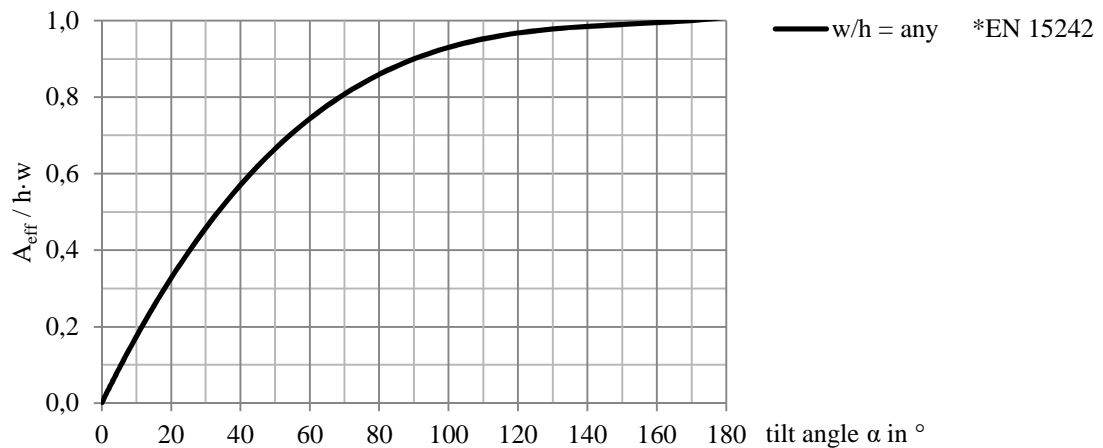


Figure 2.33: Effective area of a bottom-hung window scaled by the fully opened window with equal area according to [28].

2.7 Conclusions

A brief summary of the significant observations based on the literature survey carried out are listed as follows:

- The aim of natural ventilation is to provide good indoor air quality (with rather low air change rates) as well as good thermal comfort in summer (with increased airspeeds during daytime and high night-time air change rates).
- The recommended CO₂ concentrations should not exceed about 1000 ppm, but there is still no uniform limit. Measurements in densely populated rooms are often higher.
- With manually controlled natural ventilation, good indoor air quality cannot be guaranteed, especially in densely populated rooms (schools, offices).
- The analysis of non-residential buildings in international projects has shown that warm and moderate climates with large day/night temperature differences of 10-12 °C are suitable for natural night ventilation. In temperate climates, a good thermal comfort can be achieved by night cooling while reducing cooling loads through sun protection or similar. In hot climates with moderate night temperatures natural night ventilation can be used to reduce energy consumption of the active cooling system. Typical room temperature reductions by night ventilation are of the order 1-3 °C (up to 6 °C).

- Natural ventilation in humid climates is not recommended for cooling (with water content of air of more than 15 g/kg). Cooling by natural ventilation in buildings alone works with rather low cooling loads ($<30 \text{ W/m}^2$) and enough thermal mass ($>75 \text{ kg/m}^2$).
- Naturally ventilated buildings can also offer good thermal comfort in hot summer conditions. For example, in the summer of 2003 the office building Lamparter had less than 10% of the hours of use above $26 \text{ }^\circ\text{C}$. Atria can easily overheat.
- The air change rates achievable through natural ventilation with correct sizing of the openings are significantly higher than those with mechanical ventilation for night cooling, and without electrical energy input.
- For high-rise building shapes, the challenges in terms of designing the envelope and its openings are greater, primarily because of the building height and the width. The potential magnitudes of driving forces become bigger, and their relative magnitudes can vary over a wider range. Simple flow path configurations are not suitable due to building widths bigger than recommended for cross ventilation.
- Automatic control of openings is essential during non-occupation of office and school buildings to allow night-time ventilation.
- Depending on the ventilation strategy, typical opening cross-sections are approximately 1-3% of the floor area.
- During occupation, a complex control system, especially in open plan offices, is important; in single offices, ventilation can also be user-controlled.
- Preliminary evaluation tools and instruments for effective vent sizing are available only for a few building and ventilation designs, especially in moderate climate. Characteristics of the building and ventilation design may only be rarely adapted. They allow the prediction of maximum indoor temperatures, energy savings, and corresponding maximum removal of cooling capacity.
- Specific and systematic statements on annual energy savings achievable through natural ventilation are rare. The saved electrical energy consumption for mechanical ventilation, the possible cooling energy by night ventilation with increased air changes rates, and the energy losses due to missing heat recovery in winter as well as auxiliary energy requirements must be considered.

3. METHODOLOGY

Passive measures for cooling are employed to reduce heat gains, to store night cold in the fabric, and to naturally exhaust heat. These measures along with a simplified building operation are considered in an integrated manner at the early design stage in order to assist the delivery of a sustainable office tower design with a high energy performance rating.

A software tool named ‘HighVent’ was developed to design and size natural ventilation systems for high-rise office buildings with a relatively small number of input parameters. In two steps, this prototypical tool is capable of designing a flow path for a wide-shaped building segment up to ten floors. Optimization targets are to reach minimal system sizes with respect to the comfort and flow path criteria developed. In the first step, the electric analogy between electrical and flow circuits is used to compute opening dimensions for a given air change rate under unchanging climate and location specific boundary conditions. Off-design calculations can be conducted apart from take-off for altered boundary conditions and design specifications to check for the best suitable solutions. In the optional second step, a dynamic design day heat balance approach is used to evaluate the comfort performance in a higher flexibility of measures to also see the effect of other building design parameters (e.g., heat gains and thermal mass). A graphical visualisation of the resulting output aims to quickly access the capabilities of the passive cooling system. The validation of the results against EnergyPlus simulations in § 3.2.3 proves the calculation capabilities of the tool in the design of passive cooling in office buildings.

The tool outputs, which are primarily design parameters for the positioning and sizing of openings in the flow path, are then further used or ‘post-processed’ as inputs for detailed weekly and annual building energy performance simulations including airflow networks. EnergyPlus simulations are run to access detailed information about the comfort reached depending on the ventilation rates and to modify the output parameters of the tool when necessary. This detailed design

development also includes the model calibration and the developed natural ventilation controls. Moreover, some parametric analyses are intended to show the influence of important design parameters on the passive cooling performance of the approach developed.

3.1 Conceptual Design

For the purpose of passive cooling, in literature it is common for natural ventilation to be applied along with other measures for the reduction of heat loads. Passive cooling is therefore realised by controlled intense day and night natural ventilation, flanked by the reduction of solar heat gains, and by thermal mass activation to store night cold in the building fabric. Focusing on natural ventilation, the design presented here is especially developed for wide-shaped high-rise buildings where simple cross ventilation or single-sided ventilation is impractical to realise. The basic strategies that are available, and their limitations are described in § 2.2.2. As the inner volume of a building is an expensive resource, the design is intended to minimise the system dimensions by optimal exploitation of natural driving forces, i.e., wind and buoyancy, and by reduction in the flow resistances whenever possible.

3.1.1 Natural ventilation

Keeping the building shape in mind, and focusing on the possible flow path design, cross ventilation from one façade orientation throughout the building to the other orientation is not an option as the building type concerned is typically shaped too wide. According to § 2.2.2.2, the maximum depth (Figure 3.1 (a)) should not be higher than 5 times the ceiling height [26] (occupied space).

Another strategy option is single-sided ventilation with a maximum penetration depth of 2,5 times the ceiling height (see § 2.2.2.1). Therefore, the inner part of a wide shaped building cannot be ventilated by deploying this strategy (Figure 3.1 (b)). Assuming all the office space is assembled at the building's perimeter, single-sided ventilation could be an option to ventilate the office area, but there are some other concerns. First, single-sided ventilation is mostly based on buoyancy, and controlled natural ventilation cannot be assisted by wind forces. Openings therefore need to be sized relatively larger, which also affects the second concern, that strong

local wind turbulences without wind shielding elements (like a double skin façade) at high storey heights may cause problems.

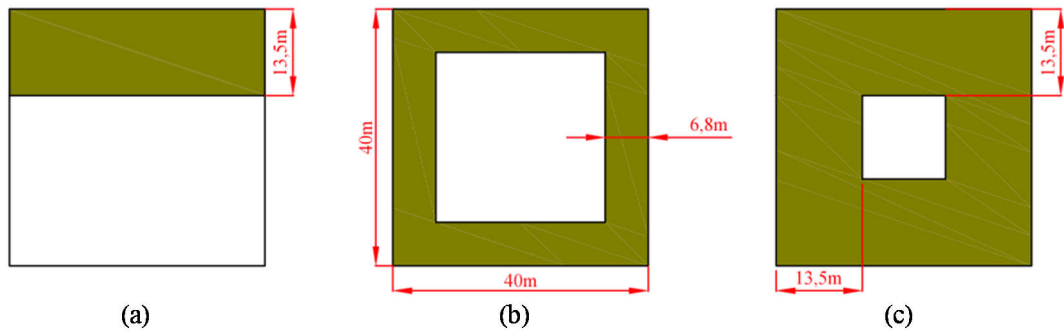


Figure 3.1: Maximum penetration depth (green area) for different ventilation strategies applied to a wide, exemplarily square shaped office-tower (plan view) with a ceiling height of 2,7 m, which are (a) wind driven cross ventilation, (b) buoyancy driven single-sided ventilation and (c) central void ventilation.

As a third alternative, a central chimney or void design as described in § 2.2.2.3 is suitable in general for wide building shapes. Buoyancy is usually the main driving force for air circulation. Central chimney or atrium design is practical for wide buildings because the occupied space is cross-ventilated towards a central void, from where the warm air rises upwards, towards a high level exhaust (Figure 3.1 (c)). To increase the driving forces, this strategy is often combined with solar heated buffer zones (e.g., atrium or solar chimney) or wind catcher, in dry climates sometimes together with evaporative cooling. To support the thermal chimney effect by wind forces, the best possible solution is positive wind pressure at the inlets together with negative wind pressure at high level outlets. As the wind pressure changes sign with the wind direction, the only way to generate positive loads at the inlet is to position all inlets at the windward façade orientation.

The initial strategy in the context of the passive approach developed here thus is an upward cross-flow ventilation design for tall buildings, for which the design idea is taken from Etheridge [40], but with further improvisations. The building is vertically segmented for different reasons. Concerning a building without segmentation and containing one single chimney for all floors, as stated by Etheridge [40]: *‘For buoyancy alone, the pressure drop is greatest at the lowest opening. For a building of height 200 m with a temperature difference of 20 °C, the pressure difference across the envelope at ground level would be 160 Pa. The forces required to open external doors and windows at the lower levels would be unacceptable.’*

Another problem considering a single segment design for buoyancy alone is that the range of opening areas required is significant. This is because the pressure drop

across the lowest storey openings can be many times than that across the highest storey openings, and to keep the flow direction on the highest floor inward, the dimensions of the outlet easily become excessive. In the present work, it has been observed that even the chimney size in terms of its cross-sectional area increases by the number of floors it supplies. With a single chimney to ventilate e.g., 25 floors, the size of the ventilation system would be too big to be realised in practice. According to Etheridge [40], a possibility to overcome these issues is the building segmentation. If the building consists of isolated segments such as shown in Figure 3.2, each segment can then be treated as a low-rise or medium-rise building.

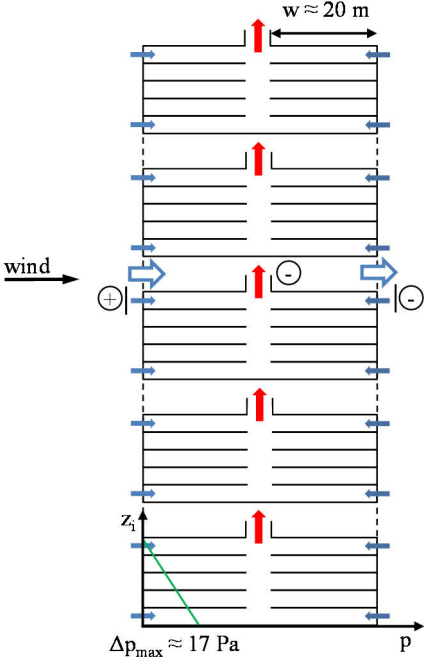


Figure 3.2: Building segmentation of a high-rise building with multiple floors for each segment (here 5 storeys each) and with a commonly used exhaust stack.

Upon further investigation of the segmented building design of one segment, the wind pressure distribution depending on the orientation becomes a design difficulty. At the inlet openings, which need to be distributed across all façade orientations, wind pressure is positive at the windward side only. At all the other orientations, the resulting wind pressure is negative and therefore counteracting the intended flow direction, from the office space to the core and then upward the chimney towards the exhaust opening. As this flow direction needs to be guaranteed, the initial design developed by Etheridge [40] needs some further adjustments to ensure a similar pressure distribution at all the inlets. Two possibilities were found, which are wind blocking devices (like a double skin façade), or a commonly used windward supply inlet. Each possibility has pros and cons but the driving forces (pressure drop from

the inlet to the outlet) would benefit more from a positive pressure inlet than from a neutral wind-blocking design. To generate a negative pressure field at the chimney exhausts is less critical since most orientations of a building create a negative pressure field (see also Figure 2.2 and wind tunnel experiments in Appendix A).

Bearing in mind all the above mentioned considerations, the adapted building is divided into modular multi-storey building segments stacked on top of each other. The derivation of the design approach is based on the building shape discussed.

The occupied space of each storey is connected to a central fresh air supply chimney and a central exhaust chimney. The stack effect in this commonly used central void pulls air from the office perimeter of each floor. Fresh air enters the offices at floor level via a sub-slab distribution system, leaving the space subsequently via openings at ceiling level to the core, and from there to the exhaust chimney.

The intermediate 'wind floors' between the segments each have two wind adapting openings in opposite direction – the windward orientation and the leeward orientation. The windward opening with a positive wind pressure field is intended as the supply inlet for the segment above, whereas the leeward opening is the exhaust of the segment below. As wind passes the building, a negative pressure field on the leeward façade orientation creates suction, further pulling the warm air from the chimney void. The wind driving forces thus support the thermally driven buoyancy forces of the warm air column within the building.

3.1.2 Solar heat gain reduction

As an accompanying measure, good shading of building fenestration is important, especially in the warm season. In summer, the higher sun can be kept from south-facing windows by overhangs. But in mornings and afternoons, the sun become hotter and reaches under overhangs. To avoid overheating, windows that face west as well as east should be well shaded according to the sun angle.

3.1.3 Thermal mass activation

Another accompanying possibility to assist passive cooling is night-time ventilation of the building mass. Whenever the night-time outdoor air temperature is low enough, ventilation can be used to cool the exposed thermal mass of a building in

order to provide a heat sink during the following day. The basic idea of the concept is described in § 2.2.4.2.

3.2 Preliminary Design and Tool Development

Achieving the required strategy is largely dependent on the flow path design and opening dimensioning for certain design conditions, such that they enable adequate control. The ‘HighVent’ design tool developed aims to ‘fast-forward’ study the natural ventilation potential and thermal comfort consequences for a passive summer approach.

It is intended to fill the gap between very simple actual tools like graphical charts from the NatVent study [16] and the detailed dynamic building energy and airflow network simulation tools as with EnergyPlus [1], both of which are found to be lacking in the ability to evaluate the functionality of controlled natural ventilation in the system design and sizing phase.

Simple design tools (such as presented in § 2.5.4) are intended to lower critical barriers for implementing natural ventilation by recommending the sizing for natural ventilation systems depending on the building concerned. However, these tools have a lot of limitations, especially in terms of flexibility in the design and consequences on comfort. They are mostly limited to a certain climate (e.g., northern European); they are restricted to simple ventilation designs like cross ventilation, single-sided ventilation or chimney ventilation for a specific small number of rooms; and they are not applicable for more complex flow paths such as multi floor chimneys with combined wind and buoyancy driving forces as shown in Figure 3.2 and Figure 6.2. They often fail to include internal flow resistances or different zone temperatures, e.g., for solar chimney applications. Moreover, other crucial parameters like internal and solar heat gains as well as the thermal mass distribution as a sink for diurnal night cooling are treated in a very simplified way. Finally, they do not consider hybrid approaches, ventilation control, and actual standards for thermal comfort in naturally ventilated buildings.

On the other hand, complex dynamic building performance simulation programs including airflow networks (see § 3.3.1) are qualified to reflect all these parameters, but they do not give any indication to the designer on how to size and locate the most

crucial parameters for a good natural ventilation design, e.g., opening sizing, flow path design, thermal mass in combination with glazing, shading devices, and internal heat gains for a specific climate. In summary, airflow networks already integrated in building energy performance simulation packages like Airnet in EnergyPlus are capable of calculating airflows but give no advice on sizing natural ventilation systems. They are thus more suitable for the detailed design analysis phase with annual simulations including the predicted energy consumption. The results of the design tool developed in this thesis are therefore especially suitable as inputs for ‘post-processing’ with complex dynamic building simulation programs.

The spread-sheet based design tool developed uses electrical circuit analogies for both ventilation and the thermal model. The tool aims to study the main parameters influencing the potentials of uncontrolled natural ventilation. It proves the functionality of a certain design, and recommends passive cooling when possible and a hybrid approach whenever needed.

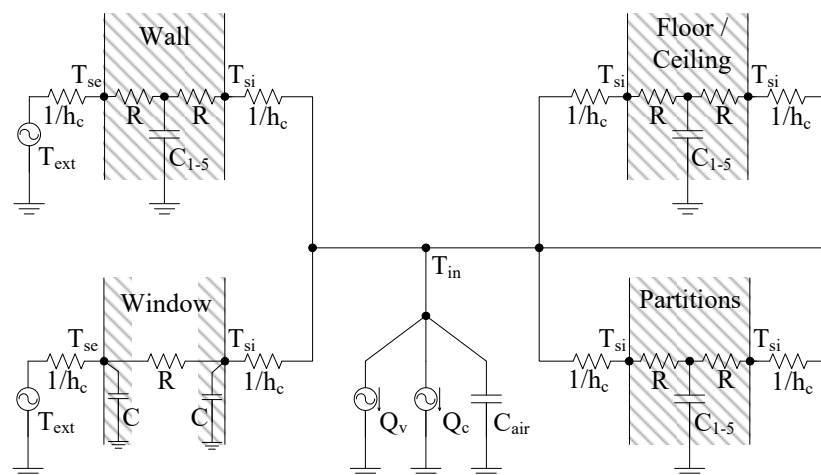


Figure 3.3: Simplified thermal-circuit model of the tool developed exclusive radiative heat transfer.

The tool targets to find an optimum passive design, neither oversizing nor undersizing the related components, that leads to minimum overheating for a specific type of building in a certain climate. It is especially intended for application in the context of high-rise office buildings as in Figure 3.2, but can also be utilised for simpler building types.

In the first step, the natural ventilation system design is realised by a newly developed steady state electric analogy model. Unchanging boundary conditions are the temperature difference between indoor and outdoor, and the wind velocity. For calculating the airflow rates, the advantage of this model compared to other

simplified analytical calculations as described in other papers by the thesis author [77,121] is that it is able to represent a multi-storey flow path, e.g., for a segment of an office tower, by calculating the pressure drops on each opening. According to the pressure distribution, openings can be sized for each cell of the model (e.g., a storey of the building or exhaust chimney) to reach a certain steady airflow rate for all cells under the boundary conditions defined.

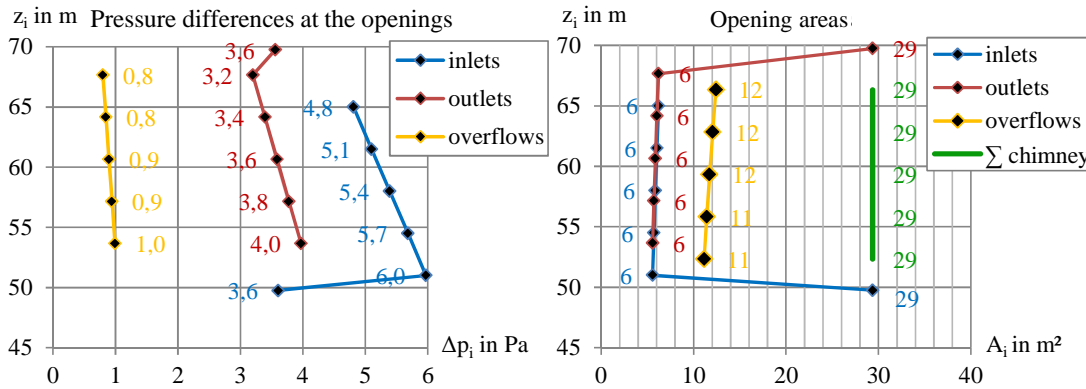


Figure 3.4: Example of the steady state ($\Delta T=3^\circ\text{C}$, $v_{\text{met}} = 5 \text{ m/s}$) ventilation design major outputs for a 5-storey building segment with a internal chimney, sized for 13 air changes per hour

In the second step, this initial natural ventilation design is originally integrated into a dynamic, thermal simulation for a specific climate, summer design day (gathered according to 5.3.3) with changing boundary conditions (e.g., external temperature). The simulation is looped (3 times iterated) to get good initial conditions. Together with other parameters, the design air change rate may here be further adapted in terms of opening sizing to fulfil the thermal comfort requirements of the maximum allowable operative cell air temperature, or to stay within psychrometric boundaries depending also on humidity levels. It is clear that the extent of the glazed area in the façade as well as the internal thermal mass directly affects the indoor ambience. Therefore, in addition to the ventilation system including basic controls, other crucial parameters must also be investigated to see their influence on the passive design. These parameters include (i) the thermal mass distribution e.g., in the walls and the floor especially for night cooling, which in the model is realised by a multi-layered lumped capacity approach, (ii) building operation and related internal heat gains, (iii) external heat gains transmitted into the cell depending on the properties of the envelope – wall and window heat resistances, glazing ratio, window solar coefficients, and external shading, and (iv) chimney heat gains, which is an optional

feature for additional solar or internal system (like data-centres) heat gains, raising the air change rates.

Due to the perceived model complexity, some parts of the calculation method were implemented in a simplified way. The dynamic thermal behaviour of the model is only analysed for one storey (cell) of the building segment analysed in step one (opening sizing). This is done due to the assumption that the heat gains, the mass distribution and the ventilation rates are equal in all storeys of the segment investigated. If heat gains differ significantly from storey to storey, the pre-design may be repeated for each floor. Another simplification is that the tool needs some amount of ‘pre-processed’ data input. This involves the typical inputs describing the simulation problem, and the solar heat gains entering the building cell, and the summer design day climatic description depending on the climatic location and adaptive comfort acceptance.

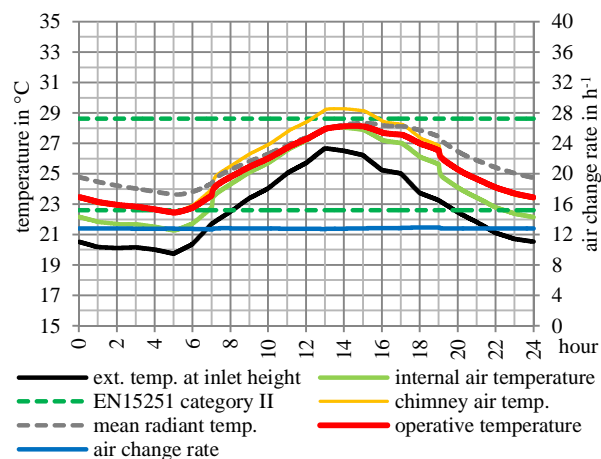


Figure 3.5: Example of the ‘HighVent’ design tool’s major thermal outputs.

In summary, the passive model (except with optional mechanical ventilation) comprises multiple major heatflow paths, keeping it simple whenever possible, but complex enough for full flexibility in the system design.

3.2.1 Ventilation model calculation method

This involves determining the sizes and positions of external and internal openings. The way chosen here is an originally compiled electric analogy model, which defines the ventilative driving forces as voltage source, the openings as resistances, and the volumetric airflow as current. By knowing the positions of the openings and their sizes, the flow pattern can be calculated for dynamic conditions with the thermal electric analogy model using the explicit method of solution. Since unsteady

conditions are important for strategies involving night cooling and free-running systems, dynamic thermal modelling is required as described in § 3.2.2.

3.2.1.1 Driving forces

As described in § 2.2.1, the driving forces for natural ventilation in rooms and buildings are pressure differences caused by buoyancy and wind. Ventilation rates are dependent on the magnitude and direction of these forces, and flow resistance of the flow path. The magnitudes of driving forces change with atmospheric variation over height.

Wind pressure difference

The pressure distribution around the building depends on pressure coefficients (see § 2.2.1.2), and the local wind speed and direction at the height of the openings. The pressure on the building at a certain height and orientation due to wind forces is:

$$p_w = 0,5 \cdot \rho_E \cdot v_z^2 \cdot C_p \quad (3.1)$$

Within the preliminary approach developed in the context of this thesis and in EnergyPlus simulations, the ASHRAE power law estimation [27] calculates the local wind speed depending on the height of the opening, the terrain roughness, and the meteorological wind speed. This is of special importance in high-rise buildings, where the wind speed significantly changes depending on the local height level of the openings.

With this approach, local wind velocities are derived from the local opening height (centroid), the wind profile coefficients δ and β (terrain characteristics), and wind speed [27,122], where 10 m is the assumed height of the meteorological station:

$$v_z(t) = v_{\text{met}}(t) \cdot \left(\frac{\delta_{\text{met}}}{10\text{m}}\right)^{\beta_{\text{met}}} \cdot \left(\frac{z}{\delta_{\text{site}}}\right)^{\beta_{\text{site}}} \quad (3.2)$$

Table 3.1: Terrain-dependent coefficients [27].

terrain	exponent β	Layer thickness δ in m
ocean	0,10	210
flat, open country, meteorological station	0,14	270
rough, wooded country, urban, industrial, forest	0,22	370
towns and cities	0,33	460

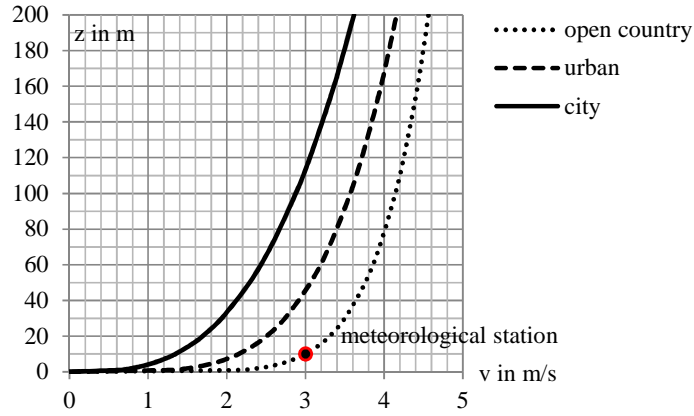


Figure 3.6: Local wind speed profiles depending on terrain, meteorological wind speed, and height.

The wind pressure difference between two façade orientations at different height levels is (see also § 2.2.1.2):

$$\Delta p_w = 0,5 \cdot \rho_1 \cdot v_1^2 \cdot C_{p,1} - 0,5 \cdot \rho_2 \cdot v_2^2 \cdot C_{p,2} \quad (3.3)$$

Stack pressure difference

Stack pressure differences due to buoyancy forces depend on the magnitude of density and height differences:

$$\Delta p_b = \Delta \rho_1 \cdot g \cdot \Delta z_i \quad (3.4)$$

The density differences are mostly affected by temperature differences. In the context of office building ventilation, the humidity ratio in kg water per kg air (HR), both outside and inside the building, can be assumed to be relatively constant. Nevertheless, a comprehensive method for determining the air density was chosen including humidity and barometric pressure.

The density of air is dependent on temperature, moisture content, and barometric pressure. The moist air density may be calculated by [123]:

$$\rho_{E,z} = \frac{p_{\text{baro},z}}{R_a \cdot T_{\text{ext},z}} \cdot \frac{1 + HR}{1 + HR \cdot \frac{R_w}{R_a}} \quad (3.5)$$

The barometric pressure is calculated at the start height of the building segment. The external temperature at local height is calculated at the height level of the openings. Including the gas constant of air and water vapour ($R_a = 286,9 \text{ J kg}^{-1} \text{ K}^{-1}$ and $R_w = 461,5 \text{ J kg}^{-1} \text{ K}^{-1}$), the equation for the moist air density of the external air density becomes:

$$\rho_{E,z} = \frac{p_{\text{baro},z}}{286,9 \frac{\text{J}}{\text{kg} \cdot \text{K}} \cdot T_{E,z}} \cdot \frac{1 + HR}{1 + HR \cdot 1,609} \quad (3.6)$$

For simplicity of the model, it is assumed that the humidity ratio of the external air is equal to the humidity ratio of the internal air (only sensible internal heat gains). Then, the internal air density becomes:

$$\rho_I = \frac{p_{\text{baro},z}}{286,9 \frac{\text{J}}{\text{kg} \cdot \text{K}} \cdot T_I} \cdot \frac{1 + HR}{1 + HR \cdot 1,609} \quad (3.7)$$

As mentioned before in § 2.2.1.1, for flow rate calculations or the sizing of opening areas it is important to use a relatively accurate value for the density difference $\Delta\rho$. The absolute value for the density is less important. Therefore, it is practicable to assume dry air conditions whenever the humidity level is unknown.

According to the U.S. Standard Atmosphere model, the external air temperature decreases with height at a rate of approximately 1°C per 150 m. In the pre-design stage, this is of minor importance when considering relatively lower height building segments. But as a side note, it should be also mentioned that 1°C lower supply air temperature will make a difference in thermal comfort aspects.

At altitude z above ground, according to the U.S. Standard Atmosphere model the external temperature is:

$$T_{E,z} = T_{\text{met}} - 0,0065 \frac{\text{K}}{\text{m}} \cdot \left(\frac{6,36 \cdot 10^6 \text{m} \cdot z_i}{6,36 \cdot 10^6 \text{m} + z_i} - \frac{6,36 \cdot 10^6 \text{m} \cdot z_{\text{met}}}{6,36 \cdot 10^6 \text{m} + z_{\text{met}}} \right) \quad (3.8)$$

With an assumed height of the meteorological station at 1,5 m:

$$T_{E,z} = T_{\text{met}} - 0,0065 \frac{\text{K}}{\text{m}} \cdot \left(\frac{6,36 \cdot 10^6 \text{m} \cdot z_i}{6,36 \cdot 10^6 \text{m} + z_i} - \frac{6,36 \cdot 10^6 \text{m} \cdot 1,5\text{m}}{6,36 \cdot 10^6 \text{m} + 1,5\text{m}} \right) \quad (3.9)$$

where $6,36 \cdot 10^6$ m is the radius of the earth and $-0,0065$ K/m is the air temperature gradient in the troposphere.

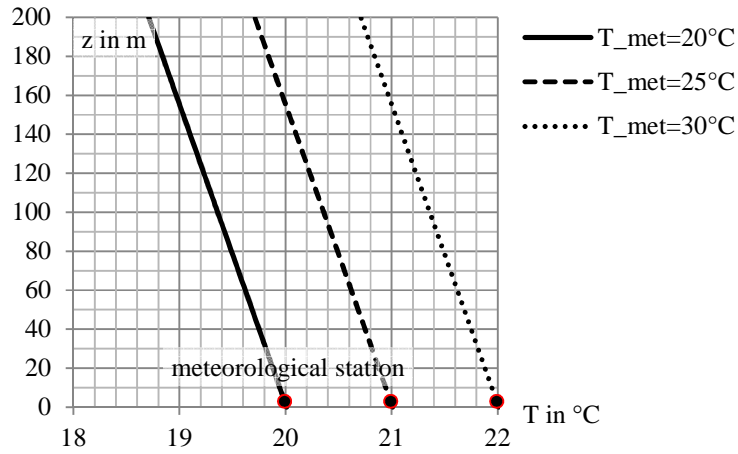


Figure 3.7: Local external temperature profiles depending on the height.

The local barometric pressure above sea level can be calculated as [122,124]:

$$p_{\text{baro},z} = 101325 \cdot \left(1 - 2,25577 \cdot 10^{-5} \cdot (z_{\text{site}} + z_i)\right)^{5,2559} \quad (3.10)$$

where 101 325 Pa is the reference pressure, which is the standard atmospheric pressure at sea level.

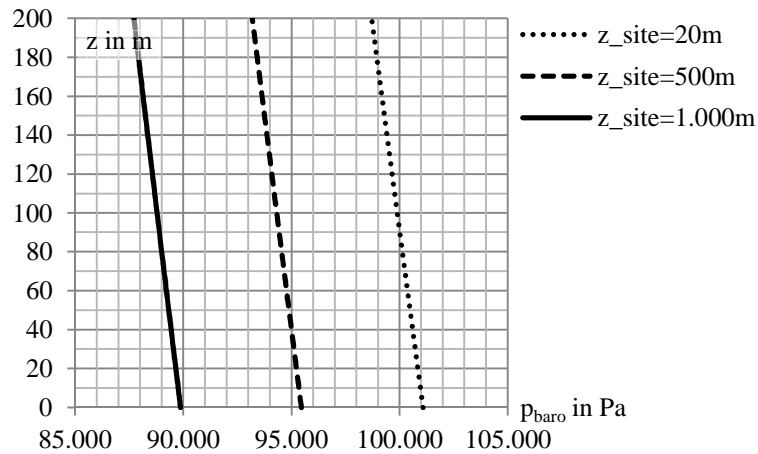


Figure 3.8: Local atmospheric pressure profiles depending on the height.

The buoyancy pressure difference between two height and temperature levels is (see also § 2.2.1.1):

$$\Delta p_b = (\rho_1 - \rho_2) \cdot g \cdot (z_1 - z_2) \quad (3.11)$$

Steady state boundaries

For the design of natural ventilation strategies, it is common practice to first design and size the system by fixed boundary conditions depending on the climate and the building location.

The wind velocity passive cooling design condition chosen is the climate specific, average wind velocity in the hottest 91 days of the year (see § 5.3.3). The local wind speed is then calculated according to the terrain and the local height of the openings.

The temperature difference chosen is 3 °C between inside and outside, which is the value recommend by CIBSE [26] for the minimum hygienic air change and for passive cooling in summer.

Optionally the chimney temperatures may be adapted. Additional chimney heats gains (to cell B Figure 3.9), usually from solar radiation or from internal heat sources, lower the chimney air density, and therefore increase the upward buoyant flow. Additional chimney heats loss (from cell A Figure 3.9), usually from mechanical cooling but could also be considered from evaporation cooling or due to underground ducts, increases the chimney air density, and in turn increases the upward buoyant flow due to higher temperature differences.

Pressure differences on each storey

Total pressure drop from the chimney inlet to the outlet (for the whole flow path):

$$\Delta p_S = \Delta p_{b,1} + \Delta p_{b,2} + \Delta p_{b,2} + \Delta p_w \quad (3.12)$$

Pressure differences due to buoyancy forces, exemplary for the 3rd storey (F) of the building segment:

$$\Delta p_{b,1} = (\rho_E - \rho_A) \cdot g \cdot (z_9 - z_1) \quad (3.13)$$

$$\Delta p_{b,2} = (\rho_E - \rho_F) \cdot g \cdot (z_{11} - z_9) \quad (3.14)$$

$$\Delta p_{b,3} = (\rho_E - \rho_B) \cdot g \cdot (z_2 - z_{11}) \quad (3.15)$$

Pressure difference due to wind forces:

$$\Delta p_w = 0,5 \cdot \rho_E \cdot v_1^2 \cdot C_{p,1} - 0,5 \cdot \rho_E \cdot v_2^2 \cdot C_{p,2} \quad (3.16)$$

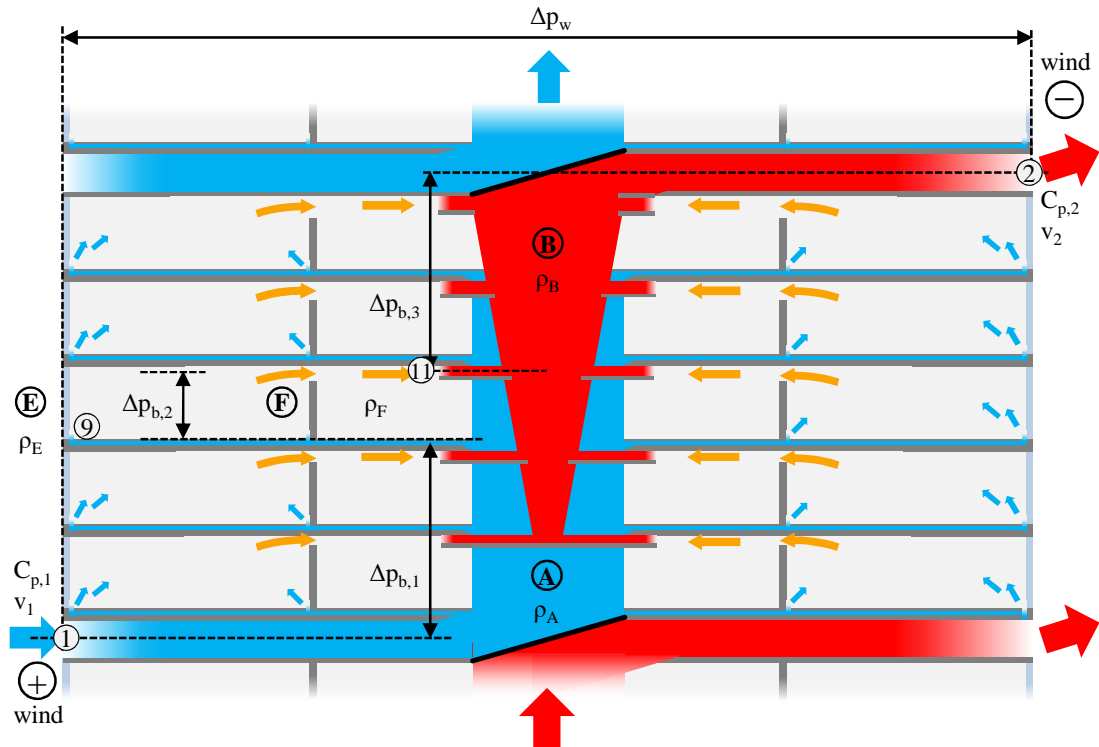


Figure 3.9: Pressure drops across the whole flow path from the supply inlet to the exhaust outlet.

3.2.1.2 Electric airflow analogy model

The building ventilation model is based on a set of resistances, generators, and flows. Pressure is analogous to voltage, electrical current is analogous to volumetric airflow rate, and electrical resistance is analogous to airflow resistance [125]. Potential differences can be generated by sources like mechanical fans or by the natural forces of wind and buoyancy.

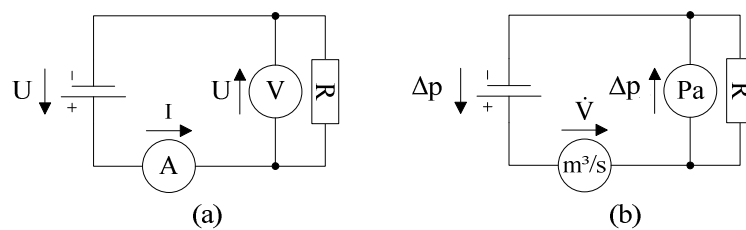


Figure 3.10: Electric circuit (a) and airflow analogy (b).

This approach provides a useful framework when developing computer software for calculating airflow through complex networks with multiple inlet and outlet openings and when internal flows occur through a network of flow paths. Models, among others, are based on electrical circuit analogies such as Kirchhoff's first and second laws, and Atkinson's equation originally published in 1886 for mine ventilation [126]. Concerning airflow circuits, Kirchhoff's first law states that the quantity of air leaving a node must be equal to the quantity of air entering the node. The second law

states that the sum of pressure drops around any closed path must be equal to zero. Atkinson's equation relates the pressure losses at an orifice at which turbulent airflow occurs proportionally to the square of the volume flow.

The use of a solver goal seeking values as available in MS visual basic integrated in Excel 2010, is very convenient for this purpose because it allows equations not to be written in an explicit form.

Model components

As described before, pressure supply sources in natural ventilation systems are buoyancy and wind:

$$\Delta p_s = \Delta p_b + \Delta p_w \quad (3.17)$$

The laminar-flow pressure losses are linear and analogous to the electric potential difference between two points according to the Ohm's law. Unlike in electrical engineering, for turbulent airflows through orifices, the Atkinson's equation relates the pressure losses in an airway proportionally to the square of the volumetric airflow rate through the airway, with the constant of proportionality being the resistance of the airway:

$$\Delta p = R \cdot \dot{V}^2 \quad (3.18)$$

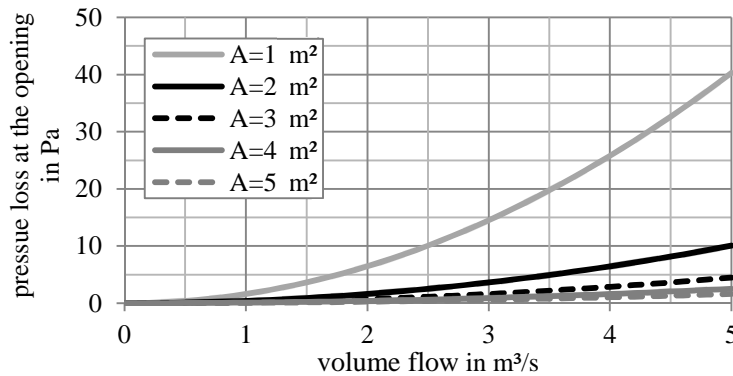


Figure 3.11: Pressure head at differently sized openings ($C_d=0,61$) depending on the volume flow according to Atkinson's equation for turbulent flow [126].

Thus, the volumetric airflow rate through an orifice such as a wall opening or window is:

$$\dot{V} = \sqrt{\frac{\Delta p}{R}} \quad (3.19)$$

Resistors are used to model pressure drops due to an orifice. The airflow resistance of orifices can be expressed in terms of their discharge coefficients, the density of air, and the effective area of the opening:

$$R = \frac{\rho}{2 \cdot C_d^2 \cdot A_{\text{eff}}^2} \quad (3.20)$$

When airflow passes through a number of sequential openings with resistances, the equivalent resistance for all the openings in series can be calculated by the sum of the individual resistances:

$$R_S = R_1 + R_2 + R_3 + \dots + R_n \quad (3.21)$$

When airflow passes through a number of parallel connected openings with resistances, the reciprocal of the equivalent resistance for all the openings in parallel can be calculated by the sum of the reciprocal individual resistances:

$$\frac{1}{R_S} = \frac{1}{R_1} + \frac{1}{R_2} + \frac{1}{R_3} + \dots + \frac{1}{R_n} \quad (3.22)$$

Considering air change rates necessary to meet the comfort criteria, the opening areas are defined according to the design air volume flow rate, the orifice resistance, the pressure drop at the opening, and the air density:

$$A_i = \frac{\dot{V}_i}{C_{d,i} \sqrt{\frac{2 \cdot |\Delta p_i|}{\rho_0}}} \quad (3.23)$$

Flow path specifications

Exemplary, for a five-storey per segment scenario, some specifications are necessary to properly size the natural ventilation system. The specifications aim to achieve a uniform airflow throughout the building and a constant cross-sectional area of the central chimney. The following rules are implemented in the ventilation model of the pre-design tool based on electric analogy:

- 1) The air volume flow rate on each storey of the building segment is defined to be equal:

$$\dot{V}_C = \dot{V}_D = \dot{V}_F = \dot{V}_G = \dot{V}_H \quad (3.24)$$

- 2) Due to the conservation of mass (Kirchhoff's first law analogy), and not modelling the infiltration, the total mass flow rate through the chimney inlet and outlet is the sum of the mass flows through each storey:

$$\dot{V}_A \cdot \rho_A = \dot{V}_C \cdot \rho_C + \dot{V}_D \cdot \rho_D + \dot{V}_F \cdot \rho_F + \dot{V}_G \cdot \rho_G + \dot{V}_H \cdot \rho_H = \dot{V}_B \cdot \rho_B \quad (3.25)$$

- 3) The chimney's vertical cross-sectional area is defined to be constant throughout the building segment. This is realised by keeping all inlet areas from the chimney to the offices of a specific storey equal to the outlet area from the offices to the chimney. For example:

$$A_3 = A_5 \quad (3.26)$$

- 4) Moreover, the chimney's air inlet from and outlet to the environment are initially defined to be equally sized as the sum of the office inlets and outlets, and is therefore equal to the internal vertical chimney's cross-section - but can be adapted by a sizing factor k . With a sizing factor other than 1, the chimney's supply opening area and exhaust opening area will be sized as bigger and smaller than the internal chimney cross-sectional area, respectively:

$$k \cdot A_1 = A_3 + A_6 + A_9 + A_{12} + A_{15} = A_5 + A_8 + A_{11} + A_{14} + A_{14} = k \cdot A_2 \quad (3.27)$$

- 5) Finally, to reduce the internal flow resistance, the area of the internal overflow openings from the offices to the core are initially set twice (factor $K = 2$) the area of storey outlets to the chimney. A high value of K will increase the overflow opening area and therefore decrease the internal flow resistance. For example:

$$K \cdot A_4 = A_5 \quad (3.28)$$

The schematic in Figure 3.12 shows the arrangement of the openings and the flow path arrangement as specified before.

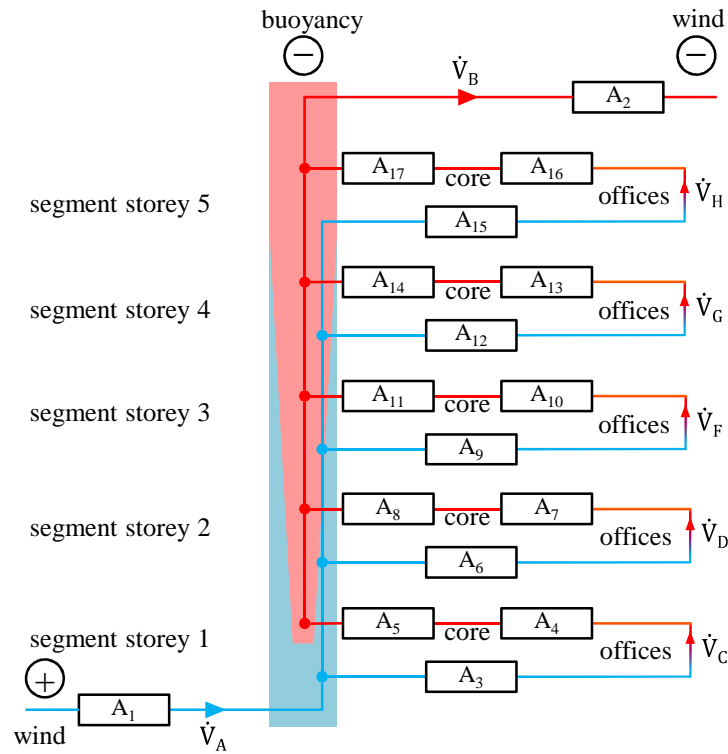


Figure 3.12: Schematic overview of the exemplary 5 storey per segment for volume flow calculations.

Flow path dimensioning / system sizing

The openings in the flow path are sized according to pressure differences, target air change rates, and flow path resistances. Planners can simply dimension openings, chimneys, and overflow air vents for the provision of fresh air and passive cooling in office buildings.

Although the tool developed can handle one to ten storeys per building segment, equations are exemplarily derived for the five-storey base-case scenario shown in Figure 3.13. This scenario is an eight-cell model with a well-mixed air assumption in each cell. The internal openings divide the envelope into seven internal cells. Overflow openings from the offices to the core area only represent an additional resistance. Cell A and Cell B can be considered as two conical stacks, one for fresh air supply and one for exhaust. The airflow rates satisfy the continuity equation for each cell and for the total envelope.

The model developed in the context of this thesis differs significantly from the envelope flow model developed by Etheridge [26]; the notation used is loosely based on that used by his models, i.e., the openings in the external envelope are denoted by lower number subscripts, the internal openings by higher numbers, and the segment cells by capital letter indices.

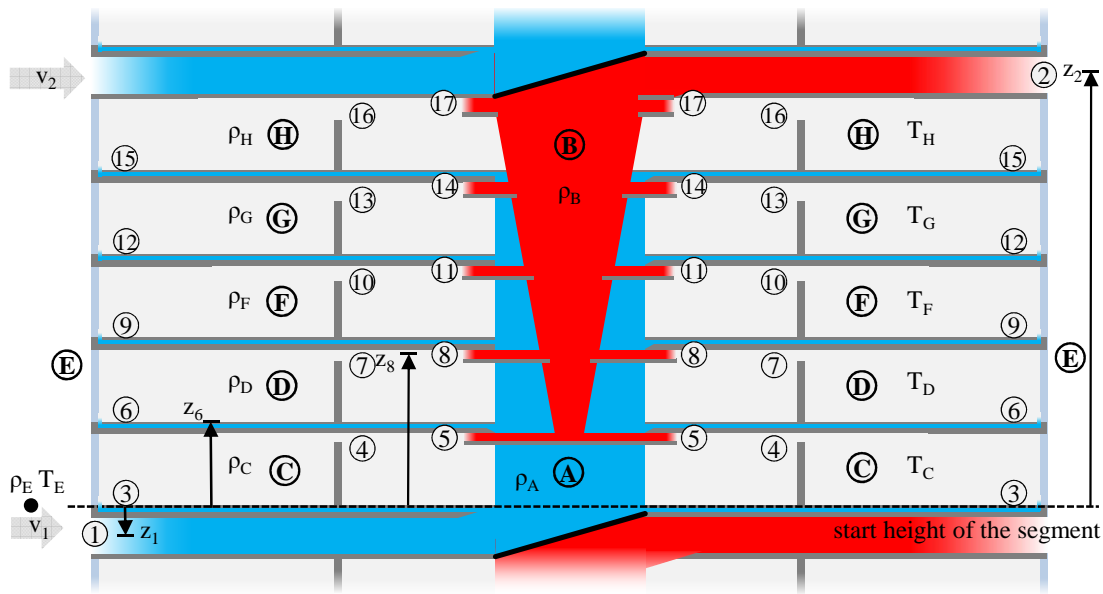


Figure 3.13: Configuration for applying the electric analogy method to upward flow ventilation of a seven-cell model of a five storey building segment.

The wind pressure share of the original equations integrates the ‘local wind speed’ (see § 3.2.1.1) on inlet and outlet opening heights instead of a constant value (without wind profile) for all openings as in the approach developed by Etheridge [26]. The external barometric pressure, the air temperature, and the density for moist air are calculated at start height of each building segment (see Figure 3.13) instead of a fixed reference external air density and temperature.

Integrating the design specification into the electric analogy model developed before, the resulting flow circuit model for an exemplary five-storey per building segment can be summarised as shown in Figure 3.14.

The resistance of flow paths for each storey is dependent on the openings’ flow resistances in series. Upon starting the iterating solvers described below, the ‘HighVent’ tool then automatically adapts the opening areas according to the design specifications to maintain the intended flow rates.

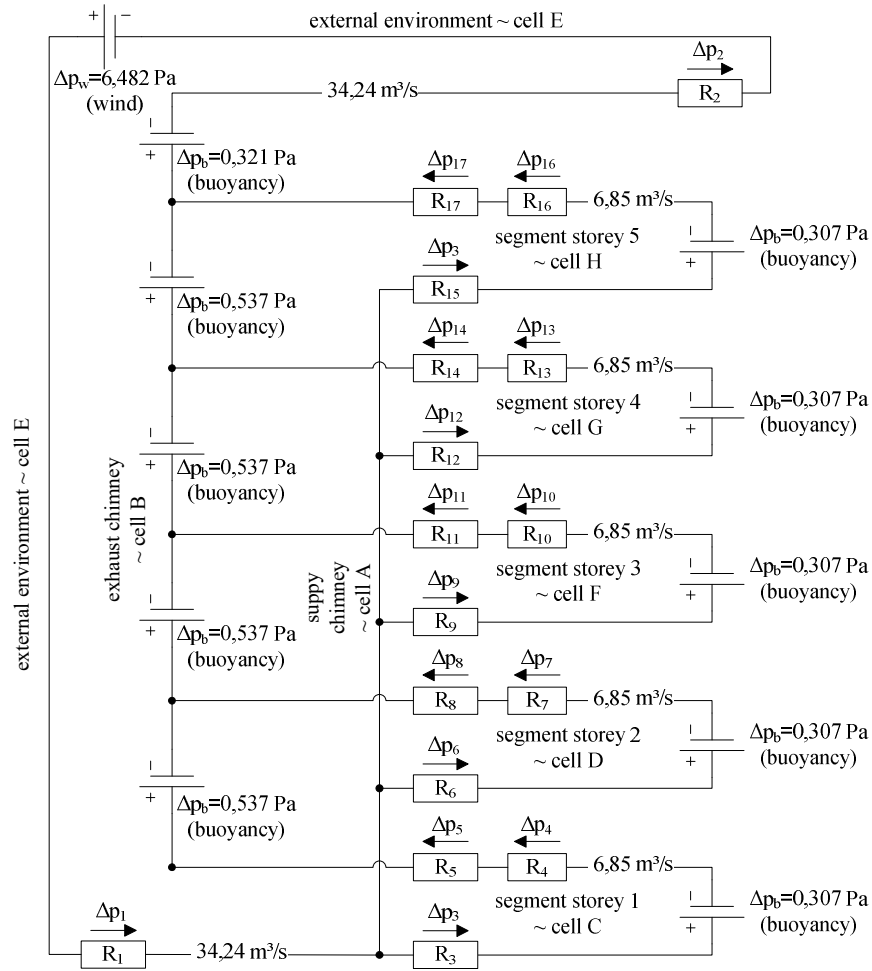


Figure 3.14: Fixed sizing boundary conditions natural ventilation model exemplarily for a segment including two chimney and five storey cells.

The solver seeks for a solution for each storey of the segment to fulfil Kirchhoff's 2nd law and the sizing specification defined before. Because each storey also influences the other storeys, the procedure is looped five times.

For the five-storey example of Figure 3.14, the changing parameters are the opening areas A_3 , A_6 , A_9 , A_{12} and A_{15} ; the other areas and all pressure drops change accordingly.

$$1^{\text{st}} \text{ storey:} \quad \Delta p_S = \Delta p_1 + \Delta p_2 + \Delta p_3 + \Delta p_4 + \Delta p_5 \quad (3.29)$$

$$2^{\text{nd}} \text{ storey:} \quad \Delta p_S = \Delta p_1 + \Delta p_2 + \Delta p_6 + \Delta p_7 + \Delta p_8 \quad (3.30)$$

$$3^{\text{rd}} \text{ storey:} \quad \Delta p_S = \Delta p_1 + \Delta p_2 + \Delta p_9 + \Delta p_{10} + \Delta p_{11} \quad (3.31)$$

$$4^{\text{th}} \text{ storey:} \quad \Delta p_S = \Delta p_1 + \Delta p_2 + \Delta p_{12} + \Delta p_{13} + \Delta p_{14} \quad (3.32)$$

$$5^{\text{th}} \text{ storey:} \quad \Delta p_S = \Delta p_1 + \Delta p_2 + \Delta p_{15} + \Delta p_{16} + \Delta p_{17} \quad (3.33)$$

where for upward flow direction, the reference density ρ_0 for the calculation of the pressure drop at the openings is

$$\text{for } \Delta p_1: \quad \rho_0 = \rho_E \quad (3.34)$$

$$\text{for } \Delta p_2: \quad \rho_0 = \rho_B \quad (3.35)$$

$$\text{for } \Delta p_{i=[3,6,9,12,15]}: \quad \rho_0 = \rho_A \quad (3.36)$$

$$\text{for all other } \Delta p_i: \quad \rho_0 = \rho_I \quad (3.37)$$

where ρ_I is the density of specific office cells.

3.2.2 Thermal model calculation method

Apart from the previously discussed air change rates, which directly influence air quality, thermal comfort is a crucial indicator in the evaluation of natural ventilation concepts. If thermal comfort can be guaranteed, then significant cooling and ventilation energy conservation can be achieved. The dynamic design day heat transfer model aims to provide guidance for the design, especially the system sizing of passive ventilated buildings by relating the system dimensions (Tool ‘Step 1’) to the comfort requirements reached (Tool ‘Step 2’). It dynamically reflects the climate, the internal and solar heat gains, the passive air driving forces, the thermal mass, the conduction through the envelope, and the impact of these parameters on internal temperatures and humidity. A matter of particular interest is the interaction of natural ventilation potentials and the diurnal cooling capacity of thermal mass with different sizing parameters, levels of heat gains, and simple control strategies for night-time ventilation only. This is in combination with fresh air for indoor air quality issues or with a strategy that allows increased air change rates even during daytime.

In this section, only a brief overview of the heat transfer models involved is given; the in-depth model description including equations is given in Appendix B. The ‘pre-processed’ summer design days referred to here are calculated according to the methodology described in § 5.3.3. A procedure with three iterations assumes that the design day is preceded by an infinite number of identical days of the same idealised weather.

3.2.2.1 Model components

Heat transfer in the model consists of a radiant share, a convective share, and a ventilative share. The radiant fraction is added to the thermal mass, which increases the surface temperature.

Internal air

The interior air space is treated as well-mixed with uniform air temperature distribution. For simplicity of the model, all heat gains or losses to the internal air are treated as sensible heat. The dynamic internal room air temperature includes the reservoir effect of the volumetric heat capacity of the cell air. The ventilative and convective fractions of the heat transfer are added to the air heat capacity, which results in the raising or lowering of internal air temperature.

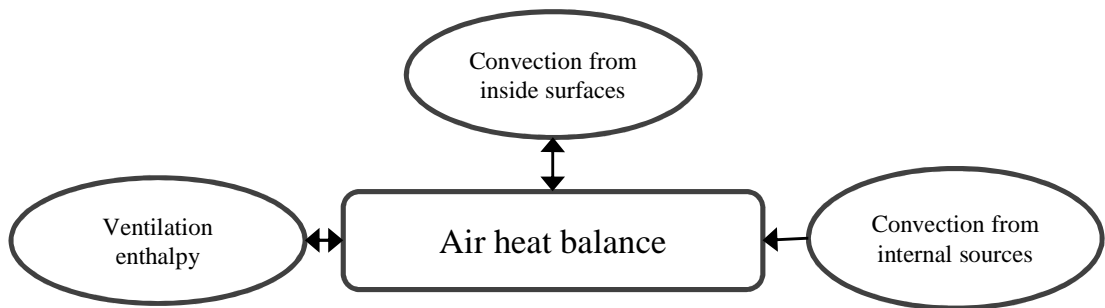


Figure 3.15: Schematic of the internal air heat balance.

Ventilation

In the dynamic thermal model of ‘Tool Step 2’, the flow rate is calculated according to fixed opening areas pre-calculated in ‘Tool Step 1’ for only one storey. Heat gains and losses due to ventilation per timestep ($\Delta t = 60$ s) are a function of the mass flow rate multiplied by the enthalpy difference between the external and the internal air. The mass flow rate per timestep is the volume flow rate multiplied by the mean air density between inside and outside.

External wall

The external wall is the opaque façade area depending on the façade's glazing ratio. A lumped capacity model manages the wall internal heat conduction and storage process, and is described below. The construction's heat gains and losses are treated according to Figure 3.16.

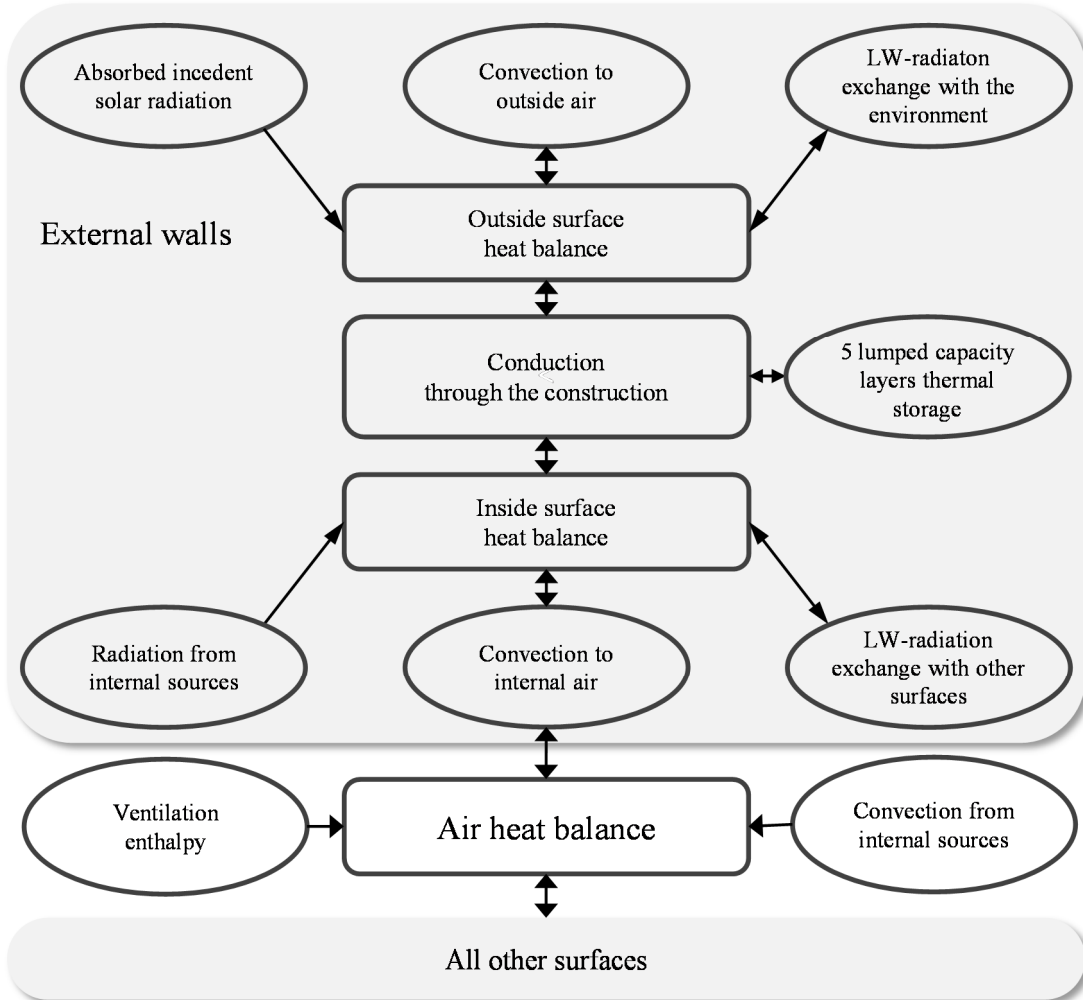


Figure 3.16: Schematic of the external wall heat balance model.

External window

All windows are combined to a single glazing model, where the window's total area is the façade area multiplied by the glazing ratio. Radiation incident on the external envelope is backcalculated from the 'pre-processed' transmitted solar radiation according to simple window indices. The construction's heat gains and losses are treated according to Figure 3.17.

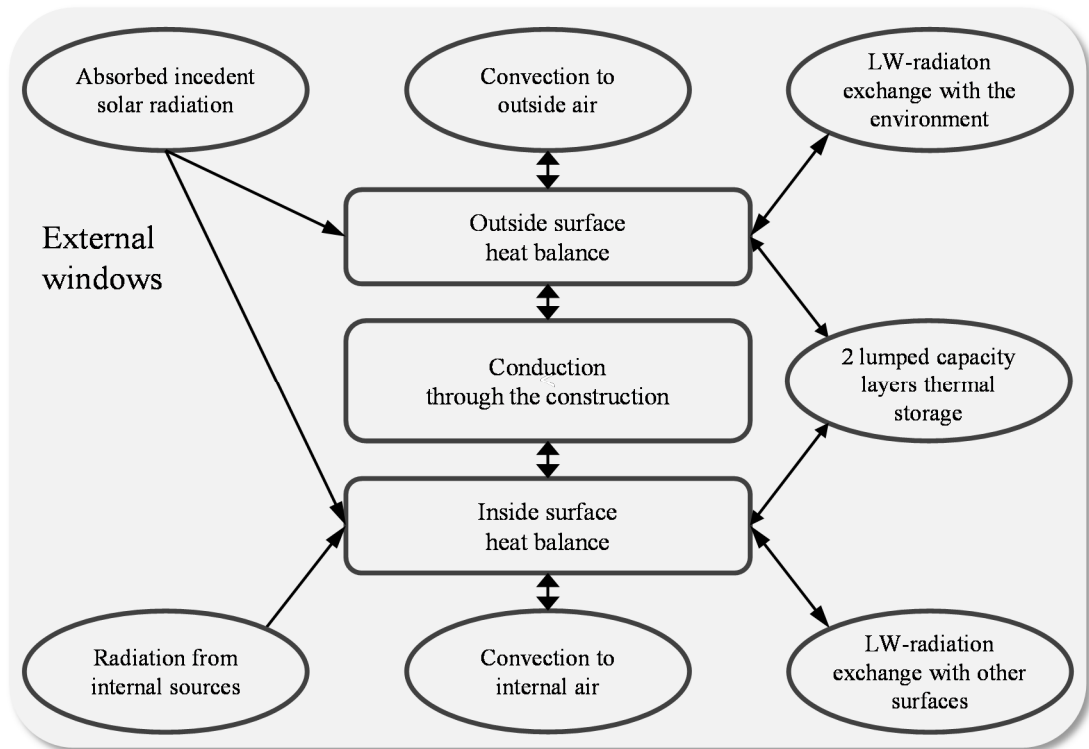


Figure 3.17: Schematic of the external window heat balance model.

The lumped capacity model for the glazing shown in Figure 3.18 has only two capacities, one for each pane. This is due to the material properties, which are high conductivity and low heat capacity of thin glass. A resistance was added between the panes to account for the thermal resistance of the gas fill, which is calculated according to the U-Value of the window minus the film coefficients on both sides of the window.

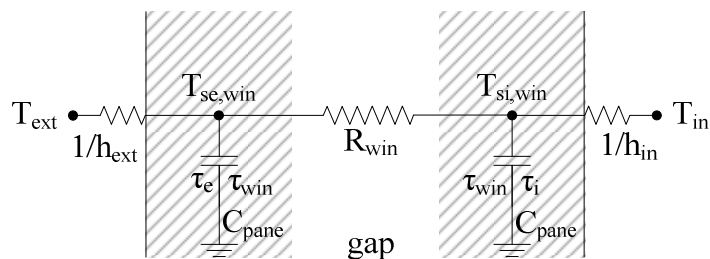


Figure 3.18: RC-model for the windows.

Internal floor / ceiling

The internal floor and ceiling of one storey are combined to one single construction with equal adjacent inside air conditions on both sides (and hence treated adiabatic). Again, a five layer lumped capacity model manages the internal heat conduction and storage process. The construction’s heat gains and losses are treated according to Figure 3.19.

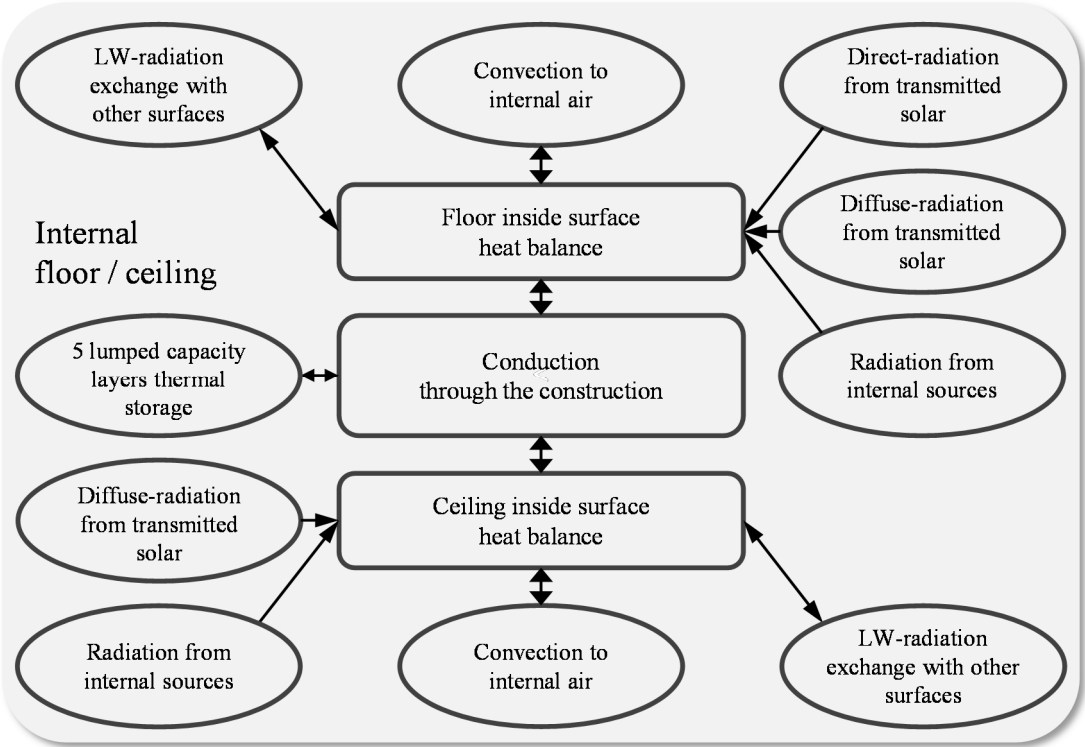


Figure 3.19: Schematic of the internal floor / ceiling adiabatic construction heat balance model.

Internal ‘additional’ mass

The tool developed also includes two ‘extra’ surfaces of one construction, which is called the ‘extra’ or ‘additional’ thermal mass construction. As an example, one of the uses of this construction would be to account for the heavyweight partitions within a space. As a general definition, the ‘extra’ thermal mass should be sized to represent all fabric within the space that is exposed to air, except the walls, the ceiling, the floor, and the windows. Figure 3.20 gives a schematic overview of the ‘extra’ mass model heat balance.

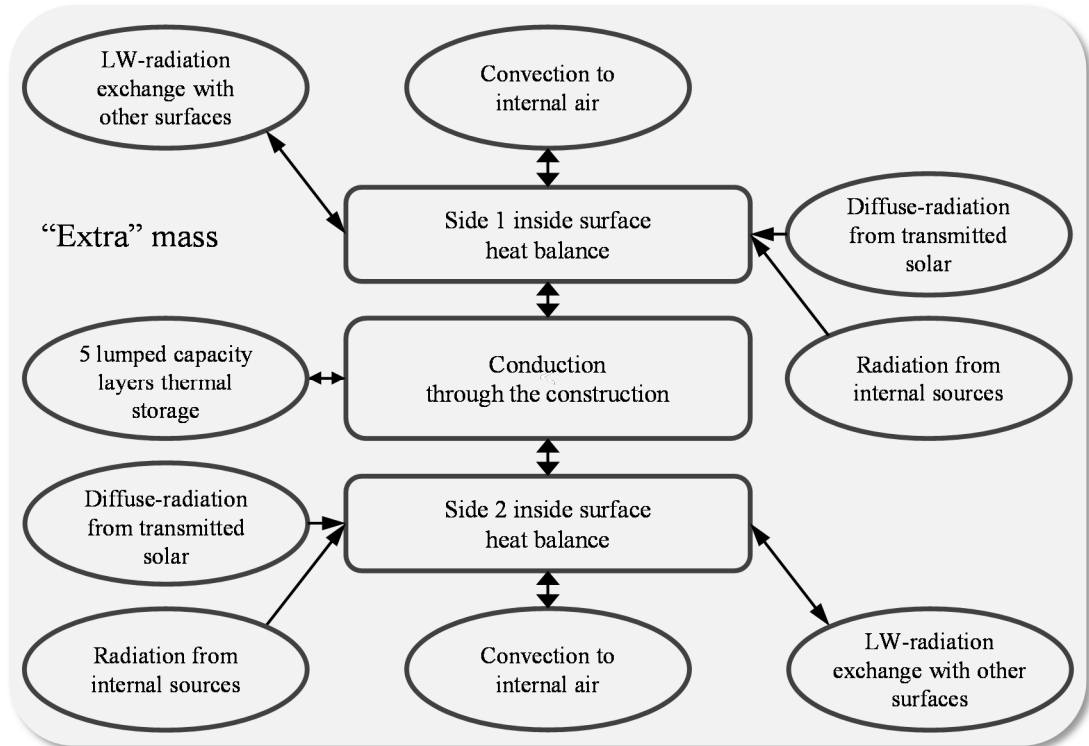


Figure 3.20: Schematic of the internal ‘extra’ mass construction heat balance model.

3.2.2.2 Heat transfer calculation methods

Convection

The surfaces’ convective heat transfer is realised by Newton’s law of cooling, which includes a constant heat transfer coefficient. The law states that the rate of heat loss of a body is proportional to the difference in temperatures between the body and its surroundings. In contrast, the convection model allows heat flow from the surroundings into the body, if the ambient air temperature is higher than the construction’s surface temperature. The external heat transfer coefficient is calculated for each timestep according to the Mobile Window Thermal Test (MoWiTT) method [127], and the internal heat transfer coefficient for each surface is a constant input value.

Radiation

Contrary to convective or conductive heat transfer, radiative heat transfer does not require any material medium for transport. The emitting rate depends on the absolute surface temperature and the surface emissivity. In the model, the grey body equation for two parallel surfaces is the governing equation, which approximates that the interaction between a given surface of a construction and the rest of the surfaces of an enclosure can be described as the interaction between the two surface elements.

One of these two surfaces has the surface temperature of the construction element, and the other surface has the mean radiant temperature of the surrounding elements, which here is the mean radiant temperature of a half sphere facing the surface. For internal heat exchange, the half sphere consists of all other construction surfaces facing the surface; for external heat exchange, the half sphere consists of the ground, the sky, and the atmosphere.

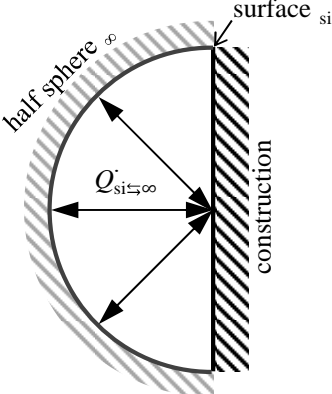


Figure 3.21: Long wave radiation exchange at the interior surfaces.

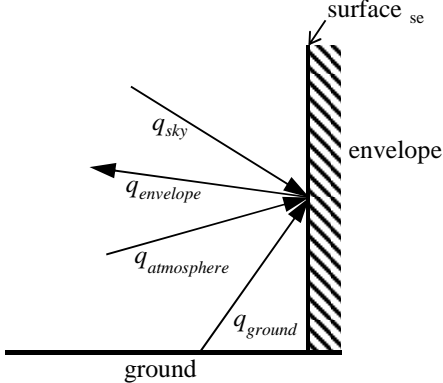


Figure 3.22: Long wave radiation exchange at the exterior surfaces.

Solar heat gains

The solar radiation incident on the construction surfaces has a direct component and a diffuse component. Surfaces either absorb or reflect a fraction of incident radiation. The transmitted solar radiation entering the cell is a ‘pre-processed’ hourly input value, which a user may gather from auxiliary building simulation programs like EnergyPlus (for inputs for the Kanyon building, see Appendix B). This is to avoid a time consuming and comprehensive calculation that includes the position of sun at each moment. Based on the position and optical properties of windows in the space, and with the consideration of multiple angular reflections, the fraction of the solar radiation entering the space that is incident on each surface is determined. 90% of the ‘pre-processed’ transmitted direct solar radiation is assumed to irradiate the floor surface. The other 10% direct solar radiation is uniformly distributed to the other internal surfaces facing the windows together with the diffuse transmitted solar radiation share. The diffuse transmitted solar radiation share is absorbed or reflected by all internal surfaces facing the windows depending on their areas and absorptance values.

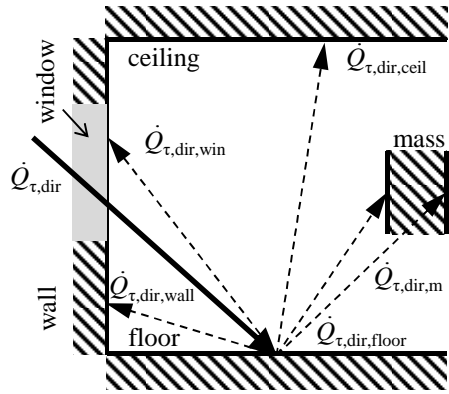


Figure 3.23: Direct solar beam distribution on interior surfaces.

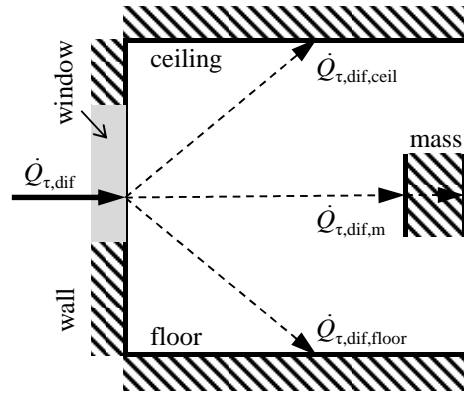


Figure 3.24: Diffuse solar beam distribution on interior surfaces.

Exterior solar radiation is absorbed, reflected, or if the surface is a window also transmitted by the surface. Values incident on the external envelope are backcalculated from the transmitted solar radiation according to simple window indices.

Internal heat gains

The internal heat sources are occupants, lights and equipment. Internal heat gains are a direct input to the design tool based on hourly value schedules, consisting of both convective and radiative shares. Internal heat gains are considered to be grey bodies that participate in the thermal radiation exchange, and sources of sensible heat for the heat and moisture balance in the room air module.

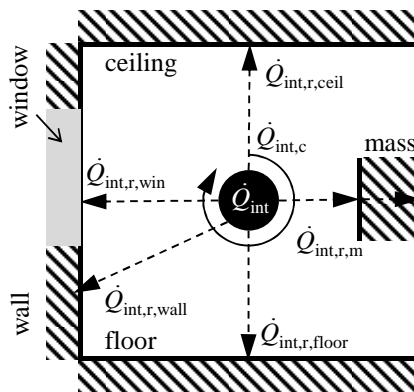


Figure 3.25: Internal heat gains distribution.

Thermal mass

Thermal mass is equivalent to thermal capacitance of a body, which is the ability to store thermal energy. Thermal mass can serve to flatten out the daily temperature fluctuations. This is because the thermal mass absorbs thermal energy when the surroundings are higher in temperature, and give thermal energy back when the

surroundings are cooler. Thus, thermal mass has the capability to time shift and lower the amplitude of indoor air peak temperatures.

The Lumped Capacitance Model (LCM) was utilised for the prediction of dynamic thermal behaviour. The model strongly reduces the complexity in the thermal model that is needed to represent the thermal response of multi-layered constructions. The LCM is however able to keep the overall accuracy of the full model, and is therefore utilised to facilitate the transient heat transfer process within a construction including mass. The LCM is an analytical one-dimensional network model, which employs the well-known analogies between the thermal and the electrical laws. With this analogy, the conductivity of the materials is interpreted as electric conductivity of a resistor, and the thermal mass as electrical capacity of a capacitor. The simple RC-network aims to solve the heat conduction/storage equation for solid layers by connecting construction layers to each other via a number of nodes (Figure 3.26).

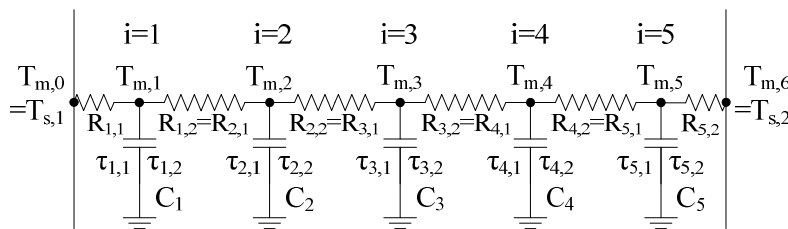


Figure 3.26: Layers of the Lumped Capacity Model (LCM) construction.

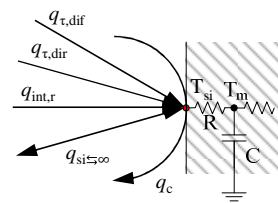


Figure 3.27: The heat flux balance at the surface node.

3.2.2.3 Adaptive comfort assessment

Operative temperature

With rising ambient air temperatures, the operative temperature is allowed to increase in naturally ventilated, non air-conditioned buildings. The average internal operative temperature of the space is the average of the internal mean air temperature and the internal mean radiant temperature [41,128]. It is a rough approximation as the influence of direct sunlight and air velocity is not reflected. Recommended operative temperatures are calculated for different comfort categories according to EN 15251 (for more details, see § 2.6.3). Because the design tool considers only one summer design day, which is out of the running timeframe context, the upper comfort limits are calculated only according to the mean external dry-bulb temperature of the design day itself. Figure 3.5 shows the adaptive comfort limits of EN 15251 category II for a typical summer design day.

Psychrometrics

The most widely used thermal comfort standards including air humidity account for the occupants of air-conditioned buildings, and have narrow thermal limits. They discourage the use of naturally ventilated passive solar buildings, where occupants have more relaxed expectations and can tolerate a wider temperature swing. The EN 15251 standard [41] accounts for personal adaptation by extending the thermal comfort limits depending on external conditions, but does not include the effect of humidity and air velocity.

To fill this gap, the design tool developed also includes psychrometric charts. A psychrometric chart graphically represents the thermodynamic properties of moist air. Humidity affects which temperatures are comfortable for the building occupants. People are most comfortable within appropriate ranges of temperature, relative humidity, and airflow. Daytime ventilation with higher indoor airspeeds directly affects the cooling sensation of building occupants when the temperature is felt as too warm. People naturally cool themselves by evaporation; higher humidity levels are more stressful.

Martinez *et al.* [129] developed extended comfort boundaries for hot summer conditions in office buildings. The occupants' adaptive behaviour has been investigated considering changes in airspeed, clothing level and transmitted solar radiation. It was found that the presence of diffuse solar radiation shifts the comfort limits towards cooler air temperatures by about 2 °C. Contrarily, increasing airspeed leads to an acceptance of warmer conditions, but this effect becomes less effective as the air velocity continues to rise. Moreover, increasing air velocities were found to be more effective in the presence of solar radiation. Figure 3.28 and Figure 3.29 show psychrometric adaptive comfort assessment limits of the tool developed according to Martinez *et al.* along with an exemplarily calculated diurnal course of internal moist air properties for a typical summer design day in Istanbul.

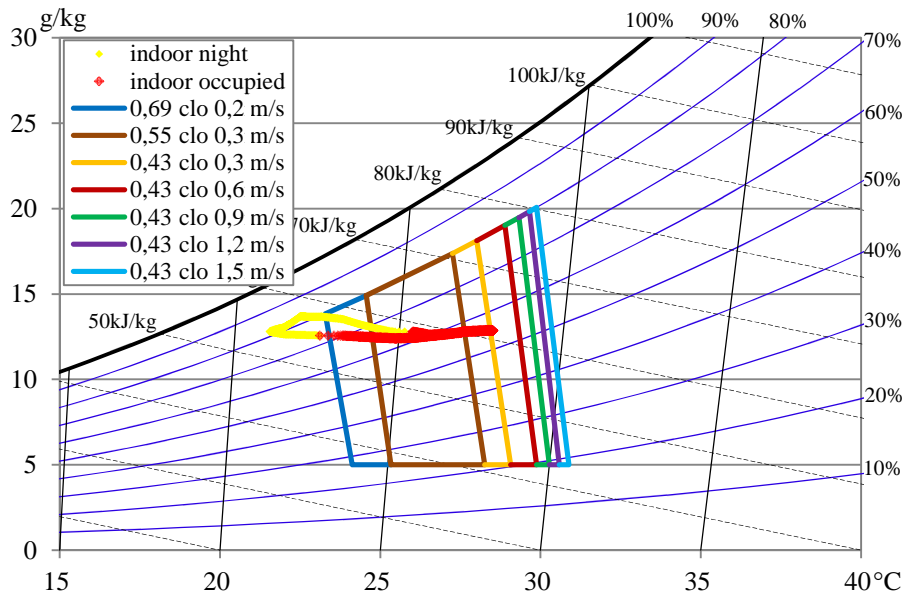


Figure 3.28: Exemplary indoor air conditions together with predicted comfort limits for 0 W/m² of solar radiation and different air velocities [129].

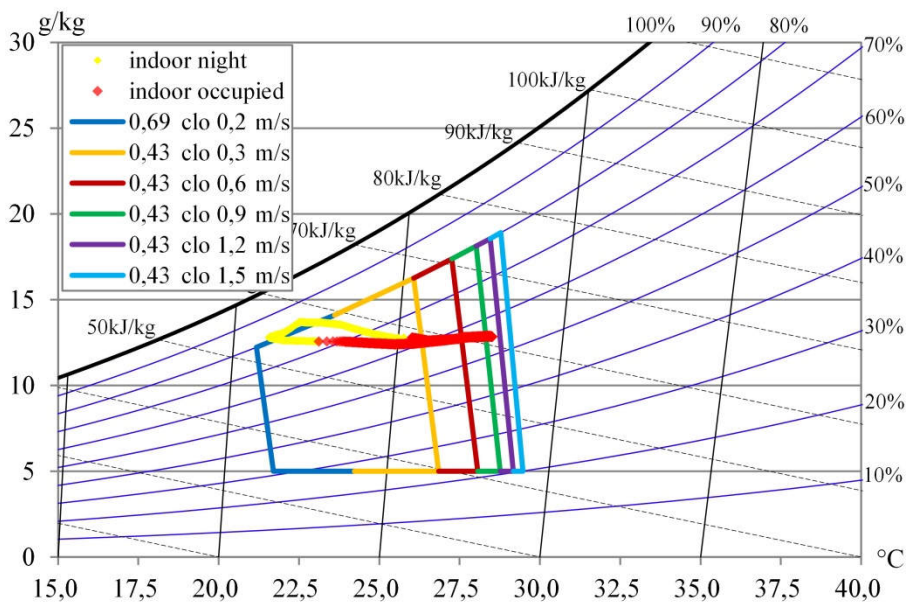


Figure 3.29: Exemplarily indoor air conditions together with predicted comfort limits for 50 W/m² of solar radiation and different air velocities [129].

3.2.2.4 Setting amounts of air for opening dimensioning

Natural ventilation serves to guarantee good indoor air quality and passive cooling in warm periods in order to achieve good thermal comfort without mechanical cooling systems. Therefore, the minimum design air change rate for a passive approach must be intense enough to guarantee the criteria defined for both IAQ and comfort (e.g., 95% of the occupied time in the category IDA II).

In terms of IAQ and according to the EN 13779 standard [55], 12,5 litres per second per person is sufficient to achieve medium air quality (IDA 2). To guarantee this hygienic volume flow rate during occupancy, the flow must also occur during the absence of wind, and design conditions are thus purely buoyancy driven.

High summer air change rates are desirable for passive ventilative cooling, e.g., removal of heat and cooling the building structure at night (according to Figure 2.19 up to 20 h^{-1} or more based on the volume of the building [43]). Here, combined wind and buoyancy forces can be assumed for the design. The amount of colder external air needed for cooling is not a fixed value but is dependent on the building, the usage, the operation, and the climate the building is located in. Therefore, to ‘fast-forward’ analyse the ventilative cooling potential of the natural ventilation system, in the ‘Tool Step 1’, the flow path is sized for a specific air change rate with unchanging boundary conditions including average local wind velocities for the hottest 91 days of the year. In the ‘Tool Step 2’, the dynamic thermal response of the building is investigated. The aim is to size the natural ventilation system in a way to stay within acceptable comfort boundaries since thermal comfort is a crucial indicator for evaluating the natural ventilation concepts. Based on the summer design days defined before (see SWMD approach in § 5.3.3), for this sizing-design assessment two requirements need to be achieved, as follows:

- The internal operative temperature stays within the category III comfort boundaries during the local climate extreme summer design day.
- The internal operative temperature stays within the category II comfort boundaries during the local climate typical summer design day.

Results of the tool can be found in passive cooling case-study application section § 6.2.

3.2.3 Tool validation

The sizing and design tool developed is validated against EnergyPlus [1] simulations. ‘Tool Step 1’ is validated against ‘pseudo’ steady state Airflow Network simulations with fixed boundary conditions, whereas ‘Tool Step 2’ is validated with dynamic design day boundaries according to § 5.3.3. Care was taken to set identical input and climate information for both the developed ‘High-Vent’ tool and EnergyPlus.

Steady state ('Tool Step 1')

To validate 'Tool Step 1' of the developed design tool, based on electric analogies against the airflow network of AIRNET (integrated into the EnergyPlus environment), a simple EnergyPlus simulation model is created for fixed boundary conditions.

As the internal and external temperatures in each simulation are stable throughout the whole run period (defined in the E+ design day object), different ventilation strategies can be analysed as if ventilation was decoupled from the building. This was realised first for the environment by setting up a design day object and then for the internal zones via 'ideal loads' – heating and cooling system objects with equal fixed setpoint temperatures.

The unchanging external wind velocities at the meteorological station are set 5,24 m/s, 2,11 m/s, and 0,85 m/s (design day values from § 5.3.3). The external air temperature is chosen as 25 °C. Including the atmospheric variation over height, the local air temperature at the inlet opening of the segment (49,75 m above ground level) is 24,68 °C. Adding the design temperature difference between inside and outside, the storey zones' air temperature is 27,68 °C and the temperature in the exhaust chimney is 28,68 °C.

To simplify the validation process, some model adaptations are equally made for both the electric analogy model and the AFN validation model. All other specifications are consistent with the design application scenario defined in § 6.3.

- Only one zone is simulated for each storey with two linkages to the inlet and the exhaust chimney. The internal flow resistance is set to zero to combine the core and the office zones into a single zone for each storey. In the electric analogy model, the factor K (resistance from office to core of each storey) was set to 1000, resulting in resistance values very close to zero. In the AFN model, the internal opening is simply not present.
- The inlet height from the supply chimney to the storeys is 0,50 m above the floor level height instead of 0,00 m to easily set up the model geometries without horizontal openings (i.e., with only vertical openings).
- The outlet opening from the storeys to the exhaust chimney are set to 3,00 m above the floor level height instead of 2,66 m.

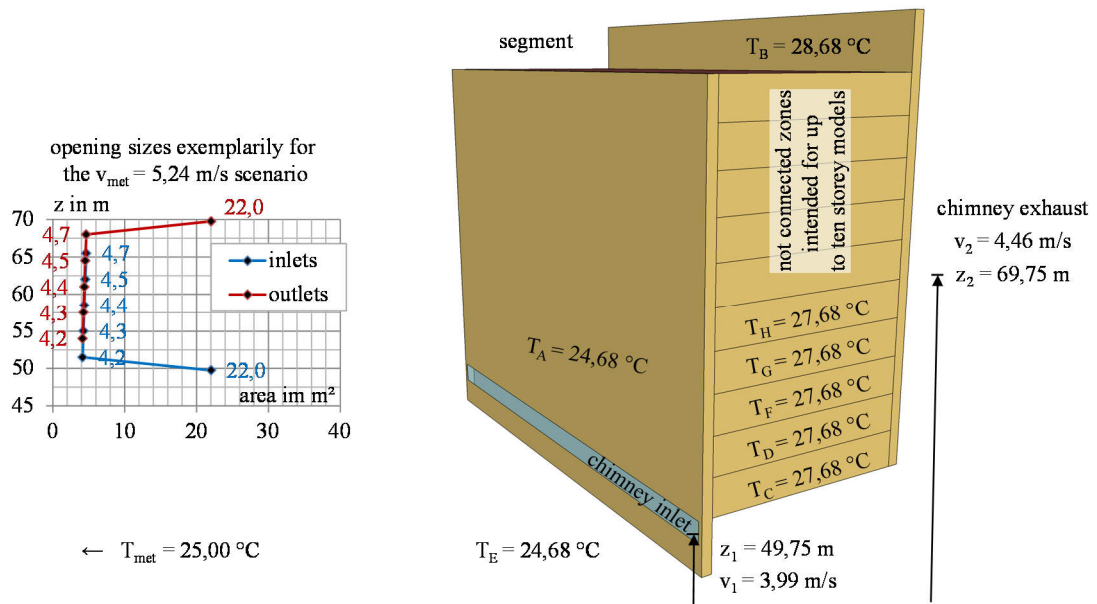


Figure 3.30: View from the inlet side on 12 zone AFN model representing one building segment.

Table 3.2: Deviation from 10 h^{-1} design air change rate (+ % indicates higher values from the AFN).

cell (storey) index I	scenario 1 $v_{met} = 5,24$ m/s	scenario 2 $v_{met} = 2,11$ m/s	scenario 3 $v_{met} = 0,85$ m/s
H	0,1%	3,3%	14,3%
G	-0,1%	1,8%	3,9%
F	-0,1%	0,8%	1,5%
D	-0,3%	0,2%	0,3%
C	-0,4%	-0,3%	-0,4%
mean deviation	-0,2%	1,2%	3,9%

The model developed fits reasonably well, especially for combined wind and buoyancy driven flows with high wind velocities as in the case of scenario 1. For buoyant flow as the main driving force, and with low exhaust stack heights for the upper storeys 4 and 5 of the segment, it was figured out that there were some problems within the EnergyPlus AFN buoyant model. Together with the EnergyPlus support team and the responsible person for the AFN⁵, it was concluded that the buoyancy forced calculations were partly buggy, and right now buoyancy alone may not always provide meaningful solutions. More precisely, a warning was given from the EnergyPlus support, that the model in some cases just gave a rough estimation. Further compounding the problem, the author of this thesis found a bug in the code. The AFN does not calculate the local temperature at the opening node height; instead, the local temperature is taken from zero height (ground level). To overcome this problem, temperature in the inlet chimney is reduced by a system of ideal loads to virtually adapt the inflow external air temperature towards the temperature at local

⁵ Staff: Lixing Gu

height. All other E+ modules except the AFN seem to consider the temperature variation over height. The EnergyPlus support is slated to fix the bug in a future E+ version.

Dynamic design day ('Tool Step 2')

To validate 'Tool Step 2' of the tool developed, another EnergyPlus simulation – a three zones, one-storey model (3rd storey of a segment at 51 m start height), is created for dynamic design day boundary conditions (from § 5.3.3) with unchanging wind velocity. More details of the simulation setup can be found in § 6.3.1.

In the first assessment, external conditions used in the developed tool are compared to the design day inputs used in the EnergyPlus simulation. As they are both based on the SWMD-approach developed before, they show identical properties as shown in Figure 3.31.

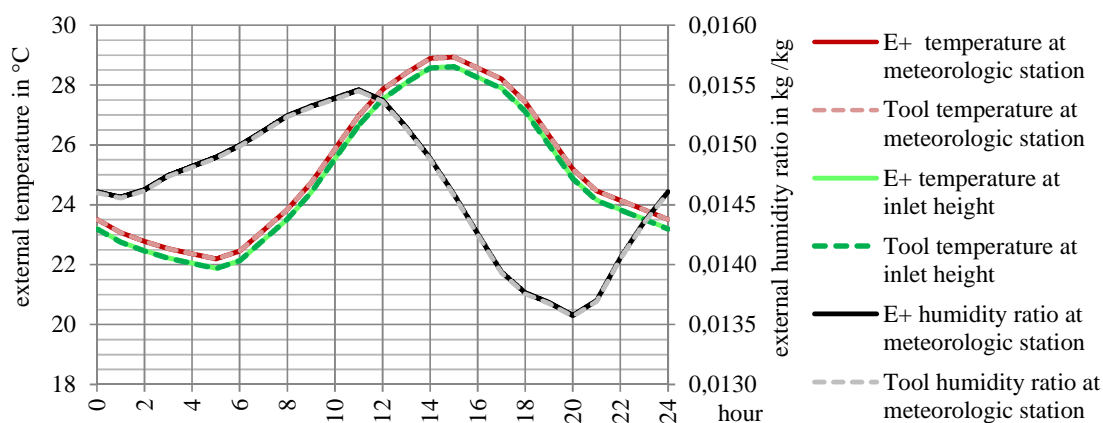


Figure 3.31: Tool validation dynamic environmental input parameters for Istanbul extreme summer design day.

The outcome of the most important test is shown in Figure 3.32. The comfort related parameters are compared to each other. Especially during occupancy, a good agreement was reached between the EXCEL-tool based simulations and EnergyPlus simulations. For Istanbul design day conditions, the most crucial parameter for system sizing, the peak internal operative temperature, has an aberration smaller than 0,1 °C. Also, the internal humidity fits well, especially during the building occupation hours.

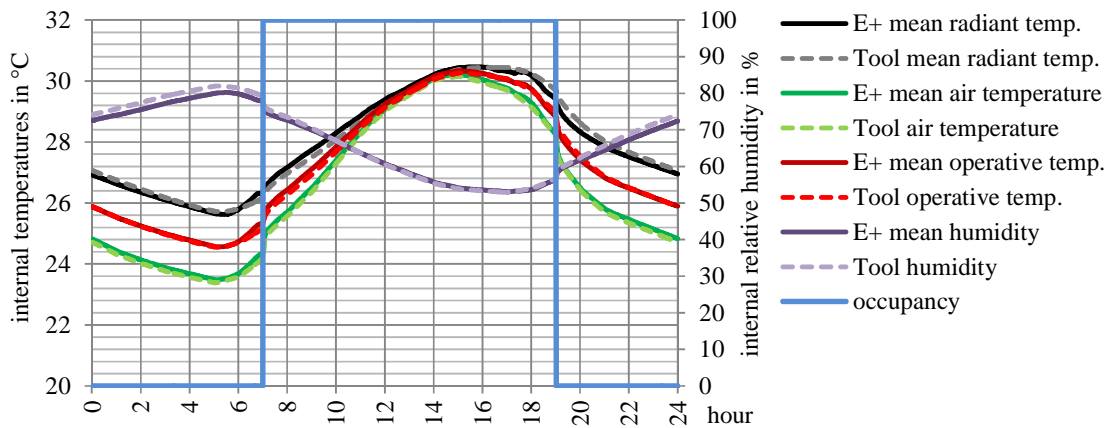


Figure 3.32: Tool validation dynamic internal output for Istanbul extreme summer design day and naturally ventilated base-case scenario.

Finally, the dynamic electric analogies model is validated against the airflow network of AIRNET. A good agreement was achieved here as well, as shown in Figure 3.33.

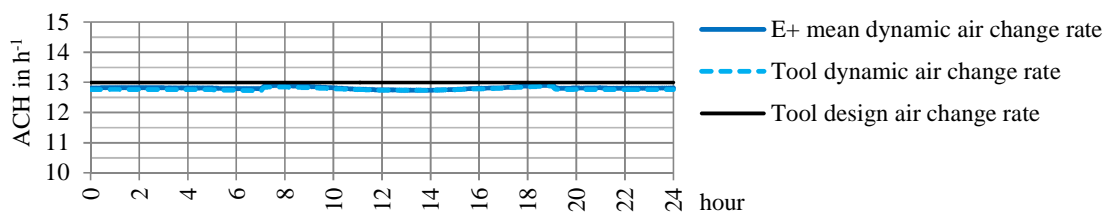


Figure 3.33: Tool validation dynamic air change rate for Istanbul extreme summer design day.

3.3 Detailed Design Development through Energy Simulation

To assess the potential of controlled natural ventilation in high-rise office buildings, the ‘HighVent’ design tool outputs, which are primarily the design parameters – the positioning and sizing of openings in the flow path, are ‘post-processed’ as inputs for detailed Building Energy Performance Simulations (BEPS) including AirFlow Networks (AFN).

BEPS tools predict the energy performance of a given building and thermal comfort for its occupants. They support the understanding of how a building operates and allows comparisons of different design alternatives. Limitations apply to almost every available program of this kind today, and hence it is necessary to understand basic principles of energy simulation.

Simulations are run to access long-term information about comfort, energy consumption and environmental impact. In contrast to the sizing tool developed, the overall annual performance for a specific climate including the mechanical systems

and controls can be considered. The simulations produce more data so that the active building performance can be compared to the passive approach developed. During the calculation process, the simulation takes into account the external climatic factors (see § 5.1), the internal heat sources, the Energy Management System (EMS) controls, the building constructions, the natural ventilation, and the mechanical systems to more accurately model the building. Building energy performance simulation therefore is a powerful method for studying the performance of buildings and for evaluating the architectural design decisions made.

Simulation outputs indicate difficulties and guide the designer to modify the initial sizing parameters gathered from the 'HighVent' design tool if necessary. This detailed design development also includes the original natural ventilation controls developed and the hybrid cooling as a design alternative.

Moreover, parametric analyses are intended to show the influence of system sizing parameters on the performance of the developed approach. The system can be resized by conducting a sensitivity analysis to study the relative impact of the design characteristics.

3.3.1 Simulation environment

The simulations are performed using the whole building energy performance simulation program EnergyPlus version 8.1. The program can model natural ventilation systems using an airflow network approach. EnergyPlus is an open source thermal simulation code developed for the United States Department of Energy. The availability of several software interfaces and the increasing number of models included contributes to the use of this tool both in design and research contexts.

3.3.1.1 Building energy performance simulation

EnergyPlus is modular in structure and uses the heat balance technique to dynamically simulate thermal loads with timesteps of less than one hour. In many aspects of the model, the level of detail is variable, e.g., calculation of solar gains and their distribution, surface convection algorithm, controls, adiabatic boundaries or full model, detailed mechanical systems or net load supply, number of timesteps per hour, etc. [122,128].

3.3.1.2 Airflow network

EnergyPlus contains a fully-integrated network model for calculating building airflows and their impact on comfort and building energy use. The Airflow Network (AFN) consists of a set of nodes linked by airflow components and represents a simplified airflow model. The flow elements correspond to openings and calculate the airflow rates, and buoyancy flows are calculated by air density differences.

The actual AFN model can be used for simulating the impacts of multi-zone airflows due to wind pressure and stack effects. The multi-zone airflow calculations are performed at the HVAC system timestep which, among other benefits, allows for modelling hybrid ventilation systems [130]. It can simulate several key components which influence airflow, e.g., cracks, ducts, fans, flow controllers, vertical large openings (windows and/or doors), horizontal openings, and passive stacks. With a well-mixed assumption, a building is subdivided into zones with homogeneous air properties.

The EnergyPlus AFN is mainly based on the algorithms AIRNET [67] and COMIS [69]. EnergyPlus program was linked in an early version with COMIS including airflow in the zone load calculations [78]. In a later version, the AIRNET/CONTAM model was introduced in EnergyPlus and replaced most of the previous links [130].

3.3.1.3 Building energy management system

Starting from 2009, the relatively new Energy Management System (EMS) feature [131] in EnergyPlus provides a way to develop custom rule-based control routines allowing fine details of how the model runs basically with defined sensors and actors (such as temperature sensors and opening damper actors). This high-level, supervisory control can override or extend some annoying predefined behaviour and therefore solve many problems faced by energy modellers. A small programming language called EnergyPlus Runtime Language (Erl) is used to describe the control algorithms.

3.3.1.4 Geometry editor

The Open Studio plug-in for Google's SketchUp was also created by the National Renewable Energy Laboratory for the U.S. Department of Energy. It is mainly a geometry editor for EnergyPlus. It allows creating the building geometry from

scratch by adding, modifying or deleting, e.g., thermal zones, heat transfer surfaces, windows, and other openings or shading surfaces. The plugin can read EnergyPlus input files, whether or not they were drawn with the plugin.

3.3.1.5 Model limitations and surface convection

There are several assumptions to be made from the program internal calculations and by the person using the simulation environment. Weather data and user input such as internal heat gains and the thermodynamic concepts for energy simulation are already based on assumptions. These assumptions are necessary so that complex interactions can be simplified and managed. The program user needs to be aware of this fact and must be able to decide whether they are reasonable for the specified simulation task. Therefore, for the generation of realistic and reliable simulation results, thermal processes need to be understood, and limitations of the programs need to be known. Easy-to-use interfaces alone therefore do not make energy analysis available to everyone. Building energy performance simulation is typically used to compare design alternatives, rather than to predict the actual energy performance of buildings. To discuss all limitations within the simulation program would exceed the scope of this thesis. Maile *et al.* [132] documented approximations, assumptions, and simplifications in Building Energy Performance Simulation. Lixing Gu [130] described the input objects, calculation procedures, model validation, and example results for the airflow network model in EnergyPlus.

For example, one parameter mainly affecting the performance of night-time ventilation is the heat transfer at the internal room surfaces. The surface convective heat transfer is simulated separately from radiation by a convective heat transfer coefficient and by the temperature difference between the room air and the internal surface. Especially, the assessment of heat transfer by convection is strongly simplified when compared to the current state of modelling of radiation and conduction [133], and is a high priority research topic [134]. BEPS programs like EnergyPlus assume isothermal surfaces, approximating a complete zone by only one air node and select an appropriate value for the convective heat transfer coefficient (CHTC) at each timestep and for each surface. Algorithms based on ACH or supply air temperature are developed for mechanical systems, and therefore have to be used with care when natural ventilation (E+ internally processed as infiltration) is applied

since the CHTC calculations might be based on wrong parameters. When simulating a building with night ventilation, this becomes increasingly problematic because convective cooling is a major parameter. Increased convection can be expected due to high forced airflow rates and the possibility of a cold air jet flowing along the ceiling, but the magnitude of these effects is hard to predict [2]. Moreover, experiments with displacement ventilation supplying the cool air at the floor level by diffusers showed that to a large extent the convective heat transfer occurs at the floor surfaces. For example, for this configuration Novoselac *et al.* [38] measured a convective heat flux at the floor surface from 51 to 82% of the total convective surface heat flux. By cooling down the floor, this surface then represents a radiative sink for the other room surfaces. Thus, correlation formulae or values are only rule-of-thumb formulae, and may not take into account the specific flow details in the regions adjacent to the walls and the spatial variability. However, Artmann *et al.* [135] found significant sensitivity to heat transfer only for total heat transfer coefficients below about 4 - 8 W/m²-K depending on the level of thermal mass.

The European standard EN ISO 13791 provides general criteria and calculation procedures for the summer thermal performance of buildings without mechanical cooling. Values for the convective heat transfer coefficients for internal surfaces are given with 2,5 W/m²-K for vertical surfaces (e.g., wall), 5,0 W/m²-K for horizontal surfaces (e.g., ceiling and floor) with upward heat flow (e.g., temp. floor > air), and 0,7 W/m²-K for horizontal surfaces with downward heat flow (e.g., temp. ceiling > air). The CIBSE traditional average value of 3 W/m²-K for all internal surfaces can be considered close but less detailed compared to the ones provided by EN ISO 13791.

However, in this study and for the adapted passive and hybrid cases as specified in the overview in Table 6.3, the convective heat transfer coefficients of the EN ISO 13791 standard are applied to the simulation model. These values are used as this study is intended to generally determine the night-cooling potential for naturally ventilated buildings, without going too much into the details of how the flow is exactly distributed (e.g., via displacement, mixing or cross ventilation). Moreover, for the horizontal surfaces the CHTC is programmed by the author of this thesis dynamically with the EMS Runtime Language, depending on the heat flow direction.

For the mechanically operated as-built reference case, the EnergyPlus default TARP [122] algorithm was employed. TARP is a comprehensive natural convection model derived by Walton [136] based on ASHRAE literature [92].

Another fundamental simplification of the thermal zone calculation method utilised is the so-called well-mixed assumption. This treats that the air in each zone is modelled as well-mixed with uniform temperature throughout. Moreover, the surface temperatures are treated to be uniform, and the long and short wave irradiation and heat conduction are one dimensional. [137]

3.3.1.6 Thermal Comfort

To assess the thermal comfort, the European CEN 15251 standard ‘Indoor environmental input parameters for design and assessment of energy performance of buildings addressing indoor air quality, thermal environment, lighting and acoustics’ [41] is applied. These parameters account for people’s clothing adaptation in naturally conditioned spaces by relating the acceptable range of indoor temperatures to the outdoor climate. EnergyPlus version 8.1 is able to report directly the thermal comfort based on the adaptive comfort criteria as output for each zone.

In addition to the CEN standard, and since air humidity is a driving factor for thermal comfort, the resulting indoor air properties during building occupancy are also analysed by psychrometric charts and by the occurrence frequency during occupancy.

3.3.2 Control strategies for the naturally ventilated offices

The control strategy for natural ventilation developed here serves to ensure acceptable air quality, compliance with the limits of comfort, and a best possible energy efficient building operation. Energy efficiency is achieved by means of passive cooling and by optimal fresh air control during winter operation. However, for the sake of simplicity, the following rule-based prediction is utilised. The EMS (Energy Management System) control algorithm is implemented in the EnergyPlus simulation model and serves the following components:

- Indoor air quality control by replacing polluted air by external air during occupation.

- Advective daytime ventilation to directly cool building interiors by replacing warm indoor air with cooler outdoor air when conditions are favourable.
- Personal daytime ventilation to directly cool building occupants by directing cool outdoor air over building occupants at sufficient velocity to enhance convective transport of heat and moisture from the occupants in the hottest season. According to Givoni [8] (see § 5.2.2), a breeze of about 2 m/s effectively enhances convective transport of heat and moisture from the occupants. Also, the external temperature should not be colder than 20 °C. As the models utilised in this study calculate the volume flow rather than the air velocities, these internal air velocities are considered here with an intense target ventilation rate of 15 h⁻¹.
- Night ventilation to precool the building's structure by exploiting cool ambient temperatures. Care must be taken not to overcool the building, especially for the next morning.

Table 3.3: Overview of the modelled natural ventilation controls.

IAQ control	advective cooling	personal cooling	precooling
enable criteria			
<ul style="list-style-type: none"> • during occupation • if hybrid systems = off 	<ul style="list-style-type: none"> • during occupation • if hybrid systems = off 	<ul style="list-style-type: none"> • during occupation • if hybrid systems = off 	<ul style="list-style-type: none"> • during non-occupation • if previous day average afternoon external air temp. > 16 °C
start operation criteria			
<ul style="list-style-type: none"> • if number of occupants > 0 	<ul style="list-style-type: none"> • if indoor temp. > min. temp. (Figure 3.35) 	<ul style="list-style-type: none"> • if indoor temp. > min. temp. (Figure 3.35) • if external air temp. > 20 °C 	<ul style="list-style-type: none"> • if indoor temp. > min. temp. (Figure 3.35) • if external air temp. > 12 °C
end operation criteria			
<ul style="list-style-type: none"> • if number of occupants = 0 	<ul style="list-style-type: none"> • if indoor temp. < min. temp. (Figure 3.35) 	<ul style="list-style-type: none"> • if indoor temp. < min. temp. (Figure 3.35) • if external air temp. < 20 °C 	<ul style="list-style-type: none"> • if indoor temp. < min. temp. (Figure 3.35) • if external air temp. < 12 °C
operation period			
<ul style="list-style-type: none"> • enable operation during entire period 	<ul style="list-style-type: none"> • enable operation during day from 7-19h 	<ul style="list-style-type: none"> • enable operation during day from 11-19h 	<ul style="list-style-type: none"> • enable operation during night from 19-7h
target air change rate			
<ul style="list-style-type: none"> • 14 litres per second per person 	<ul style="list-style-type: none"> • 0 - 10 air changes per hour 	<ul style="list-style-type: none"> • 10 - 15 air changes per hour 	<ul style="list-style-type: none"> • 0 - 15 air changes per hour

3.3.2.1 Rules on indoor air quality

This is the primary winter control mode during times of occupation. The main difficulty is to provide sufficient, but not excessive background ventilation while avoiding draughts. Moreover, ventilative heat losses should be minimised. Therefore,

to keep the ventilation rates sufficient but at a minimum level, ventilation occurs only during occupation of the office space. The amount of ventilation required is defined by 14 litres per second per person, which is the initial amount the HVAC systems control was planned for by ARUP⁶. This volume flow is at the upper limit for medium indoor air quality according to the EN 13779 standard [55], which is 15 l/s-person. So, the control does not again reflect the actual usage (2 ACH according to § 4.2.4) of the building but only the initial design values. To avoid droughts, the naturally forced incoming air in the heating season is preheated to 17 °C in the sub-floor distribution system, which is also the setback temperature setpoint of the office zones during night.

3.3.2.2 Rules on cooling

During daytime

Field tests in the RADEX-building in the context of the NatVent study [106] (see § 2.5.4) showed that the occupants would not accept frequent adjustment positions of the windows. Therefore, to avoid such frequent adjustments, the windows of the prototype developed were not controlled by simple feedback control. Instead, a predictive control system was applied, which aims to put the tilt angle of the openings in a position that is most likely the best for stabilising the internal operative temperature for the next period. Windows were adjusted only at proper moments when the office space was not occupied.

The control algorithms developed in the context of this research, to some extent are adapted from the feedforward controls described. The apertures should be opened and closed in such a way that the building can be kept between the limits of comfort, and in hot season should be able to cool the occupants by directing the cool outdoor air at sufficient velocity. However, the control can adjust every 10 minutes, which is the timestep of simulations. But because of the thermal reservoir or capacity of the office space, the control cannot end up in an on/off situation and is only slowly adapting according the internal temperature. Besides this, the opening control does not target a window opening angle with an unknown air exchange, but a target air change rate, which is based on pre-calculated pressure drops and flow resistances between the inlets and the outlets (see § 3.3.2.3 below). The maximum target air

⁶ ARUP, Kanyon office block mechanic installation report, 2003, Turkey

change rate is 15 ACH if the external air temperature is above 20 °C and 10 ACH if below 20 °C.

The ventilation rate is controlled in a way to keep internal temperature within the comfort limits. If the operative temperature exceeds the lower limit of comfort, category I ($T_{c1,min}$) [41], but not smaller than 21,75 °C (so as not to drop below the heating setpoint), ventilation for cooling is switched on. The control therefore does not target a static lower boundary setpoint but the adaptive comfort limit, depending on the weighted mean external temperature of the previous week (see § 2.6.3). The more this lower temperature limit is exceeded, the higher the target air change rate will be. Two amplifiers are intended to raise the target air change rate: one exponentially ($\varepsilon = 2$) raises the value depending on the operative temperature above the comfort lower comfort limit; the other, is linear (λ according to Figure 3.34), dependent only on the external air temperature and aims to reduce the risk of draught, and also assists to prevent overcooling:

$$ACH_{target} = \lambda \cdot (T_{op} - T_{c1,min})^2 \quad (3.38)$$

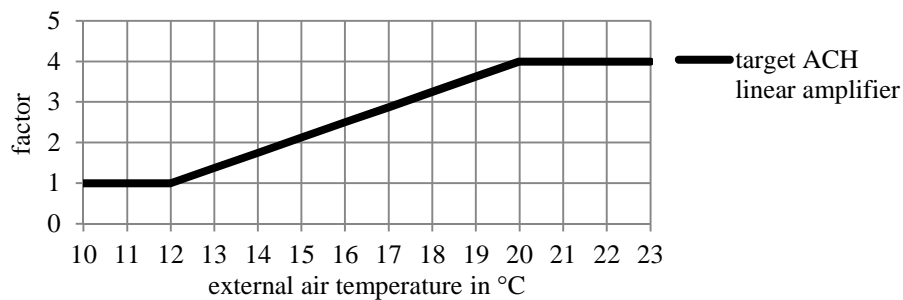


Figure 3.34: Linear amplifier correction factor λ dependent on the external temperature.

For example, if the operative indoor temperature is 1,5 °C above comfort category I and the external air temperature is 17,0 °C, then the openings are controlled in such a way as to achieve 6,5 air changes per hour.

The two amplifiers can be adapted depending on the climate, and building design and operation (e.g., heat gains from interiors and the transmitted solar radiation). Theoretically, if the occupant does not accept these air change rates, they can be manually overridden.

During night

At night with no inhabitants inside, a similar kind of algorithm is active. The opening areas are modulated in such a way that the building is pre-cooled to the extent that for

the next day the indoor climate can be kept between the comfort limits. The temperature limits are set below comfort conditions because comfort is then not a relevant factor. The control therefore first targets to keep the temperature below comfort conditions if the external conditions are suitable. External conditions are assumed as suitable only if the previous day's afternoon temperature was above 16 °C. It then raises the temperature to comfortable conditions before the morning hours so as not to create discomfort at the beginning of occupation. Again, the algorithm adapts itself to account for the colder inside air. By this procedure, the building is pre-cooled and prepared to withstand heat gains during the office hours.

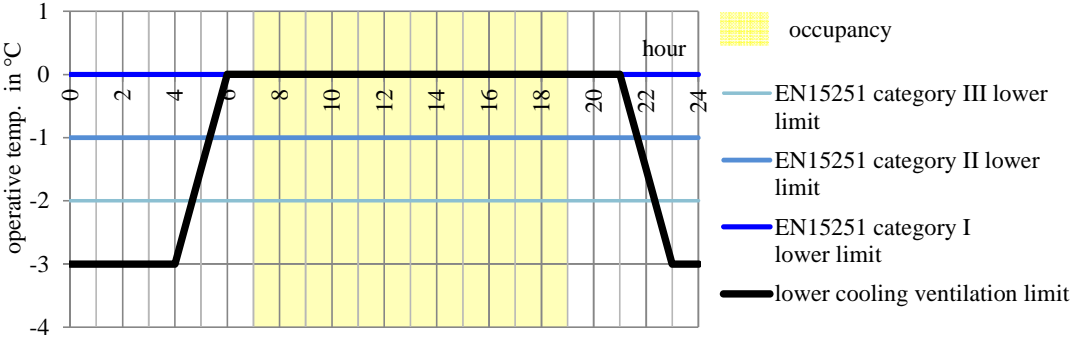


Figure 3.35: Ventilative cooling lower temperature limit for night-time ventilation in warm period.

3.3.2.3 Placement of sensors and actors

The openings are controlled by sensors and actors, included into the virtual building energy management system, which for the aim of this study is programmed inside EnergyPlus with the Runtime Language. The objective of the control algorithm is to achieve relatively constant air change rates by control of the flow resistance as described in § 3.2.1.2, and from the knowledge of actual driving forces as described in § 3.2.1.1. For predicting the dynamic driving forces (pressure differences), sensors have to be placed outside and inside the building. In the model, external sensors measure the wind speed and the temperature.

If the hybrid cooling and ventilation in the office rooms is operating, then the inlet chimney is connected to the outlet chimney by a bypass to remove the heat directly from the data centres (see Figure 3.36).

Table 3.4: List of sensors for flow control in the EMS model.

sensors	
external wind velocity	v_z m/s
external temperature	T_E °C
supply chimney temperature (if $\neq T_E$)	T_A °C
office internal temperatures	T_I °C
exhaust chimney temperature (if $\neq T_I$)	T_B °C

The wind pressure difference between the inlets and the outlets can then be calculated together with the wind pressure coefficient gathered from the wind tunnel experiments. The buoyant pressure differences are calculated according to the differences in height and temperature. With the knowledge of adjustable flow resistance or pressure drop of each opening, the volume flow can be controlled according to the target air change rates of each cell.

$$\dot{V} = C_d \cdot A_{\text{eff}} \cdot \sqrt{\frac{2 \cdot |\Delta p|}{\rho_{\text{air}}}} \quad (3.39)$$

To control the unintended infiltration through the building envelope, the openings are controlled at the inlets and the outlets of each storey. This has the advantage that the openings are controlled at low stack heights, e.g., not pulling air from the storey envelop to the high level chimney exhaust during winter operation, when buoyancy forces due to large temperature differences are very strong.

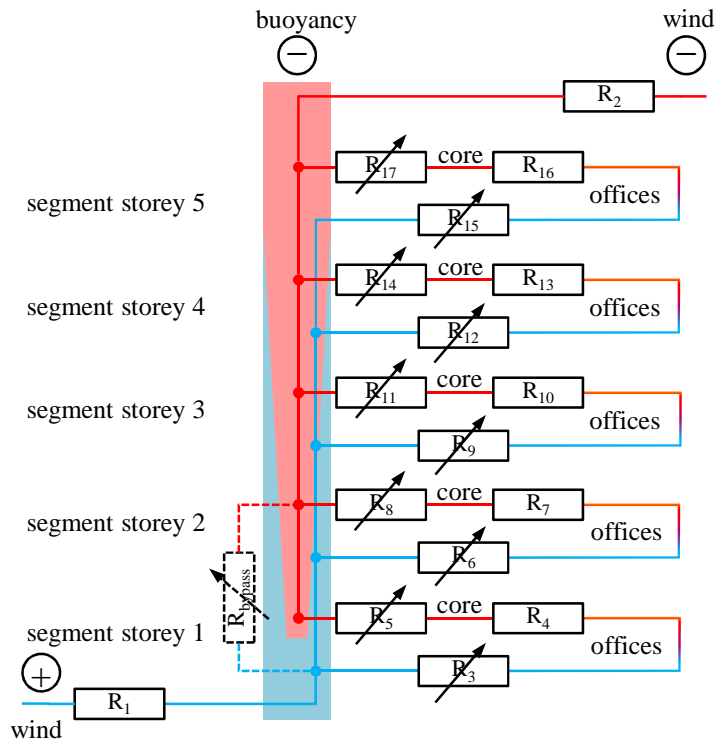


Figure 3.36: Placement of the controlled openings (actors).

In real world applications of this approach, the EMS might not have all the information necessary to predict the resulting air change rate and to control effective opening areas. In such cases, local pressure sensors may fill the knowledge gap, e.g., the local wind speed and the pressure coefficients. Also, if the external conditions are not measured locally but globally, e.g., at the top of the building, the wind sensor has to be placed in a free stream region not to be influenced by local turbulences. Global environmental sensor inputs can then be used to calculate the local conditions at the supply chimney inlet and the exhaust chimney outlet of each building segment according the method described before (see § 3.2.1.1). Internal temperature and pressure sensors have to be carefully placed, which in the dynamic EnergyPlus model is less critical due to a well-mixed air temperature assumption in each zone.

3.3.2.4 Operation Examples

Figure 3.37 and Figure 3.38 give insight into the EMS natural ventilation control over the course of typical design weeks. According to the controls described, intended natural airflow is on if (i) the building is occupied, or (ii) the internal lower operative temperature limit is exceeded. During nights, with a previous day afternoon mean external temperature above 16 °C, night ventilation operates at lower temperature limits. Ventilations rates stay low for providing fresh air only, rising fast in warm periods when the internal temperatures are high.

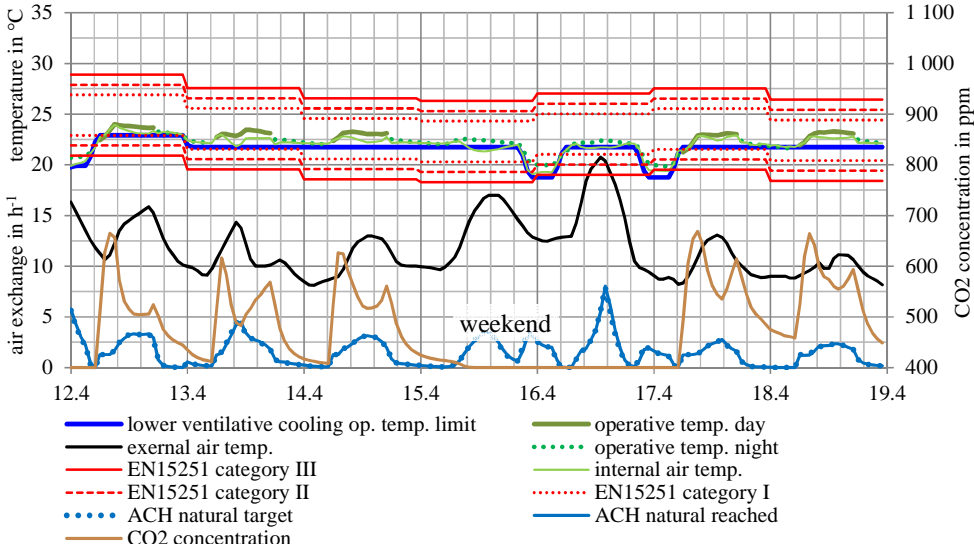


Figure 3.37: Resulting EMS controlled air change rate for a typical spring week in Istanbul.

If the natural driving forces are too small to achieve the target air change rate, the resulting air change rate corresponds to this smaller amount of air exchange as exemplarily shown in Figure 3.38.

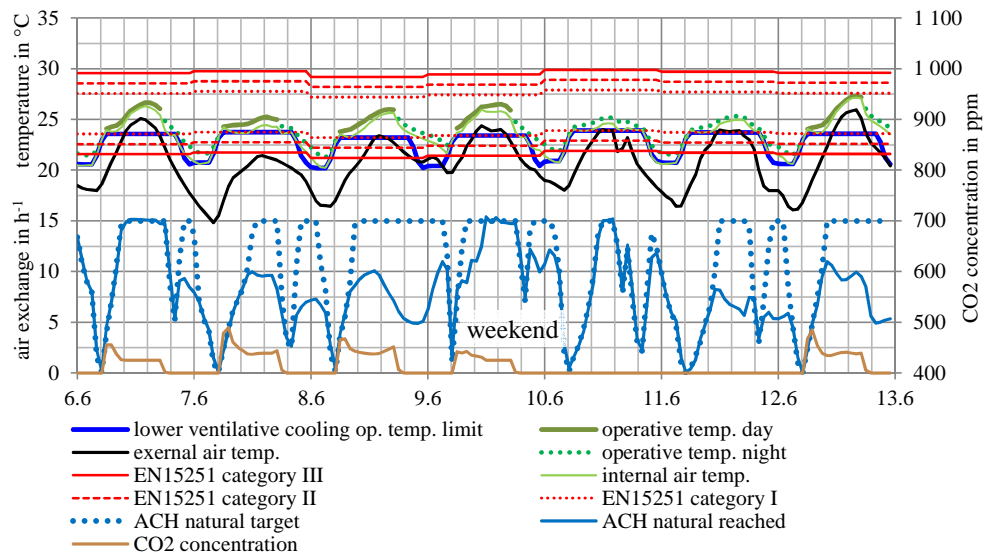


Figure 3.38: Resulting EMS controlled air change rate for a typical summer week in Istanbul.

3.3.3 Final natural ventilation system sizing

As the volume of a building is an expensive resource, the designer needs to do a weighting between the expected adaptive comfort and the size of the natural ventilation system. Design alternatives should be analysed and discussed climate specific. If a hybrid approach is applied, the mechanical system installation and energy consumption is also a parameter to be taken into consideration.

3.3.3.1 Natural ventilation potentials

Achievable air change rates depend on the climate and season, the chosen system size, and the ventilation controls. In winter, natural ventilation is mainly used to limit the CO₂ levels. For a detailed dynamic analysis of the flow potential for natural ventilation systems, the entire system including controls has to be simulated, since the ventilation is not driven just by external conditions, but by an interaction of internal and external conditions, e.g., ambient and indoor temperatures, and dynamic wind velocity (for driving forces, see § 3.2.1.1).

3.3.3.2 Adaptive thermal comfort

Apart from the air change rates, which directly influence air quality, thermal comfort is a crucial indicator for evaluating the natural ventilation concepts. The orifice

dimensions can be resized until certain comfort expectations are fulfilled by simulation.

Recommended criteria for acceptable deviations in comfort, investigated by whole year computer simulations, are given in the EN 15251 standard [41]. According to the informative Annex G in this standard, the indoor environment of the building meets the criteria of a specific category when *‘the parameter in the rooms representing 95% of the occupied space is not more than as example 3% (or 5%) of occupied hours a day, a week, a month and a year outside the limits of the specified category.’* Further, *‘By dynamic computer simulations it is possible for representative spaces in a building to calculate the space temperatures, ventilation rates and/or CO₂ concentrations. It is then calculated how the temperatures are distributed between the 4 categories. This is done by a floor area weighted average for 95 % of the building spaces.’*

3.4 Design Evaluation

The most important factors influencing passive and hybrid cooling performance are ventilation rates, controls, heat gains, building mass and climatic conditions. It can be assumed that if thermal comfort can be guaranteed without air-conditioning, then significant cooling and ventilation energy conservation can be achieved [64]. The assessment can be carried out with the help of performance indicators, and the results are intended to assist decision making in the design phase. Indicators proposed to evaluate the functionality are the energy consumption compared to that of mechanical ventilation and cooling systems, and compliance with the thermal comfort limits for users; additional aspects are the ventilation rates and the indoor air quality reached.

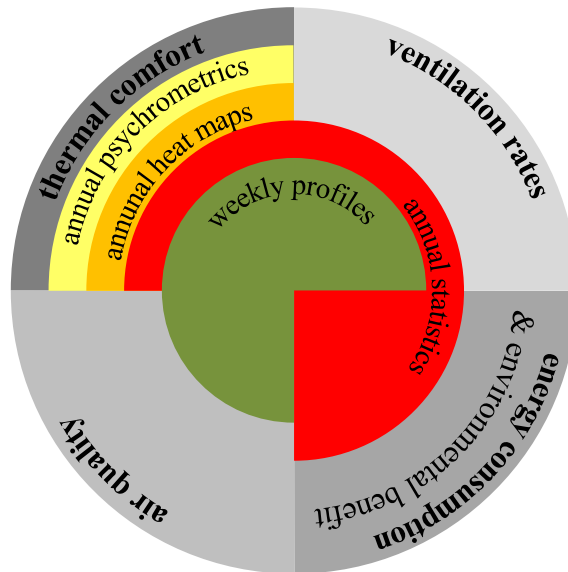


Figure 3.39: Performance evaluation wheel developed to access simulated passive cooling design.

Thermal comfort expectations (e.g., adaptive with a wider range of conditions) must be discussed and ultimately accepted by all the project stakeholders. The reference thermal comfort standard recommended as baseline is the EN 15251 standard [41], which accounts for both buildings with and without mechanical cooling systems. In this standard, in addition to the indoor operative temperatures, recommended air humidity levels are considered only if humidification or dehumidification systems are installed. Nevertheless, humidity levels have a big impact on comfort. Therefore, to support the feasibility assessment of energy efficient building design, these should also be reported for free-running situations, thus paying attention to the most important thermal comfort mechanisms for a given climate.

For the estimation of energy conservation, simulation outputs for the passive and the hybrid scenarios must be compared to those of active scenarios with mechanical ventilation and cooling systems. Based on the energy savings, the environmental benefit can be calculated from the country-specific data from the Global Emission Model for Integrated Systems (GEMIS) database [138].

The design evaluation is structured as shown in Figure 3.39:

- Weekly design profiles give insight into the functioning of natural ventilation systems and are helpful in analysing the opening control and the quality of indoor air.
- Annual assessment gives insight into the overall functionality of naturally controlled and hybrid operation throughout the year.

3.5 Conclusions

For the building type and climate considered, natural ventilation is not a stand-alone solution for good summer comfort. Instead, ventilative cooling must be brought in with other measures to reduce heat gains, and to use the building as heat sink for night-time ventilation. Hence, a building must be first conceptually adapted to reduce heat gains and to provide a sufficient amount of accessible mass for night-ventilation. Focusing on natural ventilation, a design concept was developed for wide-shaped high-rise buildings where simple cross ventilation or single-sided ventilation is impractical to realise. A central void design was found best suited, as it allows cross-ventilation of the occupied space towards a central chimney in the core, from where warm air rises upwards, towards a high level exhaust. The building is also virtually cut into modular segments to restrict the system dimensions (e.g., chimney diameter) and the peak pressure drops in winter (at high temperature differences). With a single chimney the size of the ventilation system simply would be too big to be realised in practice, but with isolated segments, each segment can be treated as a low-rise or medium-rise building. To guarantee the intended flow direction from the perimeter towards the core, besides a commonly used, leeward chimney exhaust, also a commonly used windward supply inlet is recommended. Intermediate ‘wind floors’ between the segments are outlined with two wind adapting openings in windward (positive wind pressure supply) and leeward (negative wind pressure exhaust) orientation. The central chimney is therefore designed to serve the occupied space with fresh air supply and exhaust.

The spread-sheet based ‘HighVent’ design tool was developed to size the openings of a flow path, especially in the context of segmented, high-rise office buildings. Simple electrical circuit analogies, for both ventilation and thermal models, were found to be suitable to pre-design the natural ventilation systems. This includes advice if a certain adaptive thermal comfort criteria can be reached for a summer design day. The correctness of the results could be proved by a comparative validation against the EnergyPlus building energy simulation program, which was found to be in good agreement. Considering the conceptually adapted buildings, uncontrolled design air change rates are estimated. The ventilation systems are then sized dependent on this design air change rate and average local wind velocities.

To assess the overall annual performance for a specific climate, in a next step, the building is modelled with Building Energy Performance Simulation (BEPS) along with the passive approach design adaptations developed. The 'HighVent' design tool outputs are 'post-processed' as inputs for detailed simulations including the mechanical systems. The custom natural ventilation system control, targets to achieve (i) good indoor air quality according to EN 13779 [55], and (ii) stay within adaptive comfort limits according to EN 15251 [55]. During ventilative cooling operation (day and night), the system target air change rate is increased the more the lower adaptive temperature limit (category I) is exceeded. Two amplifiers are intended to raise the target air change, one exponentially dependent on the operative temperature above the lower comfort limit; the other one is linear and dependent only on the external air temperature. At night, the system aims to precool the building by lowering the indoor temperature below comfort conditions, and raising the temperatures again before the beginning of occupation. The mean monthly air change rates are then dependent on the climate and season, and on the chosen system size. The target air change rate represents the amount of air the EMS control aims to realise, whereas the reached air change rate is the smaller amount of ventilation appearing in the simulation.

However, thermal comfort is the most crucial indicator for evaluating passive cooling concepts. Recommended criteria for acceptable deviations in comfort, investigated by whole year computer simulations are given in the EN 15251 standard [55]. The operative temperatures are distributed between the 4 categories and occupied space should not be more than 3% (or 5%) outside the limits of the specified category (defined as category II). The annual comfort distribution is first accessed for opening sizes according to the design tool outputs. By repeating the simulations without improved shadings and/or without mass activated construction elements, the influence of those measures could be investigated separately. For the final system sizing, the simulations can be repeated with different orifice sizes (flow path resistances); for example with reduced natural ventilation system sizes according to architectural sizing limits if necessary.

4. THE KANYON CASE-STUDY BUILDING

For an in-depth investigation of the objectives laid out in the thesis framework, the Kanyon high-rise office tower, situated in Istanbul (41,0°N, 28,6°E), Turkey, has been selected as the benchmark case-study building. This location has been chosen because of its highest density of high energy consuming office buildings in Turkey. Also, access to the building related data was readily provided by the management of the Kanyon-Multiplex. This chapter describes the main characteristic features of this building. The following is a generic description of the building according to the building architects⁷: *‘Kanyon, one of Europe’s largest mixed-use districts, introduces a new concept for urban living in Levent, Istanbul’s central business district. The Jerde Partnership and Tabanlıoğlu Architects designed the state-of-the-art project to combine 2.74 million sq ft of modern offices, luxury residences with local and upscale retailers in an organic, open-air design that includes an amphitheatre, plazas and rooftop park spaces where workers, residents and visitors can gather’.*

4.1 Site

The Kanyon multiplex rises on an area of 29 500 m² in Levent, Istanbul’s central business district. Its mixed-use includes 33 000 m² of residential space, 31 000 m² of office space, an 8 000 m² entertainment area including a cinema, 37 500 m² of rentable retail space, and parking for 2 300 cars (Figure 4.2 to Figure 4.4).

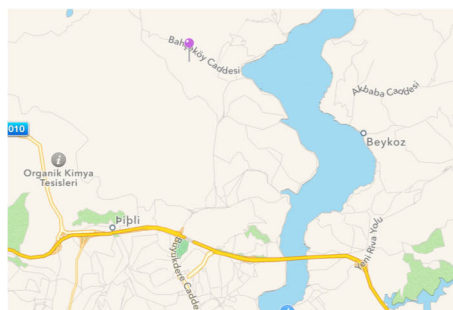


Figure 4.1: Location (purple dot in the map) of the case-study site (Source: Apple Maps).

⁷ The Jerde Partnership (<http://www.jerde.com/news/68.html>) and Tabanlıoğlu Architects

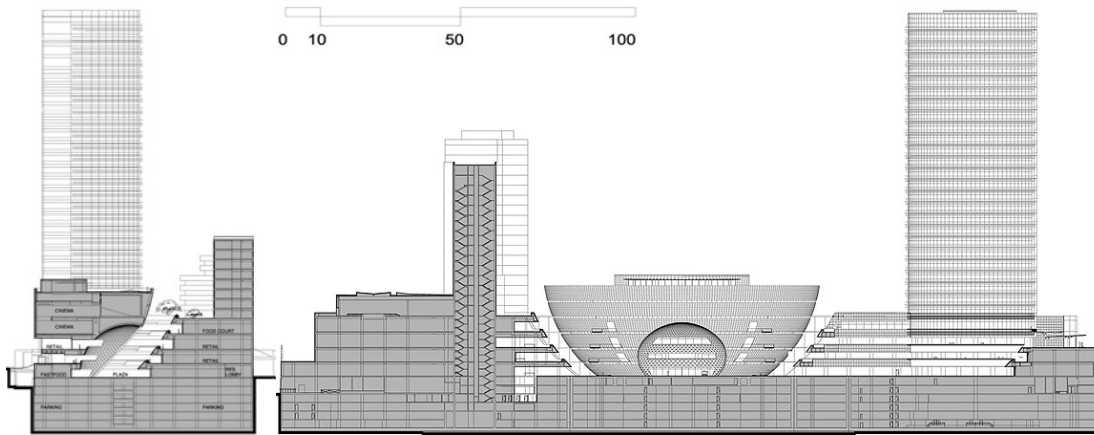


Figure 4.2: Kanyon site with the office tower cross and longitudinal sections (Source: The Jerde Partnership).

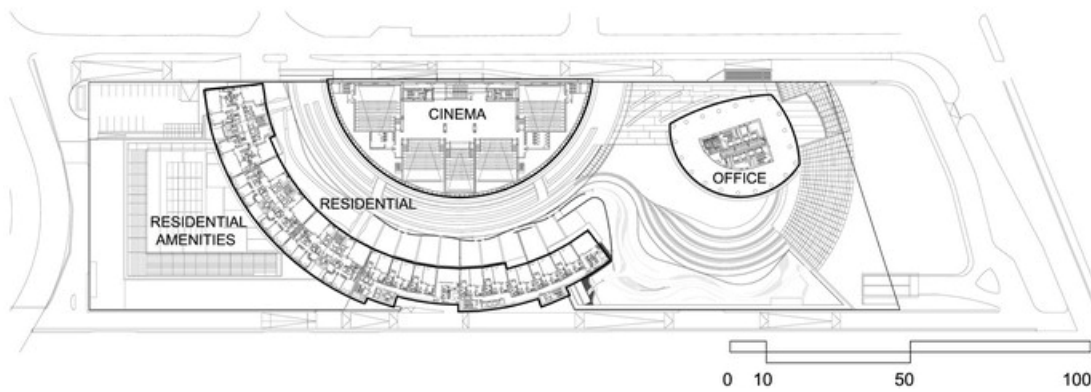


Figure 4.3: Kanyon site plan at height of the residential / cinema floor (Source: The Jerde Partnership).

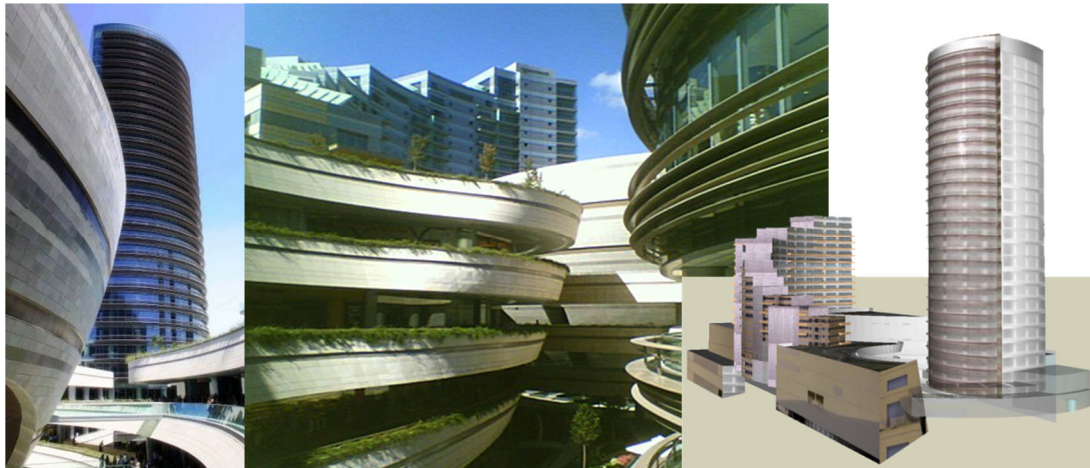


Figure 4.4: Pictures of the Kanyon multiplex including the office tower (Source: The Jerde Partnership and Google's free access building models for SketchUp).

4.2 Office Tower

Location:	Istanbul, Turkey
Architect:	The Jerde Partnership Tabanlıoğlu Architects
Engineer:	Arup Ltd.
Year of completion:	2006
Building function:	Office space
Height ⁸ :	118 m above ground
Stories:	28 above ground / 25 offices
Total gross area:	about 34 000 m ² above ground
Conditioned area:	about 28 000 m ² above ground
Gross internal area:	1 229 m ² per floor (100%)
Net internal area ⁹ :	about 1 000 m ² per floor (81%)
Gross office area:	935 m ² per floor (100%)
Net office area ⁹ :	about 850 m ² per floor (91%)
Structural material:	Concrete
Plan depth:	8 to 11 m (from central core)
Storey height:	4,00 m (office floors)
Ceiling height:	2,90 m (offices) to 3,00 m (core)

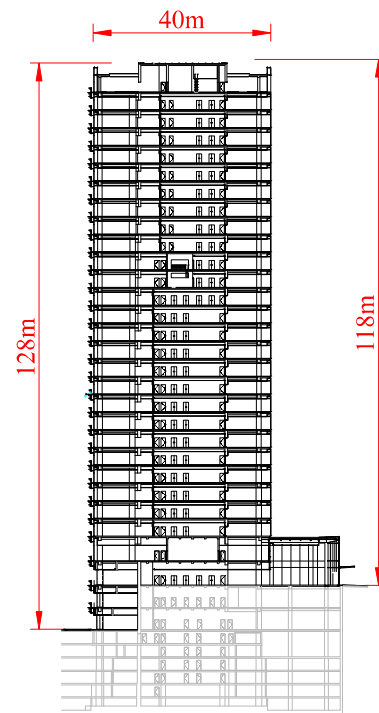


Figure 4.5: Kanyon office tower cross-section.

4.2.1 Introduction

The Kanyon office tower is a 28-level tower with a curved, highly glazed façade. The transparent glass increases visibility and offers the benefit of maximum natural light in the work areas. A shading system on the south side of the tower is intended to reduce the heat impact from the sun. The building includes modular office spaces that offer flexibility for the needs of the companies. Open plan geometry around the core (Figure 4.6) was therefore chosen to allow the floor space to be used for different sized units, i.e., for individual, combined, and open plan offices. The floor spaces are arranged around a central services core with a depth of approximately 8 to 11 m, and provide the flexibility to accommodate a range of functions. The storey height, apart from the two ground floors (5,5 m), is 4,0 m.

⁸ From the ground level at street height where also the building's main entrance is located

⁹ The floor area contained within the building measured less the floor areas taken up by the external and internal walls, enclosed machinery rooms, stairs and escalators, mechanical and electrical services, columns, ducts and risers.

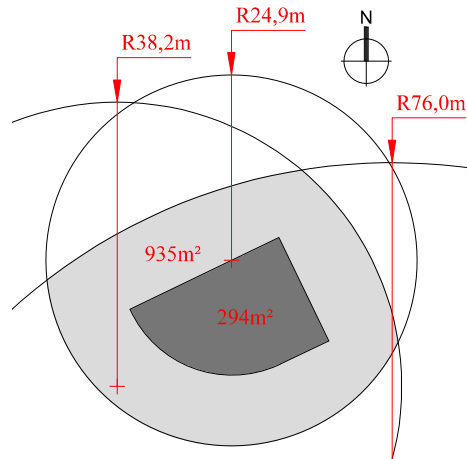


Figure 4.6: Canyon storey plan geometry (dark grey = core area / light grey = office area).

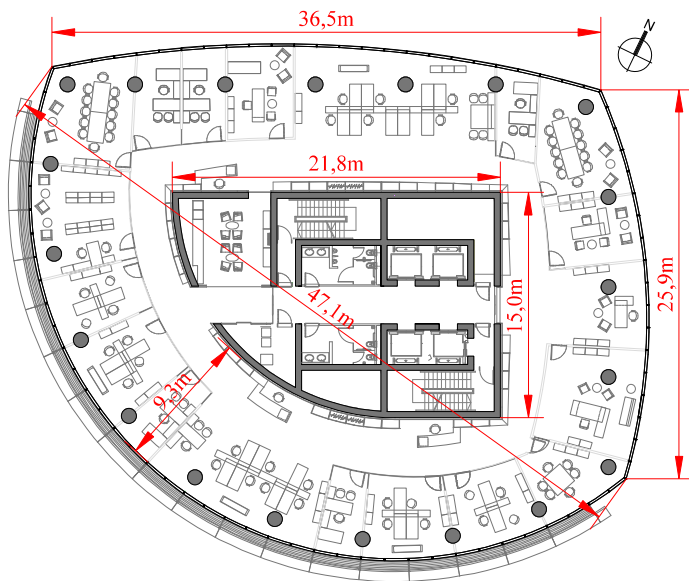


Figure 4.7: Exemplary office plan.

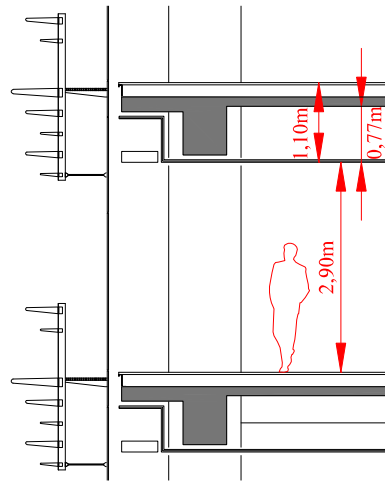


Figure 4.8: Exemplary office section.



Figure 4.9: Three pictures taken from an exemplary office storey interior (shot by the author).

4.2.2 Construction elements

Typical of the high-rise building type, the framework was built with steel and concrete from which curtain walls are suspended, rather than load-bearing walls of conventional construction. The core and the floors therefore employ a steel skeleton

construction made of reinforced concrete. The curtain wall envelope is highly glazed by Low-E double glazing with a ratio of approximately 89%.

4.2.2.1 Opaque construction elements

From the architectural drawings, the following major composite construction elements, as shown in Table 4.1, were first gathered and then specified in the building energy simulation model.

Table 4.1: Thermal properties of the building construction elements also incorporated to the model.

construction name	material name	thickness in m	layer
curtain wall u-value = 0,29 W/m ² -K	aluminium	0,0020	outside layer
	xps extruded polystyrene	0,0200	layer 2
	wall air space	0,1000	layer 3
	mw stonewool rolls	0,1000	layer 4
	stainless steel	0,0010	inside layer
internal floor u-value = 0,98 W/m ² -K	gypsum plasterboard	0,0125	outside layer
	ceiling air space	0,9900	layer 2
	concrete reinforced	0,1250	layer 3
	ceiling air space	0,1700	layer 4
	plywood	0,0300	layer 5
	carpet	0,0060	inside layer
heavyweight internal wall u-value = 1,40 W/m ² -K	oak wood	0,0130	outside layer
	wall air space	0,0250	layer 2
	concrete reinforced	0,4000	layer 3
	wall air space	0,0250	layer 4
	oak wood	0,0130	inside layer
lightweight internal partition u-value = 4,00 W/m ² -K	gypsum plasterboard	0,0125	outside layer
	wall air space	0,0500	layer 2
	gypsum plasterboard	0,0125	inside layer

The thermal properties of the building construction materials are collected from different sources and are summarised in Table 4.2.

Table 4.2: Thermal properties of the building construction materials also incorporated to the model.

name	source	conductivity in W/m-K	specific heat in J/kg-K	density in kg/m ³
aluminium	ISO 10456	160	880	2 800
XPS extruded polystyrene	Uralita S.A.	0,034	1 400	35
MW stone wool rolls	Uralita S.A.	0,040	840	30
stainless steel	ISO 10456	17	460	7 900
gypsum plasterboard	ISO 10456	0,250	1 000	9 00
concrete reinforced	ISO 10456	2,5	1 000	2 400
plywood	ASHRAE 05	0,12	1 210	544
carpet	ISO 10456	0,060	1 300	200
oak-wood	ASHRAE 05	0,17	1 630	704
name	source	thermal resistance in m ² -K/W		
wall air space	ASHRAE 05	0,15		
ceiling air space	ASHRAE 05	0,18		

4.2.2.2 Window glazing

According to the manufacturer, the highly glazed façade of the office tower was designed to provide maximum daylight transmittance for the occupants. To reduce heat gains, the tempered outer glazing was coated by invisible silver low-emittance (low-E) coating. This is a glazing type with microscopically thin and virtually invisible metal or metallic oxide layers deposited on the glazing surface, primarily to reduce radiative heat flow. An optimum low-E coating is transparent to the visible solar spectrum to provide maximum light, and reflective of long-wave infrared radiation to block solar heat gains. The design also provides the necessary resistance against high wind loads and sets a security system by preventing any injuries that would occur if a window bursts. The partly tempered inner glazing is composed of two layers of polyvinyl butyral (PVB) laminated glazing.

Table 4.3: Thermal and visual properties of the window glazing¹⁰.

LoE double glazing	initial values as specifications from the planners	catalogue values 6 mm IMF 170 + 12 mm AB + 6mm DC	adapted actual combination 8 mm IMF 170 + 16 mm AB + (4+1,52+4mm)
daylight transmittance	70%	70%	68%
daylight reflectance	10%	13%	12%
shading coefficient	0,54	0,56	0,51
solar transmission (SHGC)	0,47	0,487	0,444
U-Value (EN 673 is used)	1,4 W/m ² -K	1,7 W/m ² -K	1,4 W/m ² -K
emissivity	< 0,20	0,07	0,07

4.2.2.3 Shading devices

Both internal and external devices shade the office zones. The uniform external shading device in summer only partly shades the windows due to their size and also due to the fact that the devices were not selected according to the orientation of the windows.

External

The uniform, external shading devices are designed to allow a free view for the office occupants and to support the architectural appearance of the building composition. Less importance was given to shade the windows and to reduce the incoming heat and the risk of overheating.

¹⁰ Technical specifications from the glazing production company Trakya Cam Sanayii A.Ş.

The seven differently sized horizontal shading devices (Figure 4.10 and Figure 4.11) on each floor are mounted from south-west till south-east façade (see Figure 4.7). They are made of beige-silver coloured stainless steel and mounted by a rigid façade suspension. Because of the solar path of the sun, the highly glazed façade is only partly shaded, depending on the season, time and orientation. Horizontal shading devices generally work best for south mountings. For east and west aspects, the sun will be low in the sky for long periods. This means that the sun will come in underneath the horizontal shading devices, making them more ineffective compared to the south orientation. Therefore, with the actual shading devices a partial overheating due to intense solar beam gains occurs with clear sky from external windows.

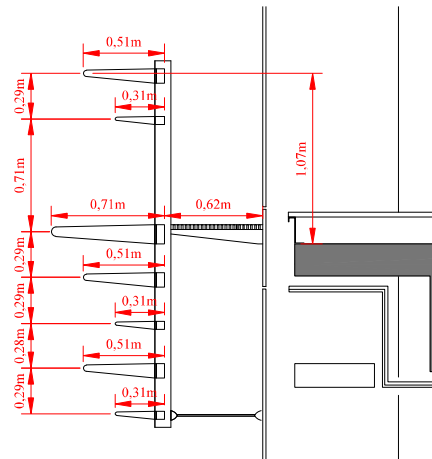


Figure 4.10: Shading devices from inside. **Figure 4.11:** External shading device drawing detail.

Simulations done in the context of this study indicate that the actual shading devices reduce the building's overall transmitted solar gains only by 11% in the cooling season (for the definition of cooling season, see § 5.1.4) compared to a case without any external shading devices.

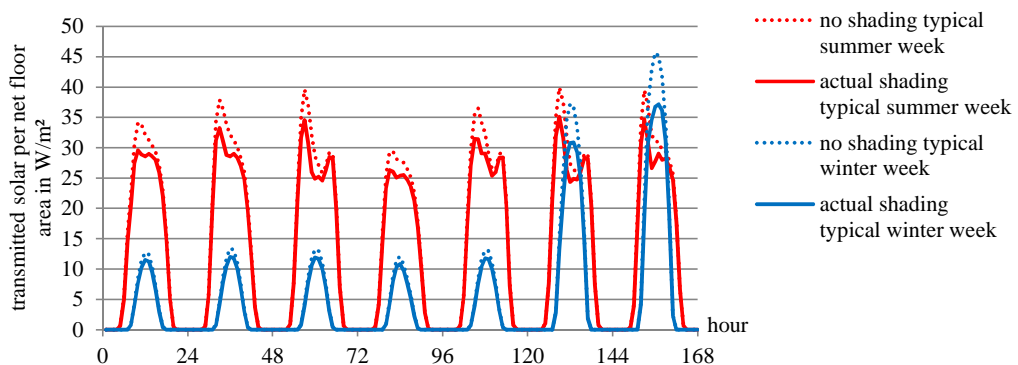


Figure 4.12: Simulated effectiveness of the actual shading devices in a typical summer and winter week period according to the ASHRAE IEWC weather data (storey net floor area = 1 000m²).

Internal

Internal vertical blinds successfully control light, block glare, and provide privacy but do not achieve effective heat control unlike external blinds. The semi-transparent rolled up interior sunblinds used in the Kanyon building are made of textile (Figure 4.9). According to the Kanyon management, the sunblinds are automatically controlled by the solar intensity, but setpoints and position of the irradiance meter are not known. For the simulation model, it was assumed that the internal shades do not significantly influence the heat balance of the building, and as such are not investigated further.

4.2.3 Internal heat gains

The building's heat balance, besides the solar heat gains, is strongly affected by its internal heat gains. From interviews with the energy management and from the energy metering data of 2007 to 2009, it can be concluded that the building has high internal heat gains. From the available data, the internal heat gains are assumed as summarised in Figure 4.13. Further information on the underlying approximations is given in the following paragraphs.

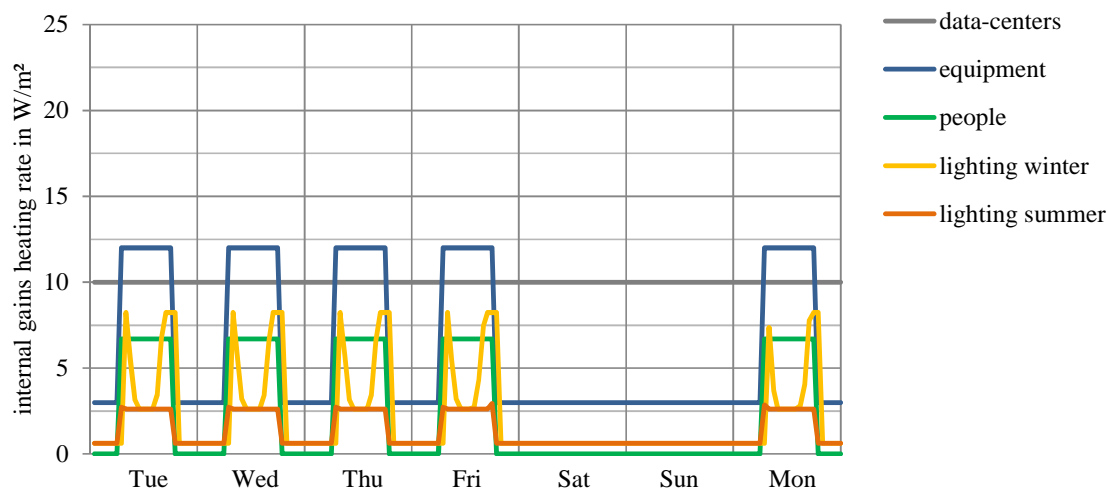


Figure 4.13: Mean actual internal heat gains modelled related to the total net storey area including the core and data centres.

People

Interviews with the Kanyon's building energy management indicated that there are approximately 62 persons working on each storey, which is a rather light occupant density per area. The heat gain rate from people working in the office is assumed to be $108 \text{ W person}^{-1}$, which is the E+ default value, and is consistent with typical office

work according to the ASHRAE HoF [27]. The radiant fraction is assumed to be 50%, which again is the E+ default value. The offices are assumed to be occupied from 7 am to 7 pm on working days.

Lights

From the available as-built drawings of the Kanyon office tower's 23rd storey, the installed approximate lighting power densities are 8,8 W/m² in the office space and 5,0 W/m² in the core space.

According to interviews with the Kanyon's management, the central energy management system controls the lights of the core and the inner part of the office area, which is a corridor around the core region, to be on from 7 am to 7 pm. At nights and during weekends, the power density is reduced to a level of about 25% in the core space and 5% in the office space.

For 80% of the office area from 7 am to 7 pm lighting is controlled by the occupants. It is assumed that the occupants turn the lights on and off at 500 lux at desk level in the centre of the office area in two steps. The first step reduces the amount of artificial light by 50% and the second step turns the light off.

Equipment

Interviews with the Kanyon's energy management team, and metering protocols from 2007 to 2009 also indicate that the equipment loads are medium heavy, even if the people density per workspace is low. Because the equipment was not separately metered, a density with 12 W/m² is taken into consideration, which is close to the medium load recommended by ASHREA HoF [27].

Table 4.4: Recommended [27]equipment load factors for various office types according to [139].

load density of the office	load factor in W/m ²	description
light	5,4	assumes 15,5 m ² /workstation (6,5 workstations per 100 m ²) with computer and monitor at each plus printer and fax. computer, monitor, and fax diversity 0,67, printer diversity 0,33
medium	10,8	assumes 11,6 m ² /workstation (8,5 workstations per 100 m ²) with computer and monitor at each plus printer and fax. computer, monitor, and fax diversity 0,75, printer diversity 0,50
medium/heavy	16,1	assumes 9,3 m ² /workstation (11 workstations per 100 m ²) with computer and monitor at each plus printer and fax. computer and monitor diversity 0,75, printer and fax diversity 0,50
heavy	21,5	assumes 7,8 m ² /workstation (13 workstations per 100 m ²) with computer and monitor at each plus printer and fax. computer and monitor diversity 1,0, printer and fax diversity 0,50

IT-Rooms

The Kanyon office tower building comprises data centre rooms for different companies. The IT equipment is mostly located in the core of the building. Even on some storeys, the companies extend the area towards the office area outside the core (see Figure 4.6). At least within the core, the IT rooms are insulated; there are no solar gains, and they are mostly unoccupied and operate 24 hours a day. The room requires no mechanical heating system due to its high internal heat gains from the computer equipment. There is an additional mechanical cooling system installed to cool the rooms when the rest of the building does not require any cooling. From the metering, 10 kW electricity load is roughly assumed as the mean IT-load for each storey.

4.2.4 Mechanical HVAC systems

The HVAC system consists of gas condensing boilers for heating, constant flow mechanical ventilation, a latent heat recovery, main water to water chiller with cooling towers, and supporting water to air chiller. The preconditioned room air temperatures can be manually set by four-pipe fan coil units. In the survey on the building's actual operation and usage, it became clear that in many situations, heating and cooling systems operate simultaneously. This is most probably due to the manual setpoint adaptation (± 3 °C) in the different rooms in combination with open doors. This circumstance is assumed to create a 'fight of the systems' by interzonal air mixing and poor internal insulation, and also from the strong effect of solar heat gains on one side of the building.

According to the management, the air-conditioning system ventilates fresh air throughout the building all day at a rate of approximately two air changes per hour. The minimum requirement according to the initial design is 14 litres per second per person¹¹. The building is conventionally ventilated in a way to supply fresh air from the exterior and to extract polluted air with a balanced mechanical ventilation system, consisting of fans and ductwork. The system also comprises filters, dampers, silencers, and heat exchangers together with the ductwork, creating a relatively high pressure drop. Such systems are able to deliver a stable supply of fresh air, which ensures an air quality and thermal comfort that is independent of outside conditions.

¹¹ ARUP, Kanyon office block mechanic installation report, 2003, Turkey

However, the ventilation system is quite complex and expensive to install and operate. A common trend towards higher indoor air quality standards has resulted in a ventilation system that requires an increasingly larger share of the building costs. The ventilation system also consumes considerable amount of electricity for fans. The complexity of such ventilation systems creates many opportunities for malfunctions.

Further details concerning the modelled building operation can be found in Table 6.3. The simulation model setup is described in § 6.3.1.

4.2.5 Metered energy consumption

The building's measured annual energy consumption for 2008 was recorded¹² as 2 040 MWh of natural gas and 7 292 MWh of total electricity. This corresponds to approximately 68 kWh gas consumption and 243 kWh electricity consumption per m² conditioned floor area. Natural gas within the office tower is exclusively used for room heating.

Unfortunately, the meters were set in a way aimed mostly at energy billing. It is therefore very difficult, if not impossible, to investigate the individual consumption for different applications, e.g., cooling or ventilation, as the consumption is often summed together with that of different other consumers.

Table 4.5: Natural-gas and electricity consumption of the Kanyon office tower in 2008.

2008	natural gas			electricity	
	m ³ *	kWh	kWh/m ² **	kWh	kWh/m ² **
Jan	38 313	418 177	14	512 500	17
Feb	41 899	457 317	15	481 000	16
Mar	28 806	314 410	10	516 000	17
Apr	19 243	210 033	7	496 500	17
May	14 830	16 1866	5	616 000	21
Jun	651	7 106	0	637 000	21
Jul	-	-	-	779 500	26
Aug	-	-	-	744 000	25
Sep	-	-	-	613 000	20
Oct	6 130	66 907	2	740 500	25
Nov	15 934	173 916	6	587 500	20
Dec	21 185	231 229	8	568 500	19
Sum	186 991	2 040 961	68	7 292 000	243

* specific calorific value of natural gas assumed with 10,915 kWh/m³

** consumption in kWh per m² conditioned space (about 30 000 m²)

¹² by the building's energy management group

4.3 Conclusions

The Kanyon office tower geometrically has a uniform building structure of 25 office storeys with a net internal area of about 1 000 m² and 2,9 m ceiling height each. The envelope is highly glazed with Low-E glazing (solar heat gain coefficient of 0,444). External shading elements only partly shade the façade in summer and reduce the building's overall transmitted solar gains by approximately 11% in the cooling season. The internal heat gains are high especially due to highly energy consuming data centres mostly situated in the core area of the building. The internal equipment loads are assumed to be 12 W and heat loads from lighting are about an average of 3 W per net floor area during building occupancy. The data centres are assumed with 10 W/m² operating for 24 hours a day throughout the whole year. All the building thermal mass, e.g., the concrete layer in the ceiling constructions, is sealed, and can thus only be poorly exploited as a heat sink (e.g., by night-time ventilation). The building internal environment is controlled by complex, high energy consuming mechanical systems. The occupant behaviour (setpoint adaptation together with open doors) tends to create a fight of the systems (cooling vs. heating) especially in the intermediate seasons when heating and cooling operate simultaneously. The mechanical ventilation rates are high (2 ACH) considering a rather light occupant density per area. The annual metered energy consumption of 243 W/m² of electricity and 68 W/m² of natural gas is high, which indicates a big potential for energy saving measures for this type of building.

5. THE CLIMATE ASSESSMENT

One of the most important issues in determining the potential of natural ventilation systems is the suitability of climate. The relevant climatic input parameters for passive system design and dynamic simulation are: ambient temperature, humidity, solar radiation, and wind velocity and direction.

In this work, the same building is considered to be situated in three different climates to evaluate the functionality of a controlled naturally ventilated high-rise office building under various external conditions (ranging from those of central to southern Europe). Besides, the building could serve as a benchmark to test if the control algorithms do a good job in different climatic regions, addressing a universal validity. The climatic charts that follow provide information from all the three climatic sites.

The main climatic location of concern is Istanbul, Turkey, as the building is actually located here. The same building model will also be positioned in Turin, Italy, which is the host university of the thesis co-adviser as well as in Stuttgart, Germany, which is the project coordination location of the Marie-Curie Research Training Network, where the research was carried out.

Figure 5.1 shows the European portion of the authoritative classification map first developed by Wladimir Köppen (1846-1940). This was updated and modified by several geographers, and continues to be a benchmark for the world climate information in use today. Its categories are based on the annual and monthly averages of temperature and precipitation. Accordingly, all the three locations considered are situated in moist mid-latitude climates with mild winters (major group C), and are considered as humid (second letter f). Only in Stuttgart, the warmest month average temperature stays below 22 °C (third letter b), whereas in Istanbul and Turin this temperature is exceeded (third letter a).

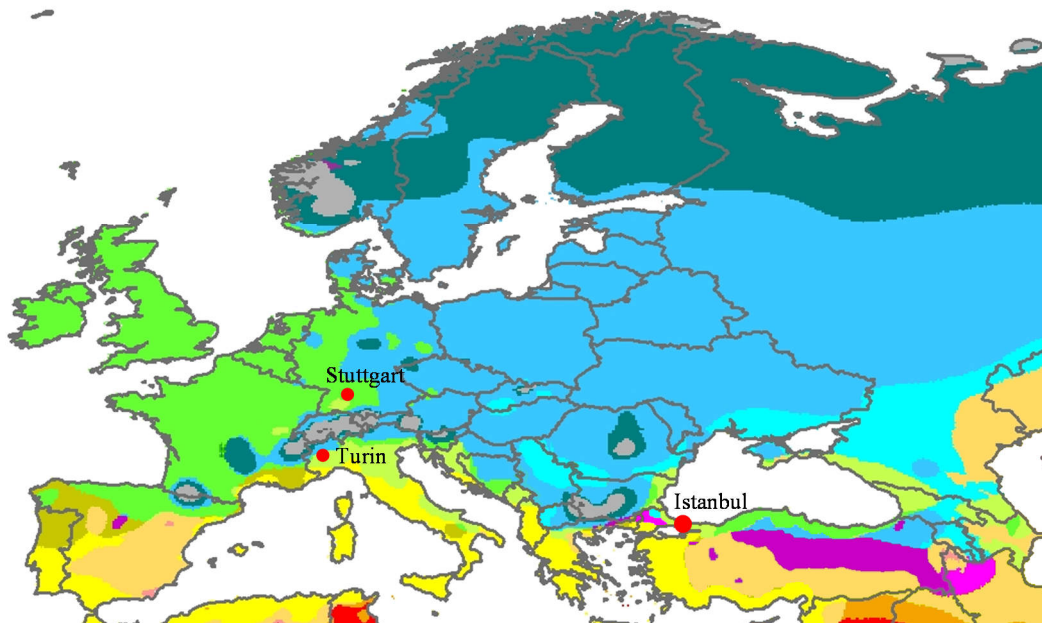
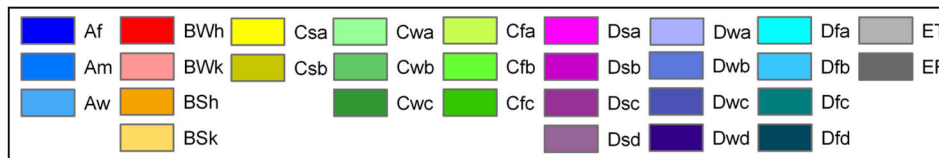


Figure 5.1: The geographical locations of Istanbul, Turin, and Stuttgart shown on a Köppen climate classification map for Europe (source: Peel *et al.* [140]).

The weather data for this study was downloaded from the EnergyPlus webpage in the EPW format. It represents a Typical Meteorological Year 2 (TMY2) weather format from ASHRAE IWEC [141]. This generic data from the weather files is usually measured at the airports, and is not further adapted in this study to account for the local microclimate or climate change, e.g., the heat island effect, the local terrain wind flow or the rising temperatures due to global warming.

As regards the wind, the shielding effect of neighbouring buildings is modelled by wind tunnel experiments and is therefore reflected by the wind pressure coefficients gathered (see Appendix A). The city centre terrain roughness will be modelled subsequently (see the method in § 3.2.1.1) by wind speed calculations at the local heights of openings. The atmospheric temperature drop with height above ground, which can be significant for high-rise buildings, is subsequently adapted according to § 3.2.1.1.

Besides the three climates, different time periods are investigated. Long term simulations, e.g., over the course of a year, are best suited for comparing the energy performance. For a general overview, monthly averages and wind occurrence values are shown for the whole year. The adaptive comfort limits, also indicating assumed

cooling periods, are calculated according to § 2.6.3, and are presented in § 5.1.4. As the focus of this thesis is on passive cooling and comfort during summer, the cooling period is further evaluated to infer the climatic cooling potentials and to address humidity effects on comfort (see § 5.2). Finally, for the natural ventilation and passive cooling preliminary design according to § 6.2, summer design weeks are analysed and then further processed to generate meaningful design days as input for the developed ‘HighVent’ design tool. A design day assessment is often used for load calculations or equipment sizing. The short-term simulations are best suited for comparing the cooling performance and can be used when quick answers are required, and where simulations using a typical meteorological year cannot be easily done or justified.

The following sections are therefore intended to provide the different climatic aspects of the three locations, and provide design day values for the sizing of passive cooling systems.

5.1 Whole Year

5.1.1 Overview

Figure 5.2 gives an overview of the three climates considered in this study. Average monthly temperatures, global horizontal radiation, and wind velocities are the highest in Istanbul. Also, Turin has a warm summer period with temperatures above 22 °C. The average relative humidity in both climates almost reaches 80% in summer, at which level constant breezes would be necessary for comfort. Stuttgart has a moist continental climate with warm summer, cold winter, and no dry season.

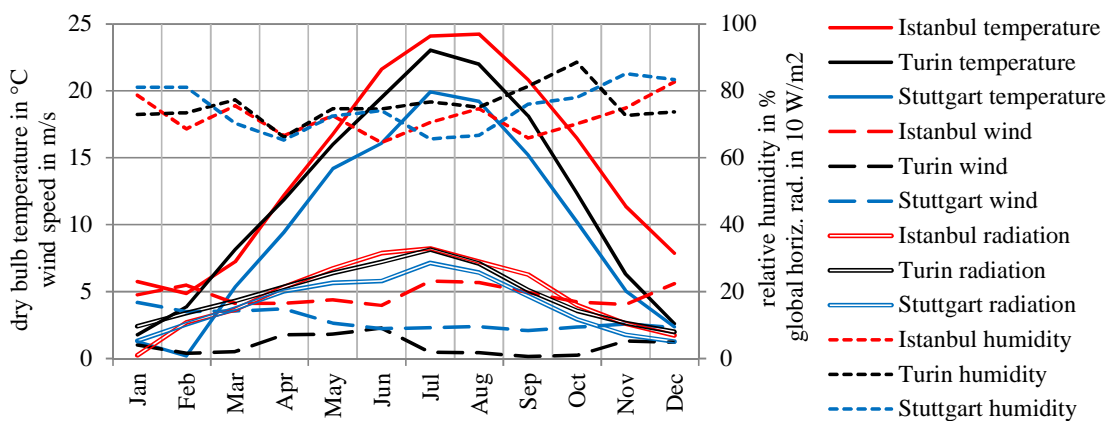


Figure 5.2: Typical monthly average temperature, wind speed, relative humidity, and solar radiation for Istanbul, Turin, and Stuttgart at meteorological station [141].

The EnergyPlus weather converter program can use a full year weather data file to calculate the ASHRE standard 90.1 Normative Appendix B [142] climatic classification. Accordingly, Istanbul can be classified as warm-marine (type 3C), Turin as mixed-humid (type 4A), and Stuttgart as cool-humid (type 5A).

5.1.2 Wind

The annual frequencies of wind velocity distribution in the three climate zones considered are summarised in Figure 5.3. The arithmetic mean wind speed values for the whole year are 4,8 m/s in Istanbul, 0,97 m/s in Turin, and 2,8 m/s in Stuttgart. The weather data from Turin seems to be broken since for 45% of the year the entries for wind speed and wind direction are zero in the weather data. This is most probably due to calm wind conditions, especially in summer, which are below the detection limit of the measurement instruments.

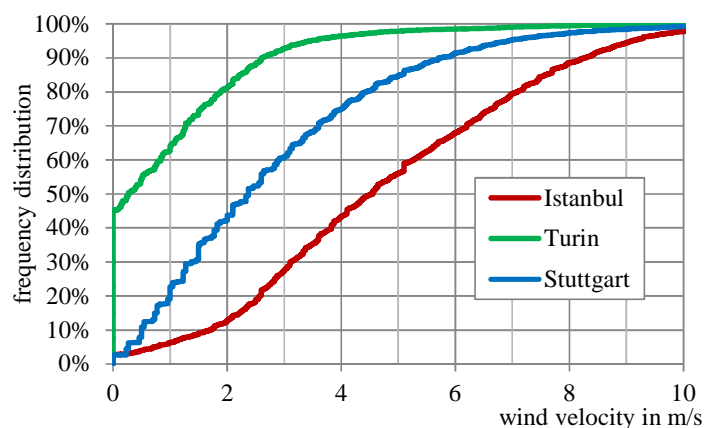


Figure 5.3: Annual wind speed frequency distribution for Istanbul, Turin, and Stuttgart [141].

Prevalent wind directions are given in Table 5.1. The knowledge of statistical wind directions is important to orient the openings towards prevailing breezes. The prevailing wind directions and average velocities for the cooling period are given in § 5.2.1.

Table 5.1: Annual wind velocity and direction statistics for Istanbul, Turin, and Stuttgart [141].

wind	from	to	annual (Jan-Dec)			wind	from	to	annual (Jan-Dec)		
Beaufort scale	m/s	m/s	Istanbul	Turin	Stuttgart	direction			Istanbul	Turin	Stuttgart
zero wind *	= 0,0		3%	45%	3%	-	-	-	3%	45%	3%
0 calm	>0,0	0,3	0%	9%	4%	north	337,5	22,5	18%	12%	5%
1 light air	0,3	1,6	7%	47%	31%	northeast	22,5	67,5	37%	7%	10%
2 light breeze	1,6	3,4	25%	34%	32%	east	67,5	112,5	8%	8%	12%
3 gentle breeze	3,4	5,5	29%	6%	22%	southeast	112,5	157,5	4%	6%	8%
4 moderate breeze	5,5	8,0	27%	2%	9%	south	157,5	202,5	9%	6%	9%
5 fresh breeze	8,0	10,8	11%	1%	2%	southwest	202,5	247,5	14%	4%	25%
6 strong breeze	10,8	13,9	1%	0%	0%	west	247,5	292,5	5%	6%	20%
7 high wind	13,9	16,9	0%	0%	0%	northwest	292,5	337,5	3%	7%	9%

* zero wind in the weather data interpreted as wind speed too low for measurement instruments

There are strong winds in Istanbul during the whole year. Though there are many winds that buffet Istanbul, there are two major ones: The Poyraz and the Lodos. The Poyraz blows from the northeast and hits the northern shores of the city. It brings cool air from off the black sea. The Lodos is a dry and warm Mediterranean wind that blows from the southwest. In Istanbul, a ventilation strategy based on wind forces is suitable if the local orography and neighbouring buildings permit this.

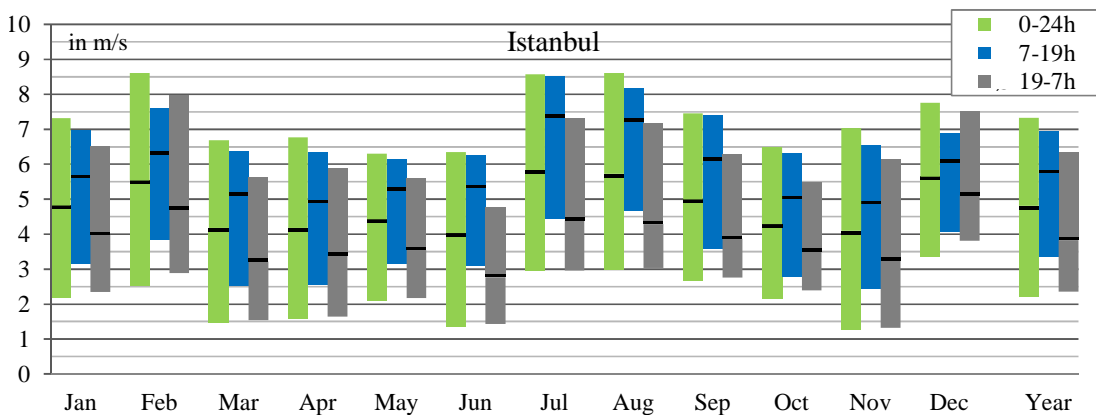


Figure 5.4: Average daily mean (black bar), daily maxima and daily minima wind velocity in Istanbul according to [141].

Turin climate is characterised by lull wind, especially in the warm cooling period from July till October. Due to these calm conditions, it would be a vain endeavour to choose a wind driven ventilation strategy.

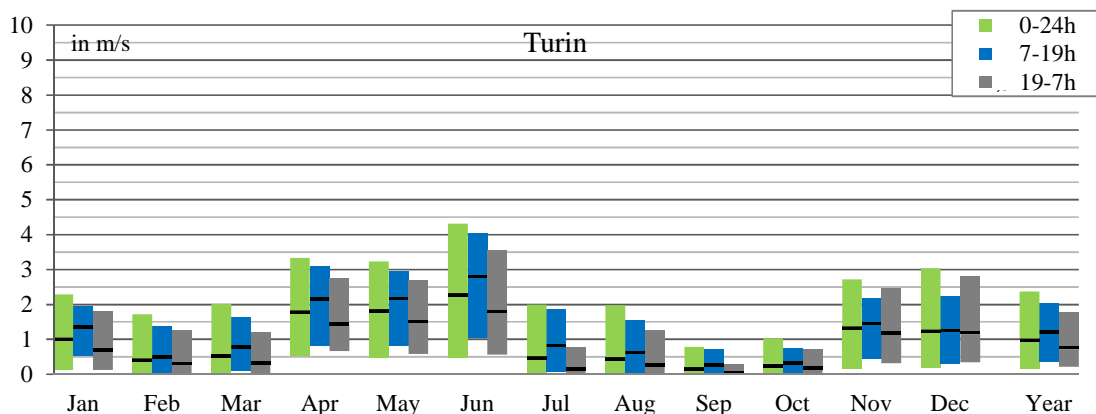


Figure 5.5: Average daily mean (black bar), daily maxima and daily minima wind velocity in Turin according to [141].

The Stuttgart climate also features wind poverty, limited not just to the valley location of the city, which is not reflected in the weather data file due to its airport location origin. The entire basin of the Neckar region is known for relative low wind speeds at a high frequency of calms. Due to the orography, the wind is very non-homogeneous. The Stuttgart Airport meteorological station is suitable to describe the

regional wind. In Stuttgart, wind forces most likely may assist natural ventilation. A ventilation strategy only based on wind is not recommended.

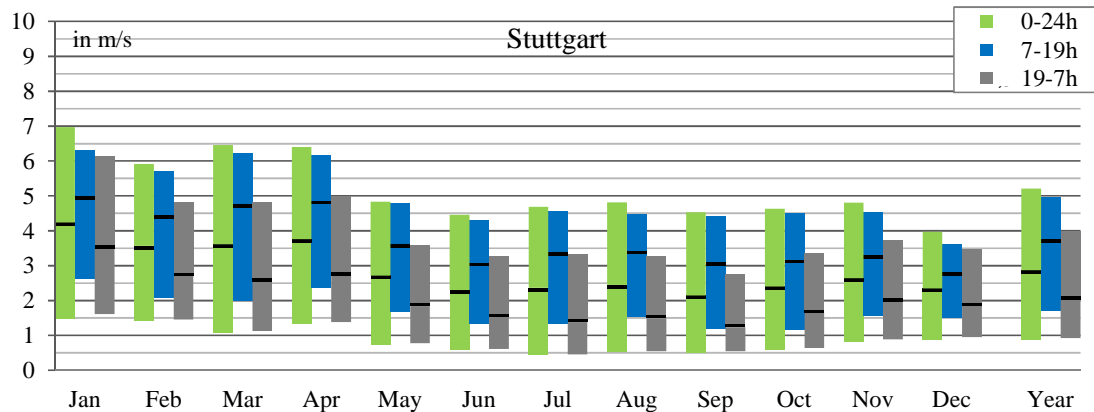


Figure 5.6: Average daily mean (black bar), daily maxima and daily minima wind velocity in Stuttgart according to [141].

5.1.3 Temperature

In addition to the monthly average temperature presented before, temperature maxima and temperature swing of the external air between day and night are meaningful information for planning the night-time ventilative cooling. As mentioned before in § 2.2.4.2, the larger the outdoor temperature swings, the bigger the potentially positive influence of thermal mass storage capacity on thermal comfort. High temperature differences are best suited for using the mass as a night-time heat sink. Figure 5.7 shows that temperature swings in summer are high in Stuttgart (>10 °C), medium in Turin (>8 °C), and relatively low in Istanbul (>7 °C).

The cooling period temperature maxima will be further discussed in § 5.2.3.

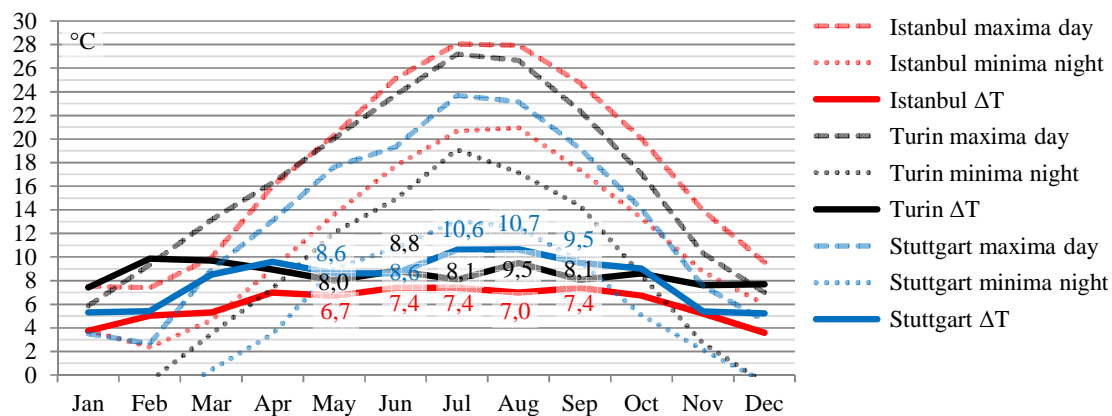


Figure 5.7: Average daily temperature swing between day and night [141].

5.1.4 Adaptive thermal comfort limits

The annual adaptive thermal comfort limits were calculated with the TMY2 climate data for the three reference locations according to the EN 15251 standard when applicable, as described in § 2.6.3. These are shown in Figure 5.8 through Figure 5.10. As regards category II, operative temperature levels of about 30 °C are temporarily allowed for hot ambient air summer conditions in Istanbul and Turin.

The term ‘cooling period’ in this study is assumed as the period from which the upper thermal comfort boundary category II is continually calculated above 26 °C. Comparing this assumption with the cooling demand for the actual case-study building in Istanbul (see Figure 6.22), this season fits reasonable well.

The basis for the passive ventilation and cooling system design in § 6.2 is the typical/extreme summer periods determined from the ASHRAE weather data statistic files, which are automatically processed by EnergyPlus while running a simulation (E+ see § 3.3.1). These summer design weeks are shown in Figure 5.8 through Figure 5.10 below. Detailed values for the summer design weeks concerned may be found in § 5.3.2.

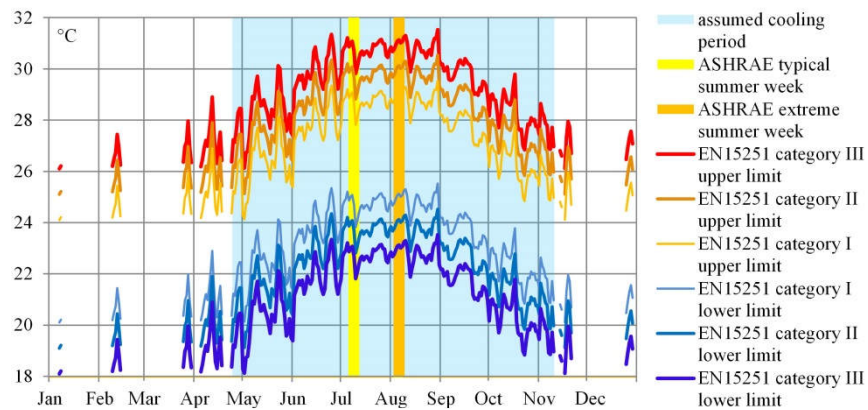


Figure 5.8: Adaptive thermal comfort boundaries according to [41] for Istanbul [141].

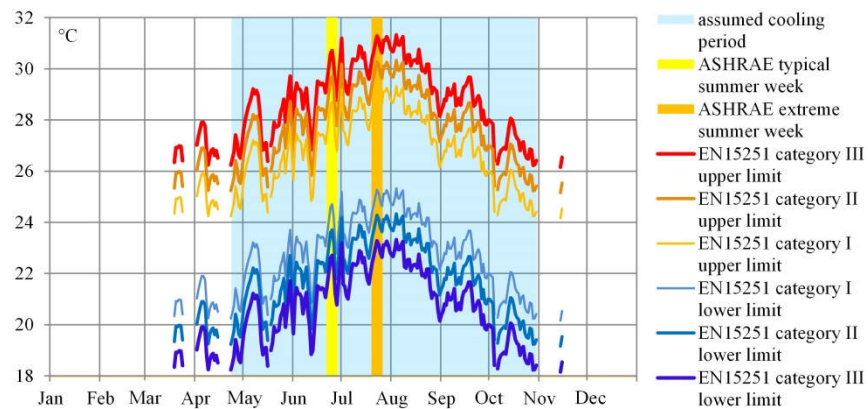


Figure 5.9: Adaptive thermal comfort boundaries according to [41] for Turin [141].

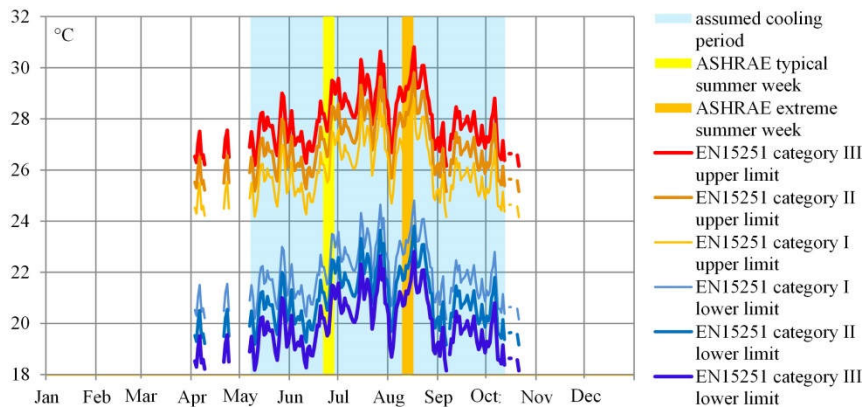


Figure 5.10: Adaptive thermal comfort boundaries according to [41] for Stuttgart [141].

5.2 Cooling Period

According to the approximation made before in § 5.1.3, a typical year’s cooling season in Istanbul is from 24th April till 10th November, in Turin from 24th April till 30th October, and in Stuttgart from 7th May till 12th October. This section gives a deeper insight into the characteristics of this season.

5.2.1 Wind

High ventilation rates due to wind pressure are of special importance for temperature control during the cooling period, when temperature differences between inside and outside are relatively low. Table 5.2 and Table 5.3 below give a detailed view on the wind conditions within the cooling period of the climates considered. As regards the determination of optimum opening orientations for cross ventilation according to the prevailing wind directions, in Istanbul they should be positioned northeast and southwest. In Turin, due to calm wind conditions the situation is less clear, and the design should rely more on a thermally driven strategy. The predominant wind directions in Stuttgart are west and east. Keeping in mind the valley location (see § 5.1.2) of the city, the ventilation design should not rely only on wind forces even though they can be responsible for higher air change rates. Summing up, only in Istanbul the ventilation design may be based on wind forces with predominant direction. Average wind velocity values for the whole cooling season are 5,1 m/s in Istanbul, 0,83 m/s in Turin, and 2,3 m/s in Stuttgart.

Table 5.2: Cooling period wind direction statistics for Istanbul, Turin and Stuttgart [141].

wind direction	from degree °	to degree °	day 7 am - 7 pm			night 7 pm -7 am		
			Istanbul	Turin	Stuttgart	Istanbul	Turin	Stuttgart
zero wind			0%	41%	1%	2%	56%	4%
north	337,5	22,5	13%	12%	5%	21%	11%	6%
northeast	22,5	67,5	45%	13%	12%	49%	5%	4%
east	67,5	112,5	10%	14%	15%	9%	4%	5%
southeast	112,5	157,5	5%	7%	7%	3%	4%	10%
south	157,5	202,5	8%	5%	9%	5%	4%	11%
southwest	202,5	247,5	14%	3%	18%	5%	3%	24%
west	247,5	292,5	4%	2%	22%	3%	6%	22%
northwest	292,5	337,5	2%	3%	12%	2%	8%	14%

Table 5.3: Cooling period wind velocity statistics for Istanbul, Turin and Stuttgart [141].

wind Beaufort scale	from m/s	to m/s	day 7 am -7 pm			night 7 pm -7 am		
			Istanbul	Turin	Stuttgart	Istanbul	Turin	Stuttgart
zero wind	= 0,0		0%	41%	1%	2%	56%	4%
0 calm	>0,0	0,3	0%	8%	1%	1%	9%	8%
1 light air	0,3	1,6	3%	44%	24%	10%	46%	48%
2 light breeze	1,6	3,4	21%	39%	42%	31%	40%	33%
3 gentle breeze	3,4	5,5	26%	8%	23%	33%	5%	10%
4 moderate breeze	5,5	8,0	32%	1%	10%	22%	1%	1%
5 fresh breeze	8,0	10,8	16%	1%	1%	4%	0%	0%
6 strong breeze	10,8	13,9	1%	0%	0%	0%	0%	0%
7 high wind	13,9	16,9	0%	0%	0%	0%	0%	0%

5.2.2 Psychrometrics

Humidity determines which temperatures are comfortable for the building occupants. People are most comfortable within appropriate ranges of temperature, relative humidity, and airflow. Psychrometric charts can show the boundaries of temperature and humidity within which comfort can be achieved at a certain indoor airspeed. Daytime ventilation with higher indoor airspeeds directly affects the cooling sensation of building occupants when temperature is felt too warm. People naturally cool themselves by evaporation; higher humidity levels are more stressful. At high humidity levels up to 90%, a breeze is needed to provide relief. Above 90% humidity, even a stiff breeze will not remove excess body heat. The simple strategy of providing high ventilation rates during occupancy is termed comfort ventilation as described in § 2.2.4.1.

Building Bio-Climatic Charts (BBCC) suggest boundaries of climatic conditions within which indoor comfort can be provided without air conditioning. Givoni [8] defined boundaries for the outdoor air temperature and humidity within which indoor thermal comfort can be provided by comfort ventilation. Diurnal comfort cooling with high flow rates in warm season is possible with external temperatures above 20 °C.

If a building is ventilated with high flow rates, the internal temperature closely follows the external temperature, but usually stays above. With higher internal temperatures, the relative humidity content will fall compared to external conditions (e.g., from 70% to 60%). Internal temperature can stay below the external by exploiting heat sinks or mechanical systems.

The following psychrometric charts in Figure 5.11 through Figure 5.13 show external boundaries within which comfort can be achieved, and also provide hourly information of the three climates considered in this study. The climatic data again is according to ASHRAE IWEC ‘typical meteorological year’ [141]. The time period investigated is the cooling period (according to § 5.1.3) during occupancy hours (7 am to 7 pm).

The humidity content of the external air in Istanbul is the highest. Especially in August, external temperatures above 25 °C are coupled with humidity values above 70%. This may restrict the applicability of a pure passive cooling approach for the building type concerned.

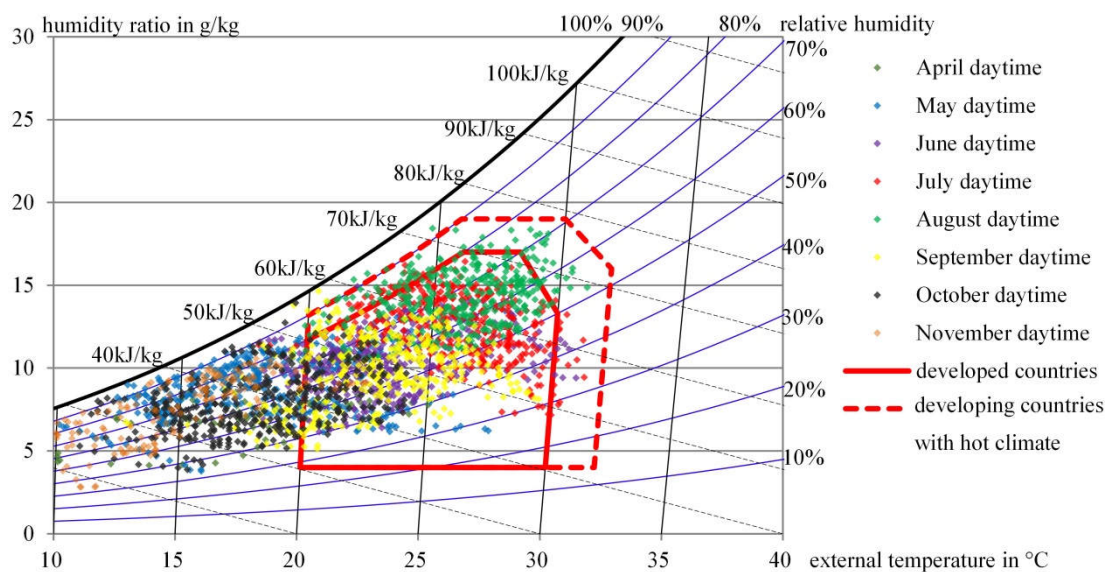


Figure 5.11: Boundaries [8] of external temperature and humidity within which indoor comfort can be provided by natural ventilation during day at high air change rates with indoor airspeed at about 2 m/s and daytime (7am-7pm) climatic data for Istanbul [141] during cooling period.

In Turin, in addition to the temperature, the humidity content in summer is a little lower than that in Istanbul, but still considerable. Especially in July and August, summer peak temperatures above 26 °C occur together with a relative humidity content above 70%.

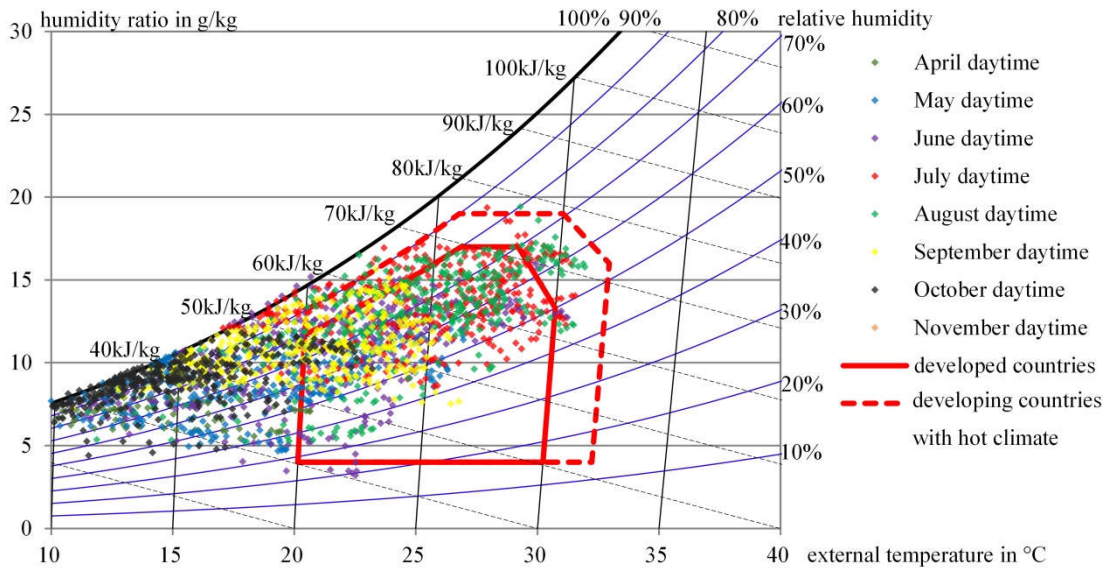


Figure 5.12: Boundaries [8] of external temperature and humidity within which indoor comfort can be provided by natural ventilation during day at high air change rates with indoor airspeed at about 2 m/s and daytime (7am-7pm) climatic data for Turin [141] during cooling period.

Stuttgart climate is less critical, where summer peak temperatures above 25 °C seldom exceed a relative humidity content of above 50%.

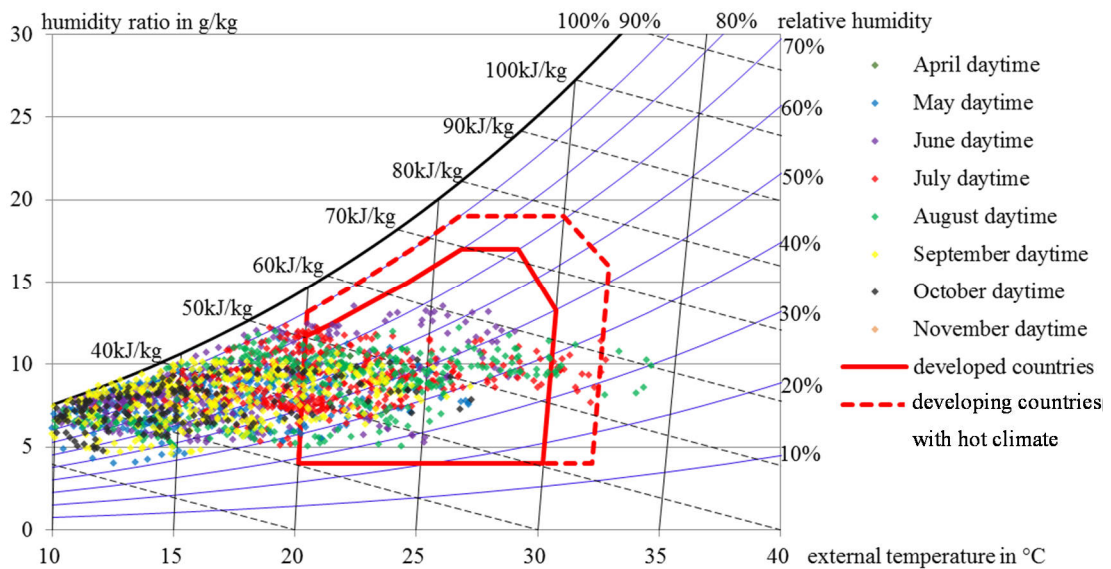


Figure 5.13: Boundaries [8] of external temperature and humidity within which indoor comfort can be provided by natural ventilation during day at high air change rates with indoor airspeed at about 2 m/s and daytime (7am-7pm) climatic data for Stuttgart [141] during cooling period.

5.2.3 Excess temperatures

Reduction of excess temperatures must be based on effective heat gain protection (e.g., solar shading), and cooling must be only a complement, not the opposite. Daytime ventilation with high flow rates cannot fully cover the impact of excess temperatures, as the internal temperature follows the external temperature but will

hardly stay below. Ventilating the building at night can reduce the rate of indoor temperature rise at day by cooling the fabric. Thus, night-time ventilation can contribute to keeping the internal temperature below the external temperature during hot summer. During occupancy, even if the inside temperature is lower, the airflow rate should not be reduced since a breeze will remove excess body heat.

Investigating the temperature excess of the three locations selected, Istanbul is the hottest, followed by Turin and Stuttgart.

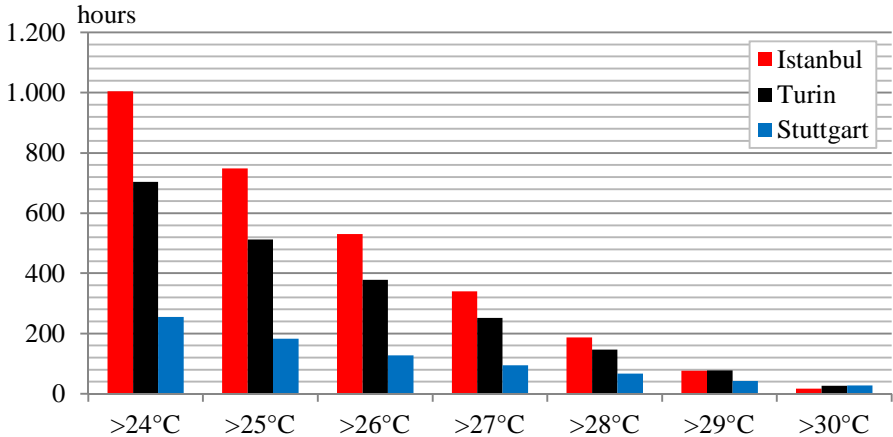


Figure 5.14: Excess frequency of fixed outdoor temperature [141] limits.

Concerning the adaptive comfort limits according to EN 15251, the excess frequency of the different locations somewhat reverses. This is due to the adaptive approach with temperature limits based on the external running mean of the previous days described in § 2.6.3. The temperature excess depends on the temperature fluctuation in summer than on external maxima. It can be concluded that people in Stuttgart need to adapt faster to the fluctuating external conditions than in the warmer and steadier climates of Istanbul and Turin.

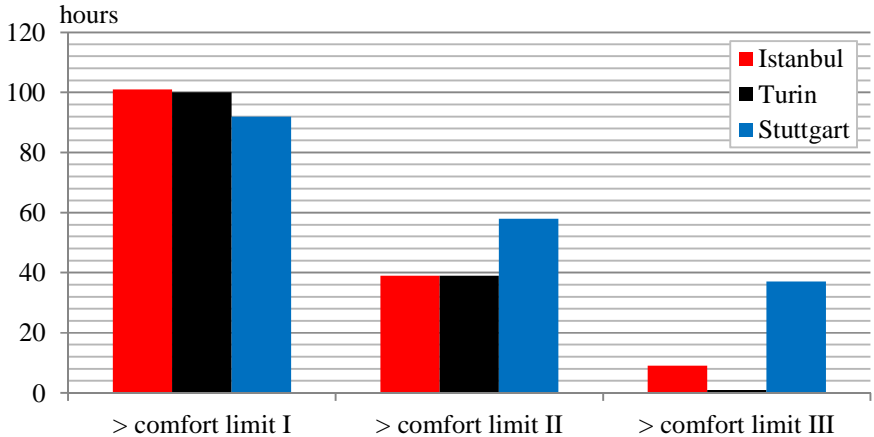


Figure 5.15: Excess frequency of outdoor temperature [141] limits above climate specific upper adaptive comfort category limits [41].

5.2.4 Cooling potentials

For a rough estimation of the climatic cooling potential due to natural ventilation, the temperature difference between the adaptive comfort limits [41] and the external air temperature in the cooling period are first considered as shown in Figure 5.16 through Figure 5.18. A distinction is made between daytime and night cooling. These diagrams indicate, depending on the period and climate, an average temperature difference during the day and during the night.

It is assumed that even the internal temperature during the day and in warm periods, due to control stays somewhere within the lower and upper adaptive comfort boundaries. The internal reference temperature for the whole cooling period is therefore the ideal indoor operative temperature, or comfort temperature, as determined by the EN 15251 adaptive comfort model.

It is also assumed that the slab temperature during the night and in warm periods also stays somewhere within the lower and upper adaptive comfort limits. For an extreme summer week period, higher internal temperatures are expected than for a typical summer week.

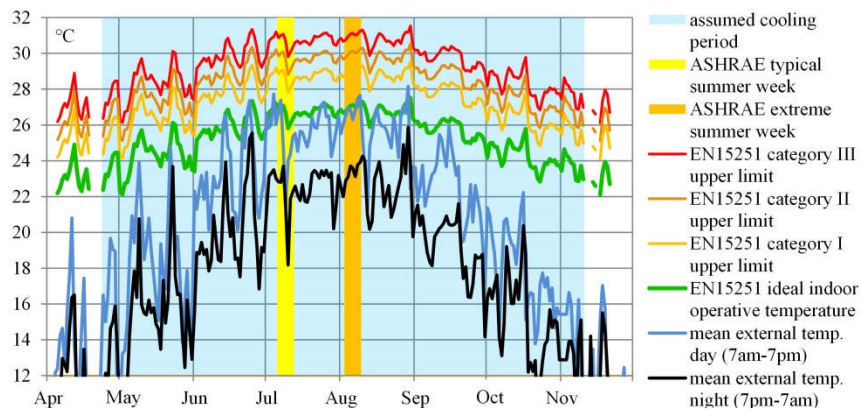


Figure 5.16: Daily cooling potentials in the cooling period for Istanbul [141].

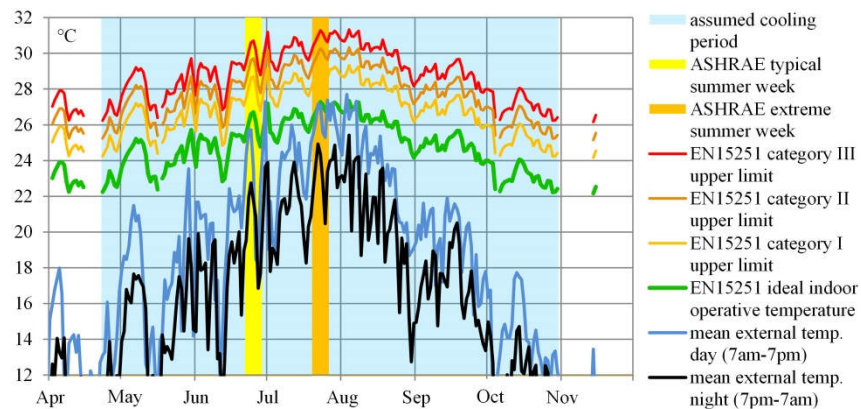


Figure 5.17: Daily cooling potentials in the cooling period for Tornio [141].

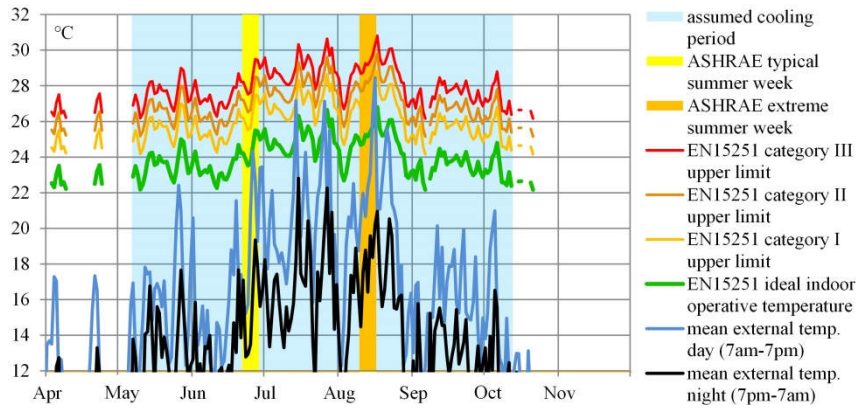


Figure 5.18: Daily cooling potentials in the cooling period for Stuttgart [141].

As summarised in Table 5.4, average temperature differences indicating the cooling potentials in Istanbul are relatively small with 3,2 to 3,8 °C during the day and with 6,6 to 6,8 °C during the night. In the Turin climate, the temperature differences during day is higher for typical summer weeks (5,2 °C) than for extreme summer weeks (3,5 °C), indicating that the extreme summer week is hot compared to the typical summer week. Night-time cooling potentials are only slightly higher than in Istanbul, indicating a relative similar diurnal temperature swing. In Stuttgart, ventilative cooling potentials are the highest. Even during extreme summer conditions considered, temperature differences at daytime (4,9 °C) are one third smaller than those for a typical summer (7,4 °C); the absolute values are significantly higher compared to the climate of Istanbul and Turin. Also, the potentials for night-time ventilation are highest indicating a large temperature swing between day and night. Therefore, in the Stuttgart climate, the air change rates may be smaller to remove the same amount of heat with a higher enthalpy difference compared to the other climates considered.

Table 5.4: Average temperature difference at day and night between external air, and indoor operative comfort criteria indicating the climatic ventilative cooling potentials.

timeperiod		Istanbul				Turin				Stuttgart			
		EN 15251 comfort category				EN 15251 comfort category				EN 15251 comfort category			
		ideal in °C	I in °C	II in °C	III in °C	ideal in °C	I in °C	II in °C	III in °C	ideal in °C	I in °C	II in °C	III in °C
day	cooling season	3,9	5,9	6,9	7,9	5,0	7,0	8,0	9,0	6,3	8,3	9,3	10,3
	typical summer	1,8	3,8	4,8	5,8	3,2	5,2	6,2	7,2	5,4	7,4	8,4	9,4
	extreme summer	0,2	2,2	3,2	4,2	0,5	2,5	3,5	4,5	1,9	3,9	4,9	5,9
night	cooling season	6,8	8,8	9,8	10,8	7,6	9,6	10,6	11,6	9,7	11,7	12,7	13,7
	typical summer	4,8	6,8	7,8	8,8	5,7	7,7	8,7	9,7	8,7	10,7	11,7	12,7
	extreme summer	3,6	5,6	6,6	7,6	3,7	5,7	6,7	7,7	7,4	9,4	10,4	11,4

5.3 Summer Design Days

In this study, design day calculations are performed in § 6.2 to size the natural ventilation systems and to obtain a quick view of the passive building systems performance under summer conditions for a specific climatic location. According to ASHRAE [27], *‘the designer, engineer, or other user must decide which sets of conditions and probability of occurrence apply to the design situation under consideration’*. Design day conditions recommended by ASHRAE were generally developed for mechanical plant sizing, in which due to strict comfort requirements, the conditions set are relatively close as for a peak load calculation. In contrast, naturally ventilated buildings can be operated with a wider comfort range as the occupants would adapt and expect stronger fluctuations in temperature and humidity [48,62,143]. The sizing of a passive cooling design analogous to mechanical systems’ climatic boundary conditions would result in highly expensive, huge dimensioned systems; or else, the comfort requirements cannot be reached. Therefore, the selection criterion addresses the balance between the need to minimise the effort and expenses for passive systems, and the number of hours of comfort requirements not met. The term passive systems here refers to the natural ventilation system, the shading devices and the amount of accessible thermal mass.

In the following chapter, it is described how a design day for passive cooling system sizing calculations can be selected for any location. The basis for the assessment is the ASHRAE International Weather for Energy Calculations (IWEC) ‘typical’ year weather data files [141], which may be downloaded without charge from the EnergyPlus webpage. The typical/extreme period determination and temperature occurrence values are gathered directly from the weather data statistic output files computed by EnergyPlus.

The design day boundary conditions gathered in § 5.3.3 will be utilised as input values for system design and sizing in § 6.2.2. The ASHREA Cooling Design Day (CDD) method is only discussed here as a basis for the SWMD approach developed, but will not be followed up by further research.

5.3.1 ASHRAE cooling design day approach

A widespread design day method used for the sizing of mechanical HVAC systems is the cooling design day approach described in the ASHRAE’s climatic design

information chapter in the Handbook of Fundamentals (HoF) [27]. The method solely covers the external dry-bulb temperature profile with a maximum temperature for a percentage cumulative frequency occurrence for one year as the period of record.

There is no recommendation for the maximum dry-bulb temperature to be utilised for passive ventilative cooling design. But in general, the maximum dry-bulb temperatures for cooling design are treated corresponding to a percentage cumulative frequency of occurrence for the hottest month. Percentages mentioned are 0,4%, 1%, 2%, and 10%. The values for the three locations concerned may be found in Table 5.5 and Figure 5.20.

Table 5.5: Cooling peak temperatures and temperature ranges [141] for design day calculations.

location	hottest month	dry-bulb range in °C	0,4% value in °C	1,0% value in °C	2,0% value in °C
Istanbul	August	7,7	31,1	30,0	28,9
Turin	July	10,1	31,0	29,8	28,3
Stuttgart	July	10,6	29,3	27,6	25,8

The environmental dry-bulb-temperature profiles can then be modelled analogous to the methodology from the ASHRAE HoF 2009. Three parameters describe the current hourly external air temperature $T_{current}$ for the design day of a specific climate location, which are the maximum peak temperature T_{max} , the temperature range T_{range} , and the range multiplier $T_{multiplier}$:

$$T_{current} = T_{max} - T_{range} * T_{multiplier} \quad (5.1)$$

The temperature range or swing is defined as the mean of the difference between the daily maximum and the daily minimum dry-bulb temperatures for the hottest month of the year. Range multipliers are designed according to the local solar time, which may be different from local time zone's time.

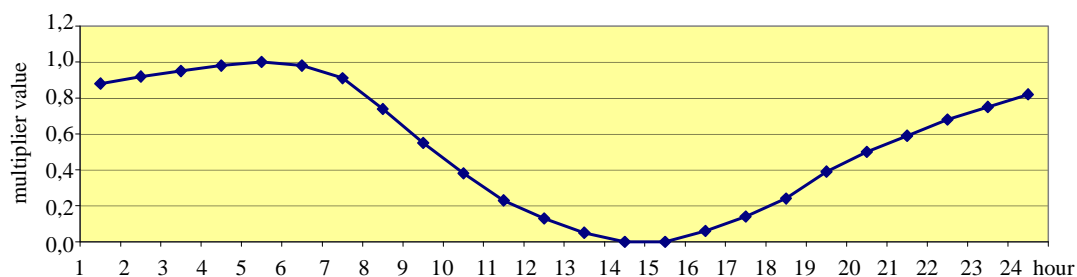


Figure 5.19: Daily temperature multiplier profile (source: [122]).

For the three climatic locations of concern, the resulting daily dry-bulb temperature profiles for 2,0% occurrence are shown in **Figure 5.20**.

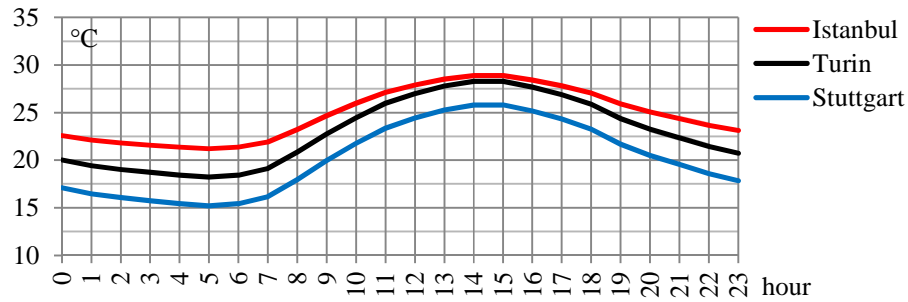


Figure 5.20: Dry-bulb temperature profile for Istanbul, Turin and Stuttgart climate according to the ASHRAE 2,0% occurrence value Cooling Design Day (CDD) approach.

However, there is no recommendation for the maximum temperature to be utilised for passive ventilative cooling design for a certain climatic location. The occurrence design values tend to oversize the equipment, and are only recommended for very temperature-critical operation. Because of the adaptive passive approach of the ventilative cooling system investigated in this study, the CDD method in general tends to unnecessarily oversize the passive systems, and is therefore not recommended.

5.3.2 ASHRAE summer design weeks

Besides the CDD design day approach, ASHRAE also recommends the utilization of summer design weeks. Typical and extreme summer 7-day periods are chosen according to the IWEC weather data statistic file, and are shown in Figure 5.21 through Figure 5.23.

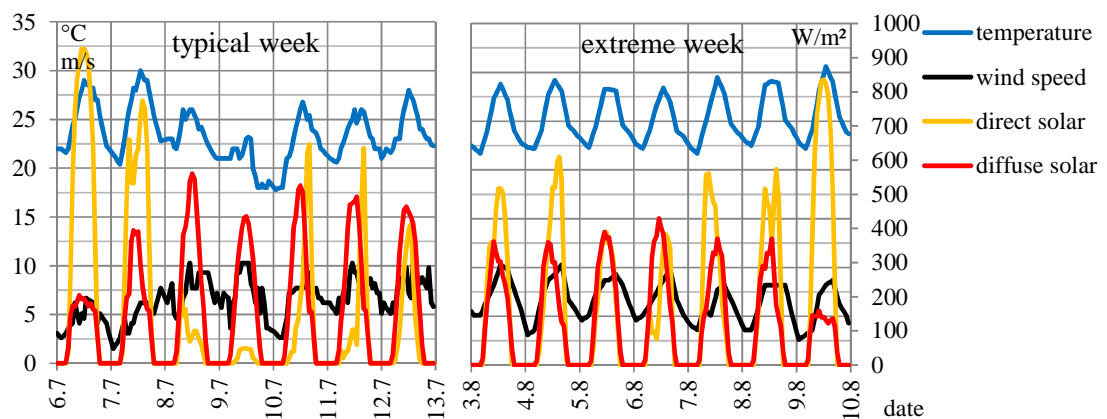


Figure 5.21: Typical/extreme period according to the ASHRAE IEWC weather data and the related statistics for Istanbul [141] climate.

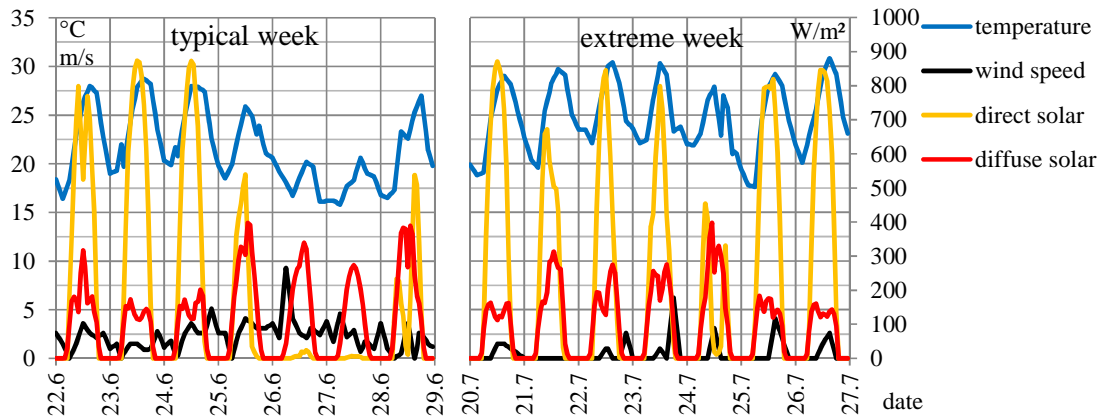


Figure 5.22: Typical/extreme period according to the ASHRAE IEWC weather data and the related statistics for Turin [141] climate.

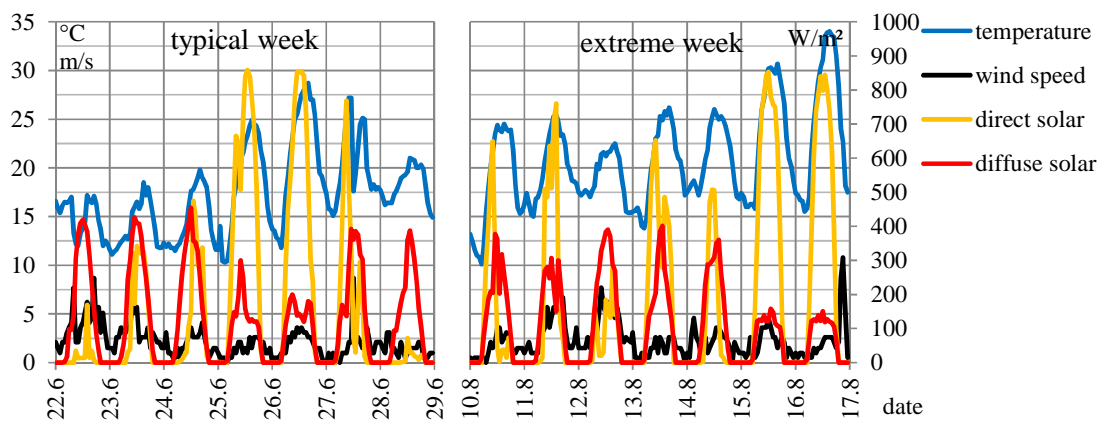


Figure 5.23: Typical/extreme period according to the ASHRAE IEWC weather data and the related statistics for Stuttgart [141] climate.

5.3.3 SWMD approach

To help passive cooling building designers evaluate the severity of climatic problems, the newly developed Summer design Week Mean Day (SWMD) approach organises average temperature, humidity, and radiation information for extreme hot and typical summer design weeks (see § 5.3.2). As the ASHRAE cooling design day, developed for mechanical HVAC system sizing was found not suitable for passive system sizing including adaptive comfort expectations, the summer design days pre-processed in this section are intended to give meaningful design boundary conditions for passive cooling, primarily system sizing. SWMD values are calculated by the mean values of the same timestep of seven days in the examined design week (Figure 5.21 to Figure 5.23). Pre-processed SWMD profiles along with further information are explained in the following paragraphs and will then be used as input for passive system design in the developed ‘HighVent’ design tool (see § 6.2).

Temperature

Design day temperature values are pre-processed for the external dry-bulb temperature at the height of the meteorological station.

Table 5.6: SWMD peak temperature and temperature range for design day calculations.

location	week	period	dry-bulb range in °C	dry-bulb maximum in °C
Istanbul	typical	6.Jun-12.Jun	7,0	29,1
	extreme	3.Aug-9.Aug	6,0	26,7
Turin	typical	22.Jun-28.Jun	8,1	25,1
	extreme	20.Jul-26.Jul	7,1	28,7
Stuttgart	typical	22.Jun-28.Jun	11,3	26,6
	extreme	10.Aug-17.Aug	8,4	21,8

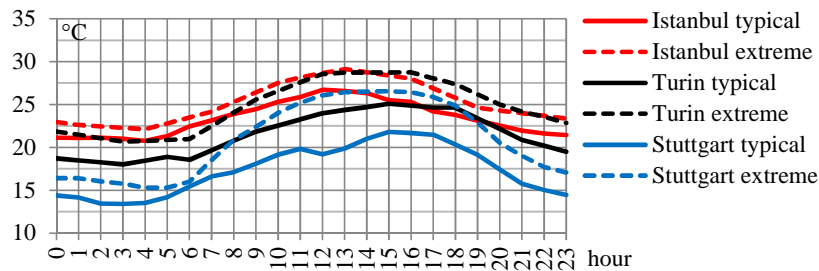


Figure 5.24: SWMD temperature profiles.

Solar radiation

Design day solar radiation values are pre-processed for direct and diffuse radiation. Besides the hourly direct-beam and diffuse radiation intensities, the sun path is of interest to further predict the solar transmitted heat gains of the glazed area. The solar position is simply derived from middle date (4th day) of the design week, and is chosen together with the geographic location.

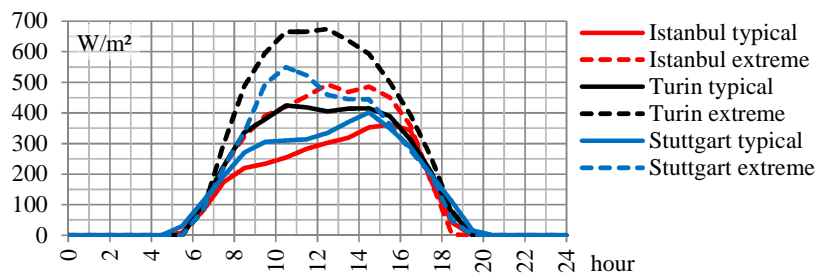


Figure 5.25: SWMD external horizontal direct solar radiation profiles.

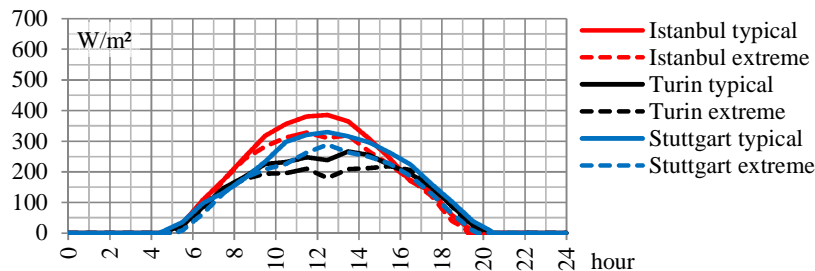


Figure 5.26: SWMD external horizontal diffuse solar radiation profiles.

Table 5.7: SWMD solar path information for design day calculations.

location	week	period	solar day used	highest solar altitude angle in °
Istanbul	typical	6.Jun-12.Jun	9.Jun	71,9
	extreme	3.Aug-9.Aug	6.Aug	65,9
Turin	typical	22.Jun-28.Jun	25.Jun	68,2
	extreme	20.Jul-26.Jul	23.Jul	64,8
Stuttgart	typical	22.Jun-28.Jun	25.Jun	64,7
	extreme	10.Aug-17.Aug	13.Aug	56,2

Humidity

Again, the humidity ratio in kg water per kg air is simply the mean daily value of the same timestep in the examined design week.

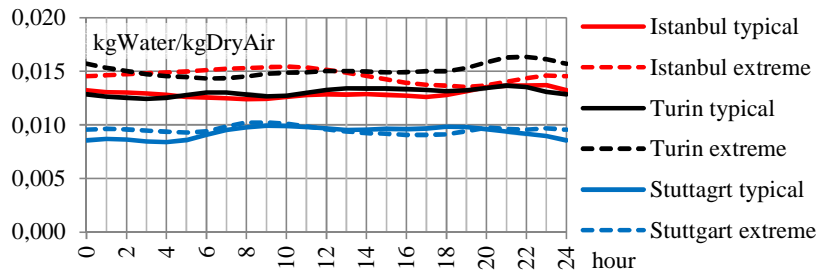


Figure 5.27: SWMD external humidity ratio profiles.

Wind speed

Because the meteorological wind speed is more of stochastic and unpredictable nature, hourly data is not interpolated as is done for temperature, radiation, and humidity. Due to a lack of suitable information in literature, a new ‘average 25% summer wind approach’ is utilised. This is intended to cover the hottest period of the year, when natural ventilation is most needed to provide thermal comfort over a term long enough so as not to account for extreme wind conditions of a specific day or week.

The approach covers the hottest 91 days of the year, which are 25% time of the year as a fragmented period of record. For these days, hourly average wind occurrence values are computed for the subsequent developed passive cooling design, and have a direct impact on the natural ventilation system sizing (e.g., opening areas).

For the three locations considered, average wind velocities for the hottest periods of the year are shown in Figure 5.28. Due to very calm conditions in Turin summer, the natural ventilation design relies mostly on thermal buoyancy forces.

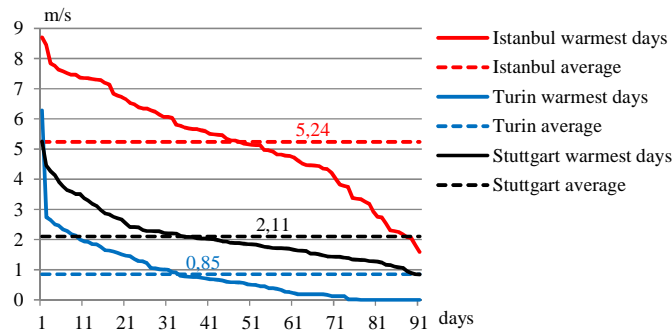


Figure 5.28: Wind speed [141] daily mean occurrence frequencies and 91 day period averages for the hottest 25% days of the year.

5.4 Conclusions

Istanbul and Turin have warm, unbearably humid periods in summer, but passive cooling is possible. In contrast, Stuttgart has less humid air during daytime. Turin and Stuttgart have extreme summer periods, significantly hotter than a typical summer, whereas Istanbul has a more stable summer with the warmest monthly average temperatures ($>24\text{ }^{\circ}\text{C}$). Average summer temperature swings between day and night are distinct in Stuttgart ($>10\text{ }^{\circ}\text{C}$), smaller in Turin ($>8\text{ }^{\circ}\text{C}$), and the smallest in Istanbul ($>7\text{ }^{\circ}\text{C}$). Considering EN standard 15251 category II, operative temperature levels of about $30\text{ }^{\circ}\text{C}$ are temporarily allowed for hot ambient air summer conditions in Istanbul and Turin. Wind velocities differ strongly: Istanbul has outstanding strong winds throughout the whole year (average about 5 m/s at the airport at 10 m height) with clear prevailing wind directions (northeast and southwest). Stuttgart has lesser wind ($2,3\text{ m/s}$ in the cooling season), and Turin is very calm, especially in hot summer periods ($0,8\text{ m/s}$ in the cooling season). Thus, ventilation strategy in Istanbul may be based on wind forces, and wind can assist in Stuttgart. In Turin, pressure differences as the driving force for natural ventilation are most likely achievable based on temperature differences.

The climatic classification design day boundary conditions are developed for passive cooling design day calculations. It is concluded that the classic design day temperatures for mechanical plant sizing are too strict for passive cooling system design as they are close to the peak values and do not reflect the adaptive comfort approach. Instead, a new summer week mean day computation method was developed for typical and extreme summer periods. The method was applied to the three climatic locations of concern, and resulting profiles for temperature, humidity, radiation, and wind are utilised as input for the ‘HighVent’ design tool in § 6.2.

6. THE APPLIED PASSIVE COOLING APPROACH

A case-study building was presented to explore an approach, which uses building simulation technology to evaluate passive cooling measures, with the main focus on natural ventilation. The approach developed in § 3 is here explained through virtual case-study integration, which is the adapted Kanyon building introduced in § 4 . The building will be evaluated for the climates of Istanbul, Turin and Stuttgart according to § 5. In § 6.1 the Kanyon case-study building is conceptually adapted towards the design presented in § 3.1, especially developed for the wide-shaped high-rise building type. In § 6.2 the ‘HighVent’ tool, developed in § 3.2, is utilized to preliminary design and size the passive system components. Finally, for the detailed development of the passive design approach including the controls, in § 6.3, a BEPS model of Kanyon tower is simulated on annual basis along with the preliminary passive design outputs from § 6.2 according the approach developed in § 3.3.

6.1 Conceptual Case-Study Design Adaptations

To assess the potential of controlled natural ventilation in high-rise office buildings, the Kanyon building is taken into account as described in § 4, and conceptually adapted towards a more sustainable naturally ventilated and cooled building design.

6.1.1 Natural ventilation

In the case of the Kanyon building, the maximum penetration depth for cross-ventilation is of only about 14,5 m (Figure 6.1 (a)); and is in case of single-sided ventilation only of about 7,3 m (Figure 6.1 (b)). A big share of the building cannot be ventilated bSimulated electricity consumption of the mechanically and passively cooledy deploying these relatively simple strategies. Therefore, a central chimney or void design as described in § 3.1.1 is chosen suitable for wide building shapes (Figure 6.1 (c)).

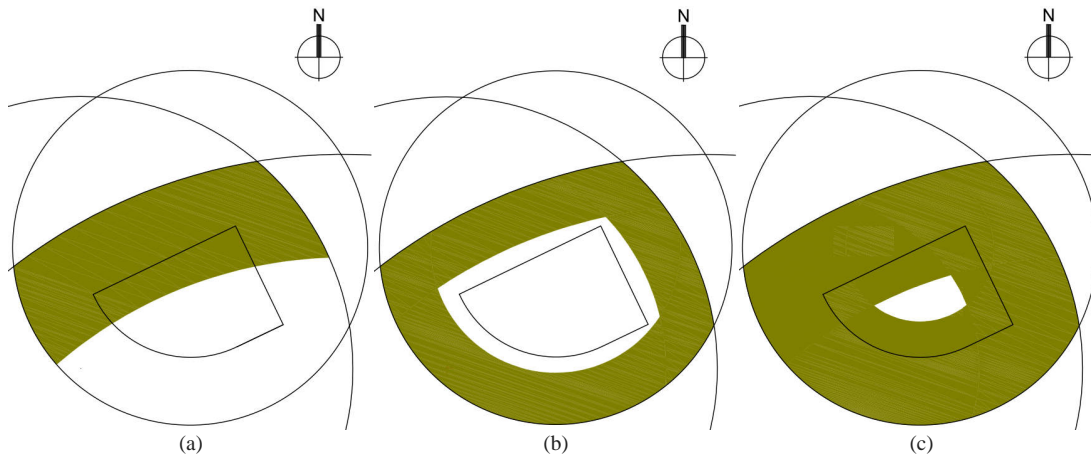


Figure 6.1: Maximum penetration depth (olive) for different ventilation strategies applied to the Kanyon, which are (a) wind (exemplarily from NNW) driven cross ventilation, (b) buoyancy driven single-sided ventilation and (c) central void ventilation.

Bearing in mind all the above considerations mentioned in § 3.1.1, the adapted Kanyon building developed is divided into modular multi-storey building segments stacked on top of each other. The derivation of the design approach is based on the building shape discussed. In the following passive cooling base-case scenarios, each segment consists of five storeys (see Figure 6.2).

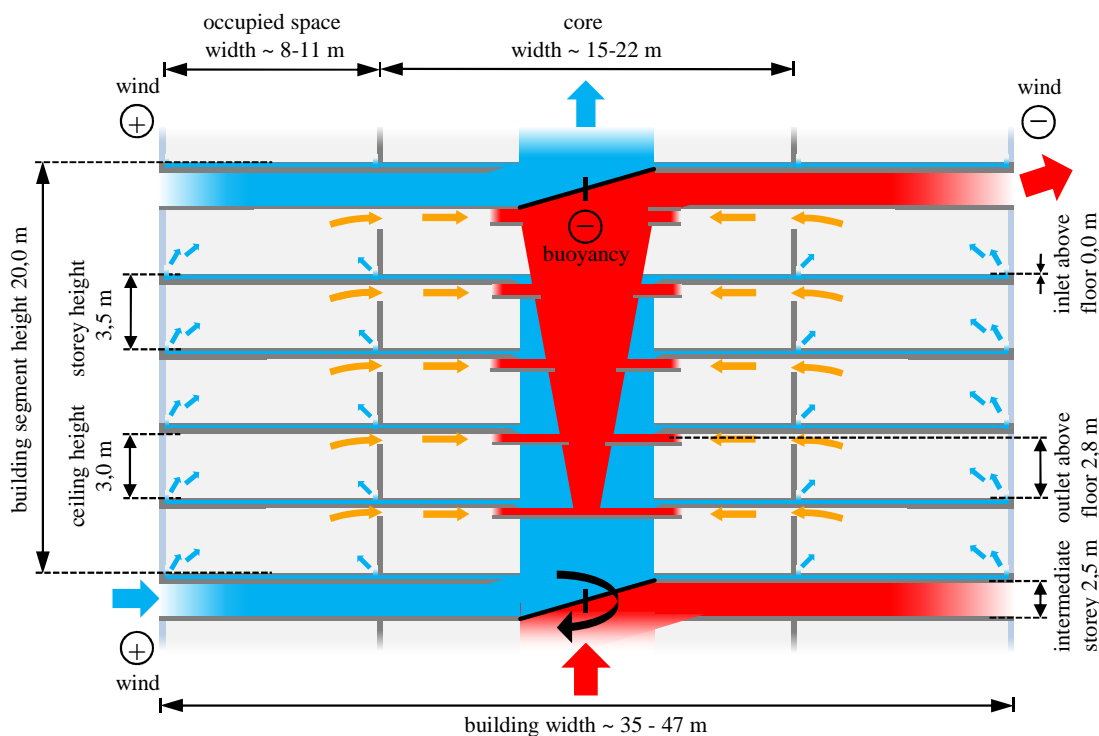


Figure 6.2: Modular five storey base-case natural ventilation building segment.

6.1.2 Solar heat gain reduction

To further reduce the transmitted solar gains, the Kanyon’s actual shading elements (see § 4.2.2.3) are virtually replaced in the adapted base-case scenarios by setpoint controlled exterior window blinds, which are a slat-type horizontal shading devices with fixed slat angle shown in Figure 6.3. The blinds are controlled in a way that the shading is on if the beam plus diffuse solar radiation incident on the façade exceeds the setpoint of 250 W/m².

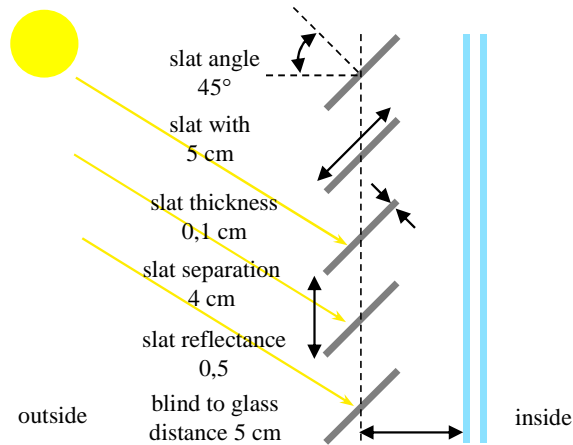


Figure 6.3: Side view of the enhanced shading window blind with horizontal slats showing slat geometry as modelled in the adapted base-case scenarios for passive cooling.

Simulations indicate that the on/off controlled blinds in the cooling period in Istanbul (cooling period see § 5.1.4) reduce the amount of solar radiation entering the window by 31% compared to the actual shading elements shown in Figure 4.11 and by 39% compared to no external shading. Figure 6.4 indicates the effectiveness of the enhanced, slat-type shading devices in comparison to the actual, horizontal shading devices over the course of a typical summer and a typical winter design week according to the ASHRAE IEWC weather data. The transmitted solar radiation in W/m² net floor area refers to the average value of the whole building.

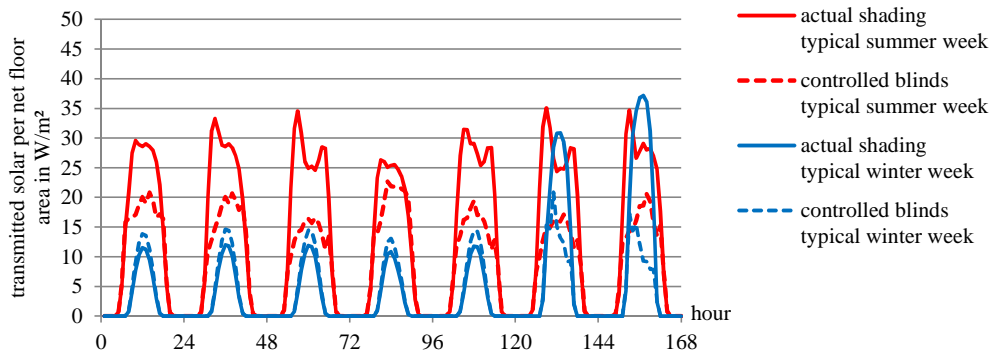


Figure 6.4: Simulated effectiveness of the controlled blinds compared to the actual shading devices in a typical summer and winter week period.

6.1.3 Thermal mass activation

Three different levels of thermal mass are defined for parametric modelling and a reverse arrangement of the ceiling/floor construction. These arrangements represent an actual as-built light-weight (suspended ceiling), a medium-weight (mass exposed concrete ceiling), a reverse medium-weight (mass exposed concrete floor), and a heavy-weight (mass exposed concrete ceiling, solid sand–lime partitions, and mass activated load bearing wall) construction. The detailed layers of the elements and the thermal properties of the building materials are given in Table 6.1. The last four columns in the table contain the total (C_m) and areal diurnal (χ_m) storage capacities of the internal construction elements when the surfaces are exposed to a varying temperature, excluding the surface resistance. The effective capacities are calculated according to the simplified calculation method in EN ISO 13786 [144], which is done by assuming a sinusoidal temperature variation with a one day time period.

Table 6.1: Thermal properties of composition elements for three different levels of thermal mass

	scenario index n	A_i in m ²	materials	d_i in m	d_T in m	ρ_i in kg/m ³	c_i in J/kg-K	C_m in J/K	C_m in Wh/Kin	χ_m in kJ/m ² -Kin	χ_m in Wh/m ² -K
suspended floor	1,2,4	1.000	carpet	0,0060,006	200	1.300	1.560.000	433	2	0	
	1,2,4	1.000	plywood	0,0300,030	544	1.210	19.747.200	5.485	20	5	
mass activated floor	3	1.000	concrete	0,1250,100	2.400	1.000	240.000.000	66.667	240	67	
suspended ceiling	1,3	1.000	plasterboard	0,0130,013	900	1.000	11.250.000	3.125	11	3	
mass activated ceiling	2,4	1.000	concrete	0,1250,100	2.400	1.000	240.000.000	66.667	240	67	
suspended internal wall	1,2,3	477	oak wood	0,0130,013	704	1.630	4.881.062	1.356	7	2	
mass activated wall	4	477	concrete	0,4000,100	2.400	1.000	81.668.640	22.686	114	32	
internal columns	1,2,3,4	163	concrete	0,5000,071	2.400	1.000	27.709.535	7.697	28	8	
light internal partitions	1,2,3,4	460	plasterboard	0,0130,013	900	1.000	5.179.500	1.439	5	1	
heavy partitions	4	460	sand–lime	0,1500,075	2000	1.000	69.060.000	19.183	69	19	
SUM n=1 (actual) $\chi_m=C_m/A_{\text{floor}}$									72	20	
SUM n=2 (ceiling activated) $\chi_m=C_m/A_{\text{floor}}$									301	84	
SUM n=3 (floor activated) $\chi_m=C_m/A_{\text{floor}}$									291	81	
SUM n=4 (heavy) $\chi_m=C_m/A_{\text{floor}}$									473	133	

Figure 6.5 shows the resulting diurnal heat storage capacity for the three different levels of thermal mass, and classifies them according to their heaviness of construction [145]. The medium level thermal mass capacity case with mass exposed ceilings (index n=2) in the following is treated as the adapted building design base-case scenario (as mentioned in Table 6.3) with a dynamic heat capacity of 84 Wh/m²-K. The light-weight case (index n=1) represents the actual as-built scenario with a diurnal heat capacity per unit floor area of 20 Wh/m²-K. The mass activated floor case (81 Wh/m²-K) and the heavy-weight case with a dynamic heat capacity of 133 Wh/m²-K serve as a scenario for the detailed design parametric analysis regarding thermal mass (see § 7.2.2.1).

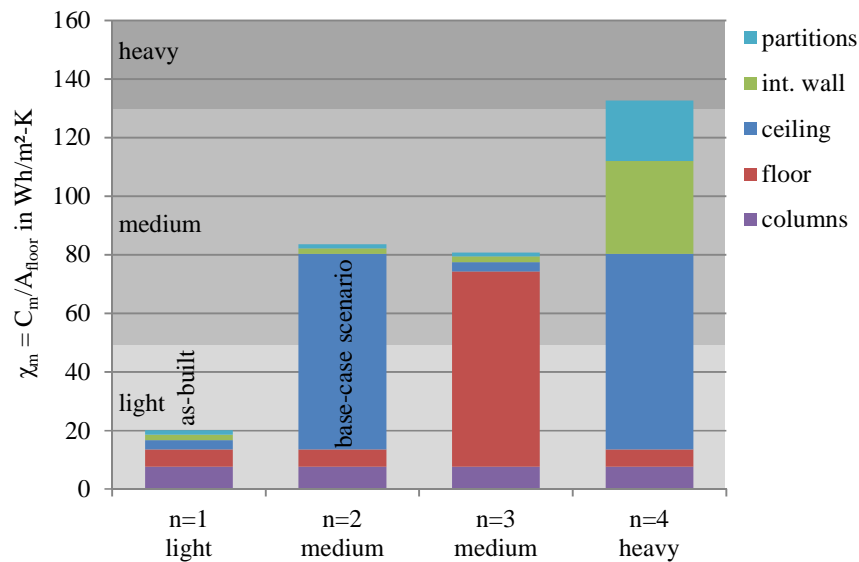


Figure 6.5: Effective heat capacity for a one day period (EN ISO 13786 [144]; excluding surface resistance) of building elements for four different levels of thermal mass and classification [145].

6.2 Preliminary Design

The ‘HighVent’ design tool developed in § 3.2, in this section is applied, to ‘fast-forward’ study the systems necessary, to passively cool the Kanyon tower. The high-rise office case-study building is situated in three different climates to size and evaluate the functionality of a naturally ventilated building under various external conditions. Optimization targets are to reach minimal system sizes with respect to the comfort and flow path criteria developed. Results are presented in detail. Examples of the application for the Kanyon building are given subsequently.

6.2.1.1 Driving forces

The wind pressure coefficients of the Kanyon tower including the neighbouring and potentially wind shielding buildings was tested in wind tunnel experiments. The lab setup including a 1:300 sized model, and the detailed results of the C_p values gathered may be found in Appendix A. Average wind pressure coefficients measured in the lab are 0,70 on the windward ($C_{p,1}$) and -0,76 on the leeward façade ($C_{p,2}$) orientations. The resulting wind pressure differences for the Kanyon building shape depending on the meteorological wind velocity and with the roughness characteristics of city centre terrain on the envelope of the 5 storey segments base-case example shown in Figure 6.2, are as shown in Figure 6.6.

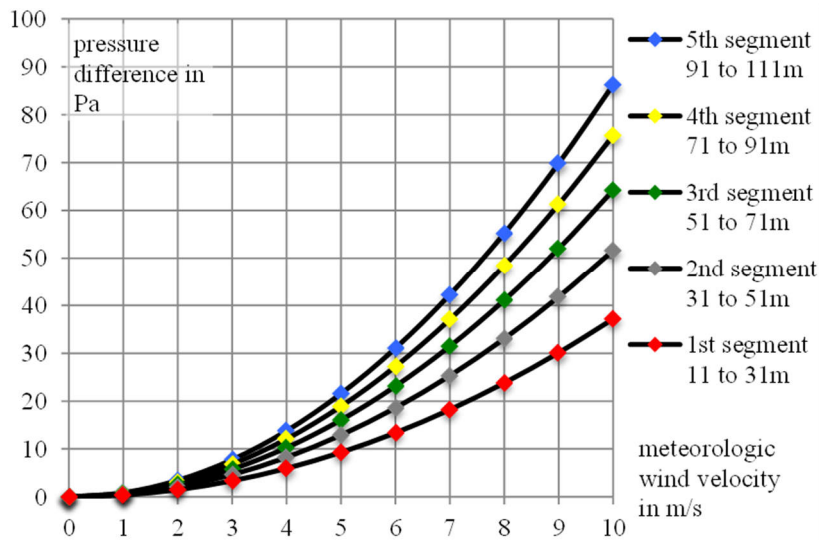


Figure 6.6: Total wind pressure difference across the flow paths from the inlet to the outlets (for the exemplary 5 building segments with a $\Delta C_p = 1,46$ and in city terrain).

Resulting stack pressure differences dependent on different exhaust chimney heights and temperature differences are assumed equal for all segments and are shown in Figure 6.7.

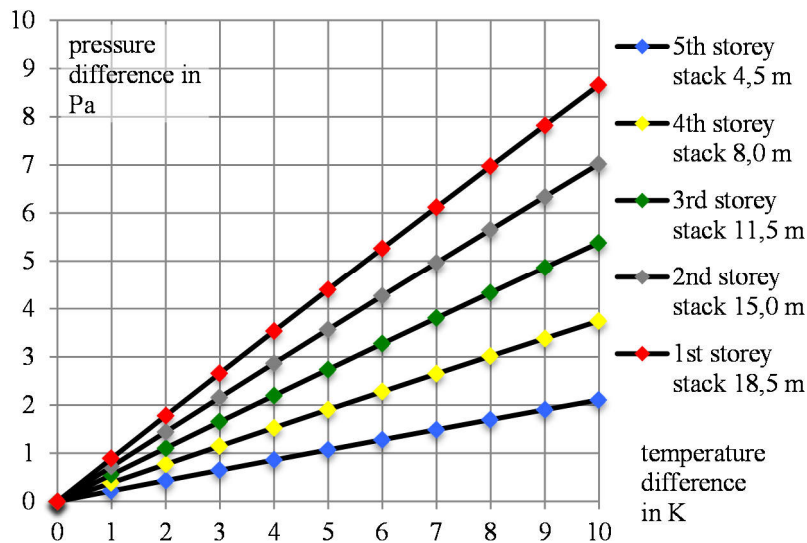


Figure 6.7: Total stack pressure difference across the flow paths from the inlet to the outlet (for the 5 storeys of each building segment).

Steady state boundaries

The wind velocity design conditions chosen for the three climates considered are the average wind velocities in the hottest 91 days of the year (see § 5.3.3), and the city centre terrain roughness. According to the weather files, the corresponding wind velocities are 5,25 m/s in Istanbul (base-case scenario), 0,85 m/s in Turin and 2,11 m/s in Stuttgart. The local wind speed is then calculated according to the terrain and the local height of the openings.

For the minimum hygienic air change and for passive cooling in summer, CIBSE [26] recommends a temperature difference of 3 Kelvin between inside and outside.

Additional chimney heats gains (to cell B), usually from solar radiation but here considered from data centres, lower the chimney air density, and therefore increase the upward buoyant flow. An increase of 1 °C is assumed in the exhaust chimney due to high heat load of the IT-systems generated in the core of the case-study building with approximately 10 kW per storey (see § 4.2.3).

Additional chimney heats loss (from cell A), usually from mechanical cooling but could also be considered from evaporation cooling or due to underground ducts, increases the chimney air density, and in turn increases the upward buoyant flow due to higher temperature differences. This temperature drop is integrated into the tool, but is not considered as a design option for the Kanyon building. Therefore, the inlet chimney has equal air properties as the external air.

Pressure differences on each storey

Figure 6.8 shows the total pressure drop from the chimney inlet to the outlet (for the whole flow path). In Turin the buoyant share is the dominating design pressure difference, whereas in Istanbul the wind pressure is far more predominant due to high wind velocities (see also § 5.3.3).

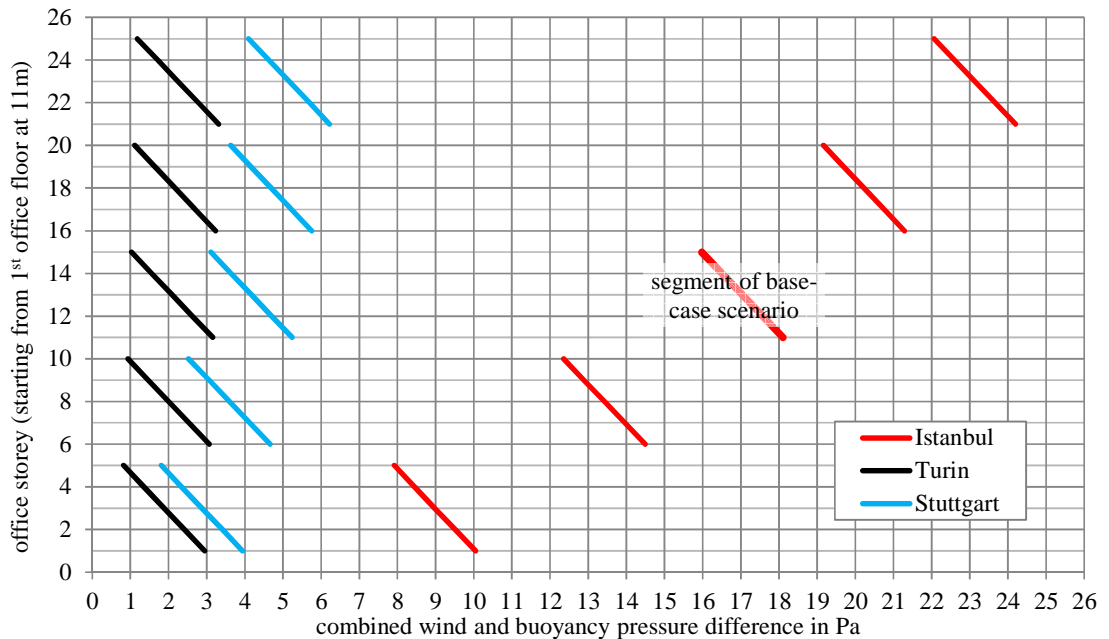


Figure 6.8: Pressure drop across the flow paths from the supply inlet to the exhaust outlet for each storey of five segments with 5 storeys each, calculated according the unchanging design boundary conditions.

6.2.1.2 Electric airflow analogy model

The following exemplary input parameters are chosen for the Kanyon building application example. The wind pressure coefficients were gathered in wind tunnel experiments, and the discharge coefficients for sharp edged openings are from literature according to § 2.2.3. The discharge coefficient for the sub-slab distribution system is a rough estimation dependent on the practical implementation, and needs further investigation.

Table 6.2: Inputs made for the flow path sizing pre-design with fixed boundary conditions.

	symbol	unit	Istanbul	Turin	Stuttgart
number of storeys per segment	n	-		5	
storey height	h	m		3,50	
ceiling height	h	m		2,90	
office cell inlet height above floor level	h	m		0,00	
office cell outlet height above floor level	h	m		2,66	
intermediate floor height (between the segments)	h	m		2,50	
meteorological summer design wind velocity	v_{met}	m/s	5,24	0,85	2,11
site terrain for wind profile	-	-		city centre	
meteorological temperature (minor relevance)	T_E	°C		25,00	
office cell temp. above supply chimney temp.	ΔT_I	°C		+ 3,00	
supply chimney temp. below external temp.	ΔT_A	°C		± 0,00	
exhaust chimney temp. above office cell temp.	ΔT_B	°C		+ 1,00	
internal overflow openings size factor	K	-		2	
chimney external openings size factor	k	-		1	
wind pressure coefficients	$C_{p,1}$	-		0,70 (windward)	
	$C_{p,2}$	-		-0,76 (leeward)	
discharge coefficients	$C_{d,1-2}$	-	0,61 (external chimney openings)		
	$C_{d,3...}$	-	0,50 (sub-slab inlet distribution)		
	$C_{d,4...}$	-	0,61 (overflows offices to core)		
	$C_{d,5...}$	-	0,61 (exhaust chimney inlets)		

The following diagrams are obtained from the design tool developed in § 3.2, and show the major outputs for a one-storey cell model (the 3rd storey of the 3rd building segment) of the case-study building. The three base-cases investigated here all include uncontrolled natural ventilation, improved shading, and activated ceiling mass. The design air change rate was adapted in 1 h⁻¹ steps until the requirements were fulfilled. So as not to oversize the system, the smallest design ACH value was taken.

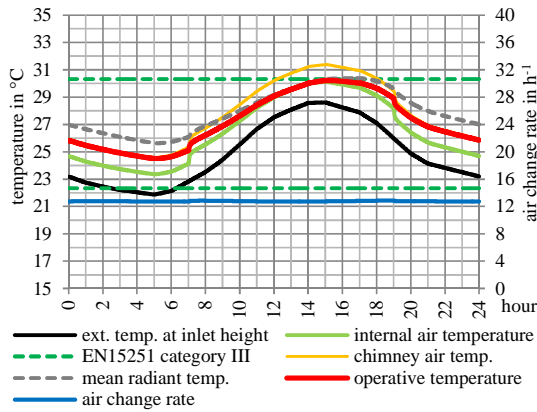


Figure 6.9: Outputs for extreme summer conditions in Istanbul sized for 13 ACH $\hat{=} A_{chi} = 29,4 \text{ m}^2$.

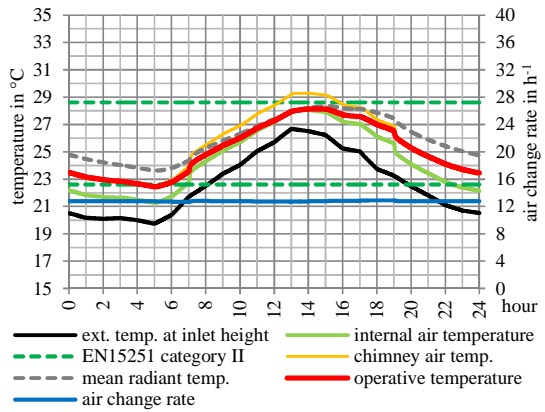


Figure 6.10: Outputs for typical summer conditions in Istanbul sized for 13 ACH $\hat{=} A_{chi} = 29,4 \text{ m}^2$.

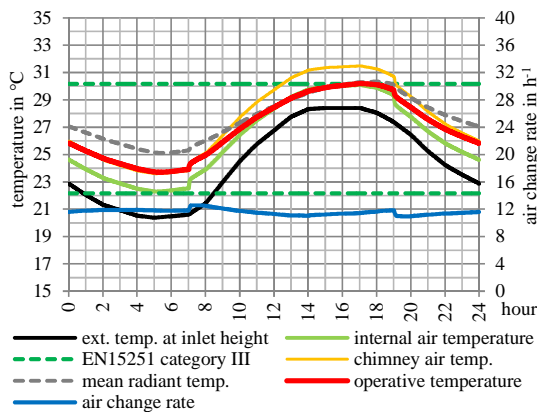


Figure 6.11: Outputs for extreme summer conditions in Turin sized for 13 ACH $\hat{=} A_{chi} = 93,4 \text{ m}^2$.

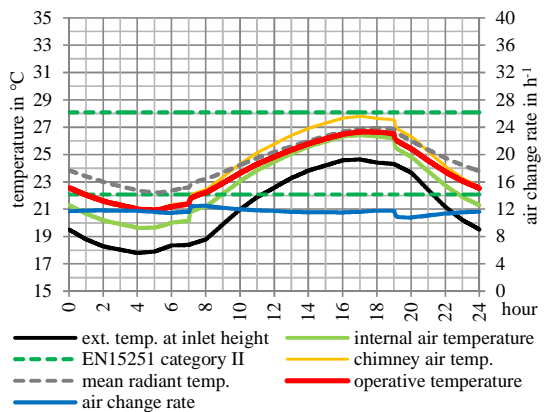


Figure 6.12: Outputs for typical summer conditions in Turin sized for 13 ACH $\hat{=} A_{chi} = 93,4 \text{ m}^2$.

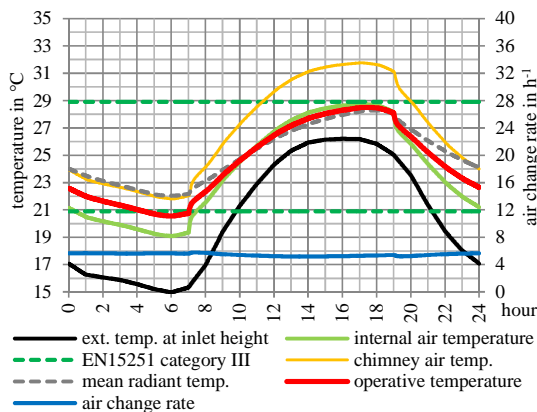


Figure 6.13: Outputs for extreme summer conditions in Stuttgart sized for 5 ACH $\hat{=} A_{chi} = 23,3 \text{ m}^2$.

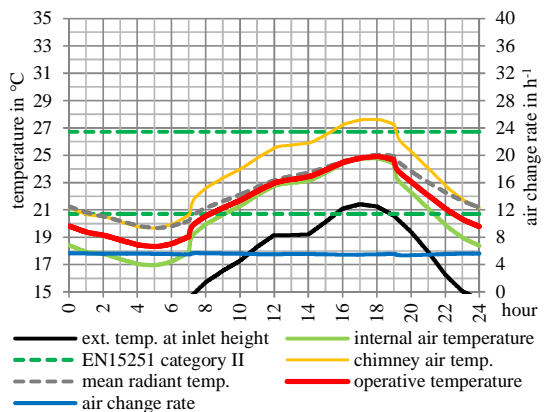


Figure 6.14: Outputs for typical summer conditions in Stuttgart sized for 5 ACH $\hat{=} A_{chi} = 23,3 \text{ m}^2$.

Istanbul is located in the hottest of the three climates considered, and hence requires significant ventilation rates with a design value at about 13 ACH to stay within the desired comfort categories. Because of high average meteorological wind velocities of about 5,2 m/s (see § 5.3.3), the ventilation system according to this first design

assessment can be sized adequately small in size. The size here first is expressed by the needed internal chimney cross-sectional area of the third building segment, which is about 29 m² (details for all the five building segments are given in § 6.2.2). Even the typical summer conditions are relatively close to the extreme and the daily external temperature swing is small; the results indicate that the size is sufficient to stay below category II comfort upper limit during a typical summer day.

Turin has a trickier climate in that it has an extremely hot summer period almost without wind (average value of 0,9 m/s). This results in a high ventilation demand identical to the one for Istanbul, but mostly driven by buoyancy forces. To achieve the ventilative objectives, the system size needs to be huge with an internal chimney cross-section of about 93 m², which is almost 10% of the net floor area. As the typical summer conditions are considerably lower in temperature than the extreme conditions, the system seems to be a bit oversized for most of the warm season. Figure 6.15 and Figure 6.16 show the outputs with reduced natural ventilation system sizes. This scenario will be further discussed in § 6.3.2.

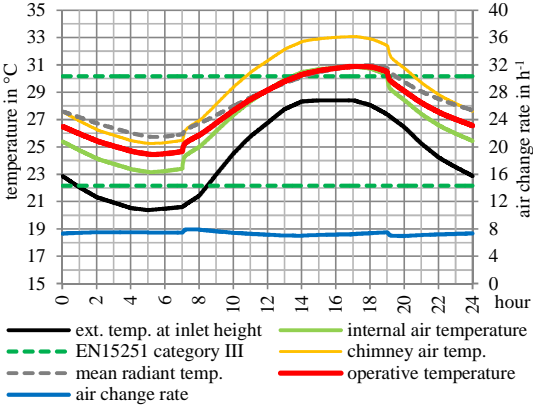


Figure 6.15: Outputs for extreme summer conditions in Turin sized for 7 ACH $\triangleq A_{\text{chi}} = 50,0 \text{ m}^2$.

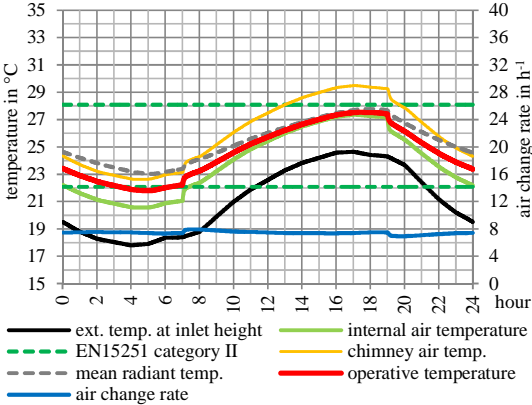


Figure 6.16: Outputs for typical summer conditions in Turin sized for 7 ACH $\triangleq A_{\text{chi}} = 50,0 \text{ m}^2$.

Stuttgart is situated in the coldest summer climate, which results in a much smaller ventilation demand of 5 ACH. Since even the average wind velocity in the hottest period of the year is less than half of that in Istanbul, the ventilation system can be sized the smallest. As the typical German summer climate is much colder than the extreme period, the second requirement can be easily fulfilled. Care must be taken not to overcool in the morning hours, which is discussed in § 3.3.2. In comparison, the Stuttgart climate seems less critical.

6.2.2 Case-study application

The approach developed is now virtually applied to all the five adapted case-study building segments at heights from 11 to 111 m, considering the summer design climates of Istanbul, Turin and Stuttgart (Kanyon building introduced in § 4, and for adaptations see § 6.1).

The size of the chimney here is assumed to be the sum of the opening areas connected to the chimney.

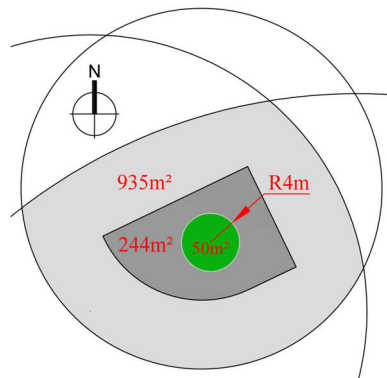


Figure 6.17: Plan view of one storey of Kanyon including an central chimney (here with 50 m² area).

Figure 6.18 gives an overview of the opening sizes calculated in ‘Tool Step 1’ and the design air change rate necessary calculated in ‘Tool Step 2’.

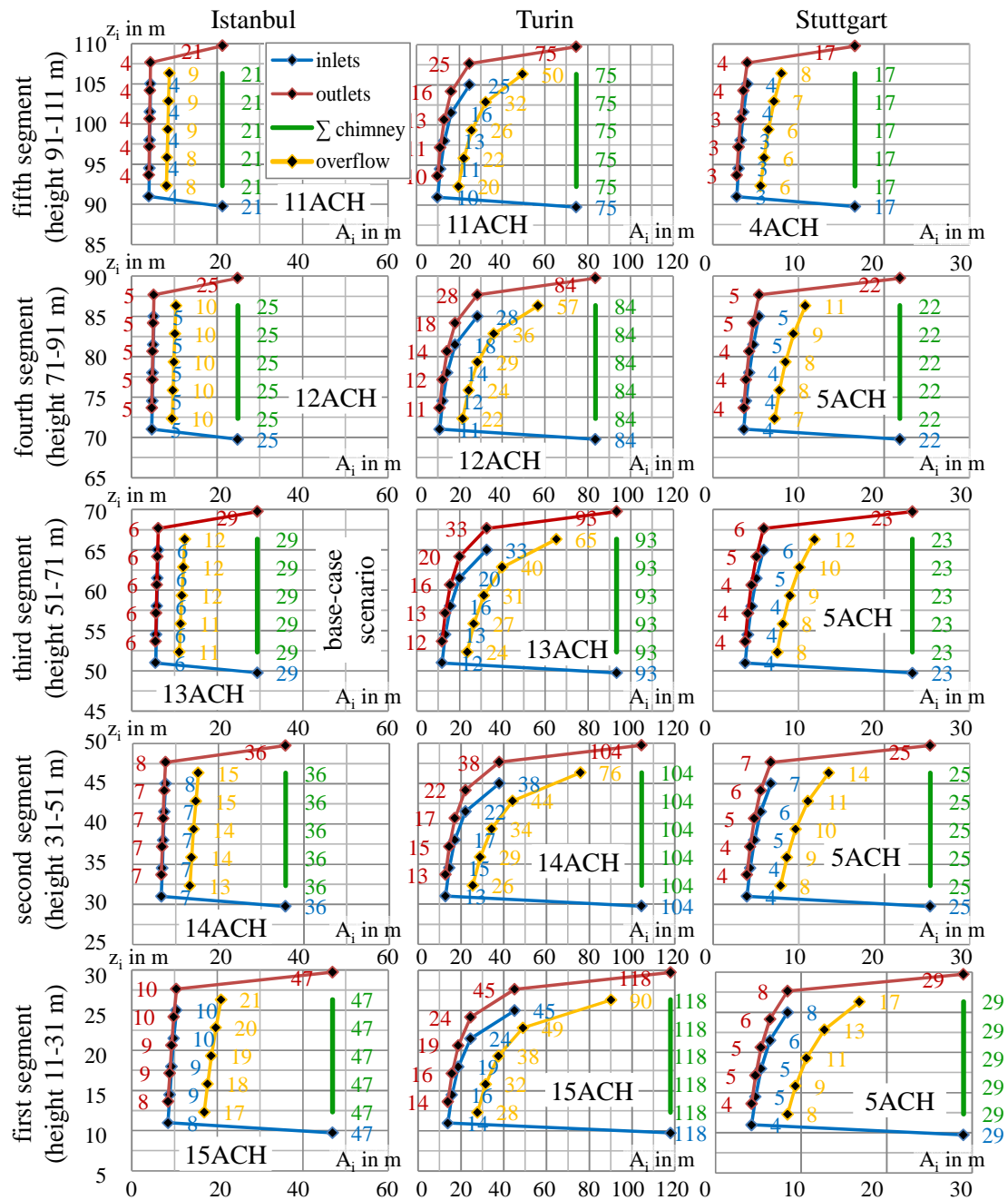


Figure 6.18: Outputs of the flow path sizing pre-design with fixed boundary conditions for each segment and the three climates considered.

Opening sizes in general get smaller at high building segment levels because of the wind profile. This circumstance is further assisted by the external temperature variation with height - also influencing the indoor thermal environment in a way it is easier to cool the space with less incoming air.

6.3 Detailed Design Development through Energy Simulation

To assess the potential of controlled natural ventilation in high-rise office buildings, an existing case-study building as described in Chapter 3 was taken and modelled along with the passive approach design adaptations developed in Section 6.1 (for an overview, see Table 6.3). The ‘HighVent’ design tool outputs from § 6.2, which are primarily the design parameters – the positioning and sizing of openings in the flow path, are ‘post-processed’ in this section as inputs for detailed Building Energy Performance Simulations (BEPS) including AirFlow Networks (AFN). Moreover, some parametric analyses are intended to show the influence of system sizing parameters on the performance of the developed approach and to support decision making.

The calibration of the as-built simulation model is necessary and crucial for the accuracy and usability of the energy simulation model, which is then adopted towards the passive design approach. The current building performance will be compared to the passive approach developed in the context of the design evaluation Chapter 7.

6.3.1 Simulation setup

The following Table 6.3 summarises the thermal properties and operation of the existing building (see also § 4), and highlights the adaptations made in the model towards a passively operated or hybrid operated building. The two adapted base-case scenarios are identical with the only difference being that one of them is purely passive cooled and ventilated, whereas the other is modelled with a hybrid backup system for summer temperature peaks. Hybrid systems are emphasised by square brackets within the right column of the adapted approach. The design adjustments of the base-case scenarios are described in more detail in Sections 6.1 through 6.2.

Table 6.3: Brief overview of the simulation setup for the as-built and the adapted scenarios.

	as-built building	base-case adapted for passive cooling
climate	Istanbul (ASHRAE IEWC 'typical' climate)	
building	Kanyon high-rise office tower with 28 storeys and 118 m height	
storeys modelled	25 office storeys from 11-111 m height	
	detailed assessment of the 3 rd segment at 51-71 m height	
storey geometry	gross internal area 1 150 m ² / 4 m storey height net usable area 1 010 m ² (850 m ² offices and 160 m ² core) / 2,9 m ceiling height	
external glazing	465 m ² /storey LoE double glazing uniform distributed to all orientations ≈ 91,8% glazing ratio / U-value 1,4 W/m ² -K / SHGC 0,444 / visible transmittance 0,68	
external wall	40 m ² metal panelled lightweight curtain wall with a U-value of 0,29 W/m ² -K	
floor / ceiling construction	sealed double floor carpet (0,006m) / plywood (0,030m) air space (0,156m) / concrete (0,125m) airspace (0,770m) / plasterboard (0,013m)	mass activated ceiling carpet (0,006m) / plywood (0,030m) air space (0,439m) / concrete (0,125m)
'additional' thermal mass	internal heavyweight but sealed partitions with an area of 373m ² (area for one side) oak wood (0,013m) / air (0,025m) / concrete (0,40m) / air (0,025m) / oak wood (0,013m)	
ventilation system	mechanical ventilation weekdays 2 ACH from 6-21h weekend 2 ACH from 8-18h max. 4 ACH during economiser operation	natural ventilation sized for passive cooling according to § 6.3.2 controlled according to § 3.3.2 [14 l/s-person during hybrid operation]
infiltration	1,0 ACH at 50 Pa pressure difference between in- and outside (n ₅₀ value 1,0 h ⁻¹)	
wind pressure coef.	mean windward C _p of 0,70 and mean leeward C _p of -0,76	
occupancy	62 people per storey during weekdays 7-19h producing 108W heat per person and 0,000000382 m ³ /W-s CO ₂	
internal equipment	12 W/m ² during weekdays 7-19h 3 W/m ² during night from 19-7h and during weekend	
external shading devices	uncontrolled horizontally attached shadings mounted on southeast through southwest façade orientations	setpoint controlled venetian blinds (on/off setpoint 250 W/m ² solar on façade) mounted on all façade orientations
lighting system	installed power density is 8,8 W/m ² in the office space and 5,0 W/m ² in the core space 18% luminous efficacy (fluorescent tube) power density reduced by 2-stepped 500 lux setpoint dimming in 80% of the office space measured in the centre of the office zones during weekdays from 7-19h power density reduced to 0,44 W/m ² in the office space and 1,25 W/m ² at night from 19-7h and during weekend	
IT-systems	10 kW per storey in the core	10 kW per storey in the exhaust chimney
heating system	central natural gas fired hot water boiler with a efficiency of 0,8 local fan coil units and preheated air from central air handling unit air temperature setpoint weekday: 22°C±3°C (6-21h) / 18°C (21-6h) weekend: 22°C±3°C (8-18h) / 18°C (18-8h)	local baseboard heating and preheated air from sub floor distribution operative temperature setpoint weekday: 21°C (6-21h) / 18°C (21-6h) weekend: 21°C (8-18h) / 18°C (18-8h)
cooling system	central water cooled (cooling tower) local fan coil units and cooled air from central air handling unit air temperature setpoint weekday: 24°C±3°C by occupants (6-21h) weekend: 24°C±3°C by occupants (8-18h)	electric chiller with a COP of 3,2 [cooled air from central air handling unit] [operative setpoint temperature] [weekday: 26°C (7-19h)] [weekend: 26°C (8-18h)]

To reduce the simulation effort to a feasible degree, only one segment of the building including five storeys and the chimney, is modelled as shown in Figure 6.19. Two horizontal cuts decouple the building segment from the rest of the building and are defined with adiabatic properties. The resulting simulation model consists of 27 zones, including 20 office zones (four per storey), 5 core zones, one air supply zone, and one air exhaust zone. The zones in the model are connected by conductive and ventilative heat transfer.

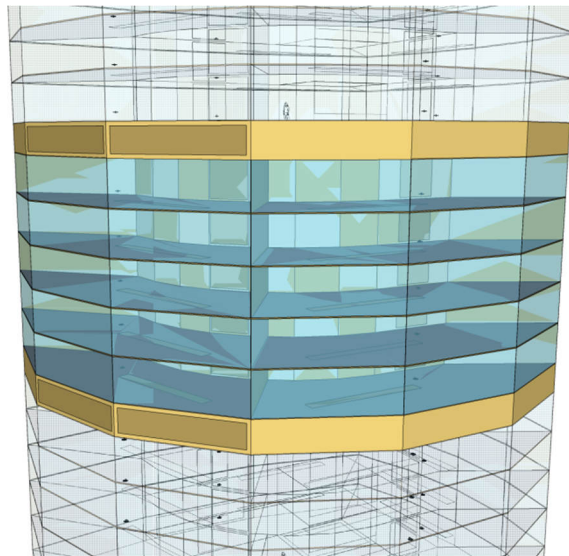


Figure 6.19: Geometrical representation of the simulation model (third building segment).

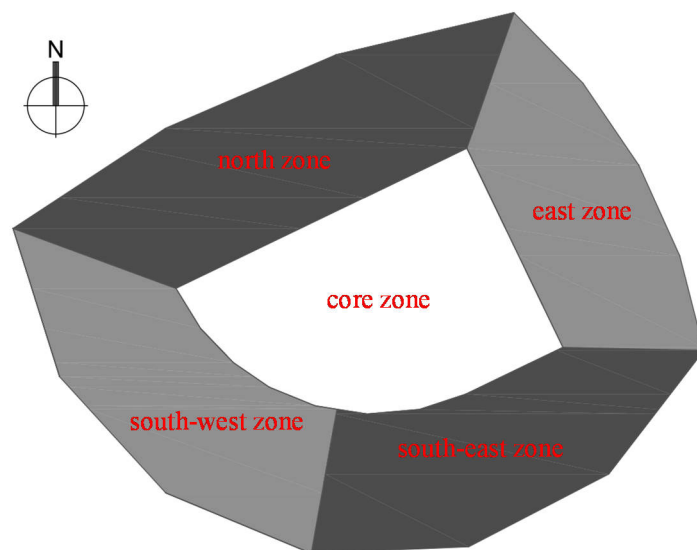


Figure 6.20: Geometrical representation of the model zones and orientation.

For the simulation of the current as-built reference case, the ventilation rate is defined outside the AFN in the ‘outdoor air design specification’ object. This object is connected to the HVAC model, which supplies heating and cooling in addition to the outdoor air according to the setpoints defined.

For the adapted models, various EMS ‘subroutine’ objects calculate a target air change rate intended to provide good comfort and air quality. Considering the dynamic driving forces for natural ventilation, the ‘venting availability’ schedules and ‘opening factors’ are then controlled in a best possible way to reach the target air change rates with a maximum value of 15 ACH. In the heating period or during hybrid cooling mechanical operation, the outdoor airflow rate with 14 litres per second per person is automatically calculated according to the occupation schedule multiplied by the number of people per zone.

6.3.1.1 HVAC systems

The building’s mechanical systems are simulated based on EnergyPlus HVAC-template objects, which provide an easy starting point for users to develop inputs with automatically generated node names. HVAC templates are not handled by EnergyPlus directly. Instead, they are pre-processed by a program called ExpandObjects [128]. There are two loops for plant equipment – a primary loop for supply equipment such as boilers and chiller, and a secondary loop for heat rejection equipment such as cooling towers.

In the context of this study, the ‘HVACTemplate:Zone:VAV:FanPowered’ simulates a variable air volume HVAC configuration with a constant minimum outdoor airflow rate during building occupation. The total pressure drop for all fans (supply, exhaust, and terminal unit) is approximated with 1 500 Pa and a primary supply air maximum design airflow rate of about 4 ACH.

The chilled water loop is supplied by centrifugal chiller with an assumed nominal Coefficient of Performance (COP) of 3,2. The condensers are water cooled, and work in conjunction with two speed cooling towers. The chilled water loop pump control type has intermittent operation.

The hot water loop is supplied by natural gas fuelled boilers with intermittent pump control. The assumed boiler efficiency is 0,8.

The rated head of the primary water pumps for chilled and hot water is set to 500.000 Pa, which is equivalent to 50 m H₂O. The rated head for the cooling towers secondary loop is set to an equivalent of 20 m.

There are some distinctions made in the HVAC simulation setup between the as-built and the adapted passive cooling scenarios (see also Table 6.3).

As-built scenario

When weather conditions are favourable, an economiser cycle is used to increase the amount of outside air introduced into the system to offset mechanical cooling energy. Local fan powered units include reheat. When heating is required, the terminal unit will activate the hot water reheat coils first, and then increase the airflow. The design outdoor air change rate during occupancy is 2 ACH. The specific setpoint temperature of a zone is controlled by the traditional approach using air temperatures. The zones are controlled by slightly different setpoints to account for the actual user behaviour and to create a fight of the systems dominated by interzonal air exchange.

Adapted scenarios

For the passive approach models developed, local fan powered units do not include reheat and are only used for cooling. Instead, the air is heated inside the naturally ventilation sub-floor distribution system using the baseboard heating option. In winter, no mechanical ventilation is applied to the model. The target outdoor air change rate here is set to 14 l/person instead of 2 ACH, which reduces the ventilation rate due to a light occupation density. The specific setpoint temperature of the zones is equally controlled by operative temperature thermostat objects. For hybrid cooling approach, the chilled water loop serves only during the cooling period (except for data centres). Hybrid systems for cooling and mechanical ventilation are operated by schedules dynamically overwritten by EMS routines.

Data centres

In contrast to the rest of the building, the cooling of data centres is modelled by the ‘HVACTemplate:Zone:FanCoil’ object. Because of the high heat gains of the IT-systems, no heating system is needed.

According to the data gathered and discussed in § 4.2.3, each of the 25 office storeys on average has approximately 10 kW equipment load from the IT-systems running for 24 h a day throughout the year. As in the case of the original Kanyon building, the data centres in the model are cooled by an independent air to air chilling system. The chilled water loop here is supplied by air cooled electric reciprocating chiller.

Again, the ‘nominal COP’ of the chiller is assumed to be consistent with the E+ default value of 3,2 W/W.

A resulting waste heat (‘chiller condenser heat transfer rate’) of approximately 12,5 kW per storey is rejected from the condensers. In the adapted natural ventilation scenarios, this waste heat is added to the air in the exhaust chimneys, and is modelled by using an internal ‘ElectricEquipment’ object. This load therefore further increases the chimney effect of each building segment by raising the air temperature. For the as-built scenarios without natural ventilation approach, the condenser heat is ejected directly to the environment.

6.3.1.2 Construction elements

Two types of construction objects are used to specify the material parameters and area of items within the space defined in § 4.2.2 and § 6.1.3.

Constructions, which are necessary geometrically, are first defined as ‘BuildingSurface:Detailed’ objects. For this type, the outside boundary condition depends on the actual surface type. Options used are outside, another surface (the backside of the construction towards another zone), or adiabatic properties. EnergyPlus will apply the same conditions to each side of the construction (inside and outside of the zone) so that there is no temperature difference across the surface. All heat transfer into the surface is a result of the dynamic response of the construction so that an adiabatic wall or floor can still store energy if the construction materials are defined to include thermal mass.

Constructions that are important to heat transfer calculations but not necessarily important geometrically, are then defined. These ‘InternalMass’ objects only exchange energy with the zone in which they are described. Concrete columns and partitions within the space are modelled as internal mass to provide good accuracy and to speed up the EnergyPlus calculations.

6.3.1.3 Airflow network

In this study, a complex AFN is used to simulate one building segment. The model consists of one air node for each zone linked by openings with additional uncontrolled cracks. Internal cracks, doors and stairways allow zone air mixing. The network is defined as a ‘multi-zone without distribution’ system, since the

mechanical ventilation system, if applied, is assumed to be without leakage losses. It can thus operate in ‘parallel’ with the AFN infiltration model. This reduces the code and the simulation time.

Large external openings such as chimney inlets and outlets as well as the overflow openings and the core to chimney exhausts are defined as ‘detailed opening’ objects with a constant discharge coefficient of 0,61. This also allows flow movement simultaneously in two different directions depending on stack effects and wind conditions. Complex geometrical properties of bottom-hung windows for the internal overflow openings with tilt angles cannot be entered in this object directly. But with application of the equations from § 2.2.3.1, they can be converted to rectangular, 2-dimensional openings with A_{eff} and h_{eff} values as geometrical input in the ‘detailed opening’ object.

For simplicity, the opening control zones are the southeast office zones, and openings in parallel are sized according to the net floor area of the zone (see also § 6.3.2).

The sub-floor distribution system on the other hand is modelled by ‘horizontal opening’ objects to account for the inlets to the office zones at floor level. Here, a constant discharge coefficient with a value of 0,50 is used as a guess, intended to account for flow resistances higher than for the other ventilation system elements.

Wind pressure coefficients are set to be input values from the wind tunnel experiments (see Appendix A), and are in the AFN structure associated with the leakage components via an ‘array’ (definition of the C_p values corresponding wind directions) and external air nodes with local height definition. At these nodes, the local wind pressure calculations are set to be calculated depending on the roughness characteristics of the surrounding terrain defined as ‘city’ in the ‘building’ object, based on the ASHRAE power-law calculation [92] (see also § 3.2.1.1).

The infiltration which is due to the building’s air tightness is realised by the definition of a ‘crack’ object. This object requires a flow coefficient (C_q in kg/s per m at 1 Pa pressure difference) and a flow exponent of 0,65, which is the E+ default value. The flow coefficient in this work is a function [128] of the expected infiltration mass flow rate at 50 Pa pressure difference between inside and outside. The expected infiltration flow rate is calculated from the net volume of a storey,

which is 2900 m³ multiplied by an n₅₀ value of one per hour¹³ at 50 Pa between inside and outside (blower-door measurement conditions). The following power law form is used, which gives infiltration airflow through the crack as a function of the pressure difference across the crack:

$$\dot{V}_{\text{inf}} = C_q \cdot \Delta p^{0,65} \cdot \rho_{\text{air}} \quad (6.1)$$

with a mass flow coefficient, which for each storey is approximated according to:

$$C_q = \frac{\dot{m}}{\Delta p^n} = \frac{\frac{1,0}{3600\text{s}} \cdot 2900\text{m}^3 \cdot 1,2 \frac{\text{kg}}{\text{m}^3}}{50\text{Pa}^{0,65}} = 0,07602 \frac{\text{kg}}{\text{s}} @ 1\text{Pa} \quad (6.2)$$

This total flow coefficient for one storey is then distributed to the four office zones according to their net floor area.

The wind driven share of the pressure difference across the crack is calculated again according to the averaged wind pressure coefficients for each zone orientation with values from wind tunnel experiments (see Appendix A), which in the airflow network are connected to the cracks in the ‘surface’ object.

Table 6.4: Mean wind pressure coefficients as AFN input for ‘crack’ infiltration calculations.

wind direction in °	SE office zone	SW office zone	N office zone	E office zone
0	-0,81	-0,85	0,63	-0,85
45	-0,80	-0,78	-0,43	0,62
90	-0,70	-0,87	-0,88	0,39
135	0,26	-0,97	-0,71	-0,74
180	0,11	-0,18	-0,78	-0,96
225	-1,10	0,65	-0,79	-0,76
270	-0,89	0,06	-0,28	-0,64
315.	-0,72	-1,22	0,67	-0,85

6.3.1.4 Model calibration and as-built assessment

The calibration of the as-built simulation model is necessary and crucial for the accuracy and usability of the energy simulation model. Within the calibration process, the results of the simulation are compared with the measured data. The simulation is tuned in a realistic range until its results closely match the measured data, especially to reflect the real user behaviour, e.g., setpoint adaptations. The results in Figure 6.21 show a reasonable agreement between the metered and the simulated energy consumption. As a limitation, it must be stated that the metered

¹³ ARUP Kanyon office block mechanic installation report, 2003, Turkey

energy consumption is from the year 2008, whereas the simulated values are for a typical year and the results of one segment are multiplied by a factor of five to account for the consumption of the whole building. Figure 6.22 is intended to give an insight into the current building's energy consumption.

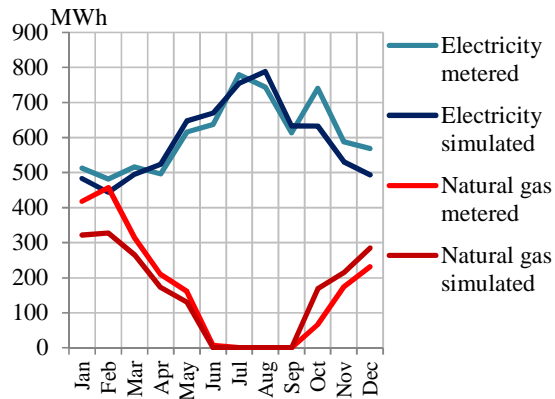


Figure 6.21: Comparison of the monthly metered (2008) and simulated energy consumption (typical year) of the as-built scenario.

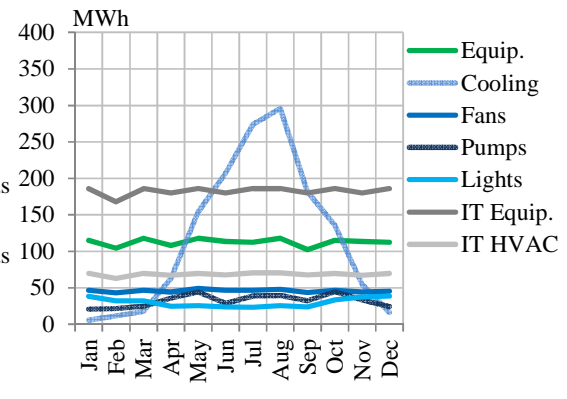


Figure 6.22: Monthly simulated electricity consumption of the different consumers.

6.3.2 Final natural ventilation system sizing

The orifice dimensions from § 6.2.2 can be resized until certain comfort expectations according to § 3.3.3.2 are fulfilled by annual simulation. For simplification in the simulation model investigated, the opening area share for the differently orientated office zones on each storey (in parallel, see § 3.2.1.2) is distributed only according to the net floor area and not according to the cooling needs. The target air change rate in the controls however is not identical for all office zones. The EMS subroutines calculate this dynamic value according to the operative temperature of each zone. Depending on the cooling needs, the passive systems (e.g., opening sizes, shading devices, and thermal mass) could also be sized in more detail for each zone, but due to complexity of the optimization solution, this was not implemented. Also, the size of natural ventilation system here is expressed only by the cross-sectional area of the internal chimney (see Figure 6.17) of the 3rd building segment. The natural ventilation system size here is restricted to a cross-sectional chimney area of 50 m², which is 5% of the net internal floor area of one storey. More detailed sizes of the openings in a flow path gathered from the design tool can be found in Figure 6.18.

6.3.2.1 Natural ventilation potentials

For a detailed dynamic analysis of the flow potential for natural ventilation systems, the entire system including controls had to be simulated, since the ventilation is not driven just by external conditions, but by an interaction of internal and external conditions, e.g., ambient and indoor temperatures, and dynamic wind velocity (for driving forces, see § 3.2.1.1). The ventilation control strategy for combined airflow and thermal simulations was described in § 3.3.2. Figure 6.23 through Figure 6.25 show how the achievable mean monthly air change rates depend on the climate and season, and the chosen system size. In winter, natural ventilation is mainly used to limit the CO₂ levels.

Air change rates increase with higher passive cooling demands in Istanbul and Turin more than in Stuttgart. The target air change rate represents the amount of air the EMS control aims to realise, whereas the reached air change rate is the smaller amount of ventilation appearing in the simulation (see also Figure 3.38). The target and the reached air change rates are in a dynamic dependence with each other. In an ideal system, both lines for the target and the reached air change rate would be identical. The longer the distance between each other, the lesser the cooling needs that can be satisfied by the system.

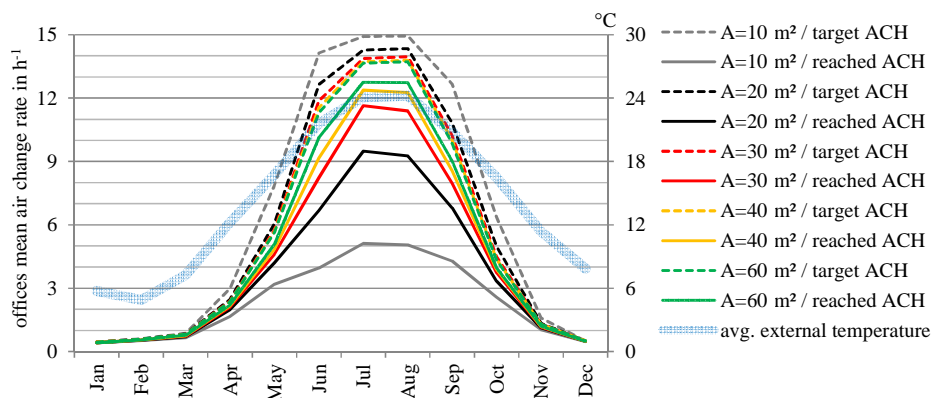


Figure 6.23: Ventilation potentials and control targets for Istanbul climate.

Because of strong wind forces in Istanbul, the ventilation potentials are high even with a small system size. Because of the warm climate, the control targets high ventilation rates. Relatively small system sizes from 20 to 40 m² already give good response to fulfill the targets.

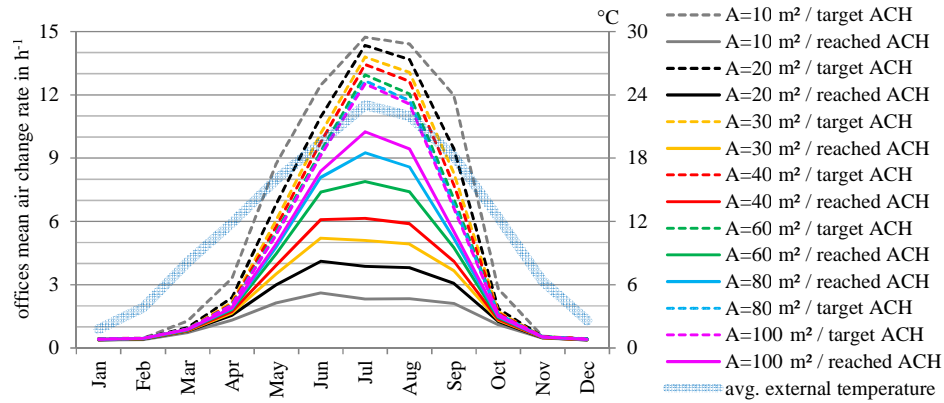


Figure 6.24: Ventilation potentials and control targets for Turin climate.

In the relatively warm Turin summer climate, the same relatively small system sizes as in the case of Istanbul, would provide only a limited air change rate, not sufficient for passive cooling. Due to the lack of wind, natural ventilation is mainly driven by thermal forces, and the systems need to be sized bigger.

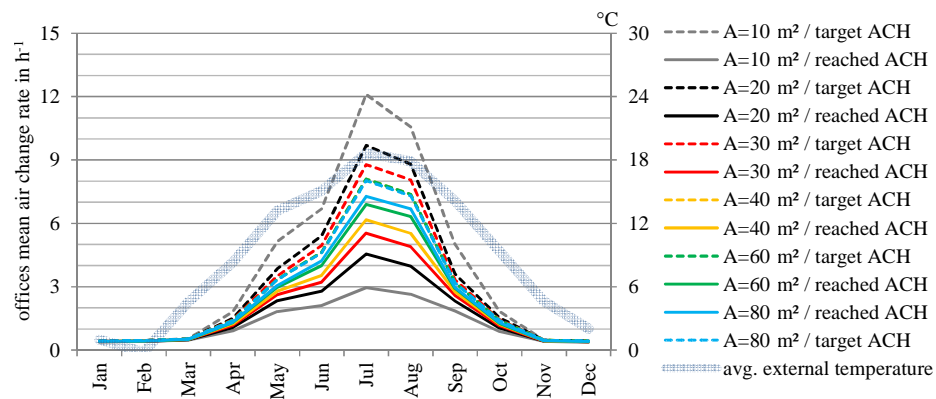


Figure 6.25: Ventilation potentials and control targets for Stuttgart climate.

In the colder climate of Stuttgart, the control targets much smaller average air change rates. For wind velocities in between those of Istanbul and Turin, the ventilation system can be sized smaller, which is sufficient for passive cooling.

Table 6.5 summarises the ventilation potentials depending on the climate and the system size. Cross-sectional chimney area bigger than 50 m² is considered to be too big, and simulation outputs are therefore written in grey.

Table 6.5: Simulated derivation between the EMS target and reached ACH in the month with the highest target ventilation rates depending on the natural ventilation system size.

	A _{chi}	10 m ²	20 m ²	30 m ²	40 m ²	60 m ²	80 m ²	100 m ²
Istanbul	Target ACH	14,94	14,65	13,95	13,80	13,72		
	Reached ACH	5,11	7,43	11,64	12,38	12,76		
	derivation	65,7%	50,2%	18,3%	11,1%	7,2%		
Turin	Target ACH	14,73	14,34	13,79	13,44	12,94	12,66	12,52
	Reached ACH	2,59	4,11	5,21	6,14	7,89	9,25	10,25
	derivation	84,3%	73,0%	63,0%	54,3%	39,0%	27,0%	18,1%
Stuttgart	Target ACH	12,10	9,69	8,78	8,40	8,10	8,02	
	Reached ACH	2,96	4,54	5,54	6,17	6,90	7,29	
	derivation	75,5%	53,1%	37,0%	26,5%	14,8%	9,2%	

6.3.2.2 Adaptive thermal comfort

Apart from the previously discussed air change rates, which directly influence air quality, thermal comfort according to § 3.3.3.2 is a crucial indicator for evaluating the natural ventilation concepts. If not explicitly stated in the result of this thesis, the mean value for all office zones in the third storey (middle) of the building segment considered is reported.

Design tool sizing inputs and conceptual design

Figure 6.26 shows the detailed simulation output of annual comfort distribution during occupancy (3.108 hours per year) in Istanbul and Stuttgart for opening sizes according to the ‘HighVent’ design tool outputs. As the natural ventilation system size is restricted to a cross-sectional chimney area of 50 m², the size for Turin was reduced according to the sizing limit shown in Figure 6.17. Scenario (a) represents the results of the adapted base-case scenario for passive cooling operation according to Table 6.3. The weighted average of all office zones stay below the 5% comfort limit benchmark mentioned, except the southwest facing zones in Turin. Also the southwest zones for the Istanbul scenario tend to be slightly closer to the benchmark due to higher solar heat gains entering these zones. Best thermal comfort is provided by the east and north zones especially in Stuttgart.

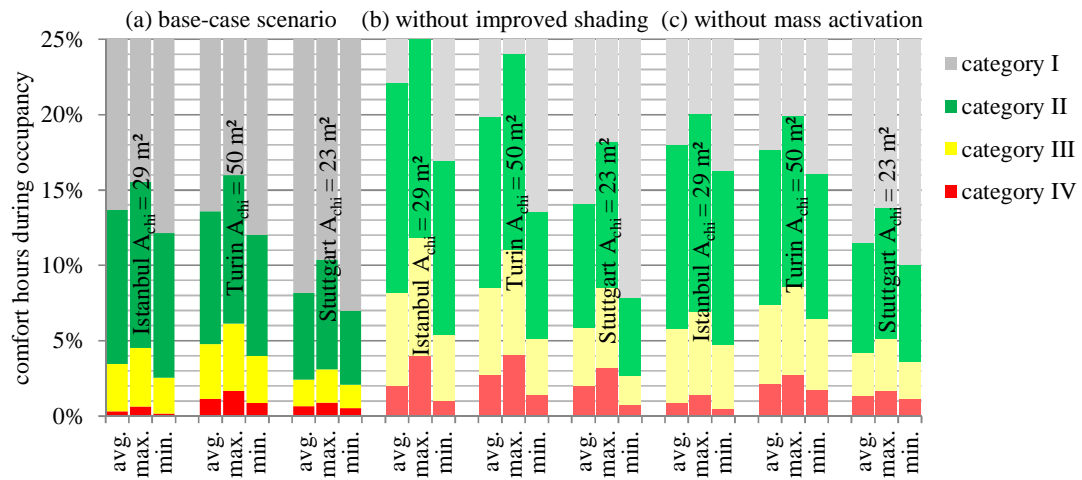


Figure 6.26: Floor area weighted average, zone minimum and zone maximum adaptive annual comfort criteria reached in respect to the three climates investigated for (a) the naturally ventilated base-case scenario, (b) a scenario without the improved shading, and (c) a scenario without the thermal mass activation at the ceiling.

To separately investigate the conceptual passive design adaptations made in terms of solar heat gain control (see § 6.1.2) and thermal mass heat sink activation (see § 6.1.3), comfort simulations are repeated without these measures. Depending on the measure and the climate, the comfort reached differs quite significantly from the passive base-case scenario investigated, and limits can no longer be maintained according to the 5% benchmark. Especially for the scenarios without improved shading devices the comfort distribution also strongly differs depending on the orientation of the office zones. For example, in Istanbul climate, category II can be maintained for 94% of the year in the north oriented zones but only for 88% in the southwest oriented zones. Therefore, if the heat balance of the building or part of the building is changed by increasing heat gains, all other passive measures have to be reconsidered, sized, and controlled accordingly; else, hybrid cooling becomes unavoidable.

Parametric sizing assessment

For each of the three climates considered, the passive cooling base-case scenario is simulated with different chimney cross-sectional areas (and associated opening areas as described in § 6.2.2). Figure 6.27 provides the annual comfort simulation outputs for this parametric analysis. Considering the 5% benchmark from EN 15251, generally good agreement is found for all the design tool sizing suggestions. The initial passive system sizes for Turin are considered to be too huge for practical implementation, and are therefore reduced to the maximum size of 50 m², but still the floor area weighted average stays within the 5% benchmark limits (Table 6.6). For

Istanbul and Stuttgart, the sizing values gathered from the design tool can be directly taken with good agreement.

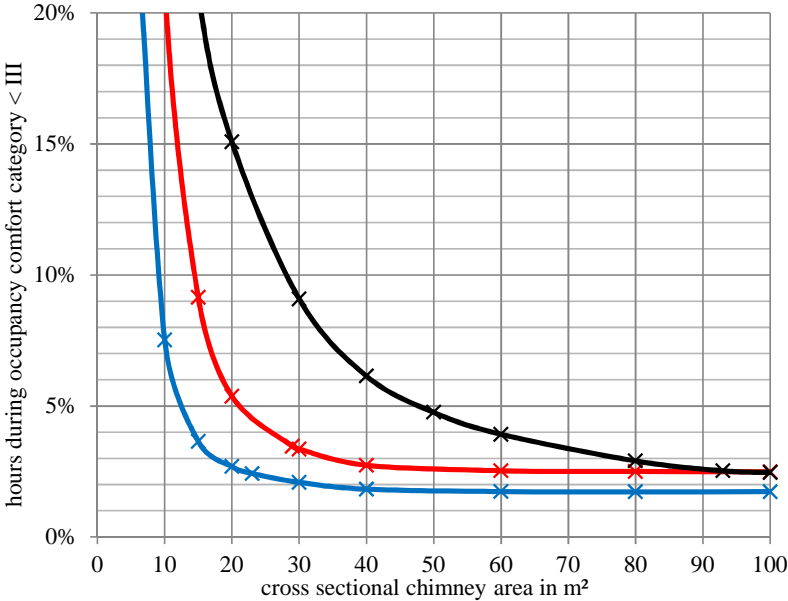


Figure 6.27: Natural ventilation system sizing sensitivity analysis in respect to the annual area weighted mean adaptive comfort distribution during occupancy (3.108 h/a).

If the 5% occurrence criterion of occupied hours per year is not reached, a hybrid cooling system is necessary (red area in Figure 6.28). Within 5% and 3%, hybrid cooling assistance is not mandatory – but is dependent on the comfort expectations of the occupants (yellow area in Figure 6.28). Optimum passive cooling, while keeping the system sizes appropriate, can be reached below 3% occurrence and 50 m² cross-sectional chimney area (green area in Figure 6.28). For a building design without proper passive cooling, the associated line in the diagram would stay outside the limits in the red zone. For example, this could be a scenario for Turin without improved shading devices as shown in Figure 6.26 (b). For Stuttgart, a building design without a mass activation at the ceiling can provide reasonable results as shown in Figure 6.26 (c).

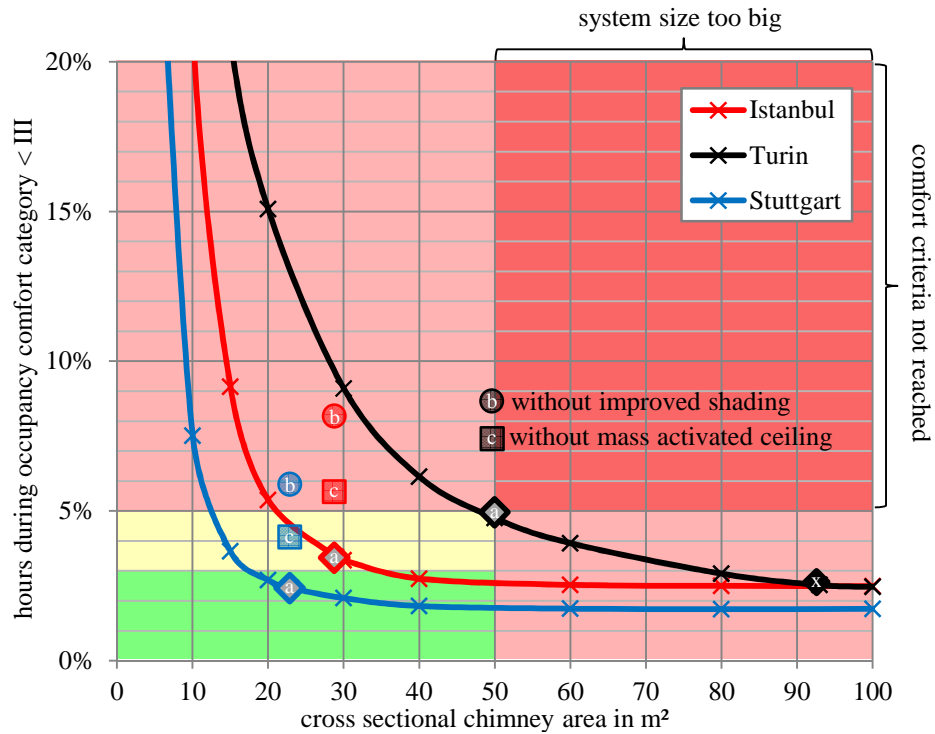


Figure 6.28: Natural ventilation system sizing sensitivity analysis in respect to the annual area weighted mean adaptive comfort distribution during occupancy.

Table 6.6 summarises the results of parametric analysis. The final sizes taken for the design evaluation (§ 7) in are marked in grey (base-case scenarios).

Table 6.6: Floor area weighted average adaptive comfort criteria reached for the adapted base-case scenario (a) during occupied hours depending on the natural ventilation system sizing.

	A_{chi}	5m ²	10m ²	15m ²	20m ²	23m ²	29m ²	30m ²	40m ²	50m ²	60m ²	80m ²	93m ²	100m ²
Istanbul	category III	30,8%	14,4%	7,2%	4,6%		3,1%	3,1%	2,6%		2,4%	2,4%		2,4%
	category IV	24,2%	6,7%	2,0%	0,8%		0,3%	0,3%	0,2%		0,1%	0,1%		0,1%
	sum	55,0%	21,1%	9,1%	5,4%		3,5%	3,4%	2,7%		2,5%	2,5%		2,5%
Turin	category III	34,1%	19,7%	12,4%	9,4%			6,2%	4,4%	3,6%	3,1%	2,4%	2,1%	2,1%
	category IV	28,0%	13,5%	8,4%	5,7%			2,8%	1,7%	1,2%	0,9%	0,5%	0,4%	0,4%
	sum	62,2%	33,2%	20,8%	15,1%			9,1%	6,1%	4,8%	3,9%	2,9%	2,5%	2,5%
Stuttgart	category III	16,8%	5,3%	2,6%	2,0%	1,8%		1,5%	1,3%		1,2%	1,2%		1,2%
	category IV	10,7%	2,2%	1,0%	0,7%	0,6%		0,6%	0,6%		0,5%	0,5%		0,5%
	sum	27,5%	7,5%	3,6%	2,7%	2,4%		2,1%	1,8%		1,7%	1,7%		1,7%

6.4 Conclusions

For the Kanyon office-tower in the three climates considered, natural ventilation is not a stand-alone solution for good summer comfort. Instead, ventilative cooling must be brought in with other measures to reduce heat gains, and to use the building as heat sink for night-time ventilation. Hence, the Kanyon building was first conceptually adapted to reduce penetration from sun by means of enhanced shading elements, and the suspended ceiling's mass was activated to let the cold night air directly circulate around the structural concrete. Focusing on natural ventilation, a

central void design allows cross-ventilation of the occupied space towards a central chimney in the core, from where warm air rises upwards, towards a high level exhaust. The building was also virtually cut into modular segments (5-storeys per segment) to restrict the system dimensions (e.g., chimney diameter) and the peak pressure drops in winter (at high temperature differences). With a single chimney to ventilate 25 floors, the size of the ventilation system simply would be too big to be realised in practice, but with isolated segments, each segment can be treated as a low-rise or medium-rise building. To guarantee the intended flow direction from the perimeter towards the core, besides a commonly used, leeward chimney exhaust, also a commonly used windward supply inlet is modelled. Intermediate ‘wind floors’ between the segments each have two wind adapting openings in windward (positive wind pressure supply) and leeward (negative wind pressure exhaust) orientation. The central chimney is therefore designed to serve the occupied space with fresh air supply and exhaust.

The spread-sheet based ‘HighVent’ design tool was developed to size the openings of a flow path in § 3.2. Considering the conceptually adapted Kanyon building inclusive of enhanced sun shading elements and mass activated ceilings, uncontrolled design air change rates necessary for passive cooling are estimated for each climate considered (13 ACH for Istanbul and Turin / 5 ACH for Stuttgart). The ventilation systems are then sized dependent on this design air change rate and average local wind velocities. Due to the lack of wind in Turin, the initial system size is 3,2 times bigger than in Istanbul. Due to the colder climate in Stuttgart (where the design air change rates are smaller) the system can be sized smallest, even when average wind velocities are relatively low. Depending on the height of the segment in the building, the chimney cross sectional area requires about 5% and 2% of the total net floor area in Istanbul, 3% and 2% in Stuttgart and 11% to 7% in Turin. The dimensioning for Turin is considered as to be too big to be realised in practice (5% maximum).

To assess the overall annual performance for a specific climate, in a next step, the Kanyon building was taken and modelled in EnergyPlus along with the passive approach design adaptations developed. The ‘HighVent’ design tool outputs were ‘post-processed’ as inputs for detailed simulations including the mechanical systems and the custom natural ventilation controls. Air change rates increase with higher passive cooling demands in Istanbul and Turin more than in Stuttgart. Because of

strong wind forces in Istanbul, the ventilation potentials are high even with a small system size. Because of the warm climate, the control targets high ventilation rates. Relatively small system sizes already give good response to fulfil the targets. In the warm Turin summer climate, the same system sizes as in the case of Istanbul would provide only a limited air change rate, not sufficient for passive cooling. Due to the lack of wind, the systems need to be sized bigger. In the colder climate of Stuttgart, the control targets much smaller average air change rates. For wind velocities in between those of Istanbul and Turin, the ventilation system can be sized smallest.

The annual comfort distribution according to the EN 15251 standard [55] was first shown for opening sizes according to the design tool outputs. For Turin, the natural ventilation system size was reduced according to the sizing limit. The results indicate that for the passive cooling base-case scenarios including improved shading devices and thermal mass activation, the comfort benchmarks barely can be reached for all zone orientations in all climates except in Turin. By repeating the simulations without improved shadings and/or without mass activation at the ceilings, the influence of those measures could be investigated separately. Only in Stuttgart the design was capable of staying within the comfort requirements with light accessible thermal mass. For the final natural ventilation sizing, the system was simulated in different sizes. Considering the 5% comfort benchmark from EN 15251 [55], generally good agreement is found for the entire design tool sizing suggestions. For Istanbul and Stuttgart, the sizing values gathered from the design tool can be directly taken with good agreement.

7. DESIGN EVALUATION

In this section, the fully mechanical as-built Kanyon building operation is compared with an operation based on the controlled passive and the hybrid cooling approach developed. The following results refer to the office tower case-study building from § 4, adapted for passive summer operation according to Table 6.3, with natural ventilation system dimensions from § 6.3.2. The most important factors influencing passive and hybrid cooling performance such as ventilation rates, controls, heat gains, building mass, and climatic conditions are evaluated according to the general approach developed in § 3.4. It is assumed that if thermal comfort can be guaranteed without air-conditioning, then significant cooling and ventilation energy conservation can be achieved [64]. Design alternatives are here analysed and discussed for different climates. Performance indicators used to evaluate the functionality are the energy consumption compared to that of mechanical ventilation and cooling systems, and compliance with the thermal comfort limits; additional aspects are the ventilation rates and the indoor air quality reached.

7.1 Weekly Profiles

Design week simulations with dynamic boundary conditions give insight into the functioning of natural ventilation systems, and are helpful for the analysis of opening controls. This section examines the performance differences for design weeks. The factors considered are the operative room temperature in relation to the limits of comfort, the room and ambient air temperatures, the CO₂ level, and the air change rates.

A good functioning is attested if the following performance indicators are satisfied:

- 1) The operative zone temperature stays within the comfort limits category 2 [41];
- 2) The internal CO₂-level stays below the IAQ limits category 2, which is 500 ppm above the external level [41,55].

Multiple simulations were performed to access information for mechanical, passive, and hybrid building operation scenarios (base-case scenarios according to Table 6.3). The focus is on passive control over comfort. Except for the three base-case scenarios, all simulations are performed with switched-off heating and cooling units. This section observes the effects of parametric changes (e.g., natural ventilation controls) on the internal comfort which utilises neither heating nor cooling. The results show the performance for one representative office zone (3rd segment / 3rd storey / southeast office zone). Except for the base-case scenarios for passive cooling, weekly profiles are evaluated only for Istanbul.

7.1.1 Mechanical approach

The mechanical operation scenarios with actual shading devices and thermal mass distribution are intended to reflect the actual building behaviour. They also indicate the internal temperatures if the mechanical heating and cooling operation are set off. The constant limits of comfort chosen from the EN 15251 standard are for buildings without natural ventilation and occupant adaptation, and are therefore independent of the external temperature.

7.1.1.1 As-built (base-case)

The first weekly profiles are simulated for the as-built scenario and are intended to reflect the actual building behaviour. The detailed simulation setup is described in § 6.3.1.

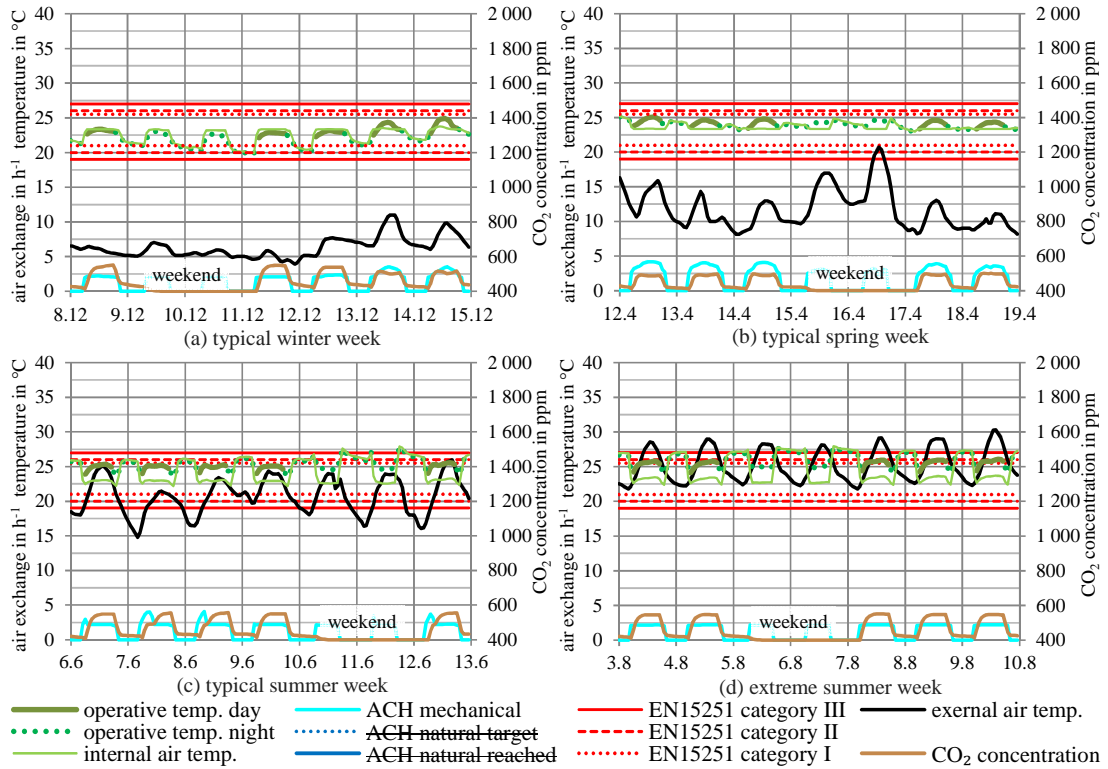


Figure 7.1: Design week simulation outputs of the as-built case in Istanbul.

The results show relatively constant room air temperatures between 22 °C and 24 °C throughout all the seasons (Figure 7.1 (a)-(d)). The small fluctuation in temperature is due to personal setpoint adaptation of the occupants together with interzonal air mixing due to open doors. The CO₂ concentration stays below 200 ppm above external level, and can be classified as low in accordance with EN 13779 (IDA 1 ≤ 400 ppm above external level). Air change rates provided by fan operation are stable at the demand driven design value of 2 h⁻¹, but sometimes exceed this value at midday (Figure 7.1 (b)) or in the morning hours (Figure 7.1 (c)) due to economiser operation at low ambient temperatures.

7.1.1.2 Ventilation only

The second scenario is intended to show weekly profiles of comfort that could be reached with only mechanical ventilation. The operation is simulated without mechanical heating and cooling. The ventilation system, besides indoor air quality control, includes an outdoor air differential economiser with a maximum ventilation rate of 4 ACH.

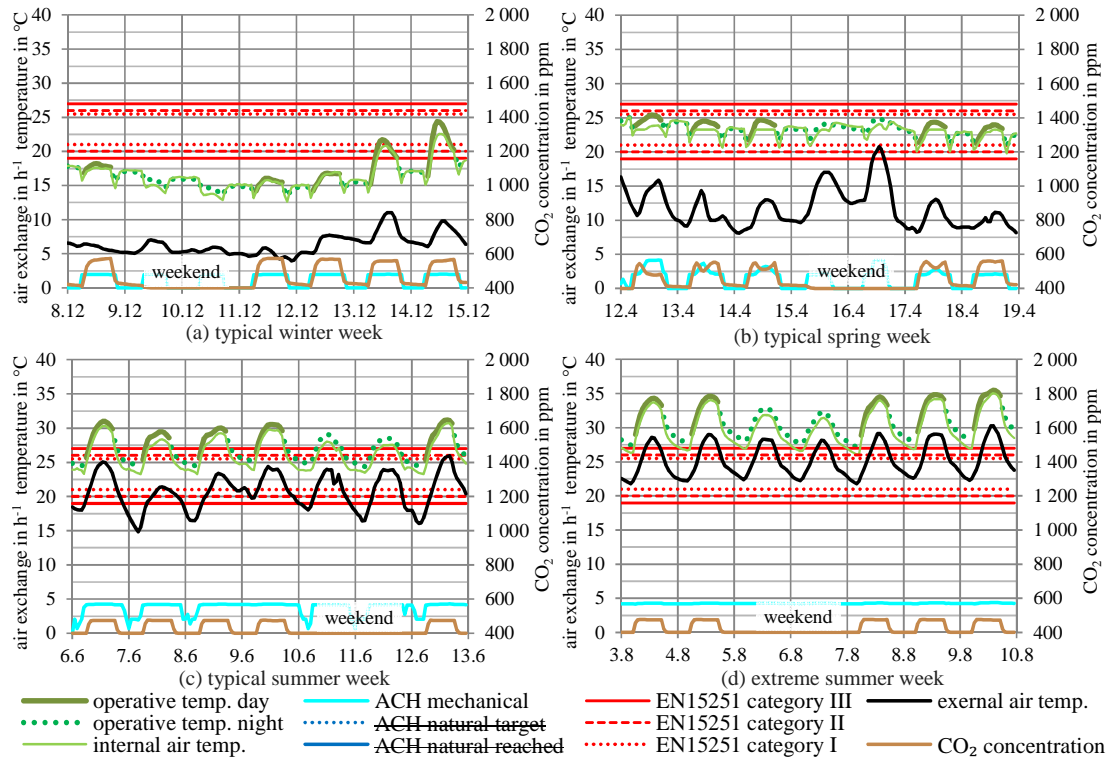


Figure 7.2: Design week simulation outputs of mechanical ventilation only case without heating and cooling in Istanbul.

As there is no cooling system available, the results show a room air temperature that is far above all the admissible comfort temperatures (Figure 7.2 (c)-(d)) for both mechanically and naturally ventilated offices [41]. The CO₂ concentration can again be classified as low. In contrast, temperatures in winter are too low without heating (Figure 7.2 (a)), but in spring (Figure 7.2 (b)) the operation is possible only with fanning.

7.1.2 Passive approach

The free-running, passive cooling scenarios include the conceptual design adaptations made for reducing solar gains and thermal mass activation at the ceilings (see § 6.1). Natural ventilation system sizes depend on the climate and correspond to the values gathered in § 6.3.2, which are simplified, expressed by the cross-sectional chimney area with values of 29 m² for Istanbul, 50 m² for Turin and 23 m² for Stuttgart. To focus on the influence of ventilation controls, simulations are conducted in the free-running mode rather than the conditioned mode. The limits of thermal comfort chosen from EN 15251 [41] are for buildings with natural ventilation and occupant adaptation, and are therefore in dynamic dependence to the external temperature whenever the adaptive approach is applicable.

7.1.2.1 Uncontrolled approach

The first scenario tested is the uncontrolled natural ventilation, which means that the orifices are 100% open throughout.

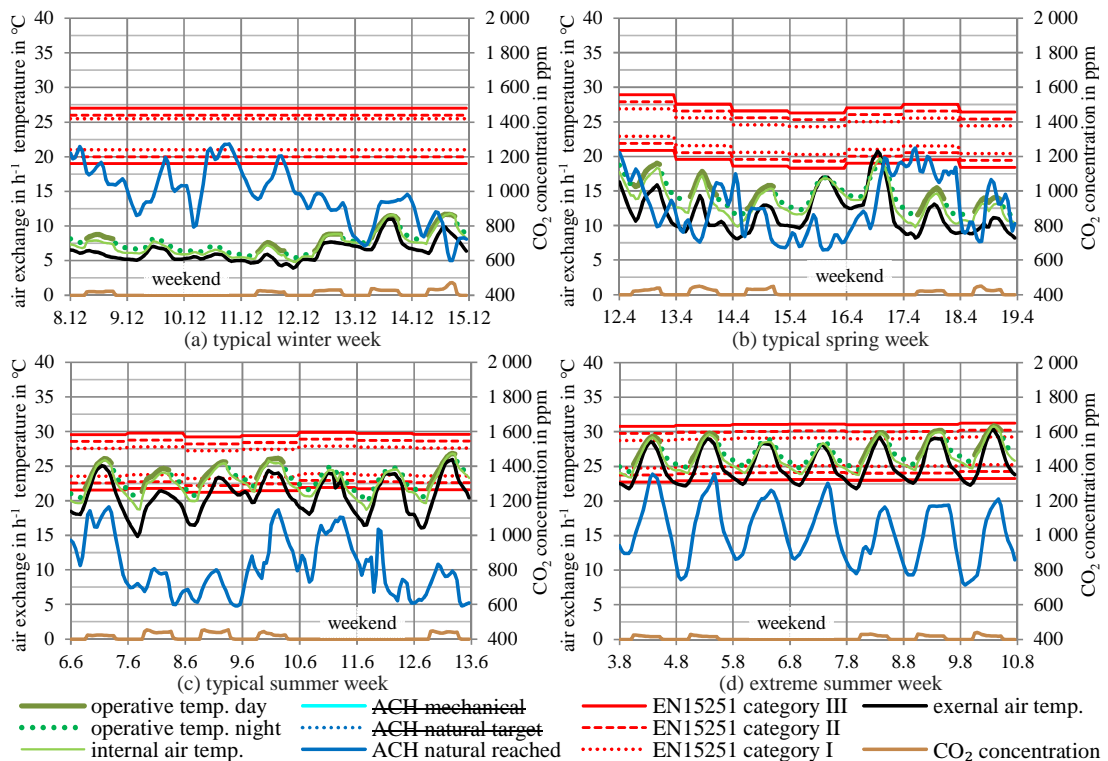


Figure 7.3: Design week simulation outputs of the base-case scenario for passive cooling but with uncontrolled ventilation and without heating in Istanbul.

Uncontrolled ventilation often results in too low indoor temperatures, especially in the mornings. The air change rates are in a range up to about 25 h⁻¹ and may cause discomfort by draughts, especially if the ambient temperature is low. The CO₂

concentrations are very low due to the increased air exchange with a maximum of about 50 to 100 ppm above the ambient level.

7.1.2.2 Controlled approach

Night-time ventilation

As a second natural ventilation scenario, the uncontrolled night-time ventilation (defined as: openings fully open during no occupancy, and closed during occupancy) is simulated.

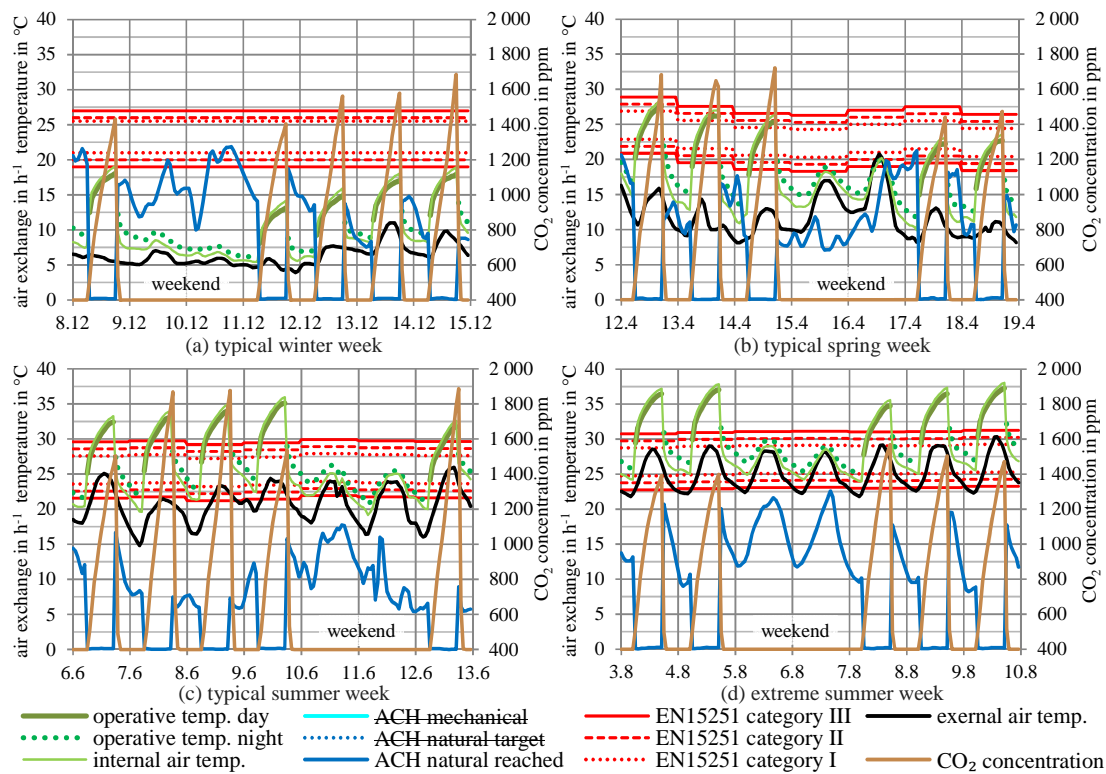


Figure 7.4: Simulation results of the base-case scenario for passive cooling but with night-time ventilation only and without heating in Istanbul.

Here, the temperatures in summer (Figure 7.4 (c)-(d)) are unacceptably high because daily heat loads are not removed by ventilation, and the thermal mass is not sufficient. Due to the closed windows during occupancy times, unacceptably high CO₂ concentrations are obtained (up to 2000 ppm above the external levels). The infiltration through the building envelope of approximately 0,1 h⁻¹ is simply not enough.

Daytime ventilation

Daytime ventilation is defined as the period in which the offices are occupied (weekdays only). The openings are opened during the day at 100 % and closed at night.

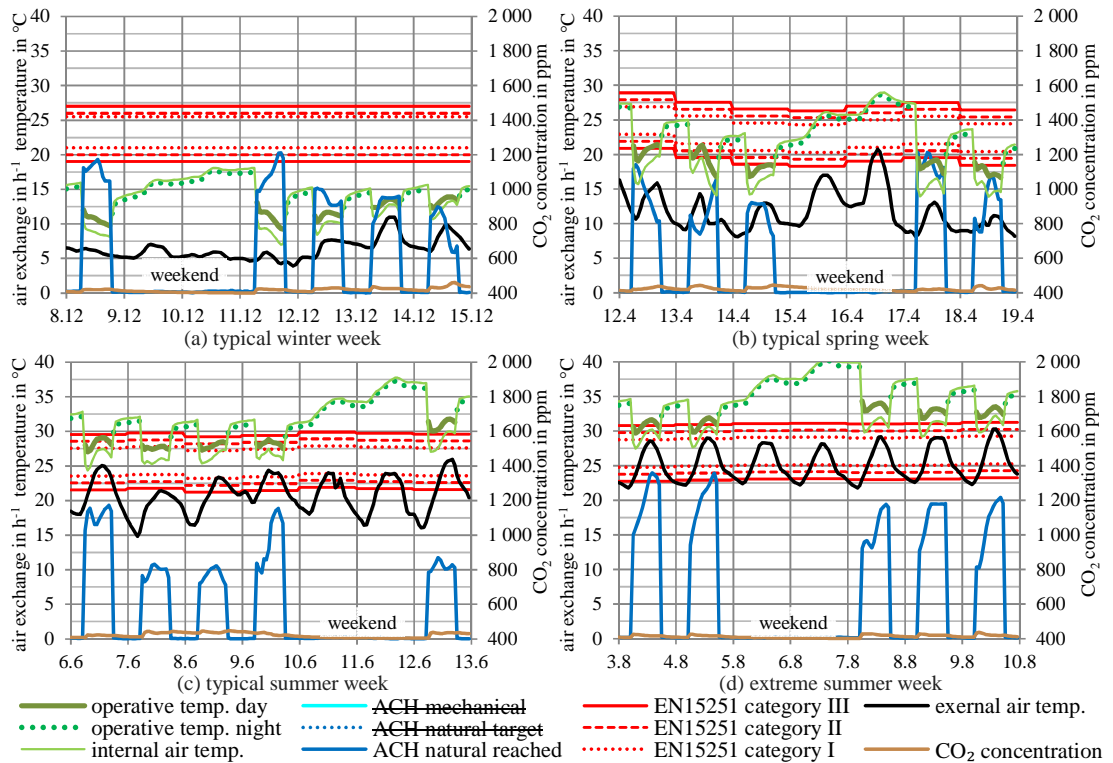


Figure 7.5: Simulation results of the base-case scenario for passive cooling but with daytime ventilation only and without heating in Istanbul.

The operative room temperatures are often outside the comfort zone in accordance with EN 15251. This is because at daytime they are always above the outdoor temperature, and heat from the fabric is not removed at night, which demonstrates the limits of natural daytime ventilation, especially at temperature peaks. In summer, the pure daytime ventilation is only suitable for building ventilation to supply fresh air to the rooms. The CO₂ concentrations are classified as low due to continuous air exchange during the occupancy at values below 100 ppm above the external level.

Fixed temperature setpoint control

The next scenario examined is a temperature-controlled scenario with fixed setpoint control. Here the ventilation openings are opened when the room temperature is higher than the ambient temperature and exceeds 20 °C.

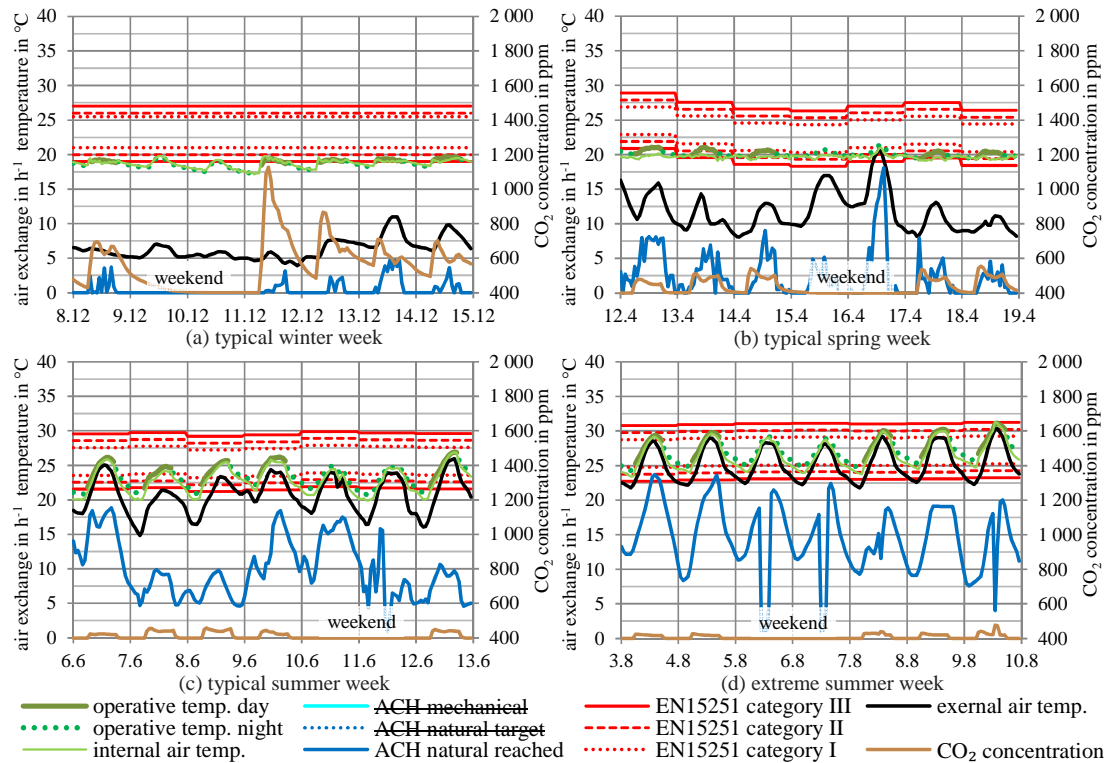


Figure 7.6: Simulation results of the base-case scenario for passive cooling but with fixed-setpoint ventilation and without heating in Istanbul.

A limitation for this simple setpoint control is that there might also occur on/off control in situations close to the 20 °C setpoint temperature. This effect is even stronger as shown in the hourly interpolated charts. The temperature limits (category II) are far less exceeded than in the other two cases before. The CO_2 levels in the warm season are constantly low but increase in the cold season. Results for a typical winter week (Figure 7.6 (a)) show that the thermal comfort can almost be provided without heating, if the air change rate is low. Since temperatures in the morning are rarely too low (Figure 7.6 (b)-(c)), this control seems to be a feasible choice for the design weeks here, but is dependent on the climate, the season, the construction, and the ventilation potential of the design.

Adaptive temperature amplifier control (base-case controls)

To overcome the above limitations and dependencies, the final controls for passive cooling are now based on adaptive comfort temperature benchmarks. The aimed air change rate is dependent on the internal and external temperatures (definitions given in Section 3.3.2). As this is the final control applied in the passive cooling models, all the three climates are evaluated.

For all the three climates, this control is more robust in terms of adapting the required flow rates for passive cooling without frequent high adjustments. In winter (Figure 7.7 (a)), the CO₂ concentrations consistently stay below 300 ppm above the external level.

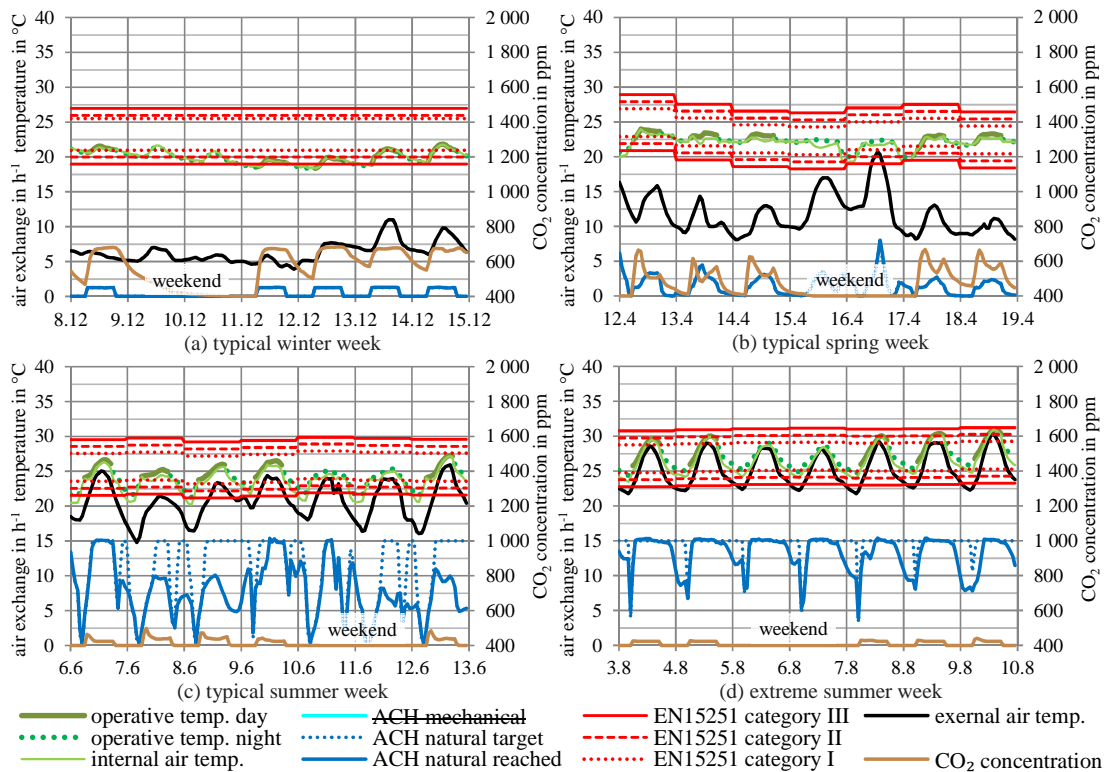


Figure 7.7: Simulation results of the base-case scenario for passive cooling with adaptive temperature amplifier control but without heating in Istanbul.

The time dependent limits for night-time and daytime ventilation ensure that the upper and the lower comfort limits in Istanbul are barely exceeded (Figure 7.7 (b)-(d)). Due to consistent high temperatures in summer (Figure 7.7 (c)-(d)), the air change rates aimed by the control are mostly high. Because of strong winds, these targets can often be reached especially in extreme summer conditions. This indicates that the flow path dimensions are sufficient. In

typical winter (Figure 7.7 (a)) the operative temperature during occupancy falls only slightly below the comfort limit, which results in a relatively small heating demand.

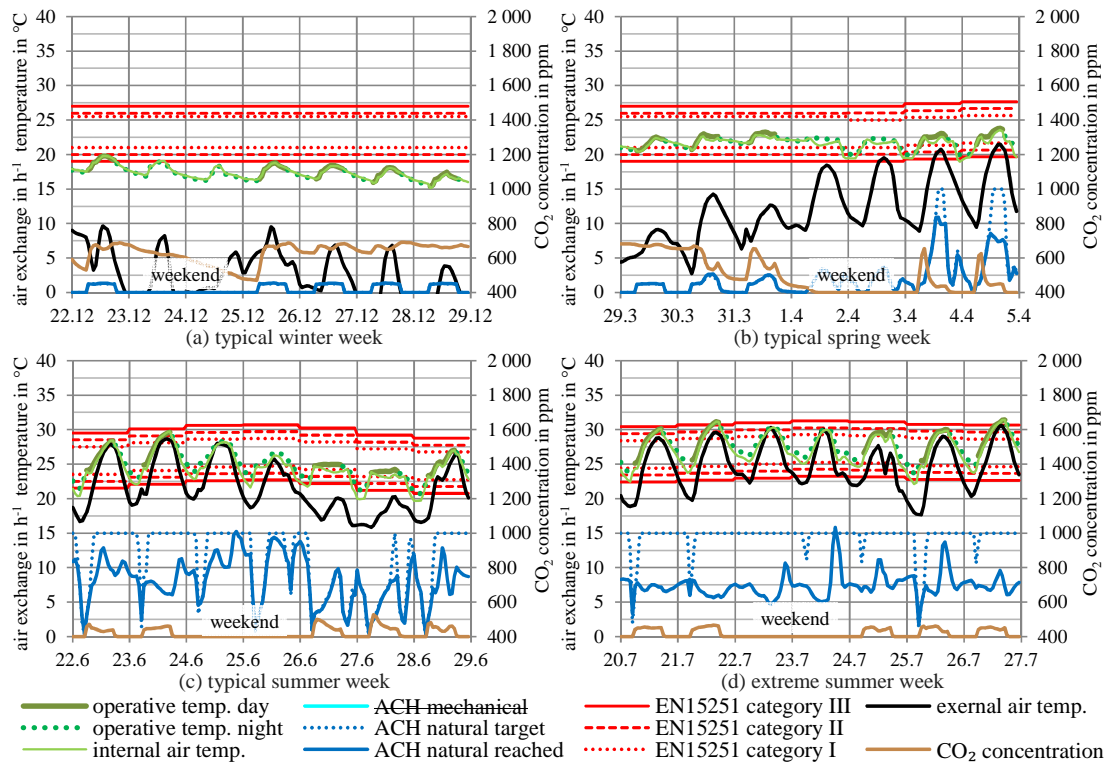


Figure 7.8: Simulation results of the base-case scenario for passive cooling with adaptive temperature amplifier control but without heating in Turin.

For the Turin climate, similar results were found except for the extreme summer design week (Figure 7.8 (d)). Due to the absence of wind, air change rates aimed by the controls to effectively cool the building cannot be satisfied by the natural ventilation system. In this relatively short period, the upper comfort boundaries are strongly exceeded (degree hours) than in Istanbul. To provide comfort, further passive cooling design adaptations or a hybrid cooling concept might be necessary. In typical winter (Figure 7.8 (a)), the indoor temperatures reached without heating are slightly lower than in Istanbul, which indicates a somewhat higher heating demand.

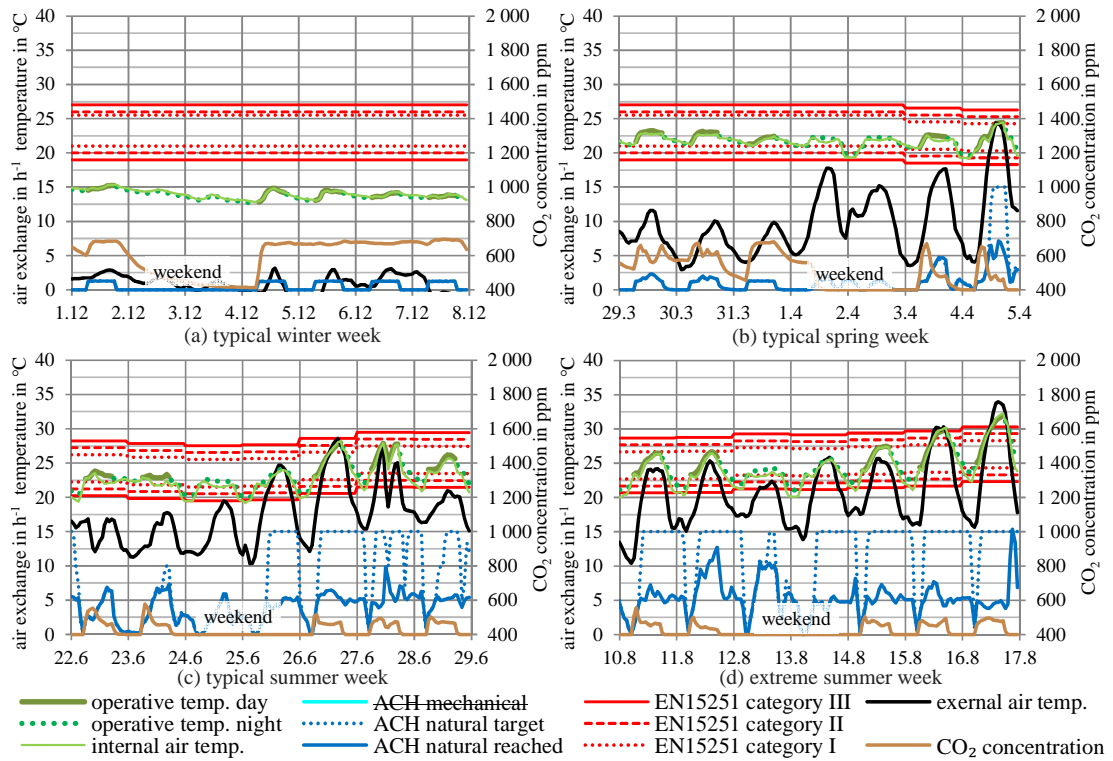


Figure 7.9: Simulation results of the base-case scenario for passive cooling with adaptive temperature amplifier control but without heating in Stuttgart.

The colder climate of Stuttgart seems best suited for passive cooling. Even smaller air change rates provided by the natural ventilation system are suitable for effectively cooling the building except for some summer days with high peak temperatures (Figure 7.9 (c)-(d)). During such days, indoor temperatures can stay below the external level because of high temperature differences between day and night. In typical winter (Figure 7.9 (a)), internal temperatures reached are lower than in Istanbul and Turin, which indicates the highest heating demand for Stuttgart.

7.1.2.3 Conceptual design adaptations

In the previous figures, the influence of conceptual design adaptations made according to § 6.1 was not shown. Nevertheless, it is worth pointing out that the enhanced solar shading elements as well as the exposed concrete ceiling were found to have great influence on the extreme summer design weeks' peak operative temperatures reached. Table 7.1 summarises these reductions. The measures are found to have the largest impact for the southwest zones in all the climates.

Table 7.1: Extreme summer operative temperature reduction by design adaptations according to § 6.1.

	adaptive shading devices				mass activated ceiling				combination of both			
	E	SE	SW	N	E	SE	SW	N	E	SE	SW	N
Istanbul	-0,73	-0,60	-1,83	-0,35	-0,42	-0,43	-0,46	-0,43	-0,95	-0,92	-2,54	-0,72
Turin	-1,31	-1,01	-2,38	-1,07	-0,78	-0,84	-1,01	-0,82	-1,55	-1,36	-3,22	-1,64
Stuttgart	-1,89	-2,35	-4,55	-1,40	-1,38	-1,56	-2,02	-1,45	-2,35	-2,82	-6,01	-2,26

Especially in Stuttgart, internal temperatures are extreme without enhanced solar shading. For all orientations in all the climates, a positive effect was found for both the measures with a peak temperature reduction minimum of 1 °C approximately, and a maximum of 6 °C approximately, depending on the climate and the orientation of the zone in the model.

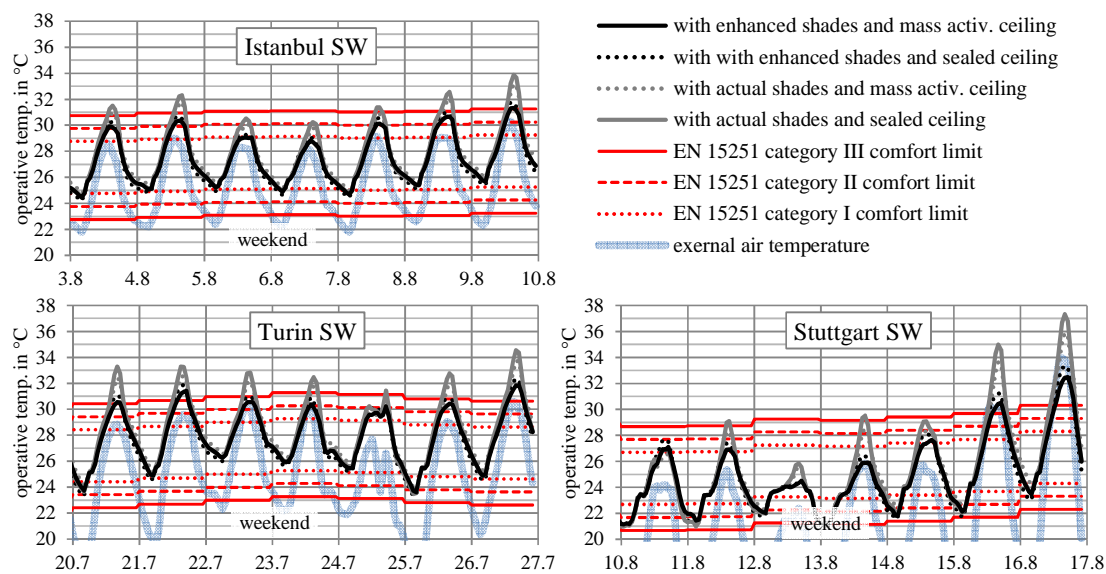


Figure 7.10: Extreme summer design week simulation results for the southwest zones indicating the effectiveness of the passive cooling conceptual design adaptations from § 6.1.

7.1.3 Hybrid approach

The mixed-mode ventilation and cooling scenarios also include the conceptual design adaptations made in § 6.1. The natural ventilation system sizes are equal to those of the passive cooling concept. Fans are smaller sized than in the as-built approach as no economiser operation is needed.

The base-case hybrid operation is controlled in a very simple way:

- 1) If the internal operative temperature exceeds 26 °C, mechanical ventilation and cooling replace passive ventilation until the end of occupancy.
- 2) If internal relative humidity exceeds 60%, natural ventilation is reduced to a level only to provide fresh air for the occupants until relative humidity again falls below 55% or the operative temperature exceeds 26 °C.

To focus on the influence of hybrid controls, the design week simulation outputs shown in Figure 7.11 are simulated in the conditioned mode. There are ongoing discussions in research and standard-making communities about the applicability of adaptive comfort approach for hybrid operated buildings that utilise a combination of natural ventilation and mechanical cooling [64]. The limits of thermal comfort plotted here are those for buildings with natural ventilation.

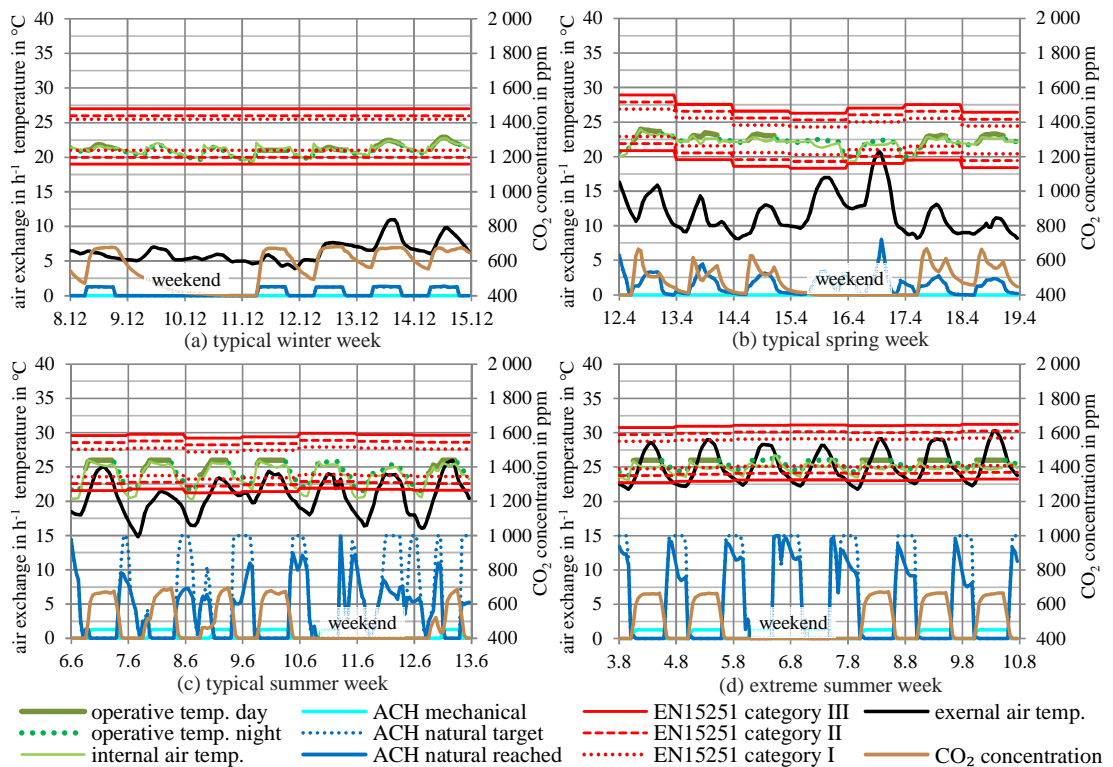


Figure 7.11: Design week simulation outputs of the base-case scenario for hybrid cooling and ventilation in Istanbul.

Hybrid operation can exploit the benefits of each mode. For example, in spring (Figure 7.11 (b)), natural ventilation with mostly low ventilation rates is sufficient to provide both thermal comfort and good indoor air quality. In summer (Figure 7.11 (c)-(d)), natural ventilation is mostly suited for night cooling, but also contributes to reduce the period of mechanical operation in the morning hours. In

contrast, passive humidity control extends the time of mechanical operation by minimising the natural ventilation rates even if cooling is needed. In Istanbul extreme summer conditions (Figure 7.11 (d)), passive cooling can only be provided when the building is not occupied. Cooling the building structure at night with natural ventilation contributes to the reduction of mechanical cooling loads. The CO₂ levels stay low in both modes. In winter (Figure 7.11 (a)), preheated fresh air is provided naturally and without heat recovery systems.

7.2 Annual Assessment

The dynamic annual simulation gives insight into the overall functionality of controlled natural ventilation throughout the year. Indicators used to evaluate the functionality are the relative energy consumption (compared to that of mechanical ventilation and cooling), and the compliance with thermal comfort limits for the users.

By dynamic computer simulations it is possible to calculate the space temperatures, the ventilation rates, and the CO₂ concentrations. The temperature distribution among the 4 categories are then calculated.

The parameters investigated are:

- cooling and ventilation strategy (full mechanical, hybrid, passive)
- climate (Stuttgart/Germany, Turin/Italy and Istanbul/Turkey)
- zone orientation (east, southeast, southwest, north)
- equipment load density of the office
- effectiveness of external solar shading devices
- levels of thermal mass (light, medium, heavy)
- convective heat transfer
- size of the ventilation system (see § 6.3.2)

The evaluation of the as-built operated case-study building with mechanical cooling and ventilation considers only the energy consumption, which can be compared with the consumption of controlled natural ventilation in order to evaluate the energy conservation. An evaluation of the thermal comfort and indoor air quality is assumed unnecessary because of a fixed mean room air temperature and an outside airflow rate control.

7.2.1 Ventilation rates

The two main functions of ventilation concepts are (i) the provision of good indoor air quality, and (ii) the improvement of thermal comfort in summer by increased daytime airspeed and high night ventilation rates. The monthly average air change rates are dependent on the following parameters:

- minimum ventilation rate to guarantee indoor air quality
- maximum ventilation rate to avoid draughts
- external dry-bulb temperature
- internal dry-bulb or operative temperature (and humidity for hybrid operation)
- optimum comfort temperature during occupancy
- driving forces (e.g. fan, wind, buoyancy pressure)
- flow path resistance (e.g. ducts, openings)

For mechanically ventilated buildings, the air change rates reached are mostly dependent on the minimum amount of fresh air necessary for indoor air quality control. If economiser operation is included, the amount of external air can rise, whenever external conditions are suitable, especially in spring and autumn. The suitability of the climate for the use of economiser ventilation for cooling also depends on the energy saved for mechanical cooling. Maximum air change rates are restricted due to relative small system sizes (4 ACH).

For naturally ventilated buildings the air change rate reached in the heating period, as in the case of mechanically ventilated buildings, is mostly dependent on the minimum amount of fresh air necessary for indoor air quality control. However, the scenario is different in the cooling period: ventilation rates for passive cooling no longer depend on the energy saved for mechanical cooling. In summer, the air change rates increase with higher passive cooling demands, and are only restricted to avoid draughts (e.g., papers flying). Natural ventilation systems are sized much bigger (10-15 ACH).

Considering hybrid ventilation, at least in this study, natural ventilation is intended for indoor air quality control, but also acts as a big sized economiser with high ventilation rates and without electricity demand for fan operation. To reduce the indoor peak temperatures in the hot season whenever passive cooling is not possible, mechanical fanning always acts together with mechanical cooling and only operates

during the building occupation. Maximum mechanical mode outdoor air change rates are restricted only to small system sizes designed for fresh air supply ($14 \text{ l}\cdot\text{s}^{-1}\cdot\text{person}^{-1}$).

For a dynamic analysis of the ventilation rates, the entire system including controls must be simulated. Figure 7.12 shows how the achievable air change rates are dependent on the climate, the type of the ventilation concept, the system sizes, and the control strategy (for natural ventilation, see § 3.3.2).

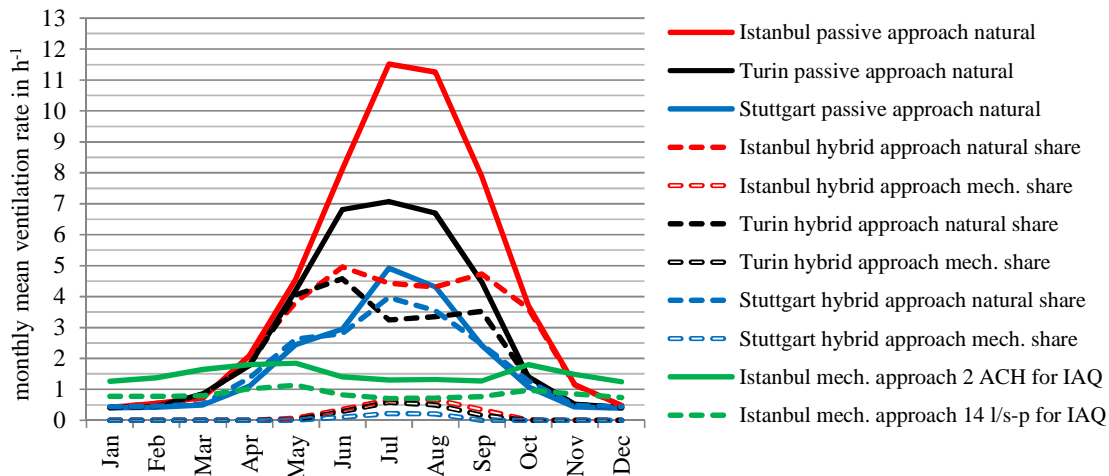


Figure 7.12: Simulated controlled air change rates (monthly averages) over the course of an year.

The seasonal variation of the air change rate was found to be highest for the natural ventilation cases and smallest for the full mechanical ventilation. In Istanbul winter, both the as-built (2 h^{-1}) and the adapted HVAC ($14 \text{ l}\cdot\text{s}^{-1}\cdot\text{person}^{-1}$) scenarios have higher ventilation rates than the naturally ventilated and the hybrid ventilated scenarios because of increased economiser operation due to the absence of proper shading devices. In summer, the natural ventilation air change rates increase more in Istanbul than in Turin and Stuttgart. In Turin climate, the biggest sized natural ventilation system provides only a limited air change rate due to relative low wind velocities. In contrast, the ventilation rates in Stuttgart are smaller mostly because of lower passive cooling demands. Hybrid operation differs from passive operation only in the hot season, most distinctive in Istanbul, where the natural ventilation share is mostly due to night ventilation. In Stuttgart, the hybrid operation mechanical share is very limited due to few hot days in summer.

7.2.2 Thermal comfort

In this work, the acceptable temperature for the naturally ventilated design scenarios were calculated following the adaptive comfort limits defined in the European standard EN 15251 [41]. In the standard, operative zone temperatures are used, which are the arithmetic mean of the zone mean air temperature and the zone mean radiant temperature. The operative temperature is allowed to increase in naturally ventilated, non air-conditioned buildings with rising ambient air temperatures according to § 2.6.3. The theory suggests that outdoor connections and control over their local environment allows occupants to adapt to a wider range of thermal conditions than is generally considered comfortable. The meaning of the different categories is also explained in § 2.6.3. The annual adaptive thermal comfort limits as well as the simulations are calculated with the ASHRAE IWEC [141] ‘typical’ climate data for the three reference locations – Istanbul in western Turkey, Turin in northern Italy and Stuttgart in southern Germany (see §5.1.4). Operative temperature levels over 30 °C are allowed for very hot ambient air summer conditions (e.g., see Istanbul in Figure 5.8).

The mechanical reference systems with active cooling and ventilation (fans) are mainly used to determine the annual energy conservation of the passive and hybrid approaches.

The more sophisticated weighted temperature excess method includes additional parameters such as air velocity, internal vapour pressure, metabolism, and clothing resistance [62]. As these values are difficult to obtain (especially the local air velocity), in this work the operative temperature excess method plotted as ‘exceeding frequency’ and ‘heat map’ charts is considered as evaluation baseline for the passive cooling approach developed.

The internal relative humidity is also plotted as ‘exceeding frequency’ chart for passive and mixed-mode operations (the fully mechanical operation will not exceed). Finally ‘psychrometric’ charts are intended to give insight into the humidity versus temperature relationship for all the scenarios including the fully mechanical-operated reference case.

7.2.2.1 Exceeding frequencies

The temperature excess method cumulates the hours with room temperatures above a given setpoint and compares them with the limiting values, for example 5% of all office hours. In designing system options, the thermal comfort analysis may indicate that a system performs very well, except for a small range of time, perhaps coinciding with an annual extreme weather event. A small percentage of hours out of the acceptability range may be permissible, but should be discussed. Recommended criteria for acceptable deviations in comfort, investigated by whole year computer simulations, are given in the EN 15251 standard [41]. According to annex G, the indoor environment of the building meets the criteria of a specific category when the rooms representing 95% of the occupied space are not more than 3% (or 5%) outside the limits of the specified category (see § 6.3.2.2).

Figure 7.13 considers the annual exceedance only for occupied hours. The average distribution in the different categories is weighted by the floor area of the different office spaces in the building. The minimum and maximum values represent the single office zone (space zoning see Figure 6.20) with the fewest and the most exceedance, respectively.

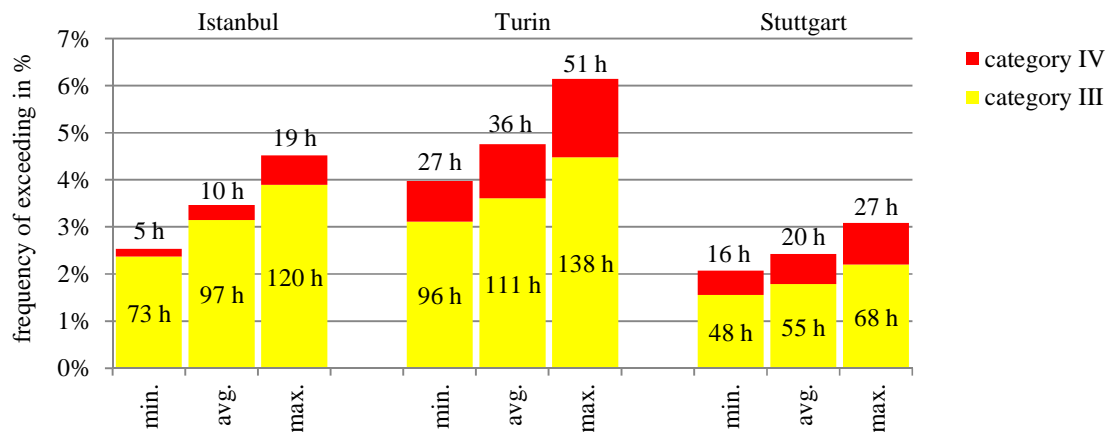


Figure 7.13: Comfort analysis for the passive cooling approach in different climates according to EN 15251 [41] comfort categories during occupancy.

For the passive cooling base-case scenario simulated with Istanbul climatic data, the frequency of exceedance in all office zones stays below the 5% benchmark with an average of 3,5% (referred to 3 084 occupancy hours per year). The zone operative temperature exceeds the EN 15251 adaptive comfort category II for 97 hours, and that of category III for 10 hours. With a value between 3% and 5%, further design adaptations or a hybrid cooling concept are reasonable but not mandatory. Turin

climate with low winds is the most critical. One of the four zones even exceeds the 5% benchmark by 1,1%. Therefore, further passive design adaptations (e.g., a smaller glazing ratio or more accessible thermal mass) or a hybrid cooling concept is recommended here. Stuttgart climate is less critical and the average frequency of exceedance stays well below 3%. Only the southwest zone very slightly exceeds with a value of 3,1%. The base-case passive cooling approach works well in the climate of Stuttgart, and no further design adaptations or hybrid cooling are necessary.

Relative humidity

To extend the picture on comfort beyond the adaptive comfort criteria of the EN 15251 standard, the internal relative humidity is also plotted as ‘exceeding frequency’. As regards the relative humidity, the standard only provides recommended design criteria for the humidity in occupied spaces if humidification or dehumidification systems are installed. These values are taken into consideration here. Figure 7.14 shows the simulation output for passive and mixed-mode operations. Since the relative humidity does not change significantly for the differently orientated zones, there is no distinction made.

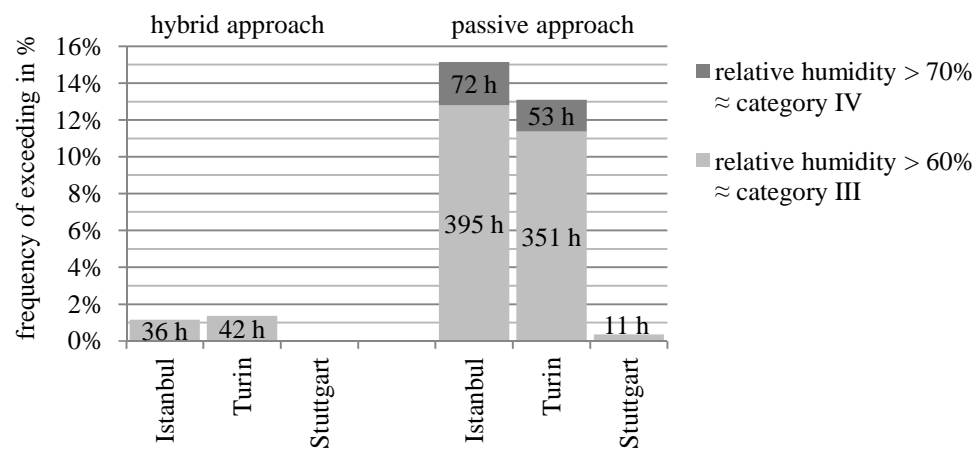


Figure 7.14: Comfort analysis for the passive and hybrid cooling approach in different climates according to the internal relative humidity level during occupancy.

In Istanbul and Turin, the passive cooling base-case scenario suffers from high humidity values mostly in the range between 60 to 70%. Humidity values above 80% are only reached for 3 hours in Istanbul. In contrast, the humidity levels reached in Stuttgart are very low. That the humidity values meet the comfort expectations must be discussed and ultimately accepted by all the project stakeholders; else, a hybrid approach might be a good alternative.

Sensitivity analysis

Sensitivity analysis is fundamental for the model development and is used in this thesis to ensure a correct use of the models, and to get insights about the subject of interest. It is also a technique for systematically changing parameters in the model to determine how the input variation affects the output, thereby indicating how the model behaves in response to changes in its inputs. It is useful in supporting decision making in terms of general design alternatives and optimization of the control strategy, and also increases the understanding of the system. In this section, deviations from the passive cooling base-case scenario are analysed. Subsequently, the base-cases for controlled natural ventilation are modified to show the influence of individual parameters (shading, internal heat gains, thermal mass, climate data, etc.) on the system functionality.

The influence of natural ventilation system size (flow path dimensions) was already discussed in § 6.3.2, and is not repeated here.

To have a higher contribution of thermal mass for good thermal comfort, the designer must take a closer look at the diurnal capacity of the mass as a heat sink, and also on the achievable heat exchange. Different levels of thermal mass (diurnal capacity) were defined for parametric modelling in the conceptual case-study design adaptations in Section § 6.1.3.

Figure 7.16 graphs the annual comfort simulation outputs for this parametric analysis, again in accordance to the benchmarks from EN 15251 [41]. Accessible thermal mass is crucial for all the simulated scenarios. Considering the convective heat transfer according to EN 13791, a mass exposed concrete floor in comparison to a mass activated ceiling results in slightly better results. A heavyweight construction for all the climates results in good thermal comfort below the 3% excess frequency benchmark.

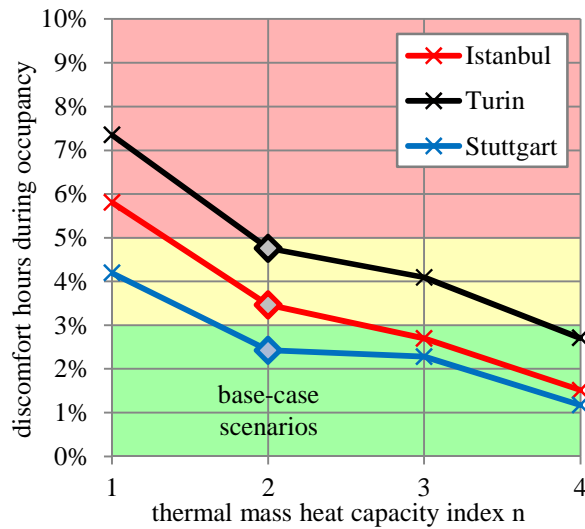


Figure 7.15: Thermal mass distribution scenarios sensitivity analysis w.r.t. the annual area weighted average adaptive comfort distribution during occupancy.

The heat exchange rate of the mass with the surrounding air is defined with Convective Heat Transfer Coefficient (CHTC) depending on the orientation of the mass, the local flow speed, the surface roughness, and the temperature differences. In the base-case scenarios, the convective heat transfer is dynamically simulated in accordance to EN 13791 (see § 3.3.1.5). The effect of different, unchanging CHTCs, equally distributed to all internal surfaces, on thermal comfort reached is shown in Figure 7.16. The CHTCs from EN 13791 give results close to a fixed value of above $\text{CHTC} = 2 \text{ W/m}^2\text{-K}$. If the CHTC could be enhanced by design measures, e.g., by better distribution of cool air flowing along the slabs, the comfort can be enhanced.

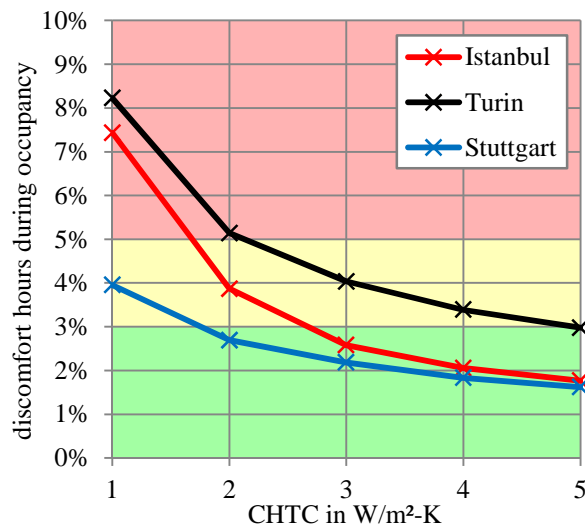


Figure 7.16: Thermal mass convective heat transfer sensitivity analysis w.r.t. the annual area weighted average adaptive comfort distribution during occupancy.

Preventive techniques are crucial for passive cooling and aim to provide protection and/or prevention of external and internal heat gains. This parametric analysis shows the effect of such techniques, and therefore indicates the permissible heat gains. Table 7.2 gives the simulated solar gain scenarios.

Table 7.2: Parametric solar gain reduction scenarios for the thermal comfort evaluation.

scenario index n	external shading on façade	facade glazing ratio
1	no shading devices	≈ 91,8%
2	actual shading devices	≈ 91,8%
3	adaptive venetian blinds	≈ 91,8%
4	adaptive venetian blinds	≈ 45,9%

Figure 7.17 shows the outputs of the thermal comfort evaluation. It indicates that enhancing the actual external solar shading devices and/or reducing the glazing ratio has great impact on the thermal comfort criteria. However, the designer needs to be aware of the reduced daylight entering the office zones and the visual aspects. The actual shading devices together with the highly glazed façade system are not a good choice for passive cooling.

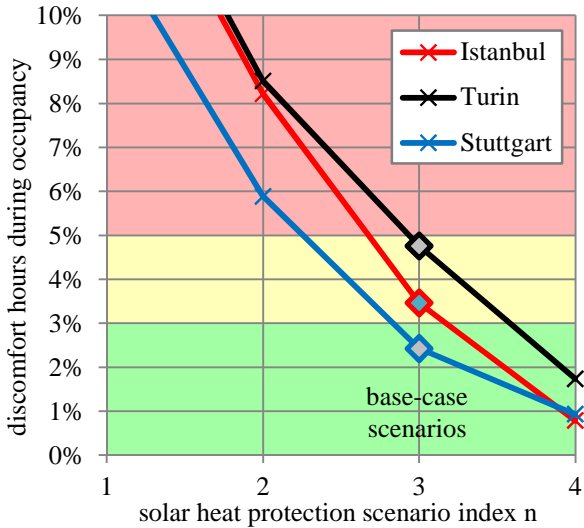


Figure 7.17: Protection of external heat gains sensitivity analysis w.r.t. the annual area weighted average adaptive comfort distribution during occupancy.

To assess the influence of internal equipment loads, loads in the office space are reduced and increased from 5 W to 30 W per net floor area. Equipment loads are defined excluding lighting loads and from 7 am-7 pm (during occupancy). At night, 25% of the daytime values are scheduled in the simulations. The equipment loads in the core area are not part of the analysis and stay constant with base-case value of 12 W/m² during occupancy, and 3 W/m² whenever the building is unoccupied. Figure 7.18 shows that the functionality of the passive cooling approach developed is

very sensitive to heat gains, especially in the warmer climate of Istanbul and Turin, where internal equipment loads above 12 W/m² are not recommended. If equipment loads above are unavoidable, other passive cooling parameters (e.g., thermal mass, sun protection, and air change rates) should be reconsidered for enhancement; else hybrid cooling is the best choice.

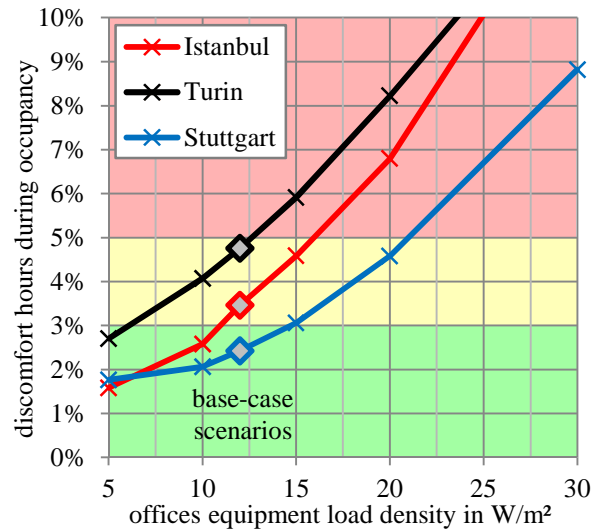


Figure 7.18: Prevention of equipment heat gains sensitivity analysis w.r.t. the annual area weighted average adaptive comfort distribution during occupancy.

7.2.2.2 Heat maps

One effective graphical option utilised to demonstrate thermal comfort results, uses a heat map of interior conditions, and is shown in Figure 7.19 through Figure 7.22. This illustrates thermal comfort performance for every hour of every day of the year with a thermal comfort colour code to represent areas when conditions are within the thermal comfort criteria, and when they are marginally or greatly outside these bounds. The colour code reports the operative temperature comfort category defined according to the adaptive comfort boundaries for naturally ventilated buildings from the European Standard EN 15251 [41]. Hours when the adaptive temperature approach is not applicable or whenever the office zones are assumed to be unoccupied are not considered (white coloured areas).

For Istanbul, all office thermal zones are chosen for review to also show the effect of different zone orientations (for space zoning, see Figure 6.20).

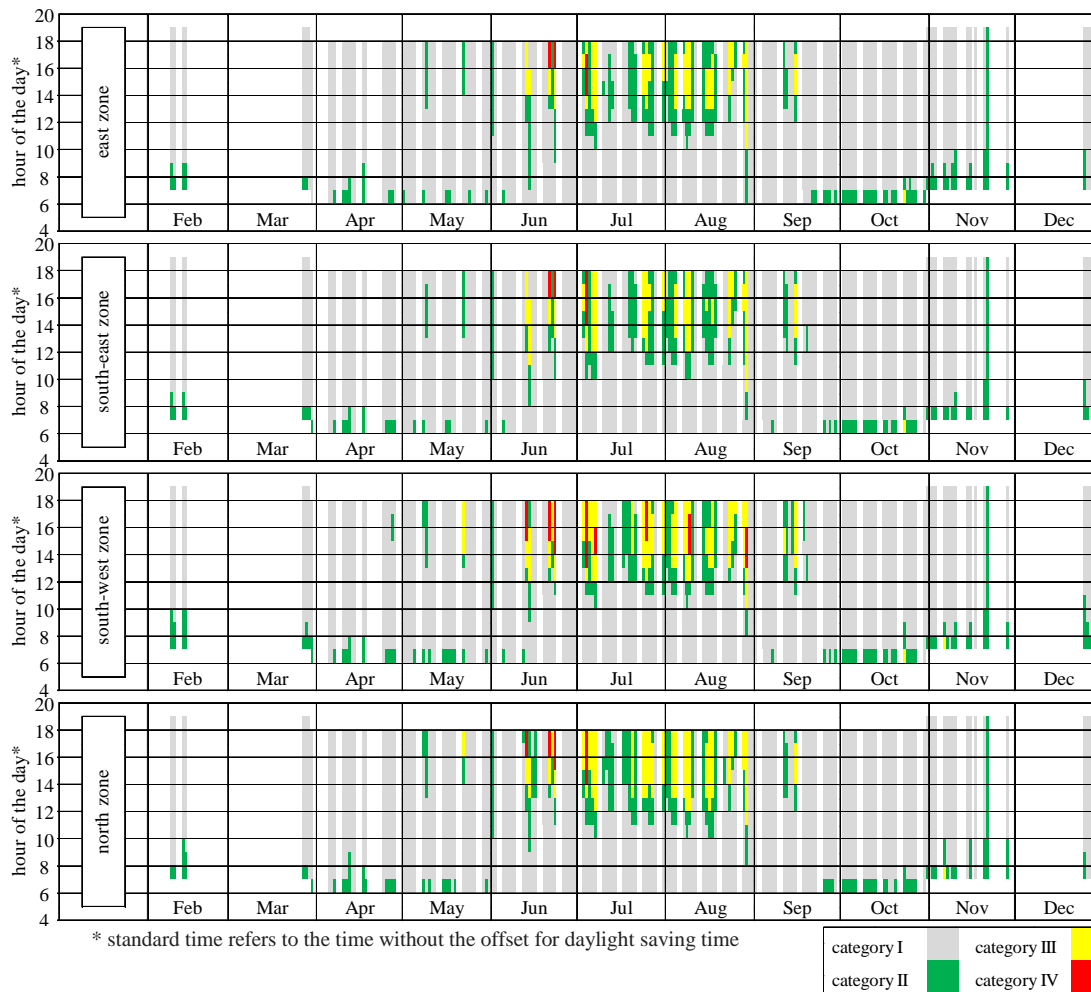


Figure 7.19: Heat maps of comfort hours for the passive cooling base-case scenario when adaptive comfort criteria from EN 15251 is applicable in Istanbul.

In the morning hours for all the orientations, the operative temperature very seldom falls below comfort category II. The controls do not tend to overcool the building. Nevertheless, a predictive control including the weather forecast, besides preventing overcooling, could also optimise the effect of night ventilation, especially in rapidly changing seasons or climates (see also weekly profiles in § 7.1.2.2).

The overheating hours in Istanbul are widely spread throughout most of the cooling period and for all orientations that take place in the afternoon. Comfort category III is far less exceeded than category II (see also Table 7.3). It is also observable that the different zones similarly often exceed comfort category II. This is because the heat gains (with setpoint controlled external blinds on all orientations) and also the thermal mass are relatively equally distributed among all the zones. Therefore, the simple flow path dimensioning only in linear dependency to the zone net floor area (and the volume) does work well here. If the zones differ significantly, a different passive approach or system sizing has to be considered for each zone.

Figure 7.20 and Figure 7.21 show the comfort distribution for the reference southeast zone located in Turin and Stuttgart. Except the flow path dimensions, all the basic parameters (base-case scenarios) are equal to those in Istanbul.

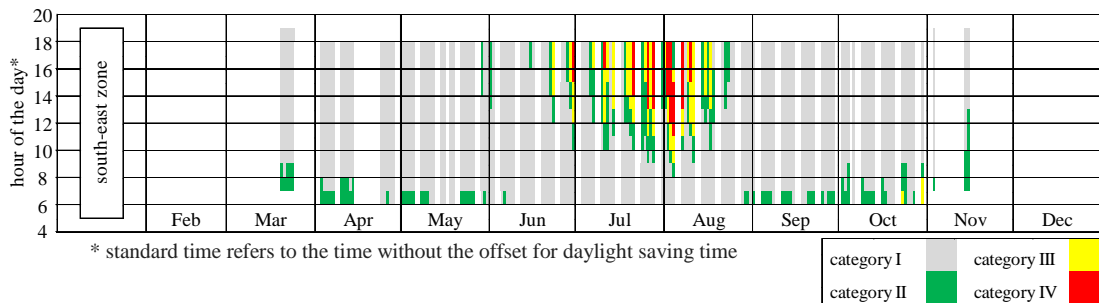


Figure 7.20: Heat map of comfort hours for the passive cooling base-case scenario when adaptive comfort criteria from EN 15251 is applicable in Turin.

For both passive cases in Turin and in Stuttgart, overcooling in the morning hours is not a problem. In Turin, the period in which heavy overheating occurs is compact and intense (end of July till mid-August). In contrast, the overheating periods in Stuttgart are much shorter but more widely distributed. This is because of the rapidly changing external temperatures in this climate.

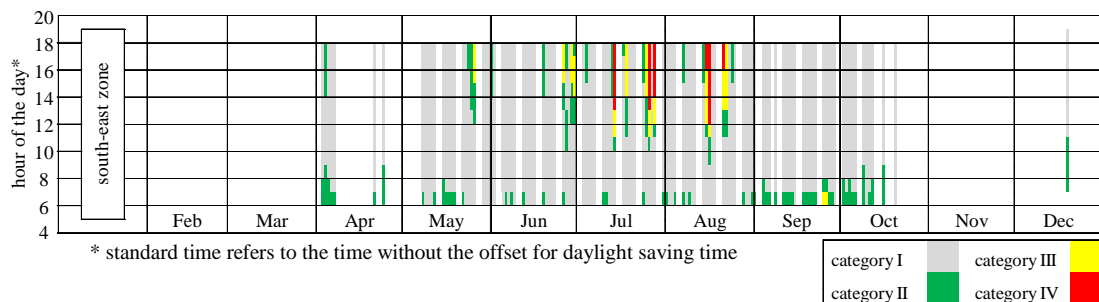


Figure 7.21: Heat map of comfort hours for the passive cooling base-case scenario when adaptive comfort criteria from EN 15251 is applicable in Stuttgart.

Table 7.3 summarises the hourly heat map values for the passive cooling base-case scenarios in all the three climates on annual basis.

Table 7.3: Passive cooling base-case comfort hours below and above category II when the adaptive temperature approach is applicable [41] for 4 office zone orientations and in 3 climates.

		Istanbul				Turin				Stuttgart			
		E	SE	SW	N	E	SE	SW	N	E	SE	SW	N
warm	category IV	5,2	6,0	19,2	8,7	27,0	35,2	51,7	29,3	16,2	19,7	27,5	16,3
	category III	65,7	74,2	99,0	102,5	66,8	73,8	83,0	69,8	31,7	36,3	39,8	32,0
cold	category III	0,5	0,2	0,3	0,3	2,5	2,7	3,7	1,0	0,3	0,5	0,8	0,2
	category IV	0,0	0,0	0,0	0,0	0,0	0,0	0,0	0,0	0,0	0,0	0,0	0,0

Finally in Figure 7.22, the simulation output is displayed for the naturally ventilated scenario in Istanbul, but without the enhanced solar heat gain reduction (with actual shading devices) and without the thermal mass activation at the ceiling (sealed

concrete). As a design scenario not suitable for implementation, the heat map indicates excessive overheating in the afternoon, spread over the whole cooling season.

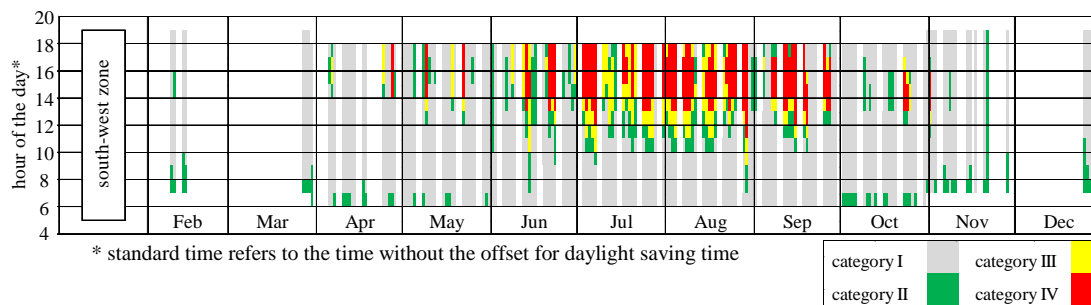


Figure 7.22: Heat map of comfort hours for an inappropriate passive cooling scenario with the actual as-built shading devices and without thermal mass activation at the ceiling when adaptive comfort criteria from EN 15251 is applicable in Istanbul.

7.2.2.3 Psychrometrics

Historically, thermal comfort in buildings has been controlled by simple internal dry-bulb temperature settings. For more sophisticated low energy building systems that make use of alternative systems such as natural ventilation, a more complete understanding of human comfort is recommended for both design and control, to determine whether local humidity effects require special consideration.

Even in this study, design evaluation is mostly based on the adaptive comfort standard EN 15251 [41]. There are other important variables not included in the standard. Besides the operative temperature (combination of the air and radiant temperatures), included are the humidity level, the air velocity, the activity level, and the clothing thermal resistance. Psychrometric charts show temperature versus humidity, and can be used to express human thermal comfort.

This evaluation provides a comparative visualisation of the different building operation strategies including the design adaptations and the climates simulated. Comfort boundaries are not shown here, but are described in § 3.2.2.3 or in the ASHRAE Standard 55 [63] (based on PMV instead of the adaptive approach).

Figure 7.23 shows the hourly simulation outputs of the office space psychrometrics (dry-bulb temperature versus humidity) during occupancy for Istanbul. The display format is intended to contrast the functionality of the different approaches with the controls incorporated. The as-built scenario Figure 7.23 (a) was simulated with full mechanical cooling and ventilation and with fixed dry-bulb temperature setpoints of

22/24 °C. The hybrid strategy (Figure 7.23 (b)) was first simulated with an operative cooling setpoint of 26 °C. If hybrid cooling is on, the air change rate is reduced to only account for fresh air supply. In the second hybrid scenario (Figure 7.23 (d)), the final hybrid cooling control including the passive humidity control is introduced (base-case controls of the hybrid approach). Natural ventilation during occupancy is now also reduced to a level only sufficient for fresh air supply (IAQ) if the internal relative humidity exceeds a level of 60%, and enhanced again if the humidity level is below 55%. Finally the result for the free running, passive cooling approach (Figure 7.23 (c)) is shown where the internal conditions are only controlled by the amount of natural ventilation. In the charts, only the internal conditions of the southeast zone are shown.

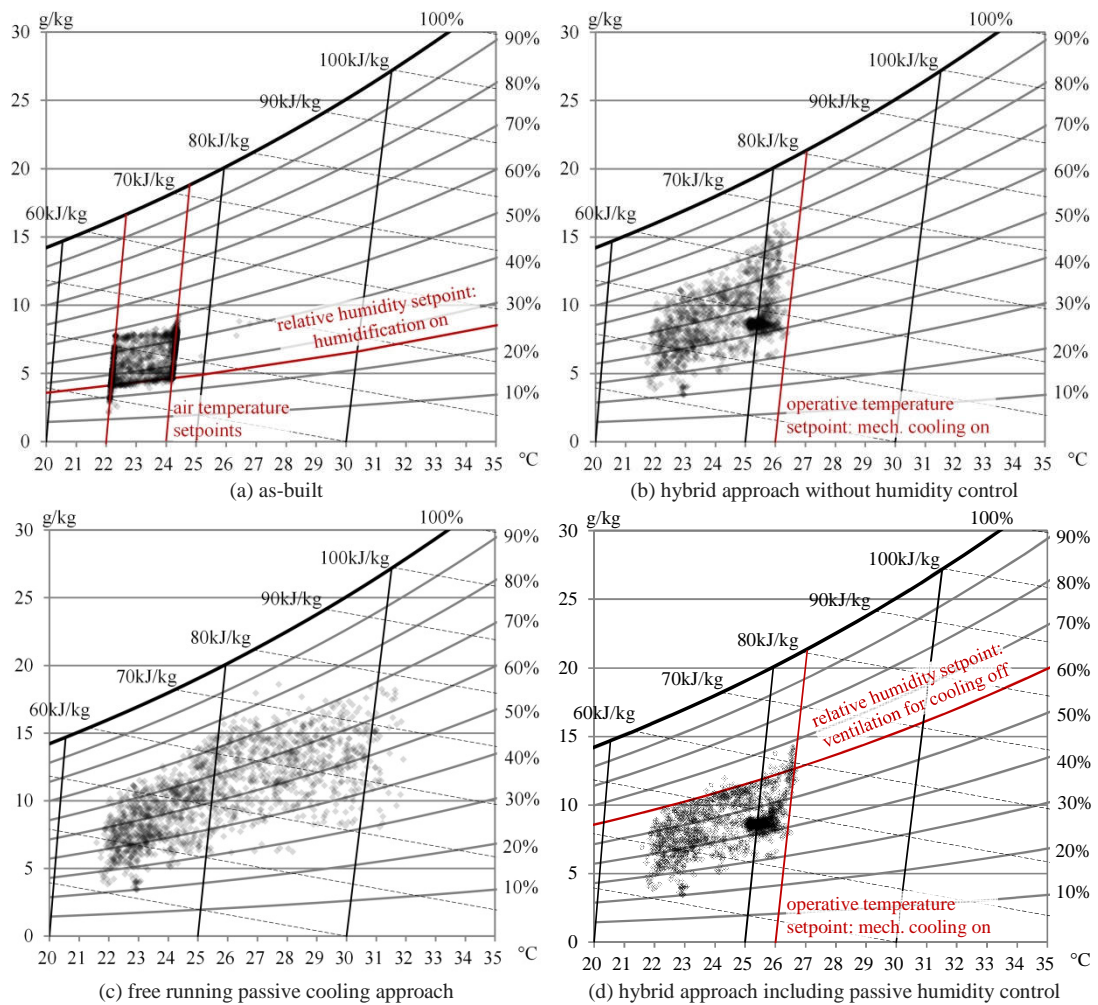


Figure 7.23: Simulation results of the office space psychrometrics during occupancy and in the cooling period for Istanbul climate.

As expected, the air temperature versus humidity dispersion is the smallest for full mechanical air-conditioning (Figure 7.23 (a)). Hybrid operation (Figure 7.23 (b) and (d)) gives the opportunity to reduce the peak temperature while

exploiting the advantages of natural ventilation whenever feasible. The introduction of passive humidity control (Figure 7.23 (d)) slightly enhances the air temperature during passive cooling operation, and drastically reduces the peak humidity levels, but is not suitable to control humidity to a specific level at any situation. Free running passive cooling operation (Figure 7.23 (c)) has by far the widest spread scatter values, and a psychrometric chart alone cannot fully indicate the functionality of the approach. But it is worth mentioning that the relative humidity in Istanbul is quite often between 60% and 70% at air temperatures between 25 °C and 30 °C. The statistical relative humidity dispersion of the different scenarios was also analysed in Figure 7.14.

Figure 7.24 and Figure 7.25 indicate the functionality of the hybrid and passive cooling approach as simulated in the climate of Turin and Stuttgart.

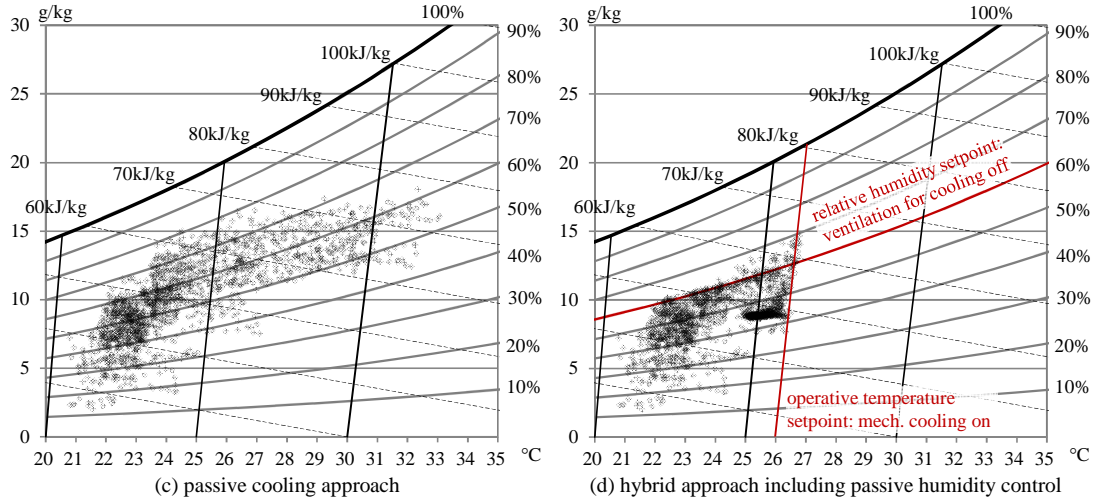


Figure 7.24: Simulation results of the office space psychrometrics during occupancy and in the cooling period for Turin climate.

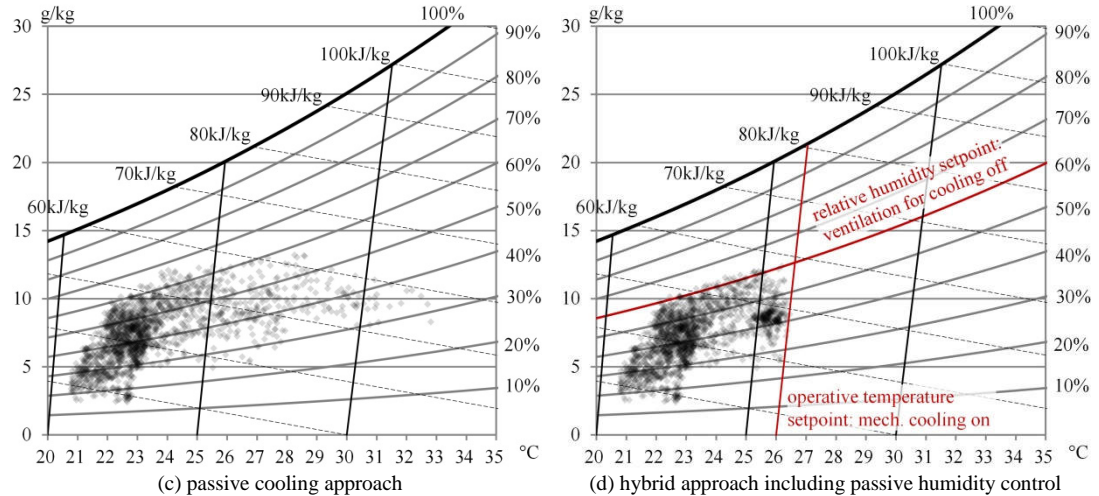


Figure 7.25: Simulation results of the office space psychrometrics during occupancy and in the cooling period for Stuttgart climate.

While passive cooling in Turin (Figure 7.24 (a)) in the hot periods (>25 °C internal air temperature) creates high internal humidity throughout ($>50\%$ relative humidity), in Stuttgart the hot period is much shorter (less scatter points) in combination with lower humidity (mostly $<50\%$).

7.2.3 Energy consumption

The model of the Kanyon office tower (according to § 4) is utilised as fully mechanical operated reference case with active cooling and ventilation (fans). To determine the associated annual energy conservation for controlled natural ventilation in moderate European climate, the passive and the hybrid cooling concepts are compared to this as-built benchmark scenario.

Energy efficiency is achieved by means of passive cooling, natural ventilation and by optimal control during winter operation. The following results refer to the parameter changes from the as-built scenario towards the hybrid and the passive base-cases defined in Table 6.3.

In addition to the simulation of the site energy demand in § 7.2.3.1, the total Primary Energy Input (PEI) and Global Warming Potential (GWP) values representing the annual building operation are calculated in § 7.2.3.2 and § 7.2.3.3. Again, the actual as-built Kanyon tower operation is compared to different adapted design scenarios in different climates. The environmental impacts are calculated using the values from the Global Emissions Model for Integrated Systems (GEMIS) [138] database, hosted by the International Institute for Sustainability Analysis and Strategy (IINAS).

7.2.3.1 Site energy input

The site energy is the amount of natural gas and electricity consumed by the building as reflected in the utility bills. Figure 7.26 shows the simulated site energy consumption of the actual Kanyon building base-case model for a typical year. The metered energy consumption was given in § 6.3.1.4.

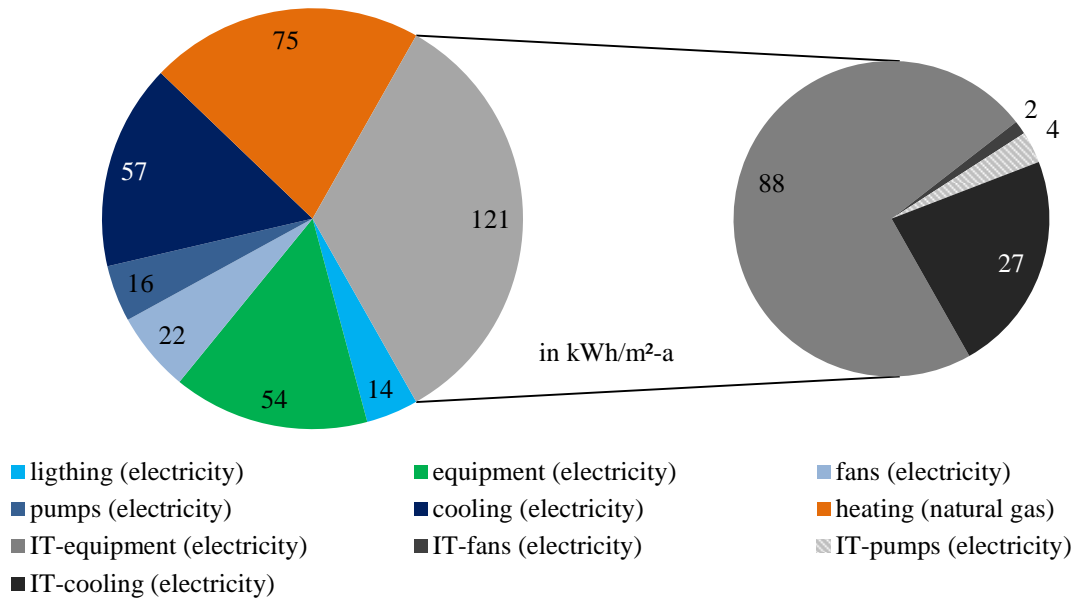


Figure 7.26: Simulated energy consumption of the as-built Kanyon building base-case.

Subsequently, in addition to the as-built case (Figure 7.27 (a)), a case without manual setpoint adaptation (see § 4.2.4) and less fresh air supply (14 l/s-p instead of 2 ACH) is simulated (Figure 7.27 (b)). This is done to demonstrate the insufficiency of actual controls and the related energy saving potential. All electrical equipment loads including the data centres and their air-conditioning are assumed to be stable throughout all the simulated scenarios. The electricity consumption for lighting, in all climates, slightly rises because of the redesigned shading elements (Figure 7.27 (c) (d)). Figure 7.27 plots the simulated annual electricity consumption of the twelve cases analysed.

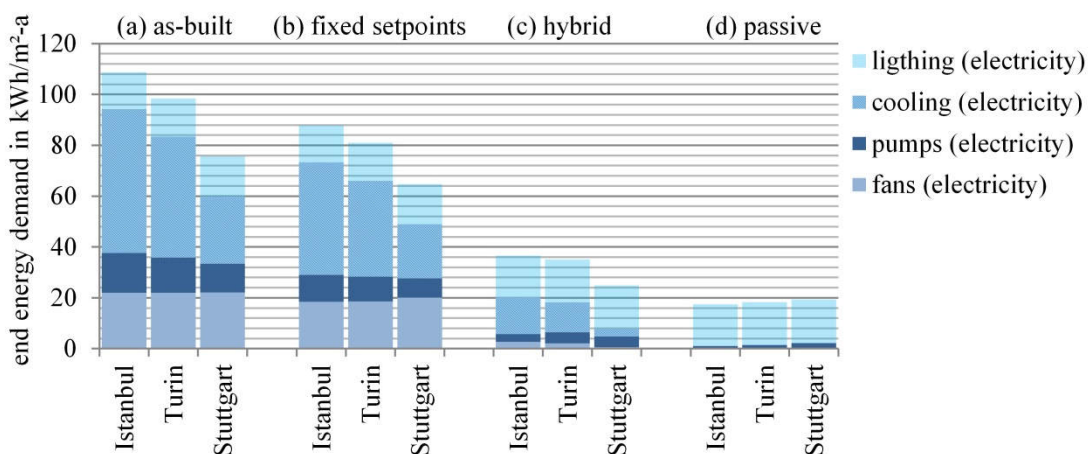


Figure 7.27: Simulated electricity consumption of the mechanically and passively cooled base-case scenarios.

Comparing the results of the hybrid (Figure 7.27 (c)) and the passively cooled (Figure 7.27 (d)) cases with those of the mechanically operated case

(Figure 7.27 (a)-(b)), energy conservation is found to be significant. In the considered and applicable cases with enhanced external shading devices and mass activated ceilings, the electricity savings, depending on the climate, are in the range between 51 to 72 kWh/m² per year for hybrid operation, and 56 to 91 kWh/m² per year for passive operation.

Included in the savings is a malfunction, which was indicated for the actual building controls. HVAC systems are fighting each other by shuttling between heating and cooling, which especially increases the natural gas consumption. With fixed heating and cooling setpoints, an increased dead band (21 °C / 26 °C instead of 22 ±3 °C / 24 ±3 °C) along with reduced fresh air supply (14 l/s and person instead of 2 ACH), the electricity consumption can be reduced by 11 to 21 kWh/m² per year.

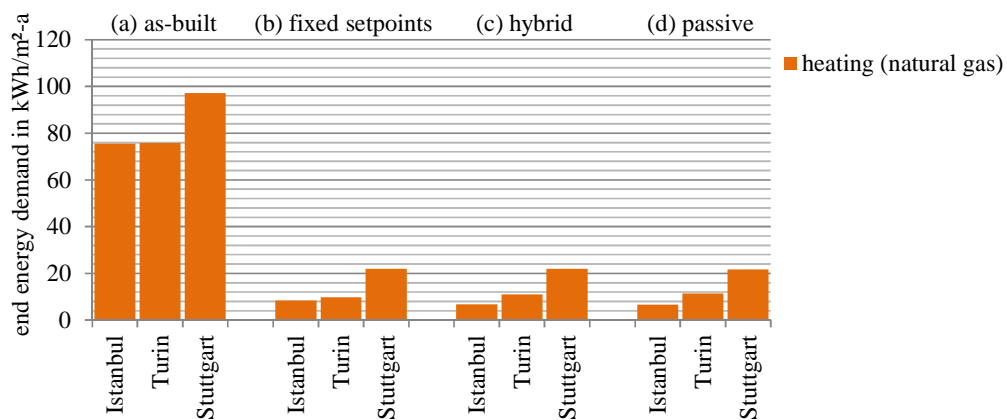


Figure 7.28: Simulated natural-gas consumption of the mechanically and passively cooled base-case scenarios.

The results of natural gas consumption mostly indicate the malfunction of the actual controls, and the climate the building is situated in (66 to 75 kWh/m² net floor area). Nevertheless, small energy savings could be achieved by reduction of fresh air supply during occupancy. Also, a small difference of gas consumption between hybrid and passive cooling is achieved due to different system sizes (e.g., pumps, boilers).

7.2.3.2 Primary energy input

The amount of energy resources required to provide the energy supply is defined as the PEI. This value refers to raw energy supply involved without any conversion or transformation processes from a life-cycle perspective. A primary energy source refers to the energy forms required by the energy sector to generate the supply of energy carriers used in building operation, such as electrical energy. To calculate the

PEI, the simulation outputs from § 7.2.3 are post-processed by multiplying the end energy usage with the PEI conversion values gathered for the three locations considered (see Table 7.4).

Table 7.4: Primary energy input of electricity and natural gas in kWh primary energy per kWh end energy usage according to GEMIS database [138].

	electricity generation (mix 2010) in kWh/kWh	natural gas in kWh/kWh
Turkey	2,15	1,18
Italy	2,24	1,12
Germany	2,71	1,11

The primary energy input for the whole building in Istanbul can be reduced by about 5 900 MWh per year by a hybrid cooling, and 6 900 MWh per year by applying a passive cooling approach (see Figure 7.29). This is a reduction of approximately 34% and 40%, respectively.

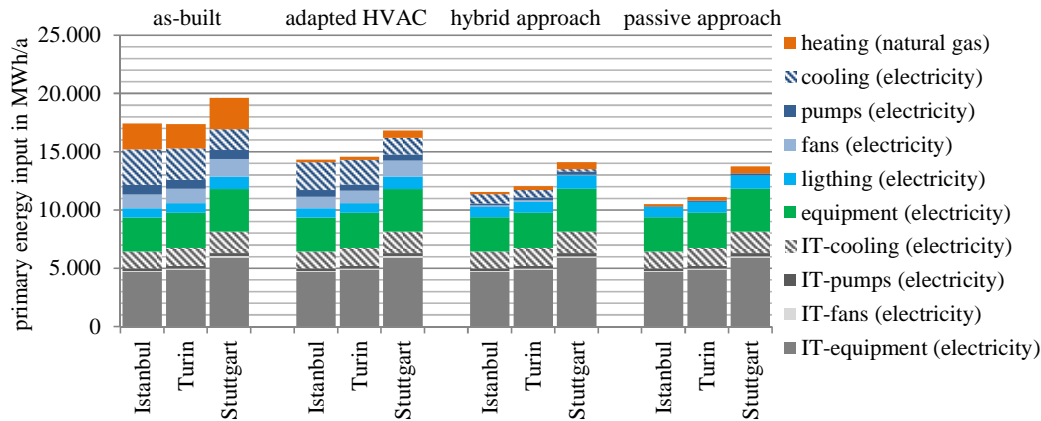


Figure 7.29: Comparative whole building annual primary energy input analysis.

Focusing on the simulated HVAC system loads in Figure 7.30, which are directly influenced not only by the free-running passive approach developed but also by the setpoint adjustments, the primary energy input is reduced by up to 97% in Istanbul.

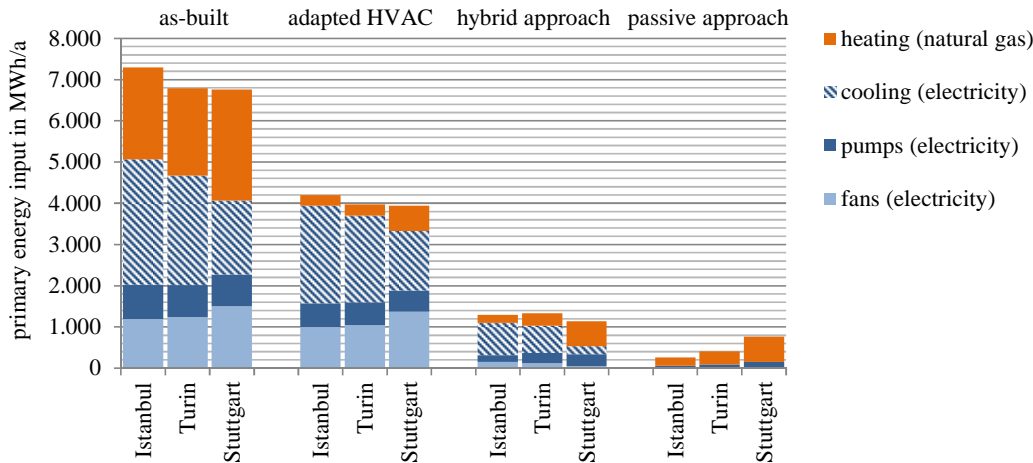


Figure 7.30: Comparative only HVAC system annual primary energy input analysis.

7.2.3.3 Global warming potential

GWP is a measurement that accounts for the relative climate effects of greenhouse gases. Carbon dioxide (CO₂), the most important greenhouse gas, is used as a reference parameter with a set GWP value of 1. The CO₂ equivalent (CO₂e) describes how much a greenhouse gas contributes to the greenhouse effect. The value depends on the gas heat absorption properties and the persistence of the gas in the atmosphere. This equivalent amount of CO₂ in kg per kWh is calculated for different energy sources, and is dependent on a life cycle assessment of each energy source incorporated. Table 7.5 summarises the electricity generation mix for Turkey, Italy, and Germany including renewable and conventional energy sources [146].

Table 7.5: Electricity generation mix in 2010 according to GEMIS database [138].

supplier	Turkey	Italy	Germany
coal	19,4%	16,3%	19,0%
brown coal	30,0%	-	23,4%
heavy oil	1,5%	5,6%	1,3%
palm oil	-	-	0,2%
natural gas	22,6%	55,2%	13,5%
furnace gas	-	1,4%	2,7%
biogas	-	-	1,9%
sewage gas	-	-	0,2%
landfill gas	-	-	0,2%
waste	-	3,9%	1,5%
nuclear	-	-	22,7%
wood waste	-	-	2,2%
geothermic	-	2,1%	0,0%
photovoltaic	-	0,6%	1,9%
wind	-	2,0%	5,9%
water	25,6%	12,8%	3,3%
biomass	0,8%	-	-

Table 7.6 gives an overview of the resulting life cycle emissions of natural gas and the electricity supply mix for these countries in 2010 [138].

Table 7.6: Global warming potential (GWP) of electricity mix and natural gas in kg CO₂e per kWh end energy usage in 2010 according to GEMIS database [138].

	electricity generation in kg/kWh	natural gas in kg/kWh
Turkey	0,586	0,199
Italy	0,506	0,199
Germany	0,588	0,201

For the calculation of environmental benefits of hybrid and passive cooling, the simulation outputs from § 7.2.3 are post-processed by multiplying the end energy usage with the GWP conversion values in kg CO₂e per kWh energy supply, gathered for the three locations considered (see Table 7.4). The CO₂ equivalent for

the whole building in Istanbul can be reduced by about 1 400 tonnes by a hybrid cooling approach, and 1 700 tonnes per year by applying a passive cooling approach (see Figure 7.31), which is a reduction of approximately 31% and 37%, respectively.

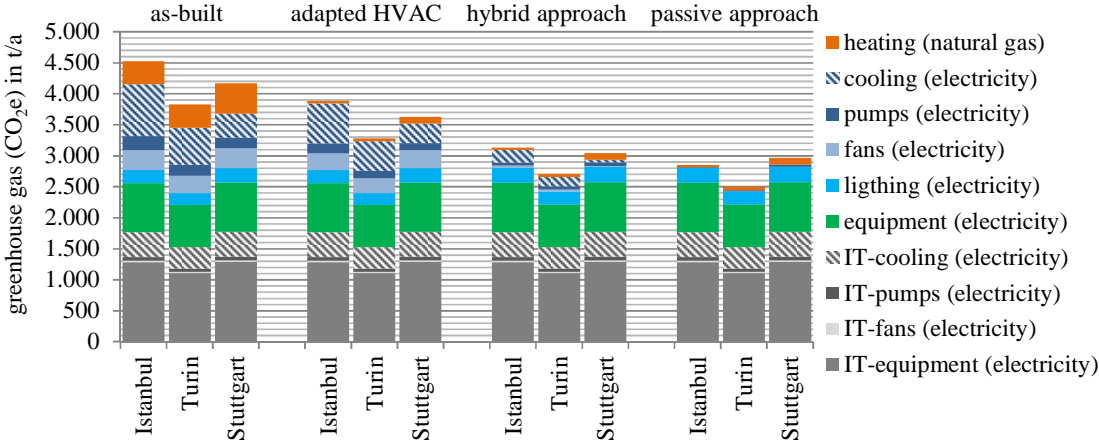


Figure 7.31: Comparative whole building annual global warming potential analysis.

Focusing on the simulated HVAC system loads, which are directly influenced by the free running passive approach developed and by the setpoint temperature adjustment, the global warming potential is reduced by up to 97% in Istanbul (see Figure 7.30).

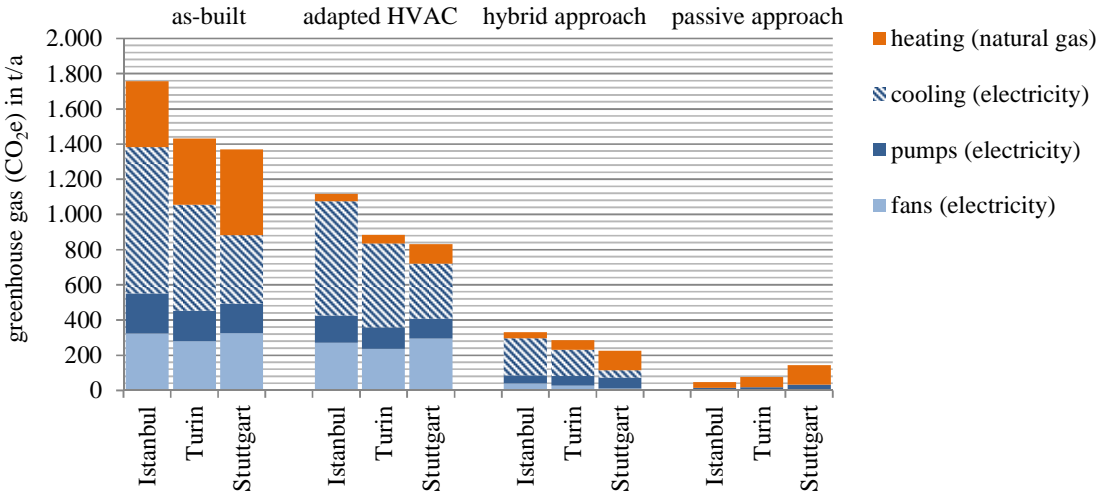


Figure 7.32: Comparative only HVAC system annual global warming potential analysis.

7.3 Conclusions

Thermal comfort

Thermal comfort plays a major role in evaluating the function of controlled naturally ventilated, passively cooled offices. Comfort was basically evaluated with the annual excess frequency (in hours) of the comfort criteria during office occupation according to EN 15251 [41]. As expected for the passive cooling approach

developed, the upper comfort limit (category II) is usually exceeded in the hottest months – July and August. Depending on the design and climatic case investigated, the comfort limit is exceeded more or less. A drop below the comfort criteria will very rarely take place throughout the year, since the opening controls prevent it, and the heating system is correspondingly controlled in the heating season.

In the base-case for Istanbul, the comfort range is exceeded by an average of 3,5%. With a value between 3% and 5%, further design adaptations or hybrid cooling are reasonable but not mandatory. Turin climate with low winds is the most critical. The southwest oriented office zone even exceeds the 5% excess frequency benchmark by 1,1%. To satisfy high comfort expectations, further passive design adaptations (e.g., smaller glazing areas, lower internal heat gains, or more accessible thermal mass) or a hybrid cooling concept is necessary here. Stuttgart climate is less critical and the average frequency of exceedance stays well below 3%. Only the southwest zone very slightly exceeds with a value of 3,1%. It can be concluded that the base-case passive cooling approach works well in the climate of Stuttgart and no further design adaptations or hybrid cooling is necessary. In Istanbul and Turin, the passive cooling base-case scenario also suffers from humidity values mostly in the range 60 to 70% at air temperatures between 25 °C and 30 °C. Humidity values above 80% are only reached for 3 hours in Istanbul. In contrast, the humidity levels reached in Stuttgart are low. That the humidity values meet the comfort expectations must be discussed and ultimately accepted by all the project stakeholders, else a hybrid operation approach might be a good alternative.

The thermal comfort simulations can be summarised as follows:

- With proper design, the use of controlled natural ventilation shows a good functionality, and the comfort limits of the EN 15251 category II are rarely exceeded.
- Night ventilation, especially in combination with a heavy building construction, along with a medium heavy construction complies significantly with the adaptive temperature limits.
- The reduction of internal (equipment) and external heat sources (solar radiation) is of crucial importance. This can be achieved through the use of external sun protection and adaptive light dimming. For the cases computed, equipment loads (without lighting) should not be higher than 10-15 W/m².

- Care must be taken to establish adequate ventilation rates. They are highly dependent on the natural ventilation design. In summer, the natural ventilation air change rates increase more in Istanbul (monthly average of 11 ACH) than in Turin (monthly average of 7 ACH) and Stuttgart (monthly average of 5 ACH). In Turin climate, the biggest sized natural ventilation system provides only a limited air change rate due to relative low wind velocities. In contrast, the ventilation rates in Stuttgart are smaller mostly because of the lower passive cooling demands. Hybrid operation differs from passive operation only in the hot season, most distinctive in Istanbul. In Istanbul, the natural ventilation share mostly results by night ventilation. In Stuttgart, the hybrid operation mechanical share is very limited due to few hot days in summer.
- Different climatic conditions for the cases considered have a great influence, but may be compensated by passive design adaptations.
- The orientation of a room affects its functionality. Proper external shading devices must be applied.

Energy conservation

Apart from thermal comfort, energy conservation plays the next major role in evaluating the function of controlled naturally ventilated offices. Energy conservation of purely passively cooled and ventilated office spaces is significant. Due to passive cooling and ventilation with controlled natural ventilation, there is no energy consumption for cooling and ventilation. In the considered applicable cases with enhanced shading devices and with mass activated ceilings, depending on the climate, the electricity savings are in a range between 51 to 72 kWh/m² per year for hybrid operation and 56 to 91 kWh/m² per year for passive operation. The hybrid strategies were found to be capable of exploiting the biggest share of passive cooling energy conservation by providing a maximum operative temperature limit of 26 °C.

Included in the savings above is a malfunction, which was indicated for the actual building controls. HVAC systems are fighting each other by shuttling between heating and cooling, which especially increases not only the natural gas consumption but also the electricity consumption. With fixed heating and cooling setpoints and an increased dead band (21 °C / 26 °C instead of 22 ±3 °C / 24 ±3 °C) along with reduced fresh air supply (14 l/s and person instead of 2 ACH during occupation), the

electricity consumption can be reduced by 11 to 21 kWh/m²-a, and the natural-gas consumption by 66 to 75 kWh/m²-a.

Without this malfunctioning, low heating loads result (8 to 22 W/m²-a) due to high-quality building façade system with low U-values, high solar transmittance, relatively high internal heat gains, and good building air tightness.

8. CONCLUSIONS

8.1 Introduction

The core premise of the thesis is that it is possible to design and construct sustainable buildings through the appropriate application of passive technologies. The existing barriers for practically implementing passive technologies in high-rise buildings can be lowered by creating a quantifiable framework that accounts for all the relevant input parameters in the design process. Towards this end, the thesis sets out to explore the concept of natural ventilation in high-rise office buildings, focusing on passive cooling in summer. A methodology has been developed for planning the natural ventilation scheme with different analysis tools and case-study integration. A sequential progression of the thesis work is recapitulated in this section.

Before natural ventilation can be widely adopted as a passive cooling and ventilation strategy, the underlying phenomena governing the flow patterns and temperature distribution had to be understood, and design concepts needed to be developed for the building type concerned. Accordingly, a literature survey was conducted. It was concluded that the preliminary evaluation tools and instruments for effective vent sizing were available only for a few building and ventilation designs, and were not suitable for complex flow path design. There was a definitive need for investigating the ventilation strategy and the size of elements involved in the flow path design. It was found that the passive cooling approach can rely not only on intense natural ventilation but also on the reduction of heat gains, and on night cold storage systems. The EN 15251 standard was found to best cover the comfort criteria for naturally ventilated buildings, and is especially suitable for whole year computer simulations.

The method was developed in three steps, including

- (i) the conceptual design considerations with focus on the architectural consequences on the building type of concern,
- (ii) the original development of a preliminary design tool based on electrical circuit analogies for sizing the natural ventilation system, and

(iii) a more detailed design development based on annual building energy performance simulations including custom ventilation control.

The applicability of the methodological approach was demonstrated and evaluated by virtually adapting the existing state-of-the art Kanyon office-tower that has high comfort expectations and high energy consuming mechanical systems.

- Through virtual monitoring, modelling, and simulation, the methodology was able to predict the temperature distribution and airflow patterns in the prototype of a naturally ventilated office-tower building.
- The results indicate that properly designed and controlled natural ventilation shows a good functionality, and the adaptive comfort limits of the EN 15251 category II are rarely exceeded.
- Comparisons were made between the resulting performance of passive, hybrid, and active operation.
- Significant reduction in the energy consumption can be noticed due to the proposed approach. The impact of different climatic conditions was brought forward through comparative performance assessment of a case-study building in three different climate locations, thus supporting the ambitious goals the European Union has set in the Energy Performance of Buildings Directive.

8.2 Summary and Conclusions from the Design Approach

Step 1 of the Design Approach

In the first step of the design methodology, a general concept was developed for passive cooling of the office tower building type. The research question concerning the effective passive cooling design approach put focus on the architectural consequences of passive cooling with intense natural ventilation. The findings are based on the investigations made for the specific building type considered, supplemented with findings from the investigation on the Kanyon case-study building in Chapter 4, and climate assessment in Chapter 5.

During the conceptual design process for wide-shaped office towers, several difficulties emerged. Design solutions addressing these challenges are summarised and discussed in Table 7.1 below. Bearing in mind all the mentioned considerations, the virtually adapted Kanyon building was designed accordingly.

Table 7.1: Design difficulties identified for passive cooling and the conceptual design adaptations proposed.

	design challenges	conceptual design solutions
natural ventilation system	<p>building width For effective ventilation, the room depth in case of single-sided ventilation should not be higher than 2,5 times the room height and in case of cross ventilation 5 times the room height.</p> <p>building height With a single chimney to ventilate an office tower, the size of the ventilation system would be either too big to be realised or the resistance of the flow path would be too high to reach high ventilation rates desired. Also the buoyant pressure drops across the envelope (e.g. at ground level), would be unacceptably high, especially in winter with high temperature differences.</p> <p>wind pressure distribution The wind pressure is not uniformly distributed at the differently orientated façade orientations. Thus, if the inlet openings are distributed directly in the façade, wind pressure is positive at the windward side only. At all the other orientations, the resulting wind pressure is negative and therefore counteracting the intended flow direction from the perimeter towards the core.</p>	<p>central chimney ventilation A void design is suitable for wide building shapes, as the occupied space is cross-ventilated from all orientations towards a central chimney, from where the warm air rises towards the exhaust.</p> <p>segmentation The building is horizontally cut into few-storey modular segments to restrict the system dimensions and peak pressure differences. As with isolated segments, each segment can then be treated as a medium-rise building.</p> <p>opposed ventilative inlet (+) and outlet (-) To guarantee the intended flow direction and to maximise the wind pressure difference, a leeward chimney exhaust and windward supply inlet is recommended. Intermediate 'wind floors' between the segments each have two wind adapting openings in windward and leeward orientation. The central chimneys serve the occupied space as fresh air supply (via sub-slab distribution) and exhaust.</p>
other passive systems	<p>solar heat gains A curtain wall envelope often is highly glazed. Measures to reduce the solar heat transmittance such as Low-E glazing and shading devices are usually inefficient to reduce the overall transmitted solar gains to practical support passive cooling. Thus, the building tends to overheat.</p> <p>thermal mass By assuming a sinusoidal temperature variation with a one day time period, suspended ceilings, floors and walls end up in a light-weight building construction. These arrangements are inefficient to provide a heat sink for night-time ventilation.</p>	<p>improved external shading Setpoint controlled exterior window blinds, which are slat-type horizontal shading devices are capable of reducing the amount of overall solar radiation entering the building in the cooling season. Thus, there is efficient protection from overheating.</p> <p>structural mass activation By exposing the structural mass (concrete) of the building, night-time ventilation can be used to cool the thermal mass. With activated concrete ceilings, the sum of all arrangements represents a medium-weight building construction.</p>
malfuctions	<p>actual control In Kanyon building, heating and cooling systems operate simultaneously by shuttling between heating and cooling, thus creating high energy demand. This is due to the manual setpoint adaptation in the rooms and due to high solar heat gains on one side of the building in combination with open doors and low internal insolation. Also, the air-conditioning system ventilates fresh air at a rate above the minimum requirement according to the initial design.</p>	<p>efficient operation Due to passive cooling and ventilation with controlled natural ventilation, there is no energy consumption for cooling and ventilation. With fixed setpoints along with adaptive comfort expectations and with reduced fresh air supply, the energy consumption can be reduced. Thus, energy conservation is significant. Hybrid strategies are found to be capable of exploiting the biggest share of passive cooling energy conservation.</p>

Step 2 of the Design Approach

In the second step of the passive cooling design approach, the 'HighVent' planning tool was introduced with the aim to determine the design air change rate and system sizes necessary for climate specific, pre-processed passive cooling summer design days. The tool is intended to replace trial-and-error evaluation of "what-if" options in building design.

- Simple electrical circuit analogies, for both ventilation and thermal models, are found to be suitable in supporting the passive system planning with emphasis on natural ventilation systems.
- The correctness of the results is proved by a comparative validation against the EnergyPlus building energy simulation program, which is found to be in good agreement.
- As it is concluded that the classic design day conditions for mechanical plant sizing are too strict for passive cooling system design and do not reflect the adaptive comfort approach, meaningful design boundary conditions have been provided by the original development of Summer Week Mean Days profiles. The approach organises average temperature, humidity, radiation, and wind information for extreme hot and typical summer periods.
- Openings can be sized automatically by the inverse solver method including an optimization process or by user-specifications of size and position. The method proposes correction factors for the terrain, and the floor height. Default pressure coefficients and flow resistances can be edited. For the Kanyon building, pressure coefficients are from wind tunnel measurements.
- The program first calculates the flow-path design for a given airflow rate with unchanging boundary conditions. These values from the first module are then provided to the thermal module, which calculates the dynamic thermal comfort. The procedure is then repeated till the system size is sufficient for passive cooling.
- The building can be described by design options such as air tightness, orientation, solar control, glazing ratio, thermal mass, site location, and internal heat gains. Dynamic design day simulations including the thermal model are carried out for a single zone model. They allow the impact assessment of the chosen ventilation strategy and size on the thermal behaviour of the building.

- The tool outputs include advice if certain adaptive thermal comfort criteria can be reached for a summer design day: in case of the extreme summer day it is category III and in case of the typical summer day the level is category II.

Step 3 of the Design Approach

In the third step of the passive cooling approach development, the annual performance of the adapted Kanyon building was exemplarily modelled with EnergyPlus building energy performance simulations including airflow networks. This includes the 'HighVent' tool preliminary ventilation design outputs, further 'post-processed' as model inputs, the conceptual adaptations made for improved shading and thermal mass activation, and the remaining features of the as-built Kanyon building in accordance with the data provided by the management as discussed in Chapter 4. It allows the users to perform sensitivity analysis for the investigation of the impact of specific parameters. The custom ventilation control was programmed with the Energy Management System (EMS) feature in EnergyPlus. The control dynamically targets to achieve (i) good indoor air quality according to EN 13779, and (ii) stay within adaptive comfort limits according to EN 15251.

- The mean monthly air change rates reached are dependent on the climate and season, and on the chosen system size. Accordingly, air exchange rates increase with higher passive cooling demands in Istanbul and Turin more than in Stuttgart.
- The target air change rate represents the amount of air the EMS control aims to realise, whereas the reached air change rate is the smaller amount of ventilation appearing in the simulation.
- Annual thermal comfort is the most crucial indicator for evaluating passive cooling concepts, and is therefore proposed for final decision making.
- During winter, the EN 15251 standard is mostly not applicable and mechanical heating is intended to raise the temperatures above a fixed temperature limit.
- The results of annual comfort distribution indicate that for the passive cooling base-case scenarios, the comfort benchmarks can be reached for all zone orientations in all climates with excess frequencies between 5% and 2%.
- Considering the 5% exceedence benchmark from EN 15251, generally good agreement is found for the entire design tool sizing suggestions.

- The natural ventilation system size gathered from the ‘HighVent’ tool was reduced to the sizing limit in cases where the initial size is considered to be too huge for practical implementation.
- As the volume of a building is an expensive resource, the designer needs to do a weighting between the expected adaptive comfort and the size of the natural ventilation system. The system can be resized by conducting a sensitivity analysis to study the relative impact of the design characteristics. If a hybrid approach is applied, the mechanical system installation and energy consumption are also the required parameters to be taken into consideration.

8.3 Summary and Conclusions from the Design Evaluation

The passive cooling design approach developed for the Kanyon office tower was further evaluated in Chapter 7. The level of functioning was attested by the usage of performance indicators to classify building energy performance simulation outputs according to categories from European standards or other benchmarks as applicable.

- Control over the openings is found to be crucial for all the cases; otherwise ventilation rates can get too high, and the office rooms tend to cool down way too much even in summer conditions. As expected for the controlled passive cooling operation, the upper comfort limit (category II) is usually exceeded in the hottest months – July and August.
- A drop below the comfort criteria will very rarely take place throughout the year, since the opening controls prevent this from happening, and the heating system is correspondingly controlled in the heating season.
- With comparative design week simulations, it is shown that the ‘adaptive temperature amplifier’ control algorithm developed is more robust than simplistic controls in terms of adapting the required flow rates for passive cooling without overcooling and frequent high adjustments.
- For all the simulated controlled cases, high indoor air quality is achieved in accordance to EN 13779, with CO₂ levels less than 400 ppm above the level of outdoor air. This is due to mechanical and natural ventilation system sizes sufficient enough to provide the required outdoor air flow rates, defined with at least 14 litres per second and person.

- The comfort criteria for passive cooling design has been mainly benchmarked by the excess frequency during office annual occupation in which adaptive comfort category II (normal level of expectation) could be reached according to the EN 15251 standard.
- It is concluded that in the climate of Stuttgart, no further design adaptations or hybrid cooling is necessary. In Istanbul, with an average excess frequency between 3% and 5%, further design adaptations or hybrid cooling are reasonable but not mandatory. However, to satisfy the comfort expectations in Turin, there is a necessity for further passive design adaptations or a hybrid cooling concept. Sensitivity analysis shows that if the glazing area or the equipment heat gains are reduced to half or a heavyweight building construction is realised, the average excess frequency in Turin can be reduced to a value below 3%.
- That the humidity values meet the comfort expectations must be discussed and ultimately accepted by all the project stakeholders, else a hybrid operation approach might be a good alternative.
- Apart from thermal comfort, energy conservation plays the next major role in evaluating the function of controlled naturally ventilated offices.

To systematically study the possible energy conservation while maintaining thermal comfort, identical buildings with different variants (passive/hybrid/active) were compared by simulation for different climates (Istanbul/Turin/Stuttgart). The energy consumption was benchmarked against the as-built scenarios.

- The primary energy input for the Kanyon office-tower building is reduced by approximately 30% to 40% for passive operation and by 28% to 34% for hybrid operation. For passive cooling including controlled natural ventilation, there is no energy consumption for cooling and ventilation, and pump operation is limited to heating season. This verifies the initial assumption that energy conservation of purely passively cooled and ventilated office spaces is significant, especially when compared to highly energy consuming state-of-the-art office towers.
- The hybrid strategies are found to be capable of exploiting the biggest share of passive cooling and ventilation energy conservation by providing a maximum operative temperature limit of 26 °C.

- The reduction in annual global warming potential accounts for approximately 1 200 tonnes CO₂ equivalents in Stuttgart, 1 300 tonnes CO₂ equivalents in Turin and 1 700 tonnes CO₂ equivalents in Istanbul.

8.4 Limitations and Ideas for Future Work

The following is a list of further research ideas to take forward the work done in this thesis:

- **Tool capabilities and integration:** The ‘HighVent’ design tool could be extended for different building types and ventilation strategies. As a computerised searching tool for passive cooling “optimisation”, it focuses on the architectural aspects of flow path design. The tool could be directly coupled to the simulation engine of EnergyPlus, which would address an extended multivariate and multicriteria “optimisation” including a large amount of modules. This along with a sophisticated graphical user interface would contribute to overcome the spreadsheet based limitations of automated optimisation along with trial-and-error evaluation in building energy performance simulation.
- **Simulation:** Further research is needed to fully validate the proposed methodology in the thesis. Energy savings by natural ventilation can mostly only be evaluated when simulation tools are used, as two identical buildings with different ventilation and climatisation strategies are rarely available for monitoring. The savings on mechanical ventilation, heating, and cooling energy can be determined by comparing natural ventilation strategies (while maintaining thermal comfort) with an identical office building for which mechanical ventilation is used. Building energy performance simulation is typically used to compare design alternatives, rather than to predict the actual energy performance of buildings. Limitations apply to almost every available program of this kind today, and hence it is necessary to understand basic principles of energy simulation.
- **Weather data:** Typical year weather data has been usually processed from measurements at the airports years ago, and is not further adapted to account for the local microclimate or climate change, e.g., the heat island effect, the local terrain wind flow, or the rising temperatures due to global warming.

- **Manual control:** Individual control should be maintained even if it can conflict with guaranteeing a specific level of indoor thermal comfort or air quality, as users are more tolerant with respect to thermal climate if controlled by themselves with rapid feedback. Automatic control is necessary to reset manual controls, especially in rooms occupied by several people. To integrate manual ventilation controls into the model, and also for real world application, further investigation is needed on the user behaviour and the control options together with the mechanisms of different strategies also supported by automatic controls. Individual controls should be outlined in a way that is easy to understand.
- **Comfort assessment:** According to the Fanger's approach, six primary factors affecting thermal sensation are either environmental or personal parameters: air temperature, mean radiant temperature, air velocity, humidity, metabolic rate, and clothing. The EN 15251 standard mainly employed in this thesis accounts for personal adaptation in naturally ventilated buildings by extending the thermal comfort limits depending on external conditions, but do not include the effect of humidity and air velocity. On the other hand, the most widely used thermal comfort standards (e.g., ISO 7730) account for the occupants of air-conditioned buildings including the effect of humidity, but have narrow thermal limits. These rigid limits do not account for the effects of expectation, personal control, and psychological adaptation. They discourage the use of naturally ventilated passive buildings, where occupants have more relaxed expectations and can tolerate a wider temperature swing. Considering buildings in warm and humid climate, adaptive comfort criteria inclusive of humidity and applicable to plot psychrometric charts in the context of building energy performance simulation needs further investigation. As the BEPS models calculate the volume flow rather than the air velocities, simple rule of thumb air velocity models based on room geometry, air change rates, and orifice dimensions could be applied to complement the scenario.

- **Flow path resistance:** The discharge coefficients for sharp edged openings are taken from the literature. Especially for complex shaped sub-slab distribution and chimney systems, the coefficients are based on a rough estimation. In reality, these coefficients are dependent on the practical implementation, and further investigation is mandated. The flow path resistances for the proposed ventilation strategy should be experimentally determined by tracer gas concentration measurements where accessible. Where configurations are not accessible, detailed CFD simulations or measurements with reduced scaled models could be employed.
- **Acoustic separation:** As a limitation, the possibilities for acoustic separation from the office areas towards the core area are relatively low since the internal openings are big in size.
- **Risk of draughts:** With insufficient and poorly positioned openings natural ventilation systems run the risk of causing draughts in winter. To avoid this risk, the incoming fresh air could be pre-heated in the e.g., central intake or sub-slab air distribution system.
- **Convective heat transfer:** One parameter mainly affecting the performance of natural night-time ventilation is the heat transfer at the internal surfaces. Algorithms based on air change rate or supply air temperature are developed for mechanical systems only, and therefore cannot be used with natural ventilation. The surface convective heat transfer for naturally ventilated buildings is typically highly simplified. Simulations in this thesis have been carried out by using heat transfer coefficients for cases without mechanical cooling according to the EN ISO 13791 standard. Increased convection can be expected due to high airflow rates and the possibility of a cold air jet flowing along a case specific surface, but the magnitude and location of these effects are hard to predict with a well-mixed zone air assumption. Thus, they are not included in actual models. When simulating a building with night ventilation, this becomes increasingly problematic because convective cooling is a major parameter and therefore a high priority research topic for the future.

- **Policy implication:** Energy efficiency in the building sector is one of the key objectives to meet the ambitious 2020 objectives of the European policies to address the challenges of energy security and climate change. Ventilative cooling however is poorly rewarded in regulations in most EU countries. To push forward the development, it is essential to give guidelines for integration of ventilative cooling in design development and energy performance calculation methods and regulations (e.g., DIRECTIVE 2010/31/EU). Policy makers and standard bodies should take steps together with the implementation of the EPBD recast to accelerate the uptake of this technology.

8.5 Conclusion

The results of this research work are intended to help the building planner in better understanding and implementing passive cooling measures. It is envisioned that the recommendations put forward in this thesis will contribute to the furthering of much needed sustainable building practices.

REFERENCES

- [1] **EnergyPlus** (Version 8.1). (2014) [Energy simulation software]. USA: Department of Energy. Retrieved from <http://apps1.eere.energy.gov/buildings/energyplus/>
- [2] **Artmann, N.** (2008). *Cooling of the building structure by night-time ventilation* (Doctoral dissertation), Aalborg University, Denmark. Retrieved from <http://www.vbn.aau.dk/>
- [3] **IEA-ECBCS Annex 35.** (2002). *State-of-the-art Review Hybrid Ventilation in New and Retrofitted Office Buildings*, A. Delsante & T. A. Vik (Eds.), Retrieved from <http://www.hybvent.civil.aau.dk/>
- [4] **UN FCCC.** (2010). *The Cancun Agreements: Outcome of the work of the Ad Hoc Working Group on Long-term Cooperative Action under the Convention*. Conference of the Parties 16, Framework Convention on Climate Change. (FCCC/CP/2010/7/Add.1). Mexico: United Nations. Retrieved from <http://www.unfccc.int>
- [5] **UN EP.** (2007). *Buildings And Climate Change: Status, Challenges and Opportunities, Sustainable Buildings and Climate Initiative*. United Nations Environment Programme. (978-92-807-2795-1). Paris, France: Renouf Publishing Company Limited. Retrieved from <http://www.unep.org>
- [6] **Wood, A., & Salib, R.** (2013). *Natural Ventilation in High-Rise Office Buildings*. Council on Tall Buildings and Urban Habitat - Technical Guides. Abingdon, UK: Routledge.
- [7] **European Parliament.** (2010). *The Council of 19 May 2010: On the energy performance of buildings (recast)*. (DIRECTIVE 2010/31/EU). Luxembourg: Official Journal of the European Union. Retrieved from <http://www.eur-lex.europa.eu>
- [8] **Givoni, B.** (1998). *Climate considerations in building and urban design*. New York, USA: John Wiley & Sons Inc.
- [9] **Mazria, E.** (1979). *The Passive Solar Energy Book: A Complete Guide to Passive Solar Home, Greenhouse and Building Design*. USA: Rodale Press.
- [10] **BS 5925.** (1991). *Code of Practice for: Ventilation principles and designing for natural ventilation*. London, UK: British Standards Institution.
- [11] **Adnot, J., Riviere, P., Marchio, D., Holstrom, M., Naeslund, J., & Saba, J.** (2003). *Energy Efficiency and Certification of Central Air Conditioners - Final Report*. Armines, France: D.G. Transportation-Energy of the Commission of the E.U.
- [12] **NatVent Project.** (1998). *Work Package 2: Performance of naturally ventilated buildings* V. Kukadia (Ed.) *Final Monitoring Report* Retrieved from <http://www.projects.bre.co.uk/natvent/>
- [13] **Santamouris, M., & Asimakopoulos, D.** (1996). *Passive cooling of buildings*. London, UK: James and James Ltd.

- [14] **Allard, F., & Santamouris, M.** (1998). *Natural Ventilation in Buildings: A Design Handbook*. London, UK: James and James Ltd.
- [15] **Klitsikas, N., Geros, V., Santamouris, M., Dascalaki, E., Kontoyiannidis, S., & Argirou, A.** (1996). *Summer: A tool for passive cooling of buildings* (Version 2.0). Greece: University of Athens.
- [16] **Van Paassen, A. H. C., Liem, S. H., & Gröniger, B. P.** (1998, September). *Control of night cooling with natural ventilation: sensitivity analysis of control strategies and vent openings*. Paper presented at the 19th AIVC conference, Oslo, Norway. Paper retrieved from <http://www.aivc.org/>
- [17] **Pfafferott, J., Herkel, S., & Jäschke, M.** (2003). Design of passive cooling by night ventilation: evaluation of a parametric model and building simulation with measurements. *Energy and Buildings*, 35(11), 1129-1143. doi: 10.1016/j.enbuild.2003.09.005
- [18] **Blondeau, P., Spérandio, M., & Allard, F.** (1997). Night ventilation for building cooling in summer. *Solar Energy*, 61(5), 327-335. doi: 10.1016/S0038-092X(97)00076-5
- [19] **Geros, V., Santamouris, M., Tsangrasoulis, A., & Guarracino, G.** (1999). Experimental evaluation of night ventilation phenomena. *Energy and Buildings*, 29(2), 141-154. doi: 10.1016/s0378-7788(98)00056-5
- [20] **IEA-ECBCS Annex 35.** (2002). *Control Strategies for Hybrid Ventilation Hybrid Ventilation in New and Retrofitted Office Buildings*, R. Jagpal (Ed.) *Technical Synthesis Report* Retrieved from <http://www.hybvent.civil.aau.dk/>
- [21] **Galli, A., & Hässig, W.** (2009). *Kontrollierte Fensterlüftung – Pilotprojekt Schulhaus Untermoos* [Controlled window ventilation - Pilot project school building Untermoos]. Zurich, Switzerland: Buildings department. Retrieved from www.stadt-zuerich.ch/nachhaltiges-bauen
- [22] **Fisch, M. N., & Zargari, M.** (2009). *Analyse und Bewertung von Atrien in Bürogebäuden* [Analysis and evaluation of atria in office buildings]. Germany: TU Braunschweig & Research Initiative 'Future Building'.
- [23] **Breesch, H.** (2006). *Natural Night Ventilation in Office Buildings: Performance Evaluation Based on Simulation, Uncertainty and Sensitivity Analysis* (Doctoral dissertation), Univeristy of Ghent, Belgium. Retrieved from <http://www.aivc.org/>
- [24] **Eicker, U., Huber, M., Seeberger, P., & Vorschulze, C.** (2006). Limits and potentials of office building climatisation with ambient air. *Energy and Buildings*, 38(6), 574-581. doi: 10.1016/j.enbuild.2005.09.004
- [25] **Li, Y.** (2009, January). *Energy efficient cities and buildings for better air environment*. Paper presented at the Workshop on Clean Energy and Environment, Tianjin, China. Presentation retrieved from <http://icee.hku.hk/>
- [26] **CIBSE.** (2005). *Natural Ventilation in Non-domestic Buildings*. Application Manual (Vol. AM10). London, UK: Chartered Institution of Building Services Engineers.
- [27] **ASHRAE.** (2009). *Handbook of Fundamentals*. Atlanta, USA: American Society of Heating, Refrigerating and Air-Conditioning Engineers.
- [28] **EN 15242.** (2007). *Ventilation for buildings - Calculation methods for the determination of air flow rates in buildings including infiltration*. Brussels, Belgium: European Committee for Standardization.
- [29] **Costola, D., Blocken, B., & Hensen, J. L. M.** (2009). Overview of pressure coefficient data in building energy simulation and airflow network programs. *Building and Environment*, 44(10), 2027-2036. doi: 10.1016/j.buildenv.2009.02.006

- [30] **Orme, M., & Leksmono, N.** (2002). *AIVC Guide 5: Ventilation Modelling Data Guide* (pp. 80). Retrieved from <http://www.aivc.org>
- [31] **Ball, P.** (2010). Termites show the way to the eco-cities of the future. *New Scientist*, 205(2748), 35-37. doi: 10.1016/S0262-4079(10)60423-X
- [32] **Awbi, H. B.** (1991). *Ventilation of Buildings*. London, UK: Taylor and Francis.
- [33] **Coley, D. A.** (2008). Representing Top-hung Windows in Thermal Models. *International Journal of Ventilation*, 7(2), 151-158. doi: 10.5555/ijov.2008.7.2.151
- [34] **Hall, M.** (2004). *Untersuchungen zum thermisch induzierten Luftwechsellpotential von Kippfenstern* [Investigations on Buoyancy Induced Ventilation through bottom hung Windows]. (Doctoral dissertation), University of Kassel, Germany. Retrieved from <http://www.uni-kassel.de/>
- [35] **IES.** (2011). *MacroFlo Calculation Methods* Virtual Environment 6.4: Integrated Environmental Solutions Limited. Retrieved from <http://www.iesve.com/>
- [36] **Hult, E., Fischer, M., & Iaccarino, G.** (2012, August). *Using CFD Simulations to Improve the Modeling of Window Discharge Coefficients*. Paper presented at the SimBuild, Madison, USA. Paper retrieved from <http://www.ibpsa.org>
- [37] **Emmerich, S. J., Dols, W. S., & Axley, J. W.** (2001). *Natural Ventilation Review and Plan for Design and Analysis Tools*. (NISTIR 6781). USA: National Institute of Standards and Technology. Retrieved from <http://fire.nist.gov/bfrlpubs/build01/art073.html>
- [38] **Novoselac, A., Burley, B. J., & Srebric, J.** (2006). Development of new and validation of existing convection correlations for rooms with displacement ventilation systems. *Energy and Buildings*, 38(3), 163-173. doi: 10.1016/j.enbuild.2005.04.005
- [39] **Gissen, D.** (2003). *Big and Green: Toward Sustainable Architecture in the 21st Century*. New York, USA: Princeton Architectural Press.
- [40] **Etheridge, D.** (2011). Design Procedures. In *Natural Ventilation of Buildings: Theory, Measurement and Design* (pp. 375-413). UK: John Wiley & Sons, Ltd. doi: 10.1002/9781119951773.ch12
- [41] **EN 15251.** (2012). *Indoor environmental input parameters for design and assessment of energy performance of buildings addressing indoor air quality, thermal environment, lighting and acoustics*. Brussels, Belgium: European Committee for Standardization.
- [42] **Etheridge, D. W., & Ford, B.** (2008, March). *Natural ventilation of tall buildings – options and limitations*. Paper presented at the CTBUH 8th World Congress, Dubai. Paper retrieved from <http://www.ctbuh.org/>
- [43] **Etheridge, D.** (2011). *Natural Ventilation of Buildings: Theory, Measurement and Design* (pp. 428). doi:10.1002/9781119951773
- [44] **Oseland, N. A.** (1998). Acceptable Temperature Ranges in Naturally Ventilated and Air-Conditioned Offices. *Ashrae Transactions*, 104(pt. 1A).
- [45] **Brager, G. S., & de Dear, R. J.** (1998). Thermal adaptation in the built environment: a literature review. *Energy and Buildings*, 27(1), 83-96. doi: 10.1016/S0378-7788(97)00053-4
- [46] **Olesen, B. W.** (2000). Guidelines for comfort. *Ashrae Journal*, 42(8), 41-46.
- [47] **Raja, I. A., Nicol, J. F., McCartney, K. J., & Humphreys, M. A.** (2001). Thermal comfort: use of controls in naturally ventilated buildings. *Energy and Buildings*, 33(3), 235-244. doi: 10.1016/S0378-7788(00)00087-6

- [48] **Olesen, B. W.** (2007). The philosophy behind EN 15251: Indoor environmental criteria for design and calculation of energy performance of buildings. *Energy and Buildings*, 39(7), 740-749. doi: 10.1016/j.enbuild.2007.02.011
- [49] **Axley, J. W.** (2001). *Application of Natural Ventilation for U.S. Commercial Buildings - Climate Suitability Design Strategies & Methods Modeling Studies*. USA: National Institute of Standards and Technology. Retrieved from <http://www.stanford.edu>
- [50] **IEA-ECBCS Annex 35.** (2002). *Principles of Hybrid Ventilation Hybrid Ventilation in New and Retrofitted Office Buildings*, P. Heiselberg (Ed.) Retrieved from <http://www.hybvent.civil.aau.dk/>
- [51] **Kolokotroni, M., & Aronis, A.** (1999). Cooling-energy reduction in air-conditioned offices by using night ventilation. *Applied Energy*, 63(4), 241-253. doi: 10.1016/s0306-2619(99)00031-8
- [52] **Kolokotroni, M.** (1998). Night Ventilation for Cooling Office Buildings. *BRE Information Paper*, 4/98.
- [53] **Martin, A. J., & Fletcher, J.** (1996). *Night Cooling Control Strategies*. Technical Appraisal (Vol. 14-96). Bracknell, UK: Building Services Research & Information Association.
- [54] **Marjanovic, L., & Eftekhari, M.** (2004). Design and simulation of a fuzzy controller for naturally ventilated buildings. *Building Services Engineering Research & Technology*, 25(1), 33-53. doi: 10.1191/0143624404bt086oa
- [55] **EN 13779.** (2007). *Ventilation for non-residential buildings - Performance requirements for ventilation and room-conditioning systems*. Brussels, Belgium: European Committee for Standardization.
- [56] **European Commission.** (2012). *Commission delegated regulation (EU) No 244/2012*. Supplementing Directive 2010/31/EU of the European Parliament and of the Council on the energy performance of buildings by establishing a comparative methodology framework for calculating cost-optimal levels of minimum energy performance requirements for buildings and building elements. Luxembourg: Official Journal of the European Union. Retrieved from <http://eur-lex.europa.eu/>
- [57] **Fromme, H., Dietrich, S., Kiranoglu, M., & Tarwella, D.** (2006). *Frische Luft an Bayerischen Schulen* [Fresh air at Bavarian schools]. Oberschleißheim, Germany: Landesamt für Gesundheit und Lebensmittelsicherheit [Bavarian Health and Food Safety Authority]. Retrieved from <http://www.lgl.bayern.de/>
- [58] **Müller, D., Eggers, I., Matthes, P., & Panaskova, J.** (2010). *Hybrid ventilation for a better learning* (Vol. 15/2010): BINE Information Service. Retrieved from <http://www.bine.info/en/>
- [59] **DIN 1946-6.** (2009). *Ventilation and air conditioning – Part 6: Ventilation for residential buildings – General requirements, requirements for measuring, performance and labeling, delivery/acceptance (certification) and maintenance* (pp. 125). Berlin, Germany: Deutsche Industrie Norm [German industry standard].
- [60] **Fanger, P. O.** (1972). *Thermal comfort: analysis and applications in environmental engineering*. New York, USA: McGraw-Hill.
- [61] **ISO 7730.** (2005). *Ergonomics of the thermal environment - Analytical determination and interpretation of thermal comfort using calculation of the PMV and PPD indices and local thermal comfort criteria*. Geneva, Switzerland: International Organization for Standardization.

- [62] **De Dear, R., Brager, G., & Cooper, D.** (1997). *Developing an Adaptive Model of Thermal Comfort and Preference* (Vol. Final report RP-884, pp. 297). Atlanta, USA: American society of heating, refrigerating and air-conditioning engineers. Retrieved from <http://www.cbe.berkeley.edu>
- [63] **ASHRAE Standard 55.** (2010). *Thermal Environmental Conditions for Human Occupancy*. Atlanta, USA: American Society of Heating, Refrigerating and Air-Conditioning Engineers.
- [64] **Cynthia, R.** (2012). *Guide to Setting Thermal Comfort Criteria and Minimizing Energy Use in Delivering Thermal Comfort* (Vol. LBNL-6131E, pp. 17). USA: Berkeley Lab. Retrieved from <http://eetd.lbl.gov/>
- [65] **Gratia, E., & De Herde, A.** (2004). Natural cooling strategies efficiency in an office building with a double-skin façade. *Energy and Buildings*, 36(11), 1139-1152. doi: 10.1016/j.enbuild.2004.05.004
- [66] **Froland-Larson, A., & Hagelskjær, S.** (2001). Energieverbrauch für Lüftung. [Energy consumption for ventilation]. *DANVAK journal*, 2.
- [67] **Walton, G. N.** (1989ff). *AIRNET A Computer Program for Building Airflow Network Modeling* [Multizone Airflow and Contaminant Transport Analysis Software]. Gaithersburg, USA: National Institute of Standards and Technology.
- [68] **Feustel, H. E.** (1999). COMIS - an international multizone air-flow and contaminant transport model. *Energy and Buildings*, 30(1), 3-18. doi: doi:10.1016/S0378-7788(98)00043-7
- [69] **Feustel, H. E., Raynor-Hoosen, A., Allard, F., Dorer, V. B., Feustel, H. E., Rodriguez Garcia, E., . . . Yoshino, H.** (1990). *Fundamentals of the Multizone Air Flow Model - COMIS*. In H. E. Feustel & A. Rayner-Hooson (Eds.), (Vol. Technical Note TN 29, pp. 115). Coventry, UK: AIVC. Retrieved from <http://www.aivc.org>
- [70] **Etheridge, D.** (2011). Steady Envelope Flow Models. In *Natural Ventilation of Buildings: Theory, Measurement and Design* (pp. 89-130): John Wiley & Sons, Ltd. doi: 10.1002/9781119951773.ch4
- [71] **Awbi, H. B.** (1996). Air movement in naturally-ventilated buildings. *Renewable Energy*, 8(1-4), 241-247. doi: 10.1016/0960-1481(96)88855-0
- [72] **Axley, J. W.** (2006). Analytical methods and computing tools for ventilation. In M. Santamouris & P. Wouters (Eds.), *Building Ventilation: The State of the Art* (pp. 39-49). London, UK: Earthscan.
- [73] **Heiselberg, P., Svidt, K., & Nielsen, P. V.** (2001). Characteristics of airflow from open windows. *Building and Environment*, 36(7), 859-869. doi: 10.1016/S0360-1323(01)00012-9
- [74] **Costola, D., & Etheridge, D. W.** (2008). Unsteady natural ventilation at model scale - Flow reversal and discharge coefficients of a short stack and an orifice. *Building and Environment*, 43(9), 1491-1506. doi: 10.1016/j.buildenv.2007.08.005
- [75] **Chiu, Y. H., & Etheridge, D. W.** (2007). External flow effects on the discharge coefficients of two types of ventilation opening. *Journal of Wind Engineering and Industrial Aerodynamics*, 95(4), 225-252. doi: 10.1016/j.jweia.2006.06.013
- [76] **Chu, C. R., Chiu, Y. H., & Wang, Y.-W.** (2010). An experimental study of wind-driven cross ventilation in partitioned buildings. *Energy and Buildings*, 42(5), 667-673. doi: 10.1016/j.enbuild.2009.11.004
- [77] **Schulze, T., & Eicker, U.** (2013). Controlled natural ventilation for energy efficient buildings. *Energy and Buildings*, 56(0), 221-232. doi: 10.1016/j.enbuild.2012.07.044

- [78] **Huang, J., Winkelmann, F., Buhl, F., Pedersen, C., Fisher, D., Liesen, R., . . . Lawrie, L.** (1999, September). *Linking The COMIS Multi-Zone Airflow Model With The EnergyPlus Building Energy Simulation Program*. Paper presented at the IBPSA Building Simulation, Kyoto, Japan. Paper retrieved from <http://www.ibpsa.org/>
- [79] **Hensen, J.** (1995, September). *Modelling coupled heat and airflow: ping pong versus onions*. Paper presented at the 16th AIVC Conference Palm Springs, USA. Paper retrieved from <http://www.strath.ac.uk/esru/>
- [80] **Wang, L., & Chen, Q.** (2008). Evaluation of some assumptions used in multizone airflow network models. *Building and Environment*, 43(10), 1671-1677. doi: 10.1016/j.buildenv.2007.10.010
- [81] **Johnson, M.-H. D.** (2010). *Assess and implement natural and hybrid ventilation models in whole-building energy simulations* (Master's thesis), University of Colorado, USA. Retrieved from ProQuest Dissertations and Theses database (UMI No. 1476951)
- [82] **Etheridge, D.** (2011). Computational Fluid Dynamics and its Applications. In *Natural Ventilation of Buildings: Theory, Measurement and Design* (pp. 257-291): John Wiley & Sons, Ltd. doi: 10.1002/9781119951773.ch9
- [83] **Sapian, A. R.** (2009). Validation of the Computational Fluid Dynamics (CFD) Method for Predicting Wind Flow Around a High-Rise Building (HRB) in an Urban Boundary Layer Condition. *Journal of Construction in Developing Countries*, 14(2), 1-20.
- [84] **Guha, T. K., Sharma, R. N., & Richards, P. J.** (2009, July). *CFD modeling of wind induced mean and fluctuating external pressure coefficients on the Texas Technical University building*. Paper presented at the 5th European & African Conference on Wind Engineering, Florence, Italy. Paper retrieved from <http://www.iawe.org/>
- [85] **Santamouris, M., & Argiriou, A.** (1997). Passive Cooling of Buildings - Results of the PASCOOL Program. *International Journal of Solar Energy*, 19(1-3), 3-19. doi: 10.1080/01425919708914328
- [86] **Flourentzou, F., Maas, J. V. d., & Roulet, C.-A.** (1996). *LESOCOOL* (Version 1996) [ventilative cooling potential assessment tool]. Lausanne, Switzerland: Ecole polytechnique fédérale de Lausanne. Retrieved from <http://leso.epfl.ch/lesocool>
- [87] **Grosso, M.** (1992). *CpCalc+* [calculation of wind pressure coefficients on buildings]. Turin, Italy: PASCOOL Research Programme.
- [88] **IEA-ECBCS Annex 28.** (1995). *Review of Low Energy Technologies Low Energy Cooling*, Anonymous (Ed.) *Subtask 1* (pp. 90). Retrieved from <http://www.ecbcs.org/>
- [89] **IEA-ECBCS Annex 28.** (2001). *Technical Synthesis Report Low Energy Cooling*, M. W. Liddament (Ed.) (pp. 32). Retrieved from <http://www.ecbcs.org/>
- [90] **IEA-ECBCS Annex 28.** (2001). *Design Tools: Technology Selection and Early Design Guidance Low Energy Cooling*, N. Barnard & D. Jaunzens (Eds.), *Subtask 2* (pp. 50). Retrieved from <http://www.ecbcs.org/>
- [91] **IEA-ECBCS Annex 28.** (2000). *Detailed Design Tools Low Energy Cooling*, H. Roel (Ed.) *Subtask 2* (pp. 200). Retrieved from <http://www.ecbcs.org/>
- [92] **ASHRAE.** (1985). Natural ventilation and infiltration. In: *Handbook of Fundamentals*. Atlanta, USA: American Society of Heating, Refrigerating and Air-Conditioning Engineers.

- [93] **Aynsley, R. M., Melbourne, W. H., & Vickery, B. J.** (1977). *Architectural aerodynamics*. London, UK: Applied Science Publishers.
- [94] **De Gids, W., & Phaff, H.** (1982). Ventilation rates and energy consumption due to open windows: a brief overview of research in the Netherlands. *Air Infiltration Review*, 4(1), 4-5.
- [95] **Givoni, B.** (1976). *Man, climate and architecture*. Architectural Science (2nd ed.). London, UK: Applied Science Publishers.
- [96] **Melaragno, M. G.** (1982). *Wind in architectural and environmental design*. New York, USA: Van Nostrand Reinhold Co.
- [97] **Gandemer, J.** (Ed.). (1992). *Guide sur la climatisation naturelle de l'habitat en climat tropical humide - tome 1: Méthodologie de prise en compte des paramètres climatique dans l'habitat et conseils pratiques*. Paris, France: CSTB.
- [98] **Ernest, D.** (1991). *Predicting Wind-induced Indoor Air Motion, Occupant Comfort, and Cooling Loads in Naturally Ventilated Buildings* (Doctoral dissertation), University of California, Berkeley, USA.
- [99] **Dascalaki, E., Santamouris, M., Argiriou, A., Helmis, C., Asimakopoulos, D. N., Papadopoulos, K., & Soilemes, A.** (1995). Predicting single sided natural ventilation rates in buildings. *Solar Energy*, 55(5), 327-341.
doi: 10.1016/0038-092x(95)00057-x
- [100] **Liddament, M. W.** (1986). *Air Infiltration Calculation Techniques: An Applications Guide* Retrieved from <http://www.aivc.org/>
- [101] **Chandra, S., Fairey, P. W., & Houston, M. M.** (1986). *Cooling with Ventilation* Solar Technical Information Program. Colorado, USA: Solar Energy Research Institute. Retrieved from <http://www.fsec.ucf.edu/>
- [102] **Chandra, S., Fairey, P. W., & Houston, M.** (1983). *A Handbook for Designing Ventilated Buildings: Final Report*. Cape Canaveral: Florida Solar Energy Center.
- [103] **Lee, B. E., Hussain, M., & Soliman, B. F.** (1980). Predicting natural ventilation forces upon low-rise buildings. *ASHRAE Journal*, 22(2), 35-39.
- [104] **Aggerholm, S.** (1998). *Perceived Barriers to Natural Ventilation Design of Office Buildings* NatVent - Overcoming technical barriers to low-energy natural ventilation in office type buildings in moderate and cold climates, Vol. WP1. *European Report* (pp. 25). Retrieved from <http://projects.bre.co.uk/natvent/>
- [105] **De Gids, W. F.** (1997). *Controlled air flow inlets* NatVent - Overcoming technical barriers to low-energy natural ventilation in office type buildings in moderate and cold climates, Vol. WP3 Act2. *An overview of the availability, performance and application of inlets for natural supply of ventilation air and the consequences on indoor air quality and comfort* (pp. 21). Retrieved from <http://projects.bre.co.uk/natvent/>
- [106] **Van Paassen, A. H. C., Broekhuizen, H. F., & Verwaal, M.** (1998). *Prototype of Night Ventilator for Cooling* NatVent - Overcoming technical barriers to low-energy natural ventilation in office type buildings in moderate and cold climates, Vol. WP3 Act4. *Smart Components and Intelligent Night Cooling* Retrieved from <http://projects.bre.co.uk/natvent/>
- [107] **Van Paassen, A. H. C., & van Galen, P. J. M.** (1995, August). *Rules for cooling through motorised vent windows*. Paper presented at the 19th International Congress of Refrigeration, Den Haag, Netherlands. Paper retrieved from <http://www.aivc.org/>

- [108] **Kolokotroni, M., Tindale, A., & Irving, S. J.** (1997, September). *NiteCool: Office Night Ventilation Pre-Design Tool*. Paper presented at the 18th AIVC Conference 'Ventilation and Cooling', Athens, Greece. Paper retrieved from <http://www.aivc.org/>
- [109] **Tindale, A.** (1993). Third-order lumped-parameter simulation method. *Building Services Engineering Research and Technology*, 14(3), 87-97. doi: 10.1177/014362449301400302
- [110] **CIBSE.** (1982). A2 Weather and Solar Data. In: *CIBSE Guide*. London, UK: Chartered Institute of Building Services Engineers.
- [111] **Irving, S. J., Concannon, P. J., & Dhargalkar, H. S.** (1995). *Sizing and location of passive ventilation openings* ETSU report (Vol. S/N5/00142, pp. 37). St. Albans, UK: Oscar Faber Applied Research.
- [112] **Irving, S. J., Concannon, P. J., & Dhargalkar, H. S.** (1995, October). *An Inverse Solver for Sizing Passive Ventilation Openings*. Paper presented at the CIBSE National Conference '95, Eastbourne, UK.
- [113] **AIVC (Ed.).** (1996). *A Guide to Energy Efficient Ventilation*. Coventry, UK: Air infiltration and Ventilation Centre.
- [114] **Santamouris, M., & Wouters, P.** (2006). *Building Ventilation: The State Of The Art*. (P. Wouters Ed.). London, UK: Earthscan.
- [115] **IEA-ECBCS Annex 35.** (2002). *The use of simulation tools to evaluate hybrid ventilation control strategies* Hybrid Ventilation in New and Retrofitted Office Buildings, A. Delsante & S. Aggerholm (Eds.), *Technical Report* (pp. 63). Retrieved from <http://www.hybvent.civil.aau.dk/>
- [116] **IEA-ECBCS Annex 35.** (2002). *Hybrid Ventilation and Control Strategies in the Annex 35 Case Studies* Hybrid Ventilation in New and Retrofitted Office Buildings, S. Aggerholm (Ed.) *Technical Report* (pp. 31). Retrieved from <http://www.hybvent.civil.aau.dk/>
- [117] **IEA-ECBCS Annex 35.** (2002). *Advanced Control Strategy* Hybrid Ventilation in New and Retrofitted Office Buildings, P. Michel & M. El Mankibi (Eds.), *Technical Report* (pp. 11). Retrieved from <http://www.hybvent.civil.aau.dk/>
- [118] **IEA-ECBCS Annex 35.** (2002). *A Simple Tool to Assess the Feasibility of Hybrid Ventilation Systems* Hybrid Ventilation in New and Retrofitted Office Buildings, G. V. Fracastoro, M. Perino & G. Mutani (Eds.), *Technical Report* (pp. 18). Retrieved from <http://www.hybvent.civil.aau.dk/>
- [119] **Crawley, D. B.** (1998). *Which Weather Data Should You Use for Energy Simulations of Commercial Buildings?* ASHRAE Transactions (Vol. 104-2, pp. 18). Atlanta, USA: American Society of Heating, Refrigerating and Air-Conditioning Engineers. Retrieved from <http://apps1.eere.energy.gov/>
- [120] **Building Research Establishment.** (1978). *Principles of Natural Ventilation*. (Vol. Digest 210). London, UK: BRE Ltd.
- [121] **Schulze, T., Eicker, U., & Yilmaz, Z.** (2013, October). *A simplified calculation methodology for controlled natural ventilation*. Paper presented at the Climamed, Istanbul, Turkey. Paper retrieved from <http://www.climamed.org/>
- [122] **EnergyPlus** (Version 8.1). (2013). *Engineering Reference* The Reference to EnergyPlus Calculations (pp. 1399). Washington DC, USA: U. S. Department of Energy. Retrieved from <http://apps1.eere.energy.gov/>
- [123] **EngineeringToolBox.** (n.d.). Density of Dry Air, Water Vapor and Moist Humid Air. Retrieved April, 2013, from http://www.engineeringtoolbox.com/density-air-d_680.html

- [124] **EngineeringToolBox**. (n.d.). Air Pressure and Altitude above Sea Level. Retrieved April, 2013, from http://www.engineeringtoolbox.com/air-altitude-pressure-d_462.html
- [125] **Aynsley, R. M.** (1997). A resistance approach to analysis of natural ventilation airflow networks. *Journal of Wind Engineering and Industrial Aerodynamics*, 67–68(0), 711-719. doi: 10.1016/S0167-6105(97)00112-8
- [126] **Atkinson, J. J.** (1886). *A Practical Treatise on the Gases Met with in Coal Mines and the General Principles of Ventilation*. Newcastle-upon-Tyne, UK: Andrew Reid.
- [127] **Yazdani, M., & Klems, J. H.** (1993). *Measurement of the exterior convective film coefficient for windows in low-rise buildings* ASHRAE Transactions (Vol. 100-1, pp. 19). Atlanta, USA: American Society of Heating, Refrigerating and Air-Conditioning Engineers. Retrieved from <http://btech.lbl.gov/>
- [128] **EnergyPlus** (Version 8.1). (2013). *Input Output Reference* The Encyclopedic Reference to EnergyPlus Input and Output (pp. 2147). Washington, DC: U. S. Department of Energy. Retrieved from <http://apps1.eere.energy.gov/>
- [129] **Martinez, D., Fiala, D., Cook, M. J., & Lomas, K. J.** (2000, July). *Predicted comfort envelopes for office buildings with passive downdraught evaporative cooling*. Paper presented at the 7th International Conference on Air Distribution in Rooms (RoomVent), Reading, UK. Paper retrieved from <http://www.reading.ac.uk/rv2000/>
- [130] **Gu, L.** (2007, September). *Airflow network modeling in EnergyPlus*. Paper presented at the IBPSA - Building Simulation, Beijing, China. Paper retrieved from <http://www.ibpsa.org/>
- [131] **EnergyPlus** (Version 8.1). (2012). *Application Guide for EMS - Energy Management System User Guide* Energy Management System User Guide (pp. 96). Washington DC, USA: U. S. Department of Energy. Retrieved from <http://apps1.eere.energy.gov/>
- [132] **Maile, T., Fischer, M., & Bazjanac, V.** (2007). *Building Energy Performance Simulation Tools a Life-Cycle and Interoperable Perspective* (Vol. Working Paper #WP107). Stanford University, USA: Center for Integrated Facility Engineering. Retrieved from <http://cife.stanford.edu/>
- [133] **Le Dréau, J., Heiselberg, P., & Jensen, R. L.** (2013). Experimental investigation of convective heat transfer during night cooling with different ventilation systems and surface emissivities. *Energy and Buildings*, 61(0), 308-317. doi: 10.1016/j.enbuild.2013.02.021
- [134] **Leenknecht, S., Wagemakers, R., Bosschaerts, W., & Saelens, D.** (2012). Numerical sensitivity study of transient surface convection during night cooling. *Energy and Buildings*, 53(0), 85-95. doi: 10.1016/j.enbuild.2012.06.020
- [135] **Artmann, N., Manz, H., & Heiselberg, P.** (2008). Parameter study on performance of building cooling by night-time ventilation. *Renewable Energy*, 33(12), 2589-2598. doi: 10.1016/j.renene.2008.02.025
- [136] **Walton, G. N.** (1983). *TARP Reference manual* Thermal analysis research program (Vol. NBSIR, 83-2655, pp. 277). Washington DC, USA: U.S. Dept. of Commerce, National Bureau of Standards.
- [137] **Crawley, D. B., Lawrie, L. K., Winkelmann, F. C., Buhl, W. F., Huang, Y. J., Pedersen, C. O., . . . Glazer, J.** (2001). EnergyPlus: creating a new-generation building energy simulation program. *Energy and Buildings*, 33(4), 319-331. doi: 10.1016/S0378-7788(00)00114-6

- [138] **Fritsche, U. R., & Schmidt, K.** (2014). *GEMIS Global Emission Model for Integrated Systems* (Version 4.93) [public domain life-cycle and material flow analysis model]. Darmstadt, Germany: Öko-Institut e.V. [Institute for Applied Ecology]. Retrieved from <http://www.iinas.org/>
- [139] **Wilkins, C. K., & Hosni, M. H.** (2000). Heat gain from office equipment. *ASHRAE Journal*, 42(6), 33-44.
- [140] **Peel, M. C., Finlayson, B. L., & McMahon, T. A.** (2007). Updated world map of the Köppen-Geiger climate classification. *Hydrology and Earth System Sciences*, 11(5), 1633-1644. doi: 10.5194/hess-11-1633-2007
- [141] **ASHRAE.** (n.d.). International Weather for Energy Calculations (IWEC Weather Files). Retrieved March, 2011, from http://apps1.eere.energy.gov/buildings/energyplus/weatherdata_about.cfm
- [142] **ASHRAE Standard 90.1.** (2007). *Energy Standard for Buildings Except Low-rise Residential Buildings*. Atlanta, USA: American society of heating, refrigerating and air-conditioning engineers.
- [143] **Richard J. de Dear, G. S. B.** (2002). Thermal comfort in naturally ventilated buildings: revisions to ASHRAE Standard 55. *Energy and Buildings*, 34(6), 549-561. doi: 10.1016/S0378-7788(02)00005-1
- [144] **EN ISO 13786.** (2007). *Thermal performance of building components - Dynamic thermal characteristics - Calculation methods*. Brussels, Belgium: European Committee for Standardization.
- [145] **Häupl, P., Homann, M., Kölzow, C., Riese, O., Maas, A., Höfker, G., . . . Willems, W.** (2012). *Lehrbuch Der Bauphysik* [Manual of Building Physics] Schall - Wärme - Feuchte - Licht - Brand - Klima (7 ed., pp. 830). Wiesbaden, Germany: Springer Fachmedien.
- [146] **Capros, P., Mantzos, L., Papandreou, V., & Tasios, N.** (2008). *European energy and transport Trends to 2030* (Vol. Update 2007, pp. 156). Luxembourg: Office for Official Publications of the European Communities. Retrieved from <http://bookshop.europa.eu/>

APPENDICES

APPENDIX A: Wind Tunnel Measurements

APPENDIX B: 'HighVent' Tool Detailed Calculations

APPENDIX A: Wind Tunnel Measurements

	<u>Page</u>
A.1 Introduction	260
A.2 Lab Setup	262
A.2.1 Wind tunnel unit	262
A.2.2 Measuring Instruments	263
A.3 Kanyon Model	266
A.4 Results	267
A.5 Discussion	270
References Appendix A	271

Nomenclature

C	: coefficient	dimensionless
p	: pressure	Pa
v	: velocity	m s ⁻¹
ρ	: density	kg m ⁻³

Subscripts

p	: pressure
w	: wind
z	: local height from start height
∞	: free stream region without any disturbance

A.1 Introduction

A wind tunnel is a tool used in aerodynamic research. It is used to study the effects of air moving past solid objects. Measurements are often carried out to study the pressure distribution at certain points of structures.

In building science, wind tunnel tests are a reliable method (e.g., [1]) for estimating wind pressure coefficients of complex buildings. Wind pressure coefficients are non-dimensional and therefore can be used in the design of natural ventilation systems for any wind speed.

The relationship between the dimensionless coefficient and the measured dimensional numbers without simulating the atmospheric boundary layer (wind profile depending on the terrain roughness) simply is [2]:

$$C_p = \frac{p}{p_\infty} \quad (\text{A.1})$$

Tests were carried out for the Kanyon building modelled with a scale of 1:300 at 98 points of the building façade structure. The points correspond to fourteen nodes on each storey, one node for each façade orientation, and on seven different storey levels. Besides the Kanyon building, adjacent buildings were also modelled to include their possible local shielding effect. The measurements were repeated for eight wind directions.

The aim of the experiment is to pre-process C_p data as an input for the developed ‘HighVent’ design tool and for dynamic AFN simulations with EnergyPlus. As stated before, the atmospheric boundary layer reflecting the terrain roughness is not simulated in the wind tunnel tests, but is added in the subsequent analysis tools. In those tools, the local pressure is dependent on the wind speed at local height and may be estimated by:

$$p_w = 0,5 \cdot \rho_{\text{air}} \cdot v_z^2 \quad (\text{A.2})$$

A.2 Lab Setup

The wind tunnel studies were realised in the Physical Environment Control Laboratory of the architectural faculty at the Istanbul Technical University under supervision of Prof. Vildan Ok. The laboratory is further supported by the mechanical engineering faculty.

A.2.1 Wind tunnel unit

The wind tunnel is an open (without return duct), sub sonic (low speed), suction tunnel with a closed test section. This so called jet Eiffel type has a total length of 12,55 m.



Figure A.1: Wind tunnel air inlet.

Figure A.2: View from the wind tunnel inside (from narrowing square down).

Figure A.3: Wind tunnel air outlet and fan.

The incoming air is introduced in the tunnel by a large bell shaped opening with dimensions of $2,50 \cdot 2,50 \cdot 0,30$ m, followed by a flow shaping module with dimensions of $2,00 \cdot 2,00 \cdot 0,92$ m. An adaptor with 1,30 m in length connects this inlet part to the observation module by a narrowing square from $2,00 \cdot 2,00$ m to $1,05 \cdot 1,05$ m in section.

The test section has dimensions of $1,00 \cdot 1,00 \cdot 3,00$ m. The side parts are made of acrylic glass and the horizontal surfaces of fibreboard.

The diffuser part behind the test section is 5,96 m in length, passing the air stream from the observation room in square section to a circular section with 1,64 m in diameter. At the very end of the tunnel, a fan is attached with a blade radius of 0,52 m. The axial fan's maximum power is 4 kW with a rotor speed of 2 905 rpm.

The placement of the wind tunnel in the laboratory is shown in plan and in section in Figure A.4 and Figure A.5.

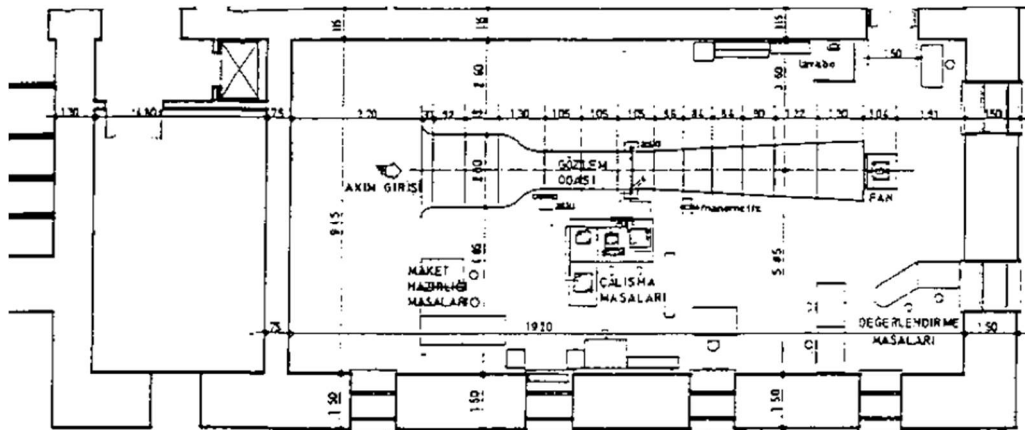


Figure A.4: I.T.U. Arch. Fac. Phy. Env. Cont. Lab. wind tunnel unit layout in plan.

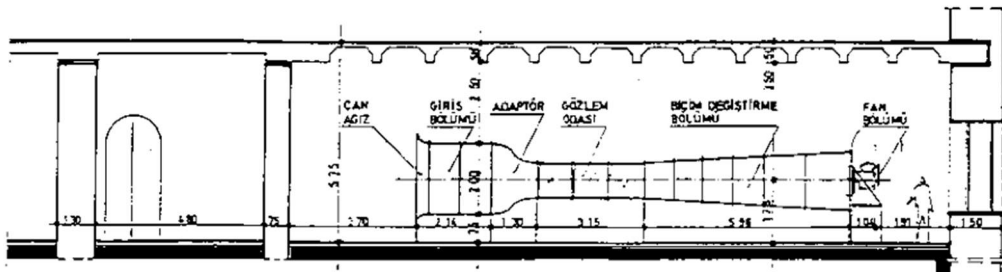


Figure A.5: I.T.U. Arch. Fac. Phy. Env. Cont. Lab. wind tunnel unit layout in section.

A.2.2 Measuring Instruments

The different instruments used for the measurements are described in detail below. Figure A.6 gives an overview of the measurement unit.

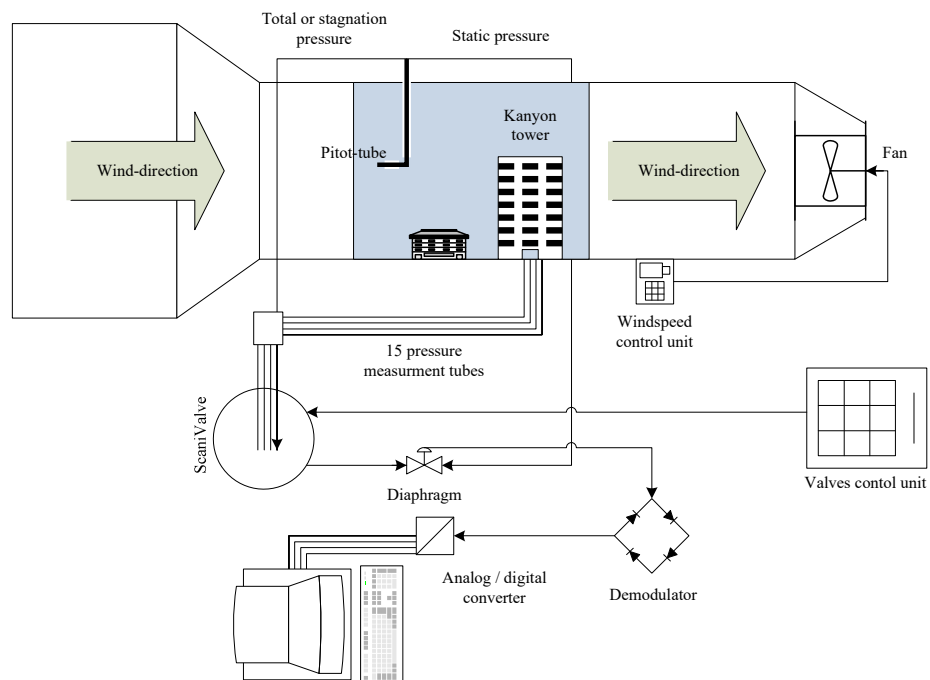


Figure A.6: Schematic measuring station layout (not true to scale).

Pitot-tube

A Pitot-tube is a pressure measurement instrument used to measure fluid pressure and flow velocity. The basic Pitot-tube simply consists of a tube pointing directly into the fluid flow. As this tube contains air, a pressure can be measured as the moving air is brought to rest. This pressure is the stagnation pressure of the air, also known as the total pressure.

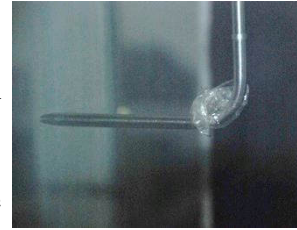


Figure A.7: Pitot-Tube.

The measured stagnation pressure cannot of itself be used to determine the dynamic pressure. But since Bernoulli's equation states that the stagnation pressure is the sum of static pressure and the dynamic pressure, the dynamic pressure can simply be derived by the difference between the stagnation pressure and the static pressure.

Diaphragm

The diaphragm pressure gauge uses the elastic deformation of a diaphragm (membrane) to measure the difference between an unknown pressure and a reference pressure.



Figure A.8: Diaphragm.

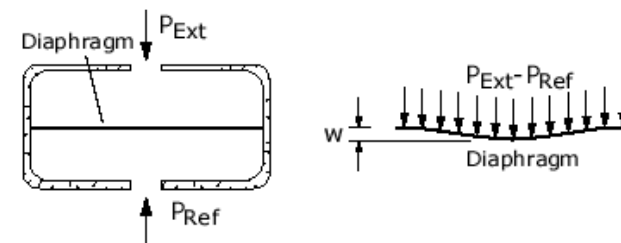


Figure A.9: Typical diaphragm pressure gauge.

A typical diaphragm pressure gauge contains a capsule divided by a diaphragm, as shown in Figure A.9. One side of the diaphragm is open to the external targeted pressure and the other side is connected to a known reference pressure. The pressure difference mechanically deflects the diaphragm.

Demodulator

Demodulation is the act of extracting the original information-bearing signal from a modulated carrier wave. The demodulator is an electronic circuit used to recover the information content from the modulated carrier wave.



Figure A.10: Demodulator.

Wind speed control unit

The wind speed control system is designed to control the wind speed in the wind tunnel. In this project, all tests are carried out keeping constant wind tunnel speed. As recommended from the staff also concerning the Reynolds Numbers, a good value for the measurements is 40% of the fan power, which corresponds to 6,6 m/s.



Figure A.11: Fan Control-Unit.

Valve control unit

This rather old control unit opens the 16 valves in the ScaniValv one by one in an interval of 5 or 10 seconds. 10 seconds was used in the experiment in order to provide enough time to average the pressure data for 5 seconds and also to manually control the software in synchronic.



Figure A.12: Valves control unit.

Analogue / digital converter

This converts the analogue electronic signal from the demodulator output to a digital signal for the computer input.



Figure A.13: Valves control unit.

ScaniValve

This tube pressure input control unit opens one out of the 16 input tubes coming from within the wind tunnel. This makes it possible to measure the pressures in a row one by one. The opened tube pressure output is sent to the diaphragm. One of the 16 pressure inputs is the total pressure measured by the Pitot-tube, and is used for the calibration of the diaphragm. The valves are controlled by the valve control unit.



Figure A.14: ScaniValve.

Computer

The PC acts as a digital interface for data collection and for data post processing, e.g. in ‘Matlab’ or ‘MS Excel’. Consequently, the computer is the last unit in the breadboard construction used for data processing and imaging.

A.3 Kanyon Model

The model was built in a scale of 1:300. For the modelling of the site including the tower, original ‘AutoCAD’ drawings were used. The neighbouring buildings were approximately modelled according to information from ‘Google Maps’ and from photos.

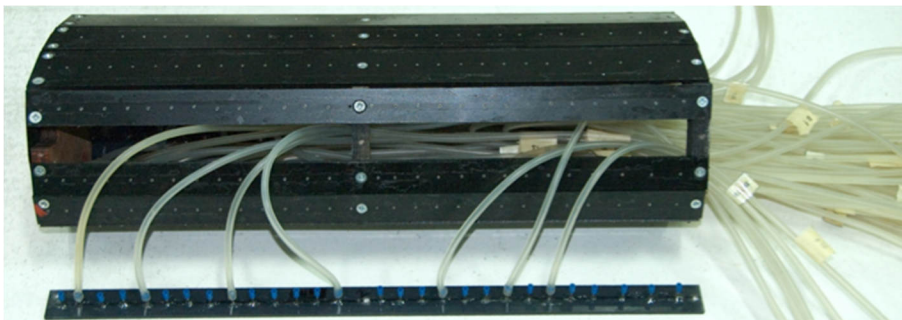


Figure A-15: The model of the tower including the measurement points and tubes.

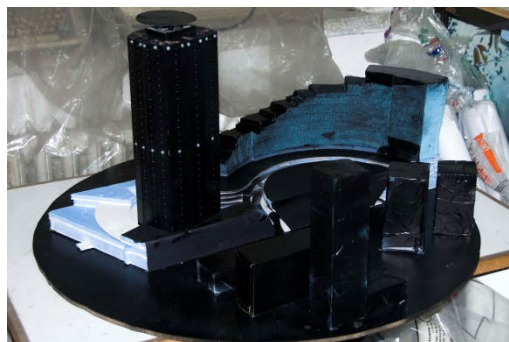


Figure A.16: Constructing the Kanyon site model on a turntable plate.

During the measurement the model was turned in 45° steps according to the wind directions north, northeast, east, southeast, south, southwest, west and northwest.

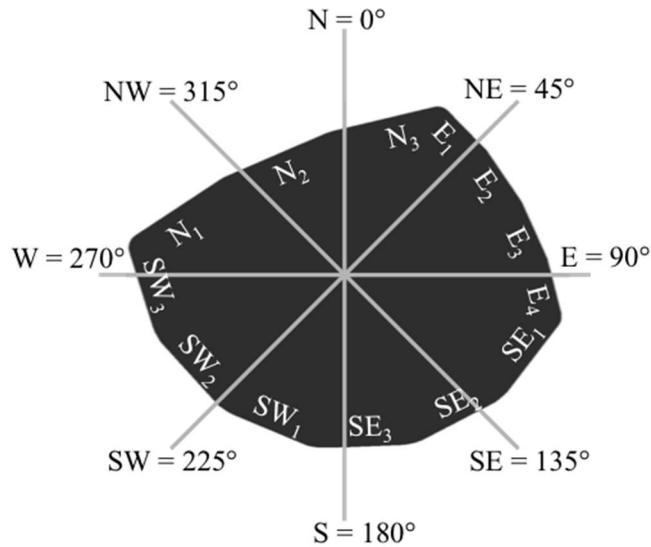


Figure A.17: Kanyon floor plan and façade orientations pertaining to the measured wind directions.

A.4 Results

The resulting wind pressure coefficient data gathered from the measurements is shown in the figures below. The coloured values indicate the wind direction, as positive values are measured at the windward side and negative values at the leeward side and the side faces. The values of the highest floor measured (at 117 m) are not coloured as they are of unpredictable nature, most probably due to the heliport modelled on the roof and local turbulences.

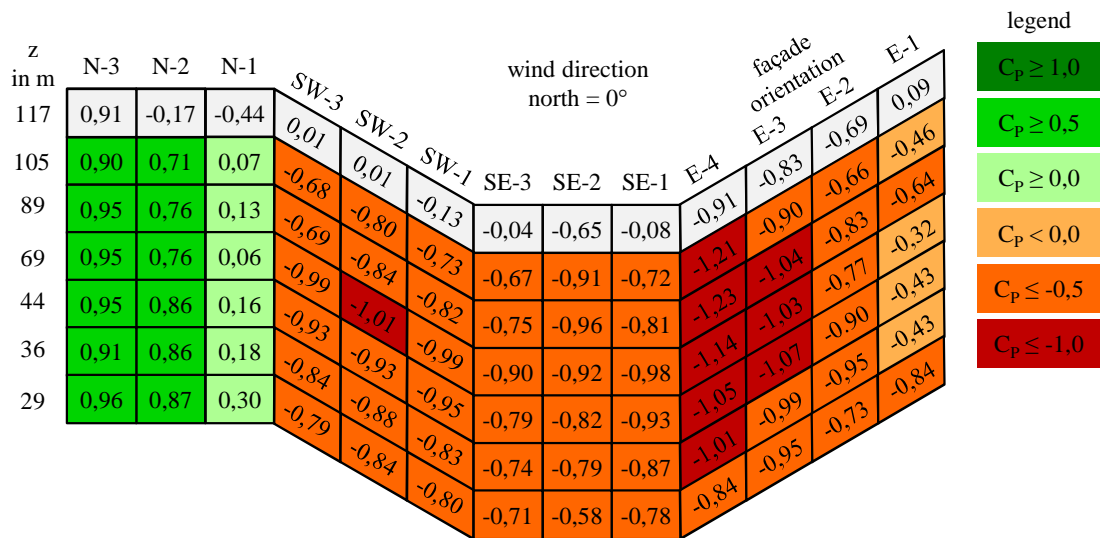


Figure A.18: Pressure coefficients measured at 0° (north) wind direction.

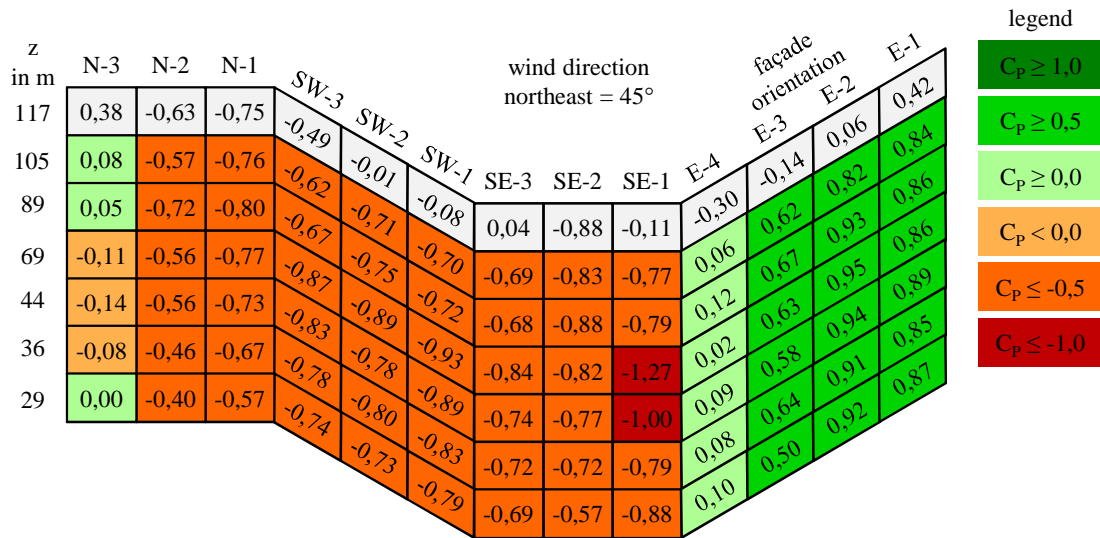


Figure A.19: Pressure coefficients measured at 45° (northeast) wind direction.

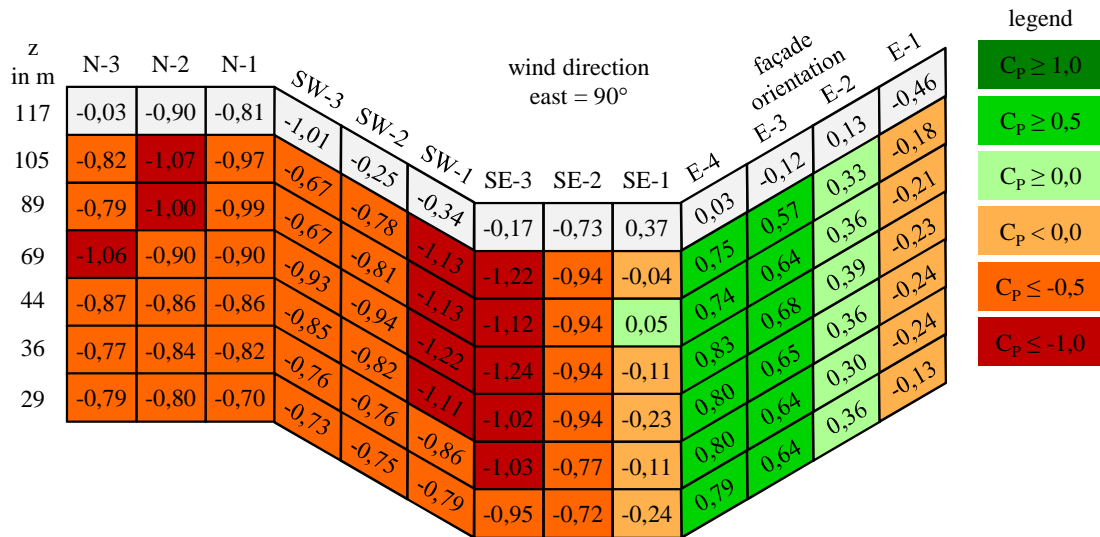


Figure A.20: Pressure coefficients measured at 90° (east) wind direction.

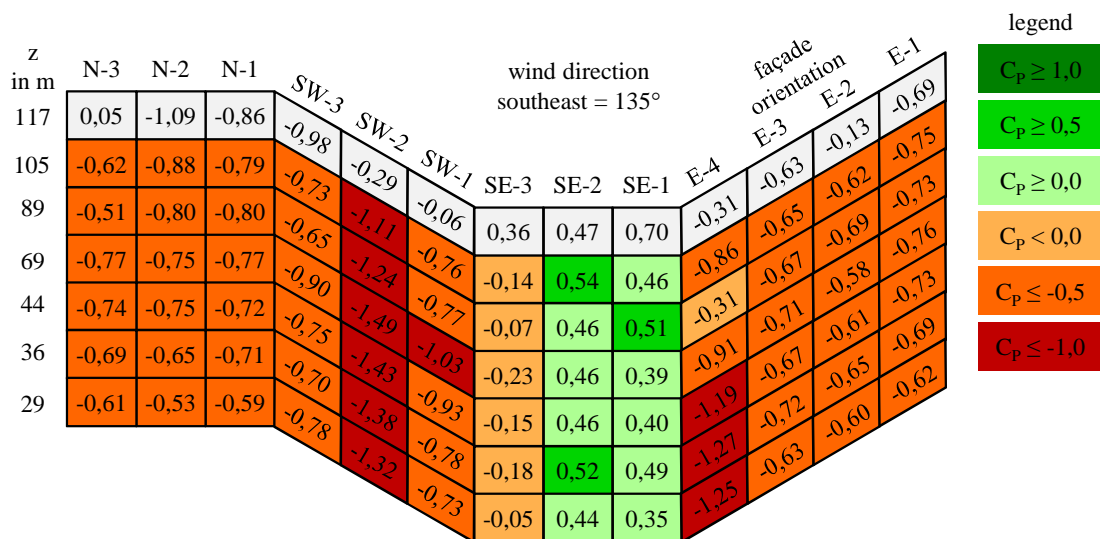


Figure A.21: Pressure coefficients measured at 135° (southeast) wind direction.

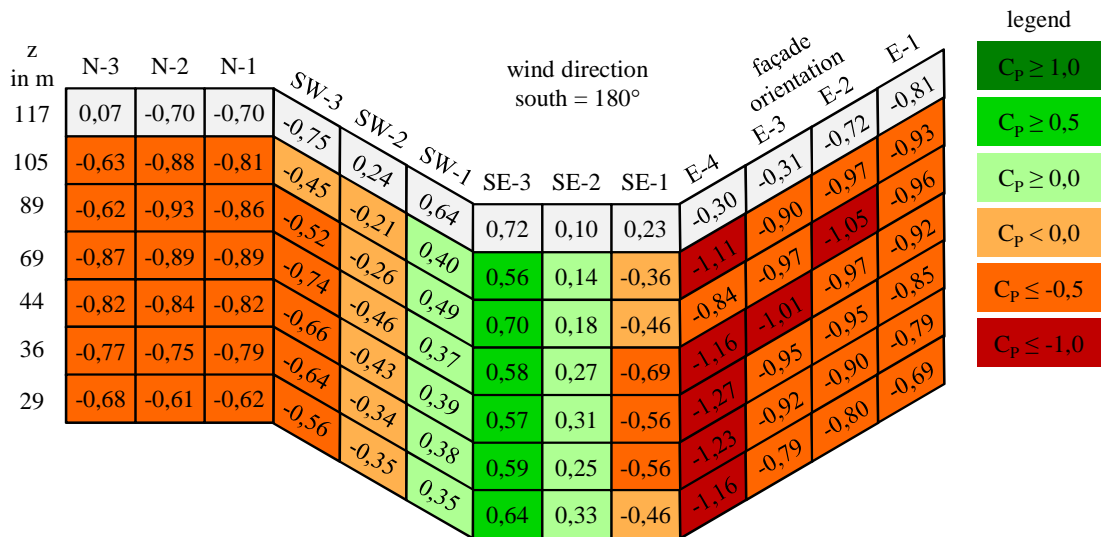


Figure A.22: Pressure coefficients measured at 180° (south) wind direction.

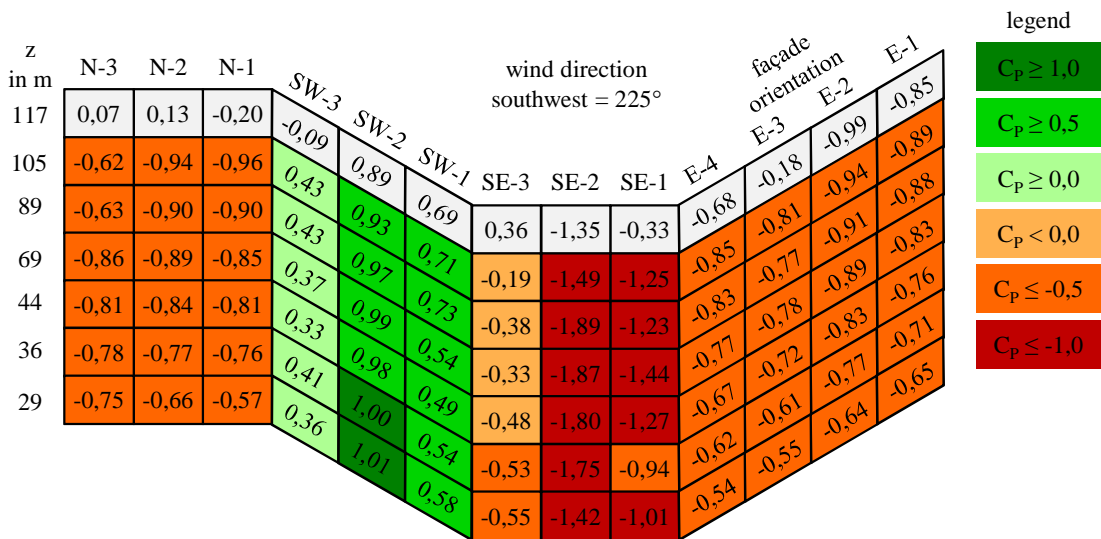


Figure A.23: Pressure coefficients measured at 225° (southwest) wind direction.

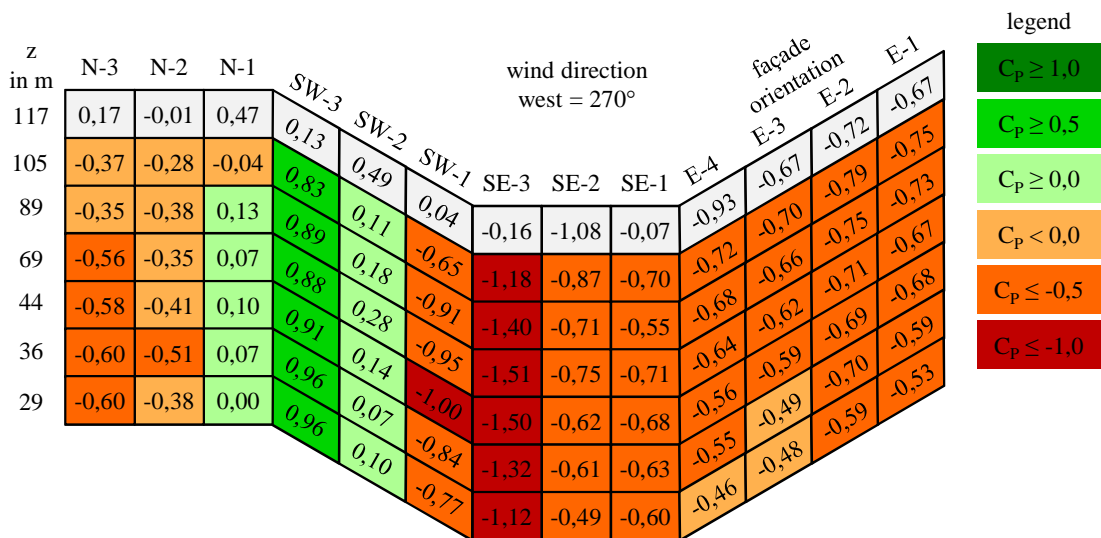


Figure A.24: Pressure coefficients measured at 270° (west) wind direction.

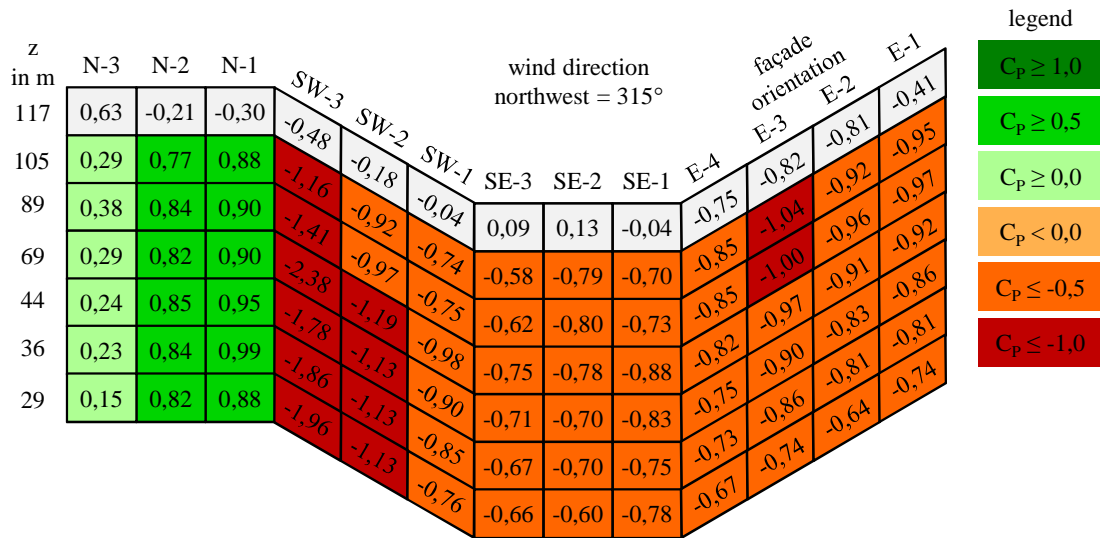


Figure A.25: Pressure coefficients measured at 315° (northwest) wind direction.

A.5 Discussion

As predicted, the wind striking the building induces a positive pressure on the windward face, and negative pressures on opposing faces and in the wake region of the side faces.

Average C_p value for the windward facing façade orientations is 0,70, and -0,76 for the opposite leeward facing façade orientations. The average here refers to mean value over the height of the building (29-105 m) of the two façade orientations closest facing the wind direction and the counterpart on the leeward side, respectively. Dependent on the wind direction, these C_p values fluctuate from 0,49 to 0,89 and from -0,60 to -0,82, respectively.

The negative values of C_p in the wake region of the side faces are even lower with average values over height from -0,92 to -1,76, depending on the wind direction.

Except in the region close to the roof, the C_p values measured are relatively consistent over the height of the building, at least at heights from above 29 m up to 105 m. Surrounding buildings therefore seem to have minor shielding influence on the wind pressure distribution.

As a limitation, it should be mentioned that the pressure distribution close to the roof and the ground would need further investigation in order to see if it is of special interest. This study did not further investigate the roof and ground regions of the building, as they are not of special interest for the natural ventilation design developed.

The derived pressure coefficients are further used as input for the ‘HighVent’ design tool developed and for the dynamic AFN-simulations with EnergyPlus.

References Appendix A

- [1] **Surry, D.** (1991). Pressure measurements on the Texas tech building: Wind tunnel measurements and comparisons with full scale. *Journal of Wind Engineering and Industrial Aerodynamics*, 38(2–3), 235-247. doi: 10.1016/0167-6105(91)90044-W
- [2] **Aynsley, R. M., Melbourne, W. H., & Vickery, B. J.** (1977). *Architectural aerodynamics*. London, UK: Applied Science Publishers.

APPENDIX B: ‘HighVent’ Tool Detailed Calculations

	<u>Page</u>
B.1 Introduction	273
B.2 Internal Air Model.....	274
B.3 Heat Transfer Models.....	276
B.3.1 Convection.....	276
B.3.2 Thermal radiation	277
B.3.3 Solar radiation	279
B.3.4 Internal gains	282
B.3.5 Thermal mass	283
B.3.6 Natural ventilation.....	287
B.4 Transmitted Solar Heat	288
B.5 Building Constructions Library.....	289
B.5.1 Floor / ceiling	289
B.5.2 External wall.....	290
B.5.3 Internal partitions	290
References Appendix B.....	292

Nomenclature

A	: area	m^2
c	: specific heat capacity	$J\ kg^{-1}\ K^{-1}$
C	: thermal capacity	$J\ K^{-1}$
d	: thickness	m
F	: thermal radiation view factor	-
h	: heat transfer coefficient	$W\ m^{-2}\ K^{-1}$
H	: enthalpy	$J\ kg^{-1}$
HR	: humidity ratio	kg water per kg air
k	: thermal conductivity	$W\ m^{-1}\ K^{-1}$
\dot{m}	: mass flow	$kg\ s^{-1}$
q	: heat flux	$J\ m^{-2}$
\dot{q}	: heat flux rate	$W\ m^{-2}$
Q	: heat transfer rate	$J/\Delta t = J/60s$
R	: thermal resistance	$m^2\ W\ K^{-1}$
SHGC	: solar heat gain coefficient	dimensionless
t	: actual timestep	-
t-1	: previous timestep	-
T	: temperature	$^{\circ}C$
U	: U-value of a construction	$W\ m^{-2}\ K^{-1}$
V	: volume	m^3
v	: velocity	$m\ s^{-1}$
\dot{V}	: volume flow	$m^3\ s^{-1}$
α	: absorptivity	dimensionless
ϵ	: emissivity	dimensionless
σ	: Stefan-Boltzmann constant, which equals to $5,67 \cdot 10^{-8}$	$W\ m^{-2}\ K^{-4}$
ρ	: density	$kg\ m^{-3}$

τ	: time constant	s
τ	: window solar transmittance at normal incidence	dimensionless

Subscripts

%	: faction
c	: convection
chi	: exhaust chimney
cell	: zone modelled in the tool
dif	: diffuse radiation share
dir	: direct radiation share
ext	: external
fab	: fabric = all internal mass objects
i	: thermal mass layer number placeholder
in	: Internal air
int	: internal gains
m	: additional thermal mass
mr	: mean radiant
r	: radiation
s	: surface
se	: surface external
si	: surface internal
sol	: solar
v	: ventilation
wi	: winter
win	: window
su	: summer
z	: local height from start height
τ	: window transmitted radiation
∞	: facing surfaces
→	: radiation emitted or reflected
←	: radiation absorbed
↔	: radiative heat exchange

B.1 Introduction

Appendix B gives supplementary information about the ‘HighVent’ tool underlying dynamic calculation method, which is not fully covered in the preliminary design tool development Section § 6.2. It provides pre-simulated solar transmitted heat gains for different shading configurations according to § 6.1.2, which are used as scheduled input for the tool. The building construction library provides lumped capacity model constructions with different levels of mass according to § 6.1.3.

B.2 Internal Air Model

The dynamic internal air temperature calculated by:

$$T_{in}(t) = T_{in}(t-1) + \frac{\dot{Q}_{c,int}(t-1) + \dot{Q}_{c,fab}(t-1) + \dot{Q}_v(t-1)}{C_{in}(t-1)} \cdot \Delta t \quad (B.1)$$

where (t-1) indicates the value from the previous timestep ($\Delta t = 60$ s). The volumetric heat capacity of the cell's air is calculated by:

$$C_{in}(t) = V_{cell} \cdot \rho_{in}(t) \cdot c_{air} \quad (B.2)$$

The chimney air temperature is optionally increased by heat gains from IT or solar.

The density of the internal moist air is calculated similar to the method described in § 3.2.1.1. For simplicity of the model, it is assumed that the humidity ratio of the external air (scheduled design day input) is equal to the humidity ratio of the internal air (only sensible internal heat gains).

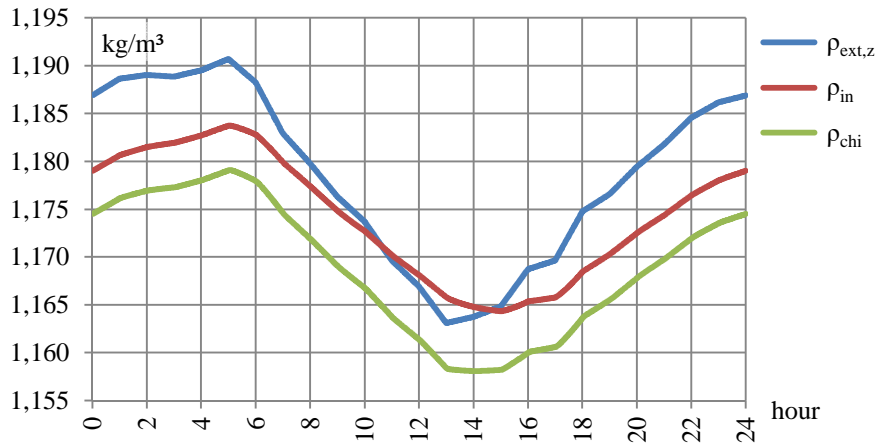


Figure B.1: Typical external, internal and chimney moist air densities.

The total convective heat gain rate from all internal sources to the cell air is:

$$\dot{Q}_{c,int}(t) = \dot{Q}_{c,peop}(t) + \dot{Q}_{c,light}(t) + \dot{Q}_{c,equip}(t) \quad (B.3)$$

The convective heat transfer rate from all internal surfaces (termed fabric) to the cell air is:

$$\dot{Q}_{c,fab}(t) = \dot{Q}_{c,si,wall}(t) + \dot{Q}_{c,si,win}(t) + \dot{Q}_{c,floor}(t) + \dot{Q}_{c,ceil}(t) + \dot{Q}_{c,m1}(t) + \dot{Q}_{c,m2}(t) \quad (B.4)$$

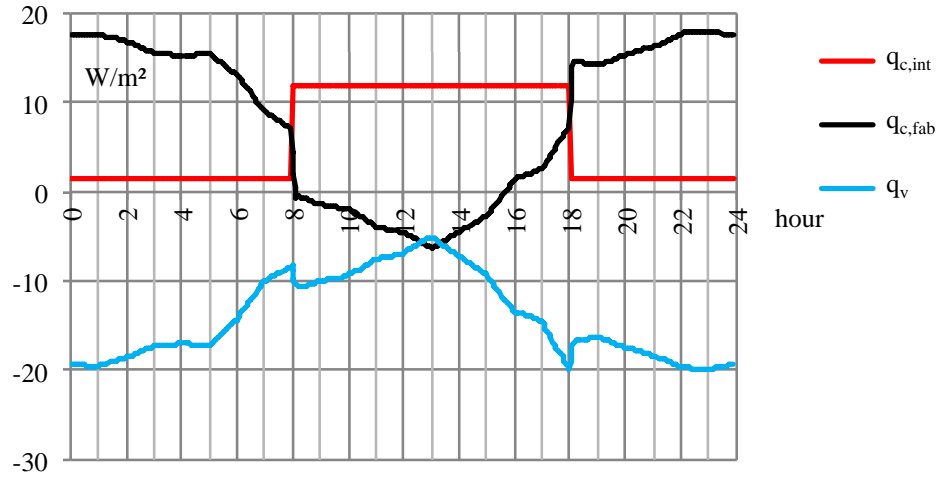


Figure B-2: Typical heat flux balance of the cell air per m² net office floor area (850 m²).

As a measure of the total energy, the enthalpy includes the sensible heat of the dry air and the latent heat of the evaporated water [1]:

$$H_{\text{air}} = c_{\text{air}} \cdot T_{\text{air}} + HR \cdot (c_{\text{wv}} \cdot T_{\text{air}} + H_{\text{we}}) \quad (\text{B.5})$$

The specific heat capacity of air (c_{air}) at constant pressure is assumed with $1\,006\text{ J kg}^{-1}\text{ K}^{-1}$, the specific heat of water vapour (c_{wv}) at constant pressure with $1\,840\text{ J kg}^{-1}\text{ K}^{-1}$, and the evaporation heat of water (H_{we}) with $2\,502\,000\text{ J kg}^{-1}$ [1].

The external air enthalpy is calculated at local height of the cell (centroid):

$$H_{\text{ext},z}(t) = 1006 \left[\frac{\text{J}}{\text{kg} \cdot \text{K}} \right] \cdot T_{\text{ext},z}(t) + HR(t) \cdot \left(1840 \left[\frac{\text{J}}{\text{kg} \cdot \text{K}} \right] \cdot T_{\text{ext},z}(t) + 2502000 \left[\frac{\text{J}}{\text{kg}} \right] \right) \quad (\text{B.6})$$

Assuming that all internal heat gains are from sensible heat, the enthalpy of the internal air is:

$$H_{\text{in}}(t) = 1006 \left[\frac{\text{J}}{\text{kg} \cdot \text{K}} \right] \cdot T_{\text{in}}(t) + HR(t) \cdot \left(1840 \left[\frac{\text{J}}{\text{kg} \cdot \text{K}} \right] \cdot T_{\text{in}}(t) + 2502000 \left[\frac{\text{J}}{\text{kg}} \right] \right) \quad (\text{B.7})$$

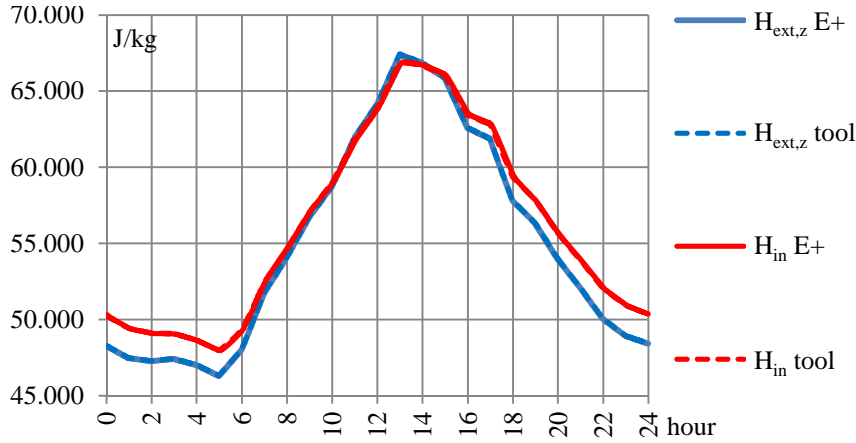


Figure B-3: Enthalpy of the external, internal, and moist air (E+ validation case).

B.3 Heat Transfer Models

B.3.1 Convection

Internal

Internal convection occurs at all construction (lumped capacity model) surfaces facing the internal air. Assuming that the cell's floor and ceiling are both internal and the temperature on each storey is equal, there is no air temperature difference across the construction, which therefore can be treated as adiabatic. All heat transfer into the surface is a result of the dynamic response of the construction, and therefore this adiabatic construction can still store or release energy. All internal convective heat exchange is dynamically computed by constant convective heat transfer coefficients:

$$\dot{Q}_{c,si}(t) = h_{c,si} \cdot (T_{in}(t-1) - T_{si}(t-1)) \cdot A_{si} \cdot \Delta t \quad (B.8)$$

External

The external convection is realised again by the classical formulation for convective heat transfer, but includes a dynamically calculated exterior surface convective film coefficient:

$$\dot{Q}_{c,se}(t) = h_{c,se}(t-1) \cdot (T_{ext,z}(t-1) - T_{se}(t-1)) \cdot A_{se} \cdot \Delta t \quad (B.9)$$

The convective film coefficient depends on the outside air temperature and on the wind velocity. It is calculated according to the Mobile Window Thermal Test (MoWiTT) method [2] for smooth surfaces. The original model has been modified according to Booten *et al.* [3] so that it is sensitive to the local wind speed which

varies with the height. For simplicity half of the façade area is treated as windward side, and the other half as leeward side, resulting in a uniform average heat exchange over the overall façade surface:

$$h_{c,se}(t) = \frac{\sqrt{\left(0,84 \cdot \left(|T_{ext,z}(t) - T_{se}(t)|\right)^{\frac{1}{3}}\right)^2 + (3,26 \cdot v_z^{0,89})^2}}{2} + \frac{\sqrt{\left(0,84 \cdot \left(|T_{ext,z}(t) - T_{se}(t)|\right)^{\frac{1}{3}}\right)^2 + (3,55 \cdot v_z^{0,617})^2}}{2} \quad (B.10)$$

B.3.2 Thermal radiation

According to ASHREA [4], it is reasonable to assume for a ‘grey body’ that emissivity and absorptivity are equal, and are constant over wavelength ($0 < \alpha = \varepsilon < 1$). The heat transferred is equal to the radiation entering minus the radiation leaving surface. The grey body equation for two parallel surfaces is the governing equation, which can be expressed as:

$$\dot{Q}_{s,1 \rightleftharpoons s,2} = \varepsilon \cdot \sigma \cdot (T_{s,1}^4 - T_{s,2}^4) \cdot A_s \cdot \Delta t \quad (B.11)$$

Most building materials (including glazing) have high emissivity of the order of 0,9. Highly reflective materials such as polished metals have emissivity of the order of 0,1. A typical value for the absorptivity of clear glass is 0,84 [3].

Internal

Assuming that all the walls forming the enclosure have the same emissivity, the grey body equation governing the internal radiative heat exchange between the surfaces is:

$$\dot{Q}_{si \rightleftharpoons \infty}(t) = \varepsilon \cdot \sigma \cdot (T_{\infty}(t-1)^4 - T_{si}(t-1)^4) \cdot A_{si} \cdot \Delta t \quad (B.12)$$

where one surface is at the surface temperature of the construction and the other is at the mean radiant temperature of all other surrounding surfaces. The mean radiant temperature of the half sphere facing the construction surface is the weighted mean radiant temperature of the surrounding elements only dependent on their areas. For simplicity, view factors representing the orientations and reflectance are not

included. Only the surfaces of the inner side of the external walls and windows are modelled as not facing each other. Typically, the weighted mean radiant temperature of the half sphere surrounding the inner side of the external wall is:

$$T_{\infty \rightarrow \text{si,wall}}(t) = \frac{T_{\text{mr}}(t) - A_{\%,\text{wall}} \cdot T_{\text{si,wall}}(t) - A_{\%,\text{win}} \cdot T_{\text{si,win}}(t)}{1 - A_{\%,\text{wall}} - A_{\%,\text{win}}} \quad (\text{B.13})$$

The equations for the other surrounding surfaces are analogous, but are not shown here.

External

The external thermal radiation exchange including few factors is a simple standard formulation essentially identical to the ones utilised in EnergyPlus [5] and TARP [6]. The external surfaces exchange heat to the sky, the air, and the ground [6,7], though the ground is assumed to be at the same temperature as the ambient air [5]. A rough approximation made for simplicity is that the sky temperature is assumed to be the ambient air temperature minus 12 °C. The total heat flux at the exterior surface (e.g., window, wall) is the total absorbed thermal radiation from the sky, the air, and the ground, minus the thermal radiation emitted:

$$\dot{Q}_{\text{se} \rightarrow \infty}(t) = (q_{\text{se} \leftarrow \infty}(t) - q_{\text{se} \rightarrow \infty}(t)) \cdot A_{\text{se}} \cdot \Delta t \quad (\text{B.14})$$

with the absorbed long wave radiation also dependent on the surface properties:

$$q_{\text{se} \leftarrow \infty}(t) = \alpha_{\text{se}} \cdot \sigma \cdot (F_{\text{sky}} \cdot (T_{\text{ext}}(t-1) - 12 [\text{K}])^4 + F_{\text{atm}} \cdot T_{\text{ext}}(t-1)^4 + F_{\text{gnd}} \cdot T_{\text{ext}}(t-1)^4) \quad (\text{B.15})$$

and the emitted long wave radiation:

$$q_{\text{se} \rightarrow \infty}(t) = \varepsilon_{\text{se}} \cdot \sigma \cdot T_{\text{se}}(t-1)^4 \quad (\text{B.16})$$

The view factors are dependent on the tilt angle of the surface [3]. For the façade the view factors are 0,500 facing the ground, 0,146 to the atmosphere and 0,354 to the sky:

$$\dot{Q}_{\text{se} \rightarrow \infty}(t) = \varepsilon_{\text{se}} \cdot \sigma \cdot (0,354 \cdot (T_{\text{ext}}(t-1) - 12[^\circ\text{C}])^4 + 0,646 \cdot T_{\text{ext}}(t-1)^4 - T_{\text{se}}(t-1)^4) \cdot A_{\text{s}} \cdot \Delta t \quad (\text{B.17})$$

The thermal radiation long wave transmittance of windows is assumed to be zero, and therefore windows can be treated like opaque walls.

B.3.3 Solar radiation

Internal

The ‘pre-processed’ total transmitted solar radiation (see § B.4) is further processed for the distribution of heat flux to all the internal surfaces. Incoming hourly transmitted radiation values are first interpolated depending on the timestep, and then further split into diffuse and direct beams according to the shading devices selected (see § B.4). Internal fabrics absorb and reflect the incoming beam, depending on their surface properties.

All entering direct beam is initially added to the floor construction’s surface only dependent on the floor’s reflectance, which is the share not absorbed. The reflected beam is treated as diffuse radiation incident on all the other surfaces including the window glazing.

The direct solar heat flux absorbed by the floor is:

$$\dot{Q}_{\tau,\text{dir},\text{floor}} = \alpha_{\text{floor}} \cdot \dot{Q}_{\tau,\text{dir}} \quad (\text{B.18})$$

The direct solar heat flux reflected by the floor and absorbed by the other surfaces is dependent on their absorptivity weighted area. The total absorption weighted area facing the reflected direct radiation by the floor surface is:

$$A_{\infty\leftarrow\text{dir},\text{floor}} = \alpha_{\text{ceil}} \cdot A_{\text{ceil}} + \alpha_{\text{si},\text{wall}} \cdot A_{\text{wall}} + \alpha_{\text{si},\text{win}} \cdot A_{\text{win}} + 2 \cdot \alpha_{\text{m}} \cdot A_{\text{m}} \quad (\text{B.19})$$

For example, the reflected direct solar heat flux absorbed by the ceiling is:

$$\dot{Q}_{\tau,\text{dir},\text{ceil}} = \frac{\alpha_{\text{ceil}} \cdot A_{\text{ceil}}}{A_{\infty\leftarrow\text{dir},\text{floor}}} \cdot (1 - \alpha_{\text{floor}}) \cdot \dot{Q}_{\tau,\text{dir}} \quad (\text{B.20})$$

The equations for the other floor facing surfaces are analogous, but are not shown here.

The diffuse beam is distributed to all the internal surfaces facing the windows, depending on their area and absorptivity. There is no reflection modelled back to the inner faces of windows or walls.

The total absorption/reflectance weighted area facing the windows for the calculation of the diffuse solar beam distribution is:

$$A_{\infty \leftarrow \text{dif,win}} = (\alpha_{\text{floor}} + \alpha_{\text{ceil}}) \cdot A_{\text{floor}} + \alpha_{\text{m}} \cdot 2 \cdot A_{\text{m}} \quad (\text{B.21})$$

The diffuse solar heat flux absorbed by the internal, window-facing surfaces is again dependent on their absorptivity weighted area. For example, for the ceiling:

$$\dot{Q}_{\tau,\text{dif,ceil}} = \frac{\alpha_{\text{ceil}} \cdot A_{\text{ceil}}}{A_{\infty \leftarrow \text{dif,win}}} \cdot \dot{Q}_{\tau,\text{dif}} \quad (\text{B.22})$$

The equations for the other window facing surfaces are again analogous, but not shown here.

External

Solar radiation absorbed by the external envelope is backcalculated from the ‘pre-processed’ transmitted solar (see § B.4) according to the simple window indices method definition in EnergyPlus [8]. This dependency was chosen due to the predominant impact of the transmitted solar energy compared to the radiation absorbed on the exterior envelope, assuming that glazed facades with relatively low U-values have good thermal insulation.

Simple window indices are converted into an equivalent single layer window. The technical procedure to determine the absorbed solar radiation by the windows is separated into four steps, where the first three steps are taken from the original method by Arasteh *et al.* [8], and the last step is newly developed to adapt the method for the approach of this tool.

Step 1: For windows with U-values smaller than 5,85, the film coefficients in winter are:

$$R_{\text{si,win,wi}} = \frac{1}{0,359073 \cdot \ln(U_{\text{win}}) + 6,949915} \quad (\text{B.23})$$

$$R_{\text{se,win,wi}} = \frac{1}{0,025342 \cdot U_{\text{win}} + 29,163853} \quad (\text{B.24})$$

The window inner resistance is:

$$R_{\text{win}} = \frac{1}{U_{\text{win}}} - R_{\text{si,win,wi}} - R_{\text{se,win,wi}} \quad (\text{B.25})$$

Step 2: For windows with U-values smaller than 3,4 and with a SHGC bigger than 0,15, the solar transmittance at normal incidence can be approximated by:

$$\tau = 0,085775 \cdot SHGC^2 + 0,963954 \cdot SHGC - 0,084958 \quad (\text{B.26})$$

Step 3: For windows with U-values smaller than 3,4 the film coefficients in summer are:

$$R_{\text{si,win,su}} = \frac{1}{199,8208128 \cdot (SHGC - \tau)^3 - 90,639733 \cdot (SHGC - \tau)^2 + 19,737055 \cdot (SHGC - \tau) + 6,766575} \quad (\text{B.27})$$

$$R_{\text{se,win,su}} = \frac{1}{5,763355 \cdot (\tau - R_{\text{si,win,su}}) + 20,541528} \quad (\text{B.28})$$

The inward flowing fraction of the absorbed solar radiation is:

$$\alpha_{\%,\text{win,in}} = \frac{R_{\text{se,win,su}} + 0,5 \cdot R_{\text{win}}}{R_{\text{se,win,su}} + R_{\text{win}} + R_{\text{si,win,su}}} \quad (\text{B.29})$$

The total solar radiation absorptivity of the windows at normal incidence is:

$$\alpha_{\text{win}} = \frac{SHGC - \tau}{\alpha_{\%,\text{win,in}}} \quad (\text{B.30})$$

Step 4: A factor of 1,2 roughly transforms the angular transmittance value to the solar transmittance at normal incidence. The factor was gathered from E+ test simulations for the Kanyon building during summer.

For simplicity in the model, half of the absorbed solar radiation is absorbed at the external pane and the other half at the internal pane of the double glazing:

$$\dot{Q}_{\text{sol,se,win}} = \dot{Q}_{\text{sol,si,win}} = 0,5 \cdot \frac{\alpha_{\text{win}}}{1,2} \cdot \dot{Q}_{\tau} \quad (\text{B.31})$$

Table B-1: Simple glazing model parameters for the Canyon Lo-E double glazing.

inputs			interim result		
U_{win}	1,400	W/m ² -K	R_{win}	0,539	m ² -K/W
SHGC	0,444	-	τ	0,360	-
			α_{win}	0,190	-

The solar radiation absorbed by external walls is calculated as a direct function of the E+ pre-processed window transmitted solar radiation. The surface mean outside face incident solar radiation absorbed is the transmitted solar radiation multiplied by a factor to convert the transmitted radiation to total radiation on the surface, further multiplied by the wall's absorption coefficient:

$$\dot{Q}_{sol,se,wall} = \frac{\dot{Q}_{\tau}}{1,2} \cdot \frac{A_{wall}}{A_{win}} \cdot \alpha_{wall} \quad (B.32)$$

B.3.4 Internal gains

Internal heat gains are based on hourly value schedules and are not interpolated. The total convective internal heat gains are:

$$\dot{Q}_{int,c} = \dot{Q}_{peop,c} + \dot{Q}_{light,c} + \dot{Q}_{equip,c} \quad (B.33)$$

The total radiative internal heat gains are:

$$\dot{Q}_{int,r} = \dot{Q}_{peop,r} + \dot{Q}_{light,r} + \dot{Q}_{equip,r} \quad (B.34)$$

The total absorption/reflection weighted area for the calculation of the internal heat gains beam distribution is:

$$A_{\infty \leftarrow int,r} = (\alpha_{floor} + \alpha_{ceil}) \cdot A_{floor} + 2 \cdot \alpha_m \cdot A_m + \alpha_{wall} \cdot A_{wall} + \alpha_{win} \cdot A_{win} \quad (B.35)$$

The heat flux absorbed by the internal surfaces is again dependent on their absorptivity weighted area. For example, for the ceiling:

$$\dot{Q}_{int,r,ceil} = \frac{\alpha_{ceil} \cdot A_{ceil}}{A_{\infty \leftarrow int,r}} \cdot \dot{Q}_{int,r} \quad (B.36)$$

The equations for the other surfaces are again analogous, but not shown here.

People

People's heat gain rates for office work are pre-set at $108 \text{ W person}^{-1}$. The radiant fraction is assumed to be 50%, which again is the E+ default value. General densities of people densities in offices per $\text{m}^2/\text{workstation}$ according to ASHRAE may be found in § 4.2.3.

Lights

Heat gain rates from the lights are scheduled values in W/m^2 net floor area. They values may be pre-processed by E+, if dimmers are applied in the case studied. The radiant fraction assumed is 37%, which is the E+ default value.

Equipment

Heat gain rates from the equipment are again scheduled values in W/m^2 net floor area. The radiant fraction assumed is 20%, which again is the E+ default value.

B.3.5 Thermal mass

In general and in rectangular coordinates, temperature is a function of space and time: $T = f(x, y, z, t)$. In a Lumped Capacitance Model LCM (also lumped system analysis), it is assumed that the temperature at any time is uniform within the body and therefore discretised in space: $T = f(t)$.

A thermal body has the properties mass, volume, density and the initial temperature T_{ini} which in the model is the temperature from the previous timestep. The body object is exposed to the outside temperature T_{∞} by the total film resistance to the outside, which depending on the type of heat transfer is the convective resistance $R_c = 1/h_c$ or the radiative resistance $R_r = 1/h_r$ plus the internal resistance from the surface to the heat capacity of the body.

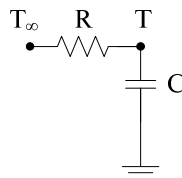


Figure B-4: Basic RC Lumped Capacitance Model.

The temperature of a solid body with capacity as a function of time is:

$$C \cdot \frac{dT}{dt} = \frac{T - T_{\infty}}{R} \quad (\text{B.37})$$

After separation of the variables and derivation:

$$\ln\left(\frac{T_{(t)} - T_{\infty}}{T_{\text{ini}} - T_{\infty}}\right) = -\frac{t}{C \cdot R} \quad (\text{B.38})$$

$$\frac{T_{(t)} - T_{\infty}}{T_{\text{ini}} - T_{\infty}} = e^{-\frac{t}{C \cdot R}} \quad (\text{B.39})$$

With the time constant (see below):

$$\tau = R \cdot C \quad (\text{B.40})$$

The basic lumped equation for the temperature of a solid with the initial condition temperature becomes:

$$T(t) = e^{-\frac{t}{\tau}} \cdot (T(t-1) - T_{\infty}) + T_{\infty} \quad (\text{B.41})$$

The LCM was utilised for the prediction of thermal behaviour in various studies like [9-14], but a full set of the formulae could not be found by the author, and is therefore given in in the following section for the simple LCM applied in the tool.

The LCM outlined for the design tool is capable of representing a five layered LCM construction as shown in Figure 3.26. This simplified model is chosen due to its low computational effort and stability, which is therefore especially suited for a dynamic spread sheet application. Because of the simplified approach, the tool must be used with care if there are several heavyweight layers in one construction, since the number of layers (in terms of heat capacity) is restricted to five and at least one layer represents the surface layer on each face. The dominant mass layer can be further subdivided into sub-layers in order to guarantee to a certain extent that the temperatures inside these sub-layers do not vary significantly in space. Therefore, it is recommended only to use constructions with an obvious thermal mass distribution (or to extend the model if necessary). In the following, the index *i* indicates the layers of the LCM from 1 to 5. ‘Pre-processed’ examples of real multi-layered constructions converted into five-layered LCMs may be found in the building constructions library § B.5.

The time constant τ is a measure of the time needed by a slab of thermal mass to react to a change in the input. The lower the time constant, the faster the heating or

cooling of a solid. Two time constants are calculated for each side of the LCM-layer with the resistance multiplied by the capacitance:

$$\tau_{i,1} = R_{i,1} \cdot C_i \quad (\text{B.42})$$

$$\tau_{i,2} = R_{i,2} \cdot C_i \quad (\text{B.43})$$

where the resistances on each side of the LCM-layers capacity are calculated by:

$$R_{i,1} = \frac{k_i \cdot d_i}{2} + \frac{k_{i-1} \cdot d_{i-1}}{2} \quad (\text{B.44})$$

$$R_{i,2} = \frac{k_i \cdot d_i}{2} + \frac{k_{i+1} \cdot d_{i+1}}{2} \quad (\text{B.45})$$

and the heat capacities of the LCM-layers are calculated by:

$$C_i = \rho_i \cdot c_i \cdot d_i \quad (\text{B.46})$$

A lumped capacitance model is valid for Biot-Numbers much smaller than 1. The Biot number Bi is an index of the ratio of the heat transfer resistances that indicates if the thermal resistance of the fluid interface exceeds that thermal resistance within the body or material. If Bi is much smaller than 1 (in literature often smaller than 0,1), then the temperatures inside a body will not vary significantly in space.

Thermal loads are raising or lowering the thermal capacitance of an LCM layer from both sides. Therefore, the temperature shift for each timestep with a certain interval (here 60s) is calculated from one side and superposed by the other side:

$$T_i(t) = e^{-\frac{\Delta t}{\tau_{i,1}}} \cdot (T_i(t-1) - T_{i-1}(t-1)) + T_{i-1}(t-1) + e^{-\frac{\Delta t}{\tau_{i,2}}} \cdot (T_i(t-1) - T_{i+1}(t-1)) + T_{i+1}(t-1) - T_i(t-1) \quad (\text{B.47})$$

where index i indicates the position of the three inner LCM layers from 2 to 4. The calculations are based on adjacent temperatures from the previous timestep.

For building internal constructions, the external LCM layers are calculated from the inner side of the body and the sum of internal heat fluxes incident:

$$T_1(t) = e^{-\frac{\Delta t}{\tau_{5,1}}} \cdot (T_1(t-1) - T_2(t-1)) + T_2(t-1) + \frac{\dot{Q}_{si \pm \infty}(t) + \dot{Q}_{int,r,si}(t) + \dot{Q}_{\tau,dir,si}(t) + \dot{Q}_{\tau,dif,si}(t) + \dot{Q}_{c,si}(t)}{C_1 \cdot A_{si}} \quad (\text{B.48})$$

$$T_5(t) = e^{-\frac{\Delta t}{\tau_{5,1}}} \cdot (T_5(t-1) - T_4(t-1)) + T_4(t-1) + \frac{\dot{Q}_{si \pm \infty}(t) + \dot{Q}_{int,r,si}(t) + \dot{Q}_{\tau,dir,si}(t) + \dot{Q}_{\tau,dif,si}(t) + \dot{Q}_{c,si}(t)}{C_5 \cdot A_{si}} \quad (\text{B.49})$$

From the solid side, the change in temperature is calculated depending on the inner temperature, the conductivity, and capacity of the body like described before. Heat exchange from the exposed side is from convection and radiation (see Figure 3.27).

The building internal surface temperatures are calculated from the closest inner mass temperature and the adjacent air temperature via the resistors in series electrical analogy. R is half the resistance of the first LCM sub-layer:

$$T_{si,1}(t) = T_1(t-1) - \frac{T_1(t-1) - T_{in}(t-1)}{\frac{k_1 \cdot d_1}{2} + \frac{1}{h_c}} \cdot \frac{k_1 \cdot d_1}{2} \quad (\text{B.50})$$

$$T_{si,5}(t) = T_5(t-1) - \frac{T_5(t-1) - T_{in}(t-1)}{\frac{k_5 \cdot d_5}{2} + \frac{1}{h_c}} \cdot \frac{k_5 \cdot d_5}{2} \quad (\text{B.51})$$

For building external constructions, the external LCM layer ($i=1$) temperature is calculated from the inner side of the body and the sum of external heat fluxes incident:

$$T_1(t) = e^{-\frac{\Delta t}{\tau_{1,2}}} \cdot (T_1(t-1) - T_2(t-1)) + T_2(t-1) + \frac{\dot{Q}_{se \pm \infty}(t) + \dot{Q}_{sol,se}(t) + \dot{Q}_{c,se}(t)}{C_1 \cdot A_{se}} \quad (\text{B.52})$$

The building external surface temperatures are calculated from the closest inner mass temperature (here for the LCM layers $i=1$) and the adjacent air temperature:

$$T_{se}(t) = T_1(t-1) - \frac{T_1(t-1) - T_{in}(t-1)}{\frac{k_1 \cdot d_1}{2} + \frac{1}{h_c}} \cdot \frac{k_1 \cdot d_1}{2} \quad (\text{B.53})$$

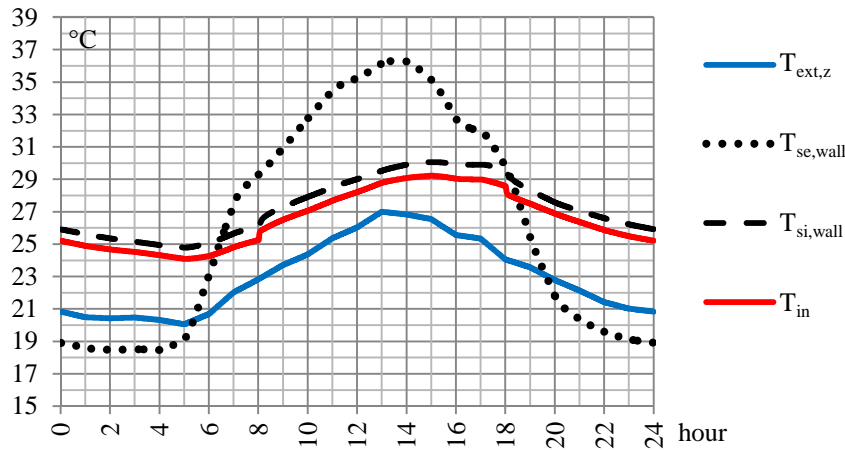


Figure B.5: Typical temperature distribution of an lightweight, insulated external wall.

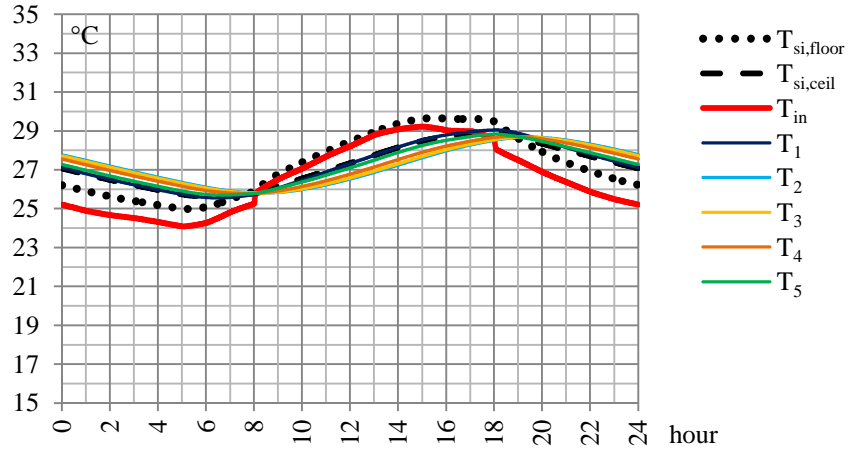


Figure B.6: Typical temperature distribution of an internal floor/ceiling LCM construction including 12,5 cm concrete as the ceiling layer and a suspended carpet/plywood tile as the floor layer.

The average internal mean radiant temperature of the internal space is a measure of the combined effects of temperatures of all the internal surfaces. It is calculated assuming that the occupant is in the centre of the cell with no weighting for any particular surface:

$$T_{mr}(t) = \frac{T_{si,wall}(t) \cdot A_{wall} + T_{si,win}(t) \cdot A_{win} + (T_{floor}(t) + T_{ceil}(t)) \cdot A_{floor} + (T_{si,m1}(t) + T_{si,m2}(t)) \cdot A_m}{A_{wall} + A_{win} + 2 \cdot A_{floor} + 2 \cdot A_m} \quad (B.54)$$

B.3.6 Natural ventilation

Heat gains and losses due to ventilation per timestep are a function of the mass flow rate multiplied by the enthalpy difference between the external and the internal air. The mass flow rate per timestep is the volume flow rate multiplied the mean air density between inside and outside:

$$\dot{Q}_v(t) = |\dot{m}(t)| \cdot (H_{ext,z}(t) - H_{in}(t)) \quad (B.55)$$

$$\dot{m}(t) = \dot{V}(t) \cdot \frac{\rho_{ext,z}(t) + \rho_{in}(t)}{2} \quad (B.56)$$

Heat losses occur if the external temperature is lower than the internal temperature.

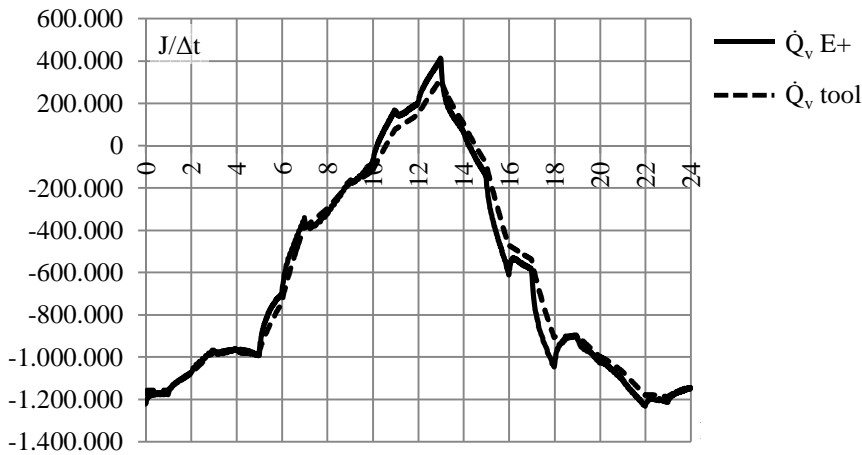


Figure B.7: Moist air total ventilative heat exchange (E+ validation case).

B.4 Transmitted Solar Heat

Pre-processed transmitted solar radiation values \dot{Q}_τ , used as design tool input, were simulated by E+ BEPS. The simulation setup was a simple one zone model (Figure B.8) using the E+ design day object including the sun path along with the scheduled SWMD solar radiation profiles from § 5.3.3.

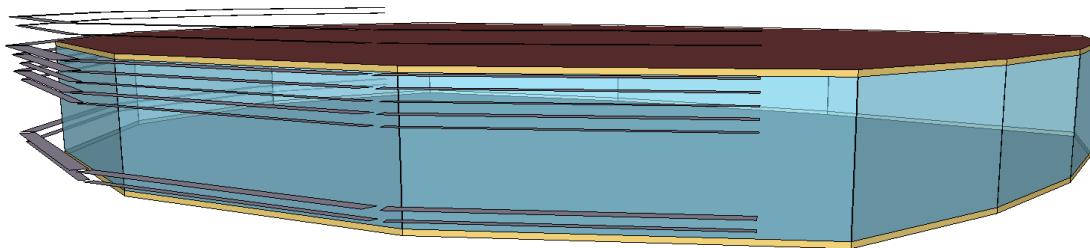


Figure B.8: EnergyPlus simulation model for gathering the transmitted solar radiation of one storey of the Kanyon building with the as-built external shading and the glazing ratio of ~ 91 % (~ SE view).

Nine cases were investigated and results are shown in Figure B.9 through Figure B.11. E+ simulations have to be repeated for each case. However the transmitted solar gains for each case are in linear dependence to the overall glazing ratio.

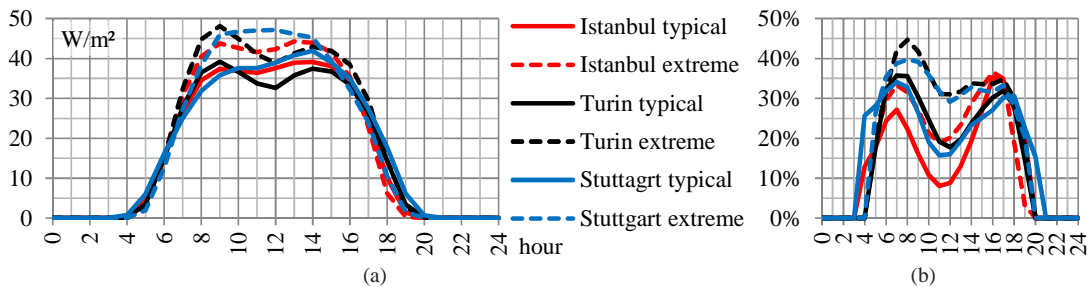


Figure B.9: Hourly SWMD (a) total transmitted solar radiation for Kanyon building without external shading devices per m^2 net office floor area and (b) the direct beam solar radiation share.

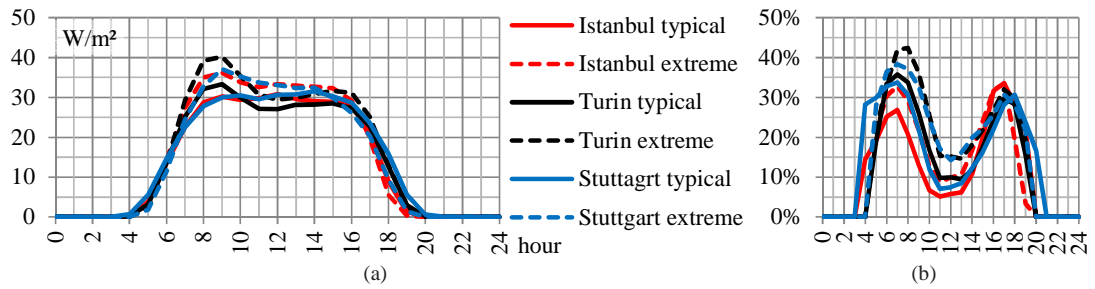


Figure B.10: Hourly SWMD (a) total transmitted solar gains for Kanyon building with the actual shading devices per m² net office floor area and (b) the direct beam solar radiation share.

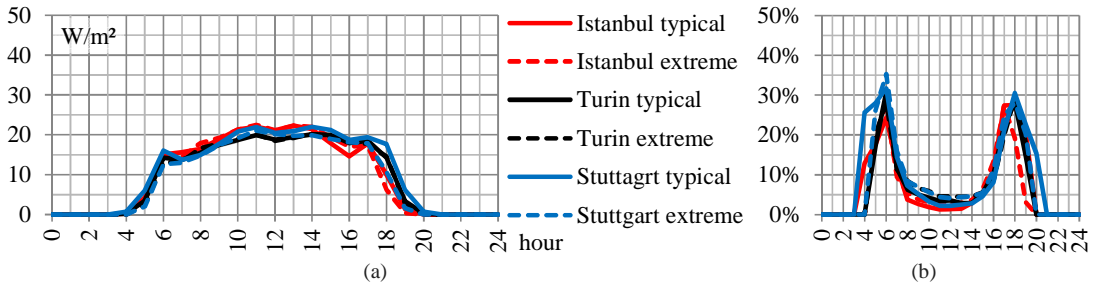


Figure B.11: Hourly SWMD (a) total transmitted solar gains for Kanyon building with adaptive blinds per m² net office floor area and (b) the direct beam solar radiation share.

Simulations showed that for the Kanyon case-study building, about 10-35% of the daily mean incoming radiation is direct beam depending on the external shading device. The more effective the shading devices are, the more they block direct radiation entering the windows. For simplicity, the fraction of transmitted direct beam solar from the total transmitted solar radiation chosen for the tool calculations is independent on time: 30% for windows without external shades, 20% for buildings with external overhangs, and 10% for buildings with adaptive setpoint controlled blinds.

B.5 Building Constructions Library

B.5.1 Floor / ceiling

Table B.2: Material properties of the floor / ceiling construction layers.

	case ¹	d in m	ρ in kg/m ³	c_p in J/kg-K	k in W/m-K	R in m ² -K/W	C in J/K-m ²
carpet	1/2	0,0060	288	1390	0,06	0,100	2.402
plywood	1/2	0,0300	544	1210	0,12	0,250	19.747
airspace	1/2	0,1700	-	-	-	0,180	-
concrete	1/2/3	0,1250	1920	840	1,10	0,114	201.600
airspace	1/3	0,9900	-	-	-	0,180	-
plasterboard	1/3	0,0125	800	1090	0,58	0,022	10.900

¹ case 1: actual floor / ceiling
 case 2: mass activated ceiling
 case 3: mass activated floor

Table B.3: LCM properties of the floor / ceiling construction calculated.

layer i	actual floor / ceiling			mass activated ceiling			mass activated floor		
	C in J/m ² -K	R in m ² -K/W	τ in s	C in J/m ² -K	R in m ² -K/W	τ in s	C in J/m ² -K	R in m ² -K/W	τ in s
1,1		0,225			0,175			0,014	
1	22 149			22 149			50 400		
1,2		0,324	7 176		0,374	8 284		0,028	1 411
2,1			21 773			18 850			1 411
2	67 200			50 400			50 400		
2,2		0,038	2 544		0,028	1 432		0,028	1 411
3,1			2 544			1 432			1 411
3	67 200			50 400			50 400		
3,2		0,038	2 544		0,028	1 432		0,028	1 411
4,1			2 544			1 432			1 411
4	67 200			50 400			50 400		
4,2		0,210	14 112		0,028	1 432		0,205	10 332
5,1			2 289			1 432			2 235
5	10 900			50 400			10 900		
5,2		0,011			0,014			0,011	

B.5.2 External wall

Table B.4: Material properties of the wall construction layers.

	case ¹	d in m	ρ in kg/m ³	c _p in J/kg-K	k in W/m-K	R in m ² -K/W	C in J/K-m ²
metal	1	0,0020	7824	500	45,280	0,000	7 824
xps extruded polystyrene	1	0,0200	35	1400	0,034	0,588	980
wall air space	1	0,1000	-	-	-	0,150	-
mw stone wool rolls	1	0,1000	30	840	0,040	2,500	2 520
metal	1	0,0010	7824	500	45,280	0,000	3 912

¹ case 1: actual lightweight wall

Table B.5: LCM properties of the wall construction calculated.

layer i	actual lightweight wall		
	C in J/m ² -K	R in m ² -K/W	τ in s
1,1		0,000022	
1	7 824		
1,2			4 225
2,1		0,540	630
2	1 167		
2,2			1 259
3,1		1,079	1 259
3	1 167		
3,2			1 259
4,1		1,079	1 259
4	1 167		
4,2			630
5,1		0,540	2 112
5	3 912		
5,2		0,000011	

B.5.3 Internal partitions

Table B.6: Material properties of the partition construction layers.

	case ¹	d in m	ρ in kg/m ³	c _p in J/kg-K	k in W/m-K	R in m ² -K/W	C in J/K-m ²
oak wood	1	0,013	1630	608	0,150	0,087	12 884
wall air space	1	0,025	-	-	-	0,150	-
concrete reinforced	1/2	0,400	1920	840	1,100	0,364	645 120
wall air space	1	0,025	-	-	-	0,150	-
oak wood	1	0,013	1630	608	0,150	0,087	12 884

¹ case 1: actual partitions
case 2: mass activated partitions

Table B.7: LCM properties of the internal partition constructions calculated.

layer i	actual partitions			mass activated partitions		
	C in J/m ² -K	R in m ² -K/W	τ in s	C in J/m ² -K	R in m ² -K/W	τ in s
1,1		0,043			0,036	
1	12 884			129 024		
1,2		0,254	3 273		0,073	9 384
2,1			54 620			9 384
2	215 040			129 024		
2,2		0,121	26 020		0,073	9 384
3,1			26 020			9 384
3	215 040			129 024		
3,2		0,121	26 020		0,073	9 384
4,1			26 020			9 384
4	215 040			129 024		
4,2		0,213	54 620		0,073	9 384
5,1			3 273			9 384
5	30 336			129 024		
5,2		0,043			0,036	

References Appendix B

- [1] **EngineeringToolBox.** (n.d.). Enthalpy of Moist and Humid Air. Retrieved April, 2013, from http://www.engineeringtoolbox.com/enthalpy-moist-air-d_683.html
- [2] **Yazdaniyan, M., & Klems, J. H.** (1993). *Measurement of the exterior convective film coefficient for windows in low-rise buildings* ASHRAE Transactions (Vol. 100-1, pp. 19). Atlanta, USA: American Society of Heating, Refrigerating and Air-Conditioning Engineers. Retrieved from <http://btech.lbl.gov/>
- [3] **Booten, C., Kruis, N., & Christensen, C.** (2012). *Identifying and Resolving Issues in EnergyPlus and DOE-2 Window Heat Transfer Calculations* (Vol. BE120104, pp. 50). Denver, USA: National Renewable Energy Laboratory. Retrieved from <http://www.osti.gov/>
- [4] **ASHRAE.** (2009). *Handbook of Fundamentals*. Atlanta, USA: American Society of Heating, Refrigerating and Air-Conditioning Engineers.
- [5] **EnergyPlus** (Version 8.1). (2013). *Engineering Reference* The Reference to EnergyPlus Calculations (pp. 1399). Washington DC, USA: U. S. Department of Energy. Retrieved from <http://apps1.eere.energy.gov/>
- [6] **Walton, G. N.** (1983). *TARP Reference manual* Thermal analysis research program (Vol. NBSIR, 83-2655, pp. 277). Washington DC, USA: U.S. Dept. of Commerce, National Bureau of Standards.
- [7] **Pedersen, C. O., Fisher, D. E., & Liesen, R. J.** (1997). Development of a Heat Balance Procedure for Calculating Cooling Loads. *ASHRAE Transactions*, 103(2), 459-468. doi: 10.2172/975375
- [8] **Arasteh, D., Kohler, C., & Griffith, B.** (2009). *Modeling Windows in Energy Plus with Simple Performance Indices* (Vol. LBNL-2804E, pp. 28). USA: Berkeley Lab. Retrieved from <http://www.osti.gov/>
- [9] **Ramallo-González, A. P., Eames, M. E., & Coley, D. A.** (2013). Lumped parameter models for building thermal modelling: An analytic approach to simplifying complex multi-layered constructions. *Energy and Buildings*, 60(0), 174-184. doi: 10.1016/j.enbuild.2013.01.014
- [10] **Kontoleon, K. J., & Bikas, D. K.** (2002). Modeling the influence of glazed openings percentage and type of glazing on the thermal zone behavior. *Energy and Buildings*, 34(4), 389-399. doi: 10.1016/S0378-7788(01)00125-6
- [11] **Kontoleon, K. J., & Eumorfopoulou, E. A.** (2008). The influence of wall orientation and exterior surface solar absorptivity on time lag and decrement factor in the Greek region. *Renewable Energy*, 33(7), 1652-1664. doi: 10.1016/j.renene.2007.09.008
- [12] **Gustafsson, J., Delsing, J., & Deventer, J. v.** (2008, April). *Thermodynamic Simulation of a Detached House with District Heating Subcentral*. Paper presented at the SysCon - IEEE International Systems Conference, Montreal, Canada. Paper retrieved from <http://ieeexplore.ieee.org/>
- [13] **Fraisse, G., Viardot, C., Lafabrie, O., & Achard, G.** (2002). Development of a simplified and accurate building model based on electrical analogy. *Energy and Buildings*, 34(10), 1017-1031. doi: 10.1016/S0378-7788(02)00019-1
- [14] **Feustel, H. E.** (1995). *Simplified numerical description of latent storage characteristics for phase change wallboard* (Vol. LBL-36933, pp. 15). USA: Lawrence Berkeley Laboratory. Retrieved from <http://www.osti.gov/>

CURRICULUM VITAE

Name Surname : Tobias Schulze

Date and Place of Birth : 03.08.1978, Munich, Germany

E-Mail : schulze-tobias@gmx.de



EDUCATION:

- 1999-2004 **Diplom-Ingenieur (FH)** German university degree in engineering (4 years), Renewable Energy Programme, University of Applied Sciences for Engineering and Economics Berlin, Germany

PROFESSIONAL EXPERIENCE:

- 2013-2015 **Research Associate** ‘KonLuft’ enhancing the energy efficiency of buildings through automatic natural ventilation, Sponsored by the Energy Optimised Construction (EnOB) Research Initiative of the German Federal Ministry of Economics and Technology, Centre for Sustainable Energy Technology (zafh.net), University of Applied Sciences, Stuttgart, Germany
- 2012-2013 **Research Assistant** ‘Plus-Energie-Schule’ study on an energy-efficient school building in Reutershagen in Rostock, Sponsored by the Energy-Oriented Improvement of the Building Fabric (EnSan) Research Initiative of the German Federal Ministry of Economic Affairs and Energy (BMWi) University of Applied Sciences, Stuttgart, Germany
- 2012 **Research Associate** Development and implementation of a tool for the dimensioning of controlled natural ventilation, Research project of the University of Applied Sciences Stuttgart in cooperation with the German Electrical and Electronic Manufacturers' Association (ZVEi)
- 2011 **Research Associate** ‘Pro Fensterlüftung’ study on controlled natural ventilation by using motorized windows, Research project of the University of Applied Sciences Stuttgart in cooperation with the German Electrical and Electronic Manufacturers' Association (ZVEi)
- 2008-2010 **Marie-Curie Actions Research Fellowship** ‘CITYNET’ Ph.D. Program on Sustainable Energy Management, Founded by the European Union, Project partners: University College Dublin, DeMontfort University, Opole Technical University, Istanbul Technical University, Strathclyde University, Polytechnic University of Turin, Rovira i Virgili University

- 2006-2008 **Project Manager** Concept Development for web-based simulation tools and technical advisor of the management of co2online gGmbH, non-profit consulting company responsible for the 'Climate Seeks Protection' campaign funded by the Federal Ministry for the Environment, SEnerCon GmbH, consulting company, Berlin, Germany
- 2005-2006 **Trainee** SEnerCon GmbH, consulting company, Berlin, Germany
- 2005 **Internship** co2online gGmbH, non-profit consulting company, Berlin, Germany
- 2002-2003 **Internship Abroad** Altertec S.A., consultancy for renewable energy systems, Managua, Nicaragua

PUBLICATIONS, PRESENTATIONS AND PATENTS ON THE THESIS:

- **Schulze, T.**, Eicker, U. & Yılmaz, Z. (2013). A Simplified Calculation Methodology for Controlled Natural Ventilation. Paper presented at Climamed 2013, Istanbul, Turkey
- **Schulze, T.** (2010). Natural Ventilation Design and Hybrid Cooling. Presented at the POLYCITY Closing Conference and CITYNET Workshop, Stuttgart, Germany
- **Schulze, T.** & Yılmaz, Z. (2010). Modeling Energy Efficient Design of a Naturally Ventilated Office Tower in Mild Climate Using EnergyPlus. Paper presented at the IAQVEC 2010, Syracuse, USA
- **Schulze, T.** (2010). et al.: Building Energy Efficient Cities. TV-Interview, In EuroNews, Sci-tech Magazine

OTHER PUBLICATIONS, PRESENTATIONS AND PATENTS:

- Erhart, T., Gürlich, D., **Schulze, T.** & Eicker, U. (2015). Experimental Validation of Basic Natural Ventilation Air Flow Calculations for Different Flow Paths and Window Configurations. Paper presented at the International Building Physics Conference, Turin, Italy
- **Schulze, T.** (2014). Passive Solar, Natural Ventilation and Daylighting of Buildings, 2b Natural Ventilation. In Eicker U. (Eds.), Energy Efficient Buildings with Solar and Geothermal Resources (pp. 67-96). UK: Wiley. ISBN: 978-1-118-35224-3
- **Schulze, T.**, & Eicker, U. (2013). Methodik zur vereinfachten Berechnung kontrollierter natürlicher Lüftung [A Methodology for the Simplified Calculation of Controlled Natural Ventilation]. *Bauphysik [Building Physics]*, 35(2), 99-106
- **Schulze, T.**, & Eicker, U. (2013). Controlled Natural Ventilation for Energy Efficient Buildings. *Energy and Buildings*, 56(0), 221-232. doi: 10.1016/j.enbuild.2012.07.044
- **Schulze, T.** & Eicker, U. (2013). Erweiterung der Lüftungskonzepte nach DIN 1946-6 zur vereinfachten Berechnung natürlicher Fensterlüftung [Extension of the ventilation concepts according to DIN 1946-6 for the simplified calculation of natural window ventilation]. Paper presented at the Bauphysikertreffen [building physicist conference], Stuttgart, Germany

- **Schulze, T. & Eicker, U.** (2012). Kontrollierte natürliche Lüftung für energieeffiziente Gebäude [Controlled Natural Ventilation for Energy Efficient Buildings]. In Pöschk, J. (Eds.), Energieeffizienz in Gebäuden, Jahrbuch 2012, Innovative Technik für mehr Energieeffizienz [Energy efficiency in buildings, Yearbook 2012, Innovative technology for increased energy efficiency] (pp. 235-250). Germany: VME Verlag und Medienservice Energie. ISBN: 978-3-936062-08-3
- **Schulze, T., Atmaca, M. & Yılmaz, Z.** (2010). Effect of Office Tower Integrated Multifunctional PV Systems on Total Greenhouse Gas Emissions and Economical Quantifying in Turkey. Paper presented at Clima 2010, Antalya, Turkey